Title
LOW ENERGY ELECTRON DIFFRACTION AND WORK FUNCTION STUDIES OF ADSORBED ORGANIC LAYERS ON THE (100) AND (111) CRYSTAL SURFACES OF PLATINUM.

Author
Gland, John Louis.

Publication Date
1973-09-01

LBL-1816
c.1

LOW ENERGY ELECTRON DIFFRACTION AND WORK FUNCTION STUDIES OF ADSORBED ORGANIC LAYERS ON THE (100) AND (111) CRYSTAL SURFACES OF PLATINUM

John Louis Gland
(Ph. D. thesis)

September 1973

Prepared for the U. S. Atomic Energy Commission
under Contract W-7405-ENG-48

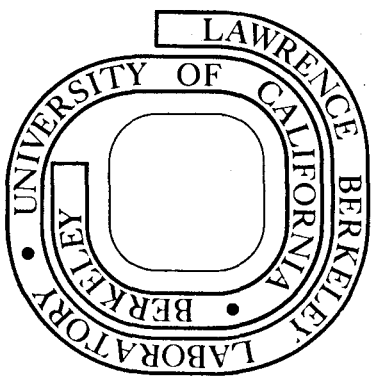

LBL-1816
c.1

DISCLAIMER

TO

Wanda Ruth Gland

"I've got a woman five feet short . . .
She's a humdinger . . . a folksinger

Table of Contents

acetylene $H-C \equiv C-H$

aniline 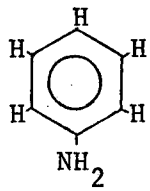

benzene 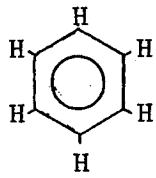

biphenyl 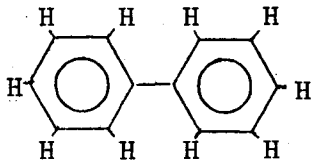

n-butybenzene 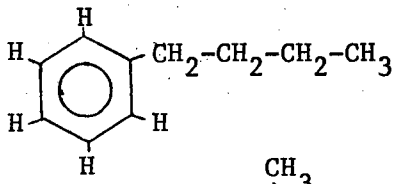

t-butylbenzene 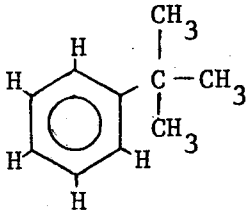

cyanobenzene 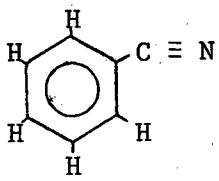

1,3-cyclohexadiene 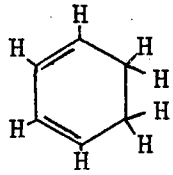

cyclohexane 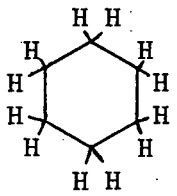

cyclohexene 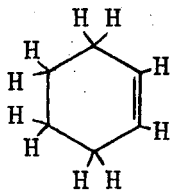

cyclopentane 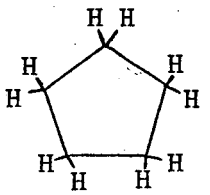

cyclopentene 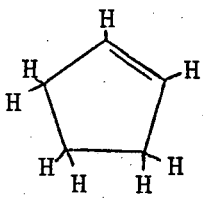

2,6-dimethylpyridine 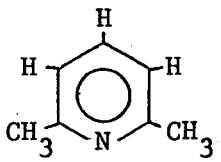

3,5-dimethylpyridine 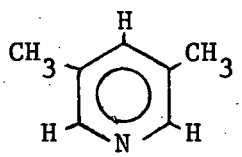

ethane CH_3-CH_3

ethylene $CH_2 = CH_2$

n-hexane $CH_3-CH_2-CH_2-CH_2-CH_2-CH_3$

isoquinoline 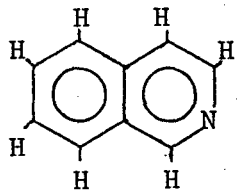

mesitylene 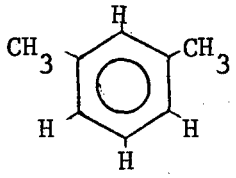

2-metylnaphthalene 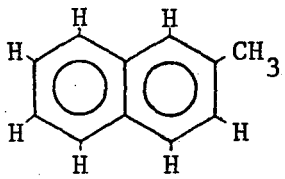

naphthalene 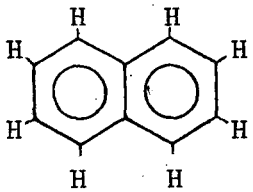

nitrobenzene 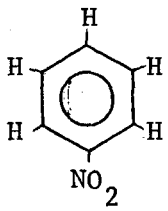

piperidine 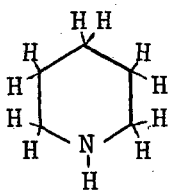

propylene $CH_3-CH = CH_2$

pyridine

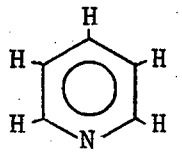

pyrrole

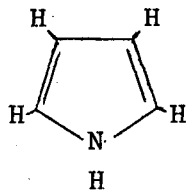

quinoline

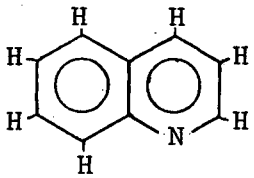

styrene

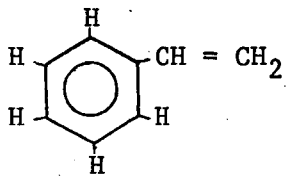

toluene

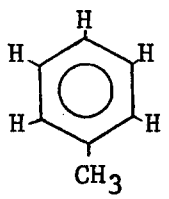

m-xylene

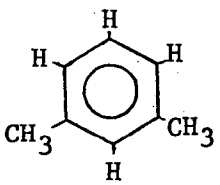

LOW ENERGY ELECTRON DIFFRACTION AND WORK FUNCTION STUDIES OF ADSORBED ORGANIC LAYERS ON THE (100) AND (111) CRYSTAL SURFACES OF PLATINUM

John Louis Gland

Inorganic Materials Research Division, Lawrence Berkeley Laboratory and Department of Chemistry; University of California, Berkeley, California

ABSTRACT

The adsorption of a group of organic compound has been studied on the platinum (100) and (111) single crystal surfaces. Low energy electron diffraction has been used to determine surface structures. Work function change measurements have been made to determine the charge redistribution which occurs on adsorption. The molecules which have been studied are acetylene, aniline, benzene, biphenyl, n-butylbenzene, t-ubtybenzene, cyanobenzene, 1,3-cyclohexadiene, cyclohexane, cyclohexene, cyclopentane, cyclopentene, 2,6-dimethylpyridine, 3,5-dimethylpyridine, ethylene, n-hexane, isoquinoline, mesitylene, 2-methylnaphthalene, napthalene, nitrobenzene, piperidine, propylene, pyridine, pyrrole, quinoline, styrene, toluene, m-xylene. All molecules studied adsorb on both the Pt(111) and Pt(100)-(5×1) surfaces. All molecules studied act as electron donors to the metal surface. The adsorbed layers are more ordered on the hexagonally symmetric Pt(111) surface than on the square symmetric Pt(100) surface. Unsaturated molecules generally adsorb on the Pt(111) and Pt(100) surface by forming π-bonds with the metal surface.

I. INTRODUCTION

A. Preface

The adsorption of organic molecules on metal surfaces is of primary importance in several areas of surface science. The adsorption of organic layers plays a large role in adhesion, friction, wear, lubrication, corrosion, and catalysis.

The properties of adsorbed layers depends on the interaction between the adsorbed molecules and the metal. This thesis reports a study of the interaction of several groups of organic compounds with platinum single crystal surfaces. Low Energy Electron Diffraction (LEED) has been used to monitor the structures of adsorbed layers on the Pt(111) and Pt(100)-(5×1) crystal surfaces. Work function changes (WFC, $\Delta\phi$) on adsorption have been used to determine the charge transfer occurring on adsorption. Both the charge transfer which occurs on adsorption and the structures formed have been used to obtain information about the nature of the interaction between the organic overlayer and metal substrate.

The predominance of ordered adsorption of low index single crystal surfaces was one of the significant findings resulting from Low Energy Electron Diffraction studies. Many of the molecules commonly used as adsorbates to date were small, with molecular dimensions less than the interactomic distance in the substrate. These adsorbed molecules can form structures with the rotational symmetry of the substrate such that the unit vectors of the surface structure are closely related to the substrate unit vector.[1,2] For large molecules with dimensions several times larger than the substrate interatomic distance, ordering

on the surface may depend on the substrate characteristics in a more complex manner. Large molecules may interact simultaneously with a large number of surface atoms, so the structures formed may be less restricted by the periodicity of the substrate. For example xenon forms an ordered xenon crystal with (111) orientation regardless of substrate rotational symmetry.[3,4,5,6] In this case we see a predominance of adsorbate-adsorbate interaction in determining the surface structure since the adsorbate-substrate interaction potential is fairly uniform across the surface.

B. Adsorption

1. Adsorption on Single Crystal Surfaces

Low Energy Electron Diffraction (LEED) can be used to determine the periodicity of single crystal sample surfaces. Auger Electron Spectroscopy (AES) can be used as a sensitive means to determine the composition of surfaces. These two techniques combined in an ultra-high vacuum system (pressure $< 10^{-8}$ Torr) allow one to perform experiments on clean, well-ordered single crystal surfaces over reasonable experimental time periods. Somorjai[1,2] has reviewed the adsorption data generated using this type of experimental procedure. This thesis reports results gathered using this type of system to study adsorption on well characterized low index platinum single crystal surfaces.

A significant amount of adsorption work has been done on platinum single crystal surfaces although some of the early work suffered from the absence of surface analysis by AES. Tucker[7] studied the adsorption of CO and O_2 on the Pt(111), Pt(100) and Pt(110) surfaces using LEED, however, the samples were cleaned by heating in vacuum exclusively (it has subsequently been shown that platinum cannot be cleaned by heating alone). Morgan and Somorjai[8] studied the adsorption of H_2, N_2, N_2O, O_2, CO, CO_2, CH_4, C_2H_6, C_2H_2 and C_2H_4 on the Pt(100)-(5×1) surface using LEED. They found that CO, H_2, C_2H_2 and C_2H_4 adsorb and form ordered structures. In a later paper Morgan and Somorjai[9] used LEED, mass spectrometry and work function change studies to characterize adsorbed layers of CO, C_2H_2, C_2H_4, C_3H_6, 1,3-butadiene and the isomeric butenes adsorbed on the Pt(111) and Pt(100)-(5×1) surfaces. They conclude that the olefins π-bond to the metal surface via their unsaturated carbon-carbon bond and that the molecules form more orderly overlayers on the hexagonal Pt(111) surface. Smith and Merrill[10] studied the adsorption of ethylene on the Pt(111) surface using molecular beam scattering and LEED. They conclude that ethylene adsorbs irreversibly with dissociation into an acetylenic species and mobile hydrogen atoms at room temperature. Clarke, Mason, and Tescari[11] have carried out LEED and high resolution Auger studies of carbon monoxide, ethylene, vinylchloride, vinylfluoride, 1,1 difluoroethylene, butadiene, propene and hexafluoropropene adsorbed on the Pt(100)-(5×1) surface. They used X-ray induced photoelectron spectroscopy to study CO adsorption which showed there is a net transfer of electrons from

platinum into carbon monoxide. They also carried out detailed analysis of the LEED diffraction information for carbon monoxide adsorption and concluded that there are two adsorption types (terminal and bridged adsorption types). They also concluded that the Auger transition energies provide no general evidence for "chemical shifts" but that chemisorption leads to significant modification of some Auger transition probabilities involving platinum valence electrons.

Bonzel and Ku[12] have studied the adsorption of CO and O_2 on the clean Pt(110)-(1×2) surface using LEED, Auger, and mass spectrometry. Their primary concern, however, was the oxidation of CO by O_2 using the Pt(110) surface as a catalyst. They found that that reaction proceeds on the Pt(110) surface, but the mechanism depends on the reaction conditions used.

Bonzel and Ku[13] have also studied the adsorption of sulfur on the Pt(110)-(1×2) surface and the effect of sulfur adsorption on subsequent CO adsorption using LEED, Auger, and mass spectrometry. They have found that sulfur interacts strongly with the surface and decreases the amount of CO adsorbed.

Weinberg, Lambert, Comrie, and Linnett[14] studied the adsorption of oxygen on the Pt(111) surface. They concluded that the initial sticking coefficient for oxygen on Pt(111) is approximately 7×10^{-7} and that carbon contamination causes larger sticking coefficients. A theoretical model (CSFO-BEEBO) is applied which correlates well with the experimental results.

Weinberg and Merrill[15] have reviewed the data for hydrogen adsorption on the Pt(111) surface. They outline the CSFO-BEEBO model and apply it successfully to the interaction between hydrogen and the Pt(111) surface.

Weinberg, Deans and Merrill[16] have studied the adsorption of ethylene and acetylene on the Pt(111) surface. They review the existing data and successfully apply the CSFO-BEEBO model to the system. They conclude that ethylene adsorbs dissociatively while acetylene remains intact on adsorption and that a second layer of reversibly adsorbed ethylene adsorbs on the dissociatively adsorbed first layer.

Lang, Joyner, and Somorjai[17] have used LEED to study the adsorption of hydrogen, oxygen, carbon, carbon monoxide, and ethylene on two high index platinum surfaces identified by the Miller indices (977) and (755) or Pt(S)-[9(111)×(111)] and Pt(S)-[6(111)×(100)]. These high index surfaces have a regular array of monatomic height steps with low index terraces separating the steps.[18] In the nomenclature given for stepped surfaces[18] the Pt(S)-[6(111)×(100)] was cut 9.5° from the (111) toward the (100) face and has monatomic (100) steps separated by (111) terraces 6 atomic units wide (measured along a close packed direction). They found that the result of adsorption on these stepped surfaces is markedly different from the results of adsorption on low index surfaces, and that there is a stronger interaction of the adsorbed gases with the stepped surfaces. They also found that carbon forms several ordered structures on these high index surfaces. (Carbon forms a disordered graphite overlayer on the low index surfaces).

Joyner, Lang, and Somorjai[19] studied the reaction n-heptane to toluene on several single crystal platinum surfaces using LEED and mass spectrometry. The reaction was studied on the Pt(111), Pt(S)-[6(111)×(100)], and the Pt(S)-[5(100)×(111)] surfaces. They found that the reaction proceeds on the stepped surfaces but not the low index surfaces and correlate the activity with the formation of ordered carbon overlayers.

Baron, Blakely, and Somorjai[20] have studied the adsorption of n-heptane, toluene, benzene, ethylene, and cyclohexane on four stepped platinum surfaces (the Pt(S)-[9(111)×(100)], Pt(S)-[6(111)×(100)], Pt(S)-[7(111)×(310)] and Pt(S)-[4(111)×(100)]) using LEED. The [4(111)×(100)] surface is unstable and facets in the presence of hydrocarbons and hydrogen. The chemisorption of hydrocarbons produces carbonaceous deposits whose characteristics depend on the substrate structure, the type of hydrocarbon adsorbed, the rate of adsorption and the surface temperature. Hydrocarbons on the [9(111)×(100)] and [6(111)×(100)] crystal faces form mostly ordered overlayers while disordered carbonaceous layers are formed on the [7(111)×(310)] surface which has a high concentration of kinks. A simple model is proposed to account for the characteristics of these surfaces.

Bernasek, Siekhaus and Somorjai[21] have studied the hydrogen-deuterium exchange reaction over the Pt(111) and Pt(S)[9(111)×(111)] surfaces using reactive molecular beam scattering. They find that the Pt(111) surface does not catalyze the exchange reaction in the temperature range 20°C to 700°C while the Pt(S)[9(111)×(111)] catalyzes the exchange reaction at all temperatures used. Further work is underway to

determine the details of the reaction mechanism on the Pt(S)-[9(111)-(111)] surface.

Recent studies by Blakely, Baron and Somorjai[22] have shown that ordered carbonaceous surface structures are important in hydrocarbon catalysis.

Recent studies by Deville and Somorjai[23] using Auger and LEED to study acetylene, isobutylene, butadiene, cyclohexane, benzene, naphthalene, n-heptane and carbon monoxide adsorption on the Pt(111) surface have shown that an inner shell Auger transition of platinum (NNN) is shifted by larger amounts with increasing unsaturation in the adsorbate. Benzene adsorbed on the Pt(111) surface gives shifts of the opposite sign with respect to clean platinum when compared to the other compounds studied. The ordered structure observed on adsorption agree with those found in this study.

Several adsorption experiments have been reported concerning adsorption of large organic molecules on low index nickel single crystal surfaces. Dalmar-Imelik and Bertoline[24] studied benzene and cyclohexane adsorption on the Ni(110) and Ni(111) surfaces using LEED and mass spectrometry. They conclude that adsorption on the Ni(110) surface causes dissociation of both molecules. Benzene and cyclohexane adsorbed on the Ni(111) surface remain unaltered up to a surface temperature of 180°C.

Edmonds, McCarroll, and Pitkethly[22] have studied benzene adsorption on the Ni(100) and Ni(111) surfaces. They conclude that the benzene adsorbs without loss of hydrogen with its ring parallel to the (111)

face, but the benzene appears to be compressed on the (100) surface which may suggest loss of aromaticity.

Maire, Anderson, and Johnson[23] have studied methane, ethane, and neopentane adsorbed on the (111), (100) and (110) nickel surfaces using LEED and photoelectric work function determinations. They conclude that all three molecules adsorbed on all of the low index nickel surfaces dissociate into CH_2 units on adsorption. The adsorbates act as electron donors to the metal surface.

2. Adsorption on Polycrystalline Surfaces

A review of polycrystalline adsorption work for metal surfaces would encompass several volumes. The interested reader is referred to several books which address this subject.[27,28,29] However, there are several topics which are particularly relevant to the work contained in this thesis. The adsorption of aromatic compounds on metals has received considerable attention in the past because of the importance of aromatic compounds.

Bond devotes a chapter in his book to the adsorption of various types of aromatic compounds.[27] Moyes and Wells in a recent review concentrate on the adsorption of benzene on metal surfaces.[30] Garnett[31] reviews homogeneous and heterogeneous exchange data for a series of unsaturated and aromatic hydrocarbons and explores the mechanistic relationship between them.

Garnett and Sollich-Baumgartner[32] review adsorption for a large number of aromatic compounds on a number of metal surfaces and review their π-complex adsorption model.

C. Surface Characterization

1. General Introduction

Somorjai[33] has reviewed the techniques commonly used for the characterization of surfaces. Surface Science[34] has recently devoted an issue to a selection of review articles concerning methods of surface characterization ranging from Low Energy Electron Diffraction to Scanning Electron Microscopy. An brief introduction to the primary techniques used in this work will now be made.

2. Low Energy Electron Diffraction

The diffraction of low energy electrons was first observed by Davisson and Germer in 1927[35,36] in an experiment which confirmed the wave hypothesis of De Broglie. It was confirmed that the distribution of the diffracted beams could be explained by assuming that the electrons have a wavelength (λ) which is related to their energy by the De Broglie relationship

$$\lambda = \frac{h}{p} = \frac{h}{mv} = \frac{h}{(2mE_p)^{1/2}} = \frac{h}{2meV_p} = \sqrt{\frac{150.4}{V_p}}$$

where

V_p = the accelerating voltage applied to the incident electrons

h = Plank's constant.

p = the momentum of the electrons

m = electron mass

Ep = eV_p = the energy of the incident electrons

e = the electronic charge

and that the scattering occurred from the periodic lattice of the surface atoms as if it were a two-dimensional diffraction grating.

Unlike comparable wavelength X-rays which penetrate deeply into the bulk of the solid, low energy electrons (< 500 V) have a large scattering cross section, and thus a substantial fraction of the incident beam is backscattered from the first few layers of the surface. Therefore these backscattered electrons are a valuable probe of surface properties From the diffraction information the size and shape of the surface unit cell can be easily determined using simple 2-dimensional grating equations. However, the orientation of the basis set of surface atoms or molecules with respect to the unit cell and the perpendicular distance between the outermost layers cannot be uniquely determined using a simple two dimensional analysis. To determine such information uniquely, scattering theory must be used to calculate diffracted intensities as a function of incident energy for the various diffracted beams. This calculated data must then be matched with experimentally measured intensities for the various diffraction beams.

Kinematic or single scattering theory used in X-ray and neutron diffraction work is inadequate for the calculation of diffracted intensities since the large scattering cross section of low energy electrons makes multiple scattering important. A number of people have developed theoretical approaches to the multiple scattering problem. These theories consider the physics of most of the processes that occur in the crystal in order to reproduce the experiments. Recently several notable successes have been achieved in correlating

theoretical calculations with experimental data. Duke, Tucker, and Larramore,[37] Marcus, Jepsen and Jona,[38] Tong and Rhodin,[39] Martin and Somorjai[40] have all demonstrated that their procedures reproduce the experimental results for the low index faces of face centered cubic aluminum. Pendry[41] working primarily with nickel, has also had substantial success in matching experimental intensity data. Several review papers have been published concerning the calculation of LEED intensities.[42,43]

The relationship between an array of scattering centers and the corresponding diffraction pattern for the case in which elastic single scattering occurs will now be briefly discussed. The results derived are applicable for the analysis of the size and shape of the surface unit cell. An incident electron beam can be described as a plane wave with an equation of motion.

$$A(r) = A(o) \exp i(\vec{k}\cdot\vec{r} - \omega t).$$

where A(r) is the amplitude at a point r, A(o) the amplitude at an origin, $\vec{k}$ the wavevector and ω the angular frequency. The wavevector $\vec{k}$ is related to the wavelength and energy of the incident beam by the equation

$$|k| = \frac{2\pi}{\lambda} = \frac{2\pi(2mE_p)^{1/2}}{h}$$

The condition of elastic scattering requires that $|k'|^2 = |k^\circ|^2$ where

$|k^\circ|$ = wavevector of the incident beam

$|k'|$ = wavevector of the scattered beam

The two dimensional diffraction conditions are

$$\vec{k}'_{\parallel} = \vec{k}^{\circ}_{\parallel} + \vec{G}_{\parallel}(h,k)$$

where

$|k^{\circ}_{\parallel}|$ = component of the incident wavevector parallel to the surface

$|k'_{\parallel}|$ = component of the scattered wavevector parallel to the surface

$|G_{\parallel}(h,k)|$ = the set of recriprocal lattice vectors which describes the regular two dimensional scattering array

If the regular two dimensional scattering array is described by the basis vectors $\vec{a}$ and $\vec{b}$ with a unit vector $\vec{z}$ perpendicular to the plane formed by the intersection of the vectors $\vec{a}$ and $\vec{b}$ and pointing into the solid.

The set of reciprocal unit vectors is determined by the equation

$$\vec{G}_{\parallel}(h,k) = 2\pi \frac{h(\vec{b}\times\hat{z})}{\vec{a}\cdot\vec{b}\times\hat{z}} + \frac{k(\hat{z}\times\vec{a})}{\vec{a}\cdot\vec{b}\ \hat{z}}$$

where h and K are integers. For a more complete review of kinematic scattering theory the reader is referred to the literature.[44]

3. The Work Function and Work Function Change on Adsorption

A number of good reviews discuss both the theory of work functions and work function changes as well as the experimental methods used for measuring them.[45,46,47] A brief synopsis of the definition of work

function and the cause of work function changes on adsorption is presented here for the sake of completeness. The material has been extracted from several primary references.[45,46,47]

The electrochemical potential $\bar{\mu}$ of electrons in a metal is defined as $(\delta A/\delta n)T,V$ where $A = E-TS$ is the Helmholtz free energy of n electrons in a volume of metal V at a temperature T. This definition is equivalent to measuring the incremental work necessary to move a small number of electrons, Δn, isothermally from infinity at rest into the constant volume V. Since one can change the potential of the interior of a conductor by changing the charge distribution outside the conductor, $\bar{\mu}$ is not only a function of the internal state of the conductor, but also depends on the condition of the surface and on external conditions. That is, any change in the electrostatic potential ($\Delta\Phi$) of the volume of metal will alter the electrochemical potential by $-e(\Delta\Phi)$ where $-e$ is the electronic charge. This effect can be isolated by defining a new quantity μ, the chemical potential, as $\mu = \bar{\mu} + e\Phi_{inner}$ where Φ_{inner} is the electrostatic potential inside the volume of metal V. The chemical potential depends only on the internal state of the volume of metal V. The work function ϕ of a uniform surface is defined in terms of the difference between the electrochemical potential of an electron inside the surface and its electrostatic energy $-e\Phi_{outer}$ at a point outside the metal where the electron is removed from significant surface interactions ($\sim 10^{-4}$ cm).

$$\phi = -\Phi_{outer} - \frac{\bar{\mu}}{e} = -\Phi_{outer} - \frac{1}{e}(\mu - e\Phi_{inner})$$

$$\phi = \Phi_{inner} - \Phi_{outer} - \frac{\mu}{e}$$

The expression ($\Phi_{inner} - \Phi_{outer}$) represents the potential difference between the inside and outside of the conductor and depends on the condition of the surface and the structure of the metal. The chemical potential μ is independent of the state of the surface.

The work function is dependent on the difference in potential between the interior of the metal sample and the potential just outside the metal surface. Adsorbates modify the charge distribution at the metal surface and hence change the work function. This effect may be evaluated in terms of the change in electrical potential caused by the redistribution of charge at the surface. Consider a sheet of uniformly charged particles each with charge q such that the density of charged species is equal to θ. A negative test charge q' experiences a force $|F| = 2\pi\theta qq'$ if the test charge is far enough away from the charged sheet so that the charge can be considered to be homogeneous. The force is attractive if the sheet is positively charged, repulsive if the sheet is negatively charged. If we now consider two oppositely charged sheets separated by a distance d with opposite but equal charge densities ($q\theta$) the test charge q' experiences a force only when it is between the two charged sheets. The repulsive and attractive interactions are additive between the plates; therefore the force experienced is $F' = 4\pi\theta qq'$. Moving the test charge from one plate to the other changes the energy by $\Delta E = 4\pi\theta qq'd$. This means that between the two sheets and in general between all points on opposite sides of the charged sheets there is a change in potential $\Delta V = \pm 4\pi\theta qd$. If we consider the arrangement of two planes to be a single dipolar plane

which contains θ dipoles per square centimeter each with a moment $M = qd$ then the change in potential is $\Delta V = \pm 4\pi\theta M$. Therefore if a dipolar layer is adsorbed parallel to the surface the work function (ϕ) will be altered by an amount $\pm 4\pi\theta M$. The minus sign is appropriate when the positive end of the dipole lies away from the surface, that is the work function decreases when the positive end of the dipole is out from the surface. One of the difficulties in applying this simple model to real adsorption systems arises because the dipole layers encountered in real situations are made of discrete dipolar elements, not homogeneously charged layers. Since the dipoles are discrete there is a depolarizing field at the position of a given dipole arising from the surrounding dipoles. This depolarization effect is included in the Topping formula for an array of point dipoles[48]

$$\Delta\phi = 4\pi M\ \theta/(1 + 9\alpha\theta^{2/3})$$

where M_o is the dipole moment perpendicular to the surface in the limit of zero coverage, α is the polarizability and θ is the density of adsorbed atoms or molecules. For comparison with experimental data Schmidt and Gomer[49] have modified the equation above to

$$\frac{\theta}{\Delta\phi}\ \left(\frac{1}{C_1}\right) + \left(\frac{C_2}{C_1}\right)\ \theta^{3/2}$$

where

$$C_1 = \left(\frac{d\Delta\phi}{d\theta}\right)_{\theta=0} = 4\pi M_o n_o$$

$C_2 = 9\alpha n_o^{3/2}$, $\theta = n/n_o$, and $n_o = 3.9\times10^{14}$ atoms/cm^2. The validity of the Topping model is then easily determined by plotting $\theta/\Delta\phi$ against $\theta^{3/2}$. The linear behavior of this characteristic determines whether the model is applicable or not. Schmidt and Gomer apply the model to potassium adsorption on several tungsten surfaces. Palmberg has also shown that this model is applicable for adsorption of xenon on Pd(100).[50]

Several papers by MacDonald and Barlow[51,52,53] have presented a more complete theortical development for the work function change expected on adsorption of polarizable polar and/or polarizable ionic species. The difficulty with the development is that there are a number of parameters which cannot be easily evaluated either theoretically or experimentally. MacDonald and Barlow[53] define a quantitity $J = \alpha/\beta^3$ where α is the polarizability and β is the distance between the electrical center of the adsorbed dipoles and the conducting surface; β might be approximated by the radius of the adsorbed atom or molecule. For values of $J \geqslant 4$, non-physical poles occur in the expression for $\Delta\phi$, the work function change. They conclude that "For any adsorbed element for which we might expect $J \geqslant 4$ in the adsorbed state, we must either conclude that the atom or molecule in question becomes wholly or partly ionized on adsorption, or that the high fields polarizing the discrete elements reduce its polarizability sufficiently that the above catastrophe does not happen." The plots of work function change ($\Delta\phi$) versus coverage which result from the variation of J show maxima in $\Delta\phi$ at small values of $\theta(< .3)$ for J

values larger than two. For benzene adsorbed parallel to the metal surface, $\alpha \sim 1.23\times10^{-23}$ cm^3[54] and $\beta \lesssim 1.7\times10^{-8}$ cm (see Appendix 1) therefore $J \sim 2.5$ for the largest reasonable distance between substrate and adsorbate. Benzene, and in fact most of the molecules studied in this thesis could easily have J values greater than four. Benzene has a maximum in its work function change versus exposure curves, however the maximum occurs after considerable exposure; thus if benzene has a high sticking coefficient up to monolayer coverage there is little similarity between this prediction and the observations.

The application of work function change theories to the systems studied is difficult because there are several factor which are unknown experimentally. The primary difficulties lie in determination of the density of adsorbed species and the separation of the metal surface and the adsorbed layer.

REFERENCES

1. G. A. Somorjai, F. J. Szalkowski, J. Chem. Phys. 54, 389 (1971).
2. G. A. Somorjai, Surf. Sci. 34, 156 (1973).
3. A. Ignaliev, A. V. Jonen, T. N. Rhodin, Surf. Sci. 30, 573 (1972).
4. P. W. Palmberg, Surf. Sci. 25, 598 (1971).
5. J. L. Lander, J. Morrison, Surf. Sci. 6, 1 (1967).
6. M. A. Chesters, J. Prilchard, Surf. Sci. 28, 460 (1971).
7. C. W. Tucker, J. of Applied Physics 35, 1897 (1964).
8. A. E. Morgan, G. A. Somorjai, Surf. Sci. 12, 405 (1968).
9. A. E. Morgan, G. A. Somorjai, J. Chem. Phys. 51, 3309 (1969).
10. D. L. Smith, R. P. Merrill, J. Chem. Physics 52, 5861 (1970).
11. T. A. Clarke, R. Mason, M. Tescari, Proc. R. Soc. Lond. A 331, 321 (1972).
12. H. P. Bonzel, R. Ku, Surf. Sci. 33, 91 (1972).
13. H. P. Bonzel, R. Ku, J. Chem. Phys. 58, 4617 (1973).
14. W. H. Weinberg, R. M. Lambert, C. M. Comeric, J. W. Linnett, Surf. Sci. 30, 299 (1972).
15. W. H. Weinberg, R. P. Merrill, Surf. Sci. 33, 493 (1972).
16. W. H. Weinberg, H. A. Deans, R. P. Merrill, submitted to Surf. Sci.
17. B. Lang, R. W. Joyner, G. A. Somorjai, Surf. Sci. 30, 454 (1972).
18. B. Lang, R. W. Joyner, G. A. Somorjai, Surf. Sci. 30, 440 (1972).
19. R. W. Joyner, B. Lang, G. A. Somorjai, J. Catalysis 27, 405 (1972).
20. Kenneth Baron, D. W. Blakely, G. A. Somorjai, Surf. Sci. to be published.

21. S. Bernasek, W. A. Seikhaus, G. A. Somorjai, Phys. Rev. Letters 30, 1202 (1973).

22. D. W. Blakely, K. Baron, G. A. Somorjai, presented at ACS National Meeting, April 9, 1973, Dallas, Texas.

23. J. P. Deville, G. A. Somorjai, Surf. Sci, to be submitted.

24. G. Dalmai-Imelik, J. C. Bertolini, Journal of Vacuum Science and Technology 9, 677 (1972).

25. T. Edmonds, J. J. McCarrol, R. C. Pitkethly, paper presented at the Discussion on Carbon Deposition on Metals, Glasgow, March 1972.

26. G. Maire, J. R. Anderson, B. B. Johnson, Proc. Roy. Soc. Lond. A 320, 227 (1970).

27. G. C. Bond Catalysis by Metals (Academic Press, New York, 1962).

28. Trapnell Chemisorption (Butterworth Press, London, 1964).

29. Chemisorption and Reactions on Metallic Films, ed. J. R. Anderson (Academic Press, New York, 1971)

30. R. B. Moyes, P. B. Wells, Advan. Catal. 23, 121 (1973).

31. J. L. Garnett, Catal. Rev. 5, 229 (1971).

32. J. L. Garnett, W. A. Sollich-Baumgartner, Advan. Catal. 16, 95 (1966).

33. G. A. Somorjai, Principles of Surface Chemistry, (Prentice-Hall, Englewood Cliffs, New Jersey, 1972).

34. Surface Science 25, 1971

35. C. Davisson, L. H. Germer, Nature 119, 558 (1927).

36. C. Davisson, L. H. Germer, Phys. Rev. 30, 705 (1927).

37. G. E. Larramore, C. B. Duke, Phys. Rev. B 5, 267 (1972).

38. D. W. Jepsen, P. M. Marcus, F. Jona, Phys. Rev. B 5, 3933 (1972).

39. S. Y. Tong, T. N. Rhodin, Phys. Rev. Lett. 26, 711 (1971).

40. M. R. Martin, G. A. Somorjai, Phys. Rev. B 7, 3607 (1973).

41. J. B. Pendry, J. Phys. Chem. 4, 2501 and 2514 (1971).

42. G. A. Somorjai, H. H. Farrell, in Advances Chem. Phys. 20, A. Prigogine, S. A. Rice, eds (John Wiley and Sons, New York 1971).

43. P. J. Estrup, E. G. McRae, Surf. Sci. 25, 1 (1971).

44. M. J. Bueger, Crystal Structure Analysis (John Wiley and Sons, New York 1960).

45. Conyers Herring, M. H. Nichols, Rev. Modern Physics 21, 185 (1949).

46. F. C. Tompkins, in Gas-Surface Interactions, E. A. Flood ed. (Marcel Dekker, New York 1967).

47. J. C. Reviere, in Solid State Surface Science, M. Green ed. (Marcel Dekker, New York, 1970).

48. A. R. Miller, Proc. Cambridge Phil. Soc. 42, 292 (1946).

49. L. D. Schmidt, R. Gomer, J. Chem. Phys. 45, 1605 (1966).

50. P. W. Palmberg, Surf. Sci. 25, 598 (1971).

51. J. Ross MacDonald, C. A. Barlow, J. Chem. Phys. 39, 412 (1963).

52. J. Ross MacDonald, C. A. Barlow, J. Chem. Phys. 44, 202 (1966).

53. J. Ross MacDonald, C. A. Barlow, Surf. Sci. 4, B81 (1966).

54. Landolt-Borstein Zahlenwerte und Fanklionen aus Physik, Chemie, Austronomic, Geophysik, und Technik 6th ed. 1(3), 509 (Springer-Verlag, Berlin, 1951).

II. EXPERIMENTAL

A. Apparatus

1. Vacuum System and Gas Inlet System

A modified Varian Leed apparatus was used in these studies. It is equipped with an isolatable, 240 ℓ/sec. Vacion pump, a water cooled titanium sublimation pump and an auxiliary 8 liter/sec. Vacion pump. Typical ambient pressures for the system are 1 to 2×10^{-9} Torr during periods of daily use.

A rotatable capillary tube was used to introduce all gases onto the crystal surface from a distance of 5 mm. This system was used so that introduced gases would have a higher incident flux on the sample surface than background gases. This is possible because the system is operated as a flow system during adsorption experiments. Photographs of the system are shown in Fig. II-1a, b & c; a simplified schematic is shown in Fig. II-2.

Fluxes at the surface can only be approximated since the ion gauge used to record the pressure was in the mouth of the ion pump. The pumping speed of the system is difficult to estimate because of the titanium sublimation pump. A lower bound for the effective pressure, P, at the surface can be calculated from the recorded pressure, p, by the equation[1]

$$P_{Torr} \gtrsim \frac{p^{T}}{39+7.08\ (T/M)^{1/2}}$$

for our experimental geometry and a minimal pumping speed (using the rated pumping speed of the ion pump). [This ignores the pumping

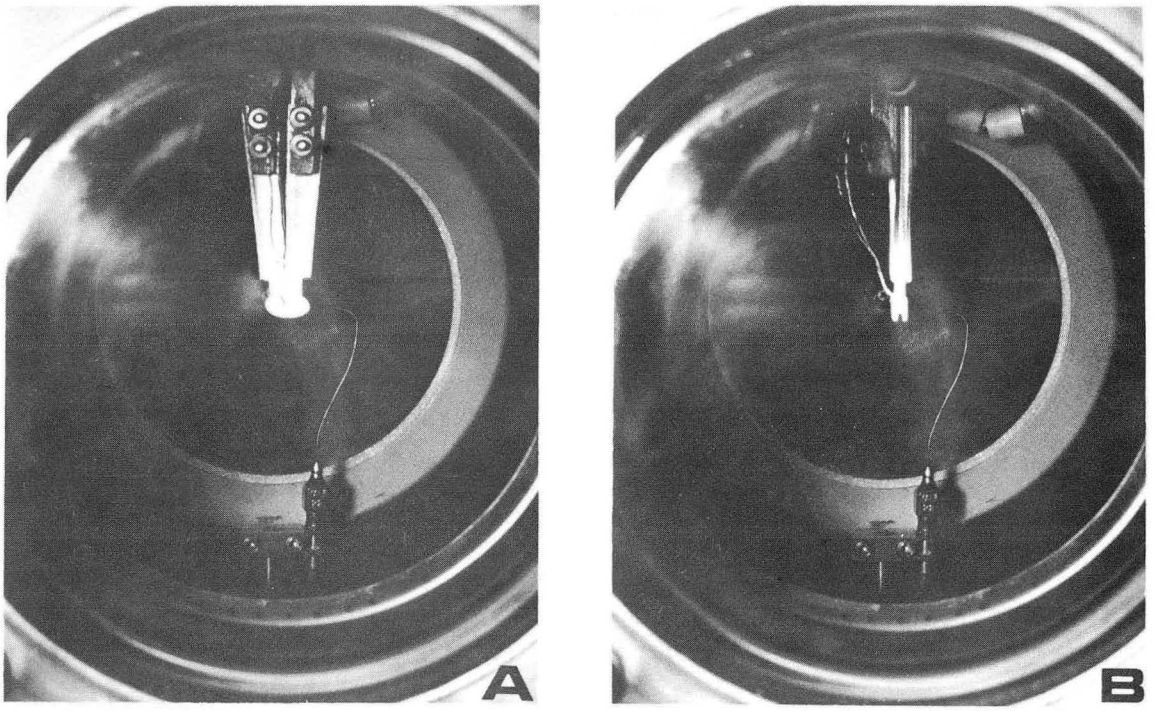

XBB 736-4125

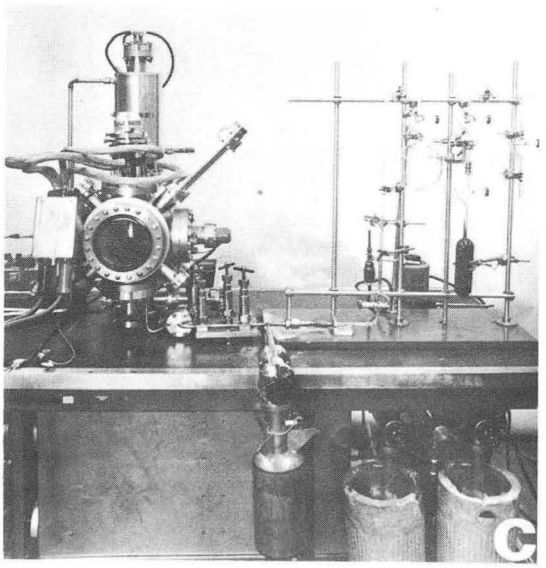

Fig. II-1. a) A photograph of the single crystal samples and the gas inlet capillary. b) A photograph of the single crystal samples showing a profile of the dual sample mount and the gas inlet capillary. c) A photograph of the vacuum chamber (notice the hot samples) and the gas manifold used for liquid and solid samples.

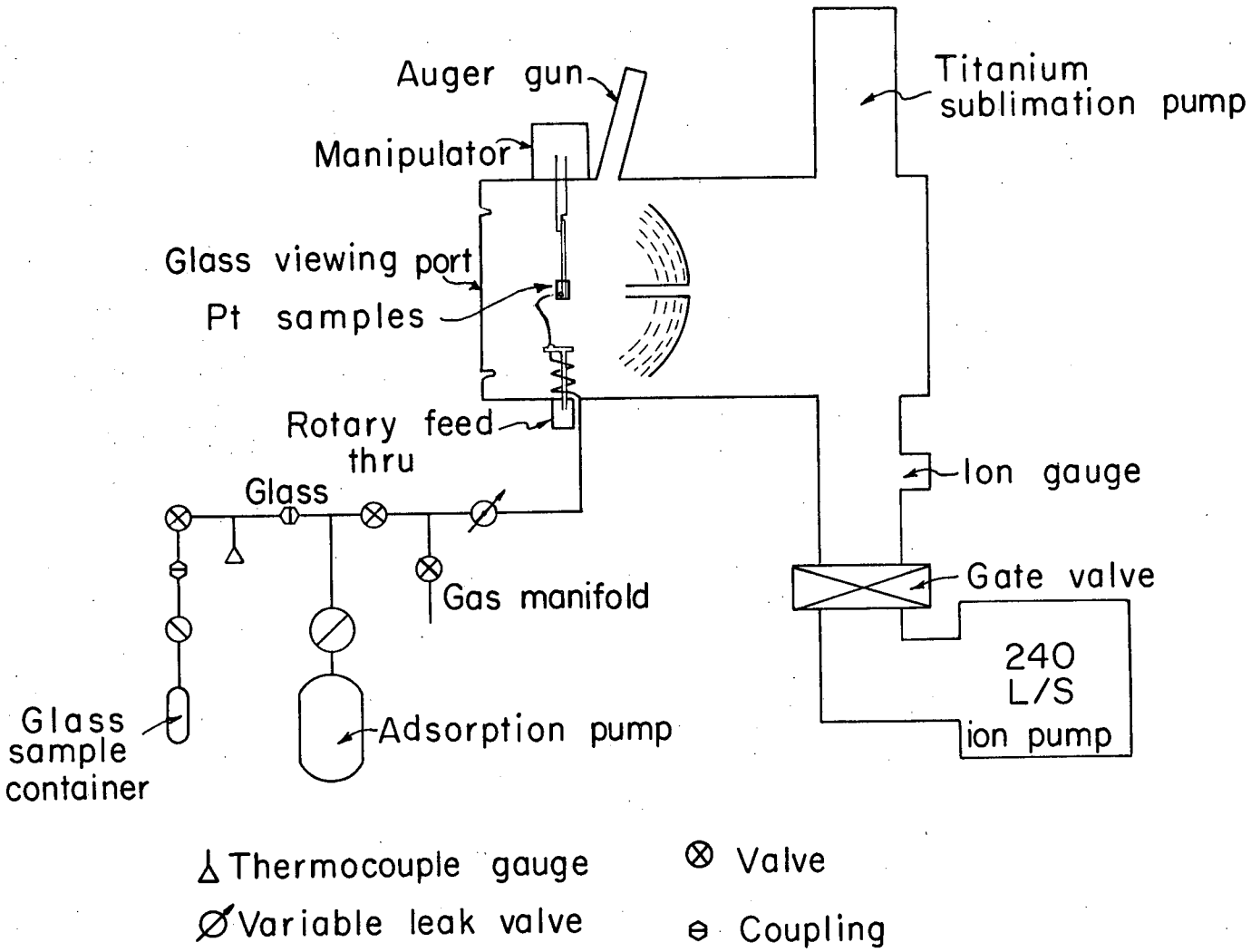

Fig. II-2. A schematic diagram of the ultra-high vacuum system and gas manifold used in the adsorption studies.

speed of the sublimation pump and the walls of the chamber.] This equation was derived assuming isotropic hemispherical effusion from a point source. M is the molecular weight of the gas being considered; T is the temperature in °K; and the constants reflect the geometry of the system. At 300°K this equation becomes

$$P \gtrsim \frac{p}{.13 + .41(M)^{-1/2}} \quad .$$

For benzene and pyridine at this temperature the equation becomes $P \gtrsim 5.7p$; for naphthalene $P \gtrsim 6p$. These equation are approximate and hold only for the case for which molecular flow predominates.

2. Electron Diffraction Optics

The apparatus was equipped with a Varian four-grid LEED optics which uses the post acceleration technique to display the diffraction patterns on a fluorescent screen. The electron beam is produced by an indirectly heated bariated nickel cathode. An electrostatic lens focuses the beam which operates in voltage range 10 to 500 V with a nominal dispersion of .2 V. The grid assembly allows only the elastically scattered electrons to penetrate and be accelerated into the fluorescent screen. The first grid is grounded to maintain the field free region around the sample. The second and third grids are coupled at or near the cathode potential, thus they repell the inelastic electrons which have lost energy in their collision with the sample. The fourth grid is grounded so that the + 5000 V potential on the fluorescent screen will not affect the retarding voltage on the second

and third grids. The elastically scattered electrons, after going through the grid assembly are accelerated through a 5000 V potential drop unto the phosphor screen where their energy is converted into light by the phosphor. This phosphor screen is then photographed through the front window of the vacuum chamber. The diffraction patterns were photographed using a Crown Graphic camera equipped with a Polaroid back. Type 57 film (3000 ASA) was used since even with an aperature of f4.5, four to eight minute photographic exposures were required to produce good photographs of the diffraction patterns. Long photographic exposures are required because the electron current produced by the electron gun was decreased since the electron gun was deliberately poisoned by heating in acetylene to 10^{-4} Torr. The poisoning was done so that the electron emission of the gun would be stable during exposures to organic vapor flux (at 5×10^{-7} Torr) and work function change measurements could be taken.

B. Samples and Sample Preparation

1. Platinum Single Crystals

The platinum single crystals used in these studies were electron beam zone refined samples purchased from Materials Research Corporation. They were aligned (± .5°) using the Laue back reflection technique, spark cut and polished with a series of abrasives. The final polish was carried our with 0.5μ Al_2O_3 powder. They were etched for 30 minutes in 1:1 diluted aqua regia at 100°C immediately prior to insertion into the vacuum system. The samples are discs 6 mm in diameter with

a thickness of .85 mm. The samples were spot welded to polycrystalline platinum holders (99.99% pure), 1 mm thick, 3 mm wide and 5 mm long. These platinum holders were supported by two tantalum bars 6 mm by 6 mm in cross section. Heavy holders were used so that the position of the sample would be constant with repeated heating and cooling and so that the samples would be the hottest part of the system. Two samples were mounted back to back on separate polycrystalline holders. Thus LEED observations could be made and work function measurements taken for both single crystal samples under identical experimental conditions by simply rotating the sample by 180°. Heating and cooling were carried out simultaneously on both crystal faces. Direct current resistance heating has been used. At a temperature of 1000°C (approximately 120 to 140 amps heating current) the crystals had 5° temperature gradients across their surfaces while the two sample surfaces were within 20° of each other (temperatures taken with a calibrated optical pyrometer). Temperatures quoted herein were measured with a platinum/platinum-10% rhodium thermocouple spot welded to the top edge of the Pt(100) sample.

2. Gas Samples

Oxygen used for cleaning was research grade O_2 (99.99%) used without further purifaction. The organic adsorbates used were specified as 99% pure by the manufacturer (Typically Baker analyzed grade), and used without further purification. They were degassed by alternate freezing and thawing in vacuum in an auxiliary glass teflon vacuum system. The vapor pressures of the organic molecules studied were

high enough to permit the use of a simple glass inlet system with teflon valves. When changing adsorbates the inlet system has been cleaned by a combination of three methods. The first involved heating the inlet system to 100°C and flowing dry nitrogen at atmospheric pressure through the inlet system and venting the nitrogen into a hood for several hours. The second step involved pumping on the inlet system with the auxiliary ion pump until pressures less than 10^{-6} Torr were attained. The inlet system was then rinsed repeatedly (a minimum of three times) by filling the inlet system with the adsorbate to the vapor pressure of the adsorbate and then pumping the inlet system out with either the auxiliary ion pump (for low vapor pressure compounds) or a sorption pump (for case where the vapor pressure $\gtrsim$ .1 Torr). As a further precaution the inlet system was always evacuated and refilled within 30 minutes of the beginning of adsorption experiments.

C. Work Function Change Measurements

The work function changes (WFC) were measured using a variation of the retarding field method as outlined by Chang.[3] A schematic of the system is shown in Fig. II-3. Essentially the WFC measurement was made by comparing the contact potential between the electron gun and the sample before and after adsorption. The work function reference was obtained before adsorption by recording a group of current through the crystal (i_c) versus cathode voltage (V_c) curves for a series of bucking voltages (V_b) as shown in Fig. II-4. The

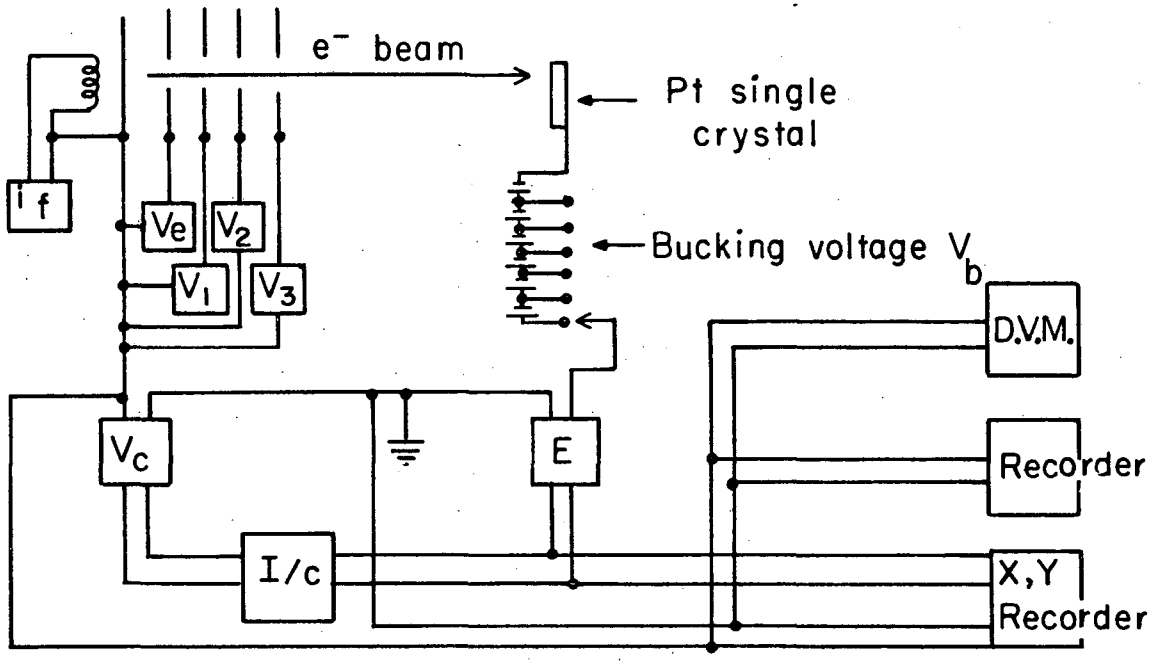

E	Electrometer (current to the crystal)	V_2	Second grid supply
V_c	Cathode voltage supply	V_3	Third grid supply
i_f	Filament current supply	I/c	Inverter/comparator
Ve	Extractor voltage supply	DVM	Digital voltmeter
V_1	First grid supply		

XBL 7210-4212

Fig. II· 3. A schematic diagram of the system used for work function change measurements.

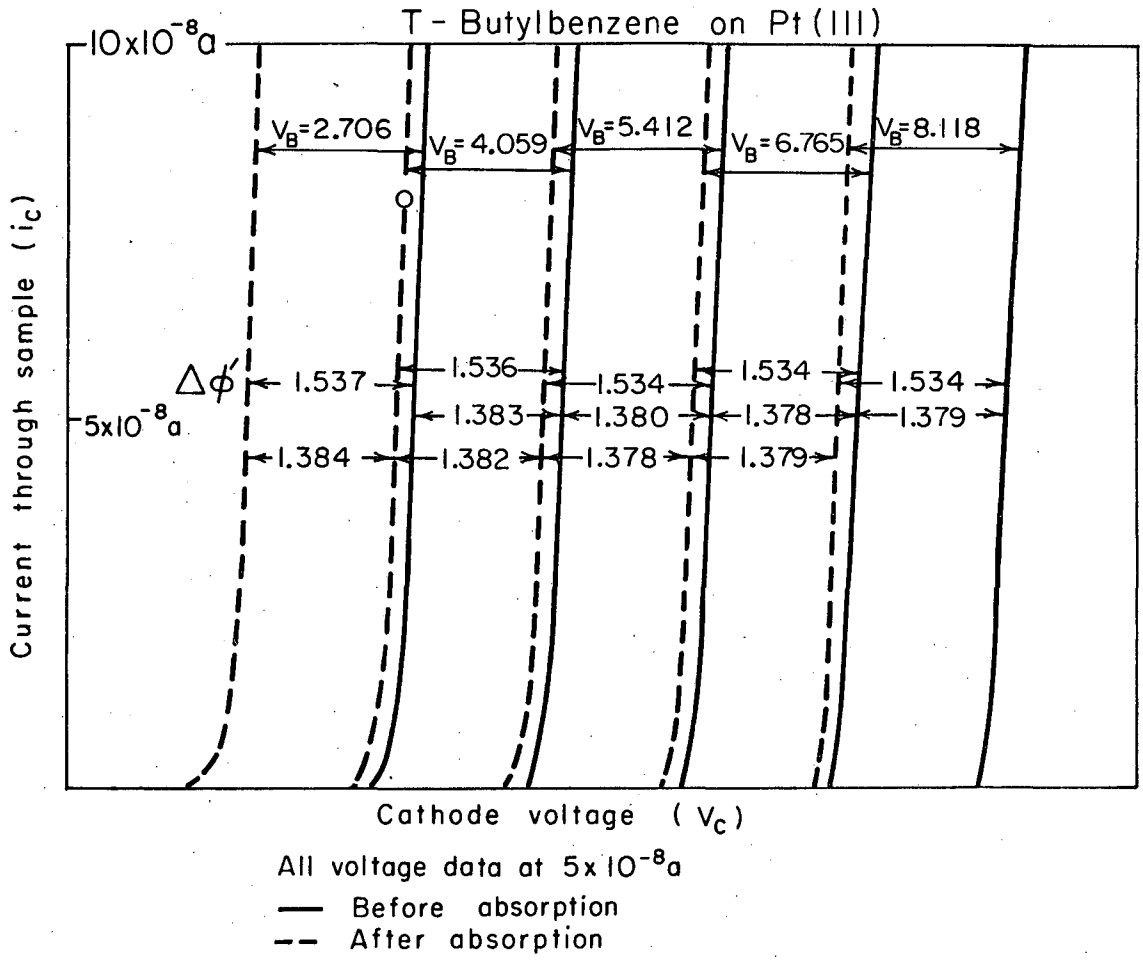

XBL737-3384

Fig. II-4. A typical set of current through the crystal (i_c) versus cathode voltage (V_c) curves taken at a series of bucking voltages (V_B) before and after adsorption of t-butylbenzene of the Pt(111) surface. The gain for this particular set of curves is $\frac{1.380}{1.353} = 1.020$.

bucking voltage is a negative voltage applied between the sample and ground. The same set of measurements were made after adsorption. The voltage difference between a parallel set of curves (for the same bucking voltage) before and after adsorption is the uncorrected work function change $\Delta\phi'$ as shown in Fig. II-4.

Data was taken for a series of bucking voltages both before and after adsorption, and since the bucking voltages are known they are used as internal voltage standards for the system. The bucking voltages used were supplied by a series of ten 1.353 V mercury batteries. A simple switching arrangement allowed sequential addition of batteries so that the bucking voltage could be easily changed by integer multiples of 1.353 V as shown in Fig. II-3. Initially the bucking voltages were measured directly using a calibrated four digit digital voltmeter; the difference between adjacent bucking voltages is ΔV_b actual (1.353 V for new batteries). The bucking voltages were then connected between the crystal and ground. A series of parallel current through the crystal (i_c) vs cathode voltage (V_c) curves were then taken with a series of known bucking voltages (Fig. II-4). The distance between these parallel curves is measured and this is ΔV_b experimental (it would be 1.353 if the gain of the system were unity). For the example shown in Fig. II-4 the average ΔV_b experimental before adsorption = 1.380 V, the average ΔV_b experimental after adsorption = 1.381 V. The gain of the system is defined as

$$\frac{\Delta V_b \text{ experimental}}{\Delta V_b \text{ actual}}$$

Since the samples are conductors we known the voltage changes introduced by the bucking voltage changes are actual surface potential changes. The measured ΔV_b experimental is divided by the gain to yield ΔV_b actual. Likewise all values of the WFC reported here have been divided by the gain. Typically for Pt(111) the gain = 1.03, for Pt(100) gain = 1.08, however the measured gain varied with the experimental geometry. As the crystal was moved up from the center of the chamber the gain increased. The crystal was positioned so that any spurious contribution to the WFC from the polycrystalline holder or edges of the crystal would be minimized. However a gain of unity could not be achieved in this configuration as was the case in the studies by Chang.[3] The gain depends on the shape of the beam and the position of the beam on the crystal. A gain of one could not be achieved with the optimum crystal position since the beam was focused on the low part of the crystal and was deflected downward. The gain is a characteristic of the system geometry and thus remains constant during adsorption. In fact the gain remains constant (within ± 1%) for a given geometry from day to day even though the external magnetic field was not compensated for and the filament temperature is not known precisely. The Varian LEED gun was used for the WFC measurements but the voltages on the gun elements and the filament heating current are supplied by auxiliary regulated power supplies stable to .2% over several days. The electron gun was also deliberately aged (poisoned) by heating in acetylene at 10^{-4} Torr for several hours. This aging was necessary so that the

electron emission of the gun would remain stable during exposures to organic vapor flux at 5×10^{-7} Torr. The stability of the gun was confirmed by running a long low pressure exposure of acetylene (1×10^{-8} Torr) to produce a stable surface. The pressure was then increased to 6×10^{-7} Torr with no change in recorded work function indicating gun stability. The current measurements were taken using a Keithley Electrometer Model 610B. Typically data was collected at bucking voltages of - 1.353 V to - 8.118 V since the gain was generally constant over this voltage range and V_c versus i_c curves were parallel for the above bucking voltages over a typical current range - 2×10^{-8}a to - 1.0×10^{-7}a. The cathode voltages, V_c, used ranged from - 7 V to - 25 V. During calibration periods for each experimental setup, data was taken by plotting the cathode voltage (V_c) versus current to the crystal (i_c) curves for a series of bucking voltages before and after adsorption using an X,Y recorder. A typical i_c vs V_b curve is shown in Fig. II-4. Data was taken in general, by recording the voltage V_c required to achieve a given current (usually 5×10^{-8}A) using a digital voltmeter and a time base recorder to measure V_c for a fixed bucking voltage usually 2.606 V. An automatic system controls V_c so that the current to the crystal was constant. This method allows a continuous monitoring of work function during adsorption and subsequent exposure. The automatic system uses a comparator on the unity gain output of the electrometer to control the cathode voltage so that a constant current is incident on the crystal surface. Gain measurements were taken before and after each adsorption by measuring a series of cathode voltages

at fixed current to the crystal for a series of bucking voltages. A typical data set is shown in Fig. II-4. The slope of the V_c vs i_c is effected by changes in the secondary emission characteristic of the surface; no such effects have been observed during these adsorption studies. The homogeneity of the surface can be estimated by comparing the gain (or WFC) recorded at different bucking voltages since the beam moves along the crystal surface as the bucking voltage is changed. During these studies this effect has been seen on surfaces known to be inhomogeneous by LEED.

D. Experimental Procedure

Prior to each adsorption experiment the platinum samples have been treated with oxygen at pressures of 1 to 3×10^{-5} Torr for 60 minutes at 1000°C to remove the carbon impurities present on the surface. During this treatment the capillary gas inlet was rotated so that oxygen flowed over each surface for 30 minutes. The auxilliary 8 liter/second ion pump was used for pumping the oxygen. After terminating the gas flow, the system was pumped down to a pressure of 1×10^{-8} Torr using the large ion pump and titanium sublimation pump; the electron guns were then degassed and warmed up. The single crystal samples remained at 1000°C for a period of 30-45 minutes in vacuum. The crystals and chamber (hot from radiant heating) are then allowed to cool. Measurement of the work function change made a 5 hour stabilization period for the LEED gun mandatory. Following gun stabilization, the crystals were heated to 1000°C for 5 minutes.

The crystal surfaces produced in this manner were clean within the limit detectable by Auger electron spectroscopy as shown in Fig. II-5. The crystal surfaces produced displayed the characteristic Pt(111)-(1×1) and Pt(100)-(5×1) diffraction patterns. The crystals were then allowed to cool to 25-40°C in a background pressure of 1×10^{-9} Torr. The cooling takes approximately 20 to 40 minutes. The organic vapor flux was then introduced at the desired pressure. During the course of the experiments each surface was alternately exposed to the incident flux for the same time period. The condition of the surface not being exposed at the time was monitored by LEED and WFC measurements. That is, the capillary gas inlet was positioned in back of the set of crystals with respect to the electron gun and the gas flowed over the sample surface not being examined by WFC or LEED.

The WFC and LEED data reported at elevated temperatures were taken by heating the samples for 10 minutes in flux and alternately exposing both surfaces to the flow of gas. The heating was followed by cooling to 20-40°C (15-20 min) in vapor flux (exposing both sides alternately). After the cooling period LEED and WFC measurements were taken. This procedure was used to minimize the possibility of changes of surface coverage due to desorption at elevated temperatures.

E. Reproducibility and Experimental Difficulties

The LEED results quoted are for three different sets [(111) and (100) orientation] of single crystal samples cut from different rods for benzene, naphthalene, pyridene, toluene, t-butylbenzene, aniline,

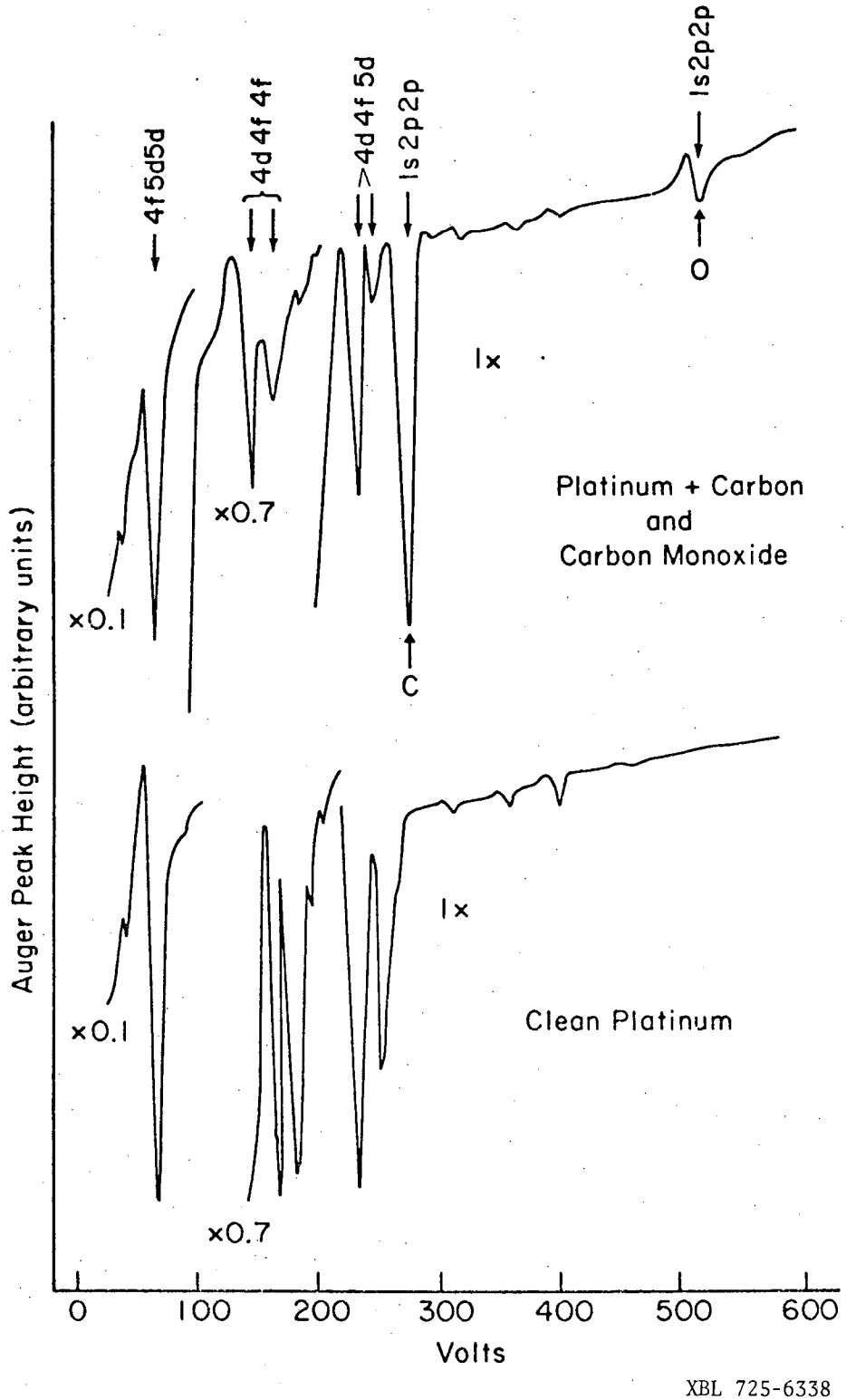

Fig. II-5. An Auger spectrum of the Pt(100) surface before and after cleaning.

nitrobenzene, cyanobenzene, ethylene, and acetylene. LEED observations have been made on two sets of single crystals for cyclohexane, cyclohexene, cyclopentane, cyclopentene. The WFC results for the above set of compounds have been taken on two sets of single crystal samples. No significant variation was observed between different single crystal samples if comparisons were made between adsorption runs under similar conditions (i.e., pressure, temperature). All other adsorbates have been studied on a single set of samples.

The LEED patterns and WFC observed on adsorption vary with contamination of the single crystal surfaces. The LEED results are difficult to reproduce without titanium sublimation pumping because of the problem of carbon monoxide contamination of the Pt crystal surfaces at room temperature. If the single crystal surfaces are not heated sufficiently in vacuum to remove adsorbed oxygen (used for removing carbon) the results are not reproducible. Even slight carbon contamination of the surface leads to irreproducible results. With carbon contamination the WFC observed on adsorption decreases in magnitude. Slight misalignment of the low index surface, resulting in a high density of monatomic height steps results in a marked change in the adsorption characteristics. The WFC observed on adsorption increases in magnitude and the LEED patterns observed are altered.[4,5]

Experiments have indicated that that adsorption at higher pressures (10^{-7} Torr) may cause marked changes in the interaction between substrate and adsorbate.

REFERENCES

1. S. Dushman, Scientific Foundations of Vacuum Techniques, ed. J. M. Lafferty, 2nd ed. (Wiley and Sons, New York, 1962).
2. T. Earl Jordan, Vapor Pressure of Organic Compounds (Interscience Publishers, New York, 1954).
3. C. C. Change, Ph.D. dissertation (Cornell University, Ithaca, New York, 1967).
4. B. Lang, R. W. Joyner, G. A. Somorjai, Surf. Sci. 30, 454 (1972).
5. Kenneth Baron, D. W. Blakely, G. A. Somorjai, to be published in Surface Science.

III. RESULTS

A. Introduction to Results

1. Generalizations

All organic compounds studied adsorb on both the Pt(111) and Pt(100)-(5×1) surfaces. The results of adsorption are shown in Table III-1. In general the adsorbed layer formed is more ordered on the Pt(111) surface than the Pt(100)-(5×1) surface. In general the adsorbed layer is more ordered and causes a larger work function change (WFC, $\Delta\phi$) on adsorption if the incident flux rate is lower. All compounds studied act as electron donors to the Pt surfaces.

Several compounds undergo pressure dependent transformations (usually above 10^{-6} Torr surface pressure) on the platinum surfaces studied; in fact the transformations occur over unexpectedly long time periods. For instance at a surface pressure of approximately 10^{-6} Torr typical transformation times involve several thousand seconds of exposure. The compounds studied which undergo transitions at 20°C as indicated by changes in WFC and diffraction information are benzene, 1,3 cyclohexadiene (benzene on the surface) cyclohexane, n-hexane, cyclopentane and mesitylene.

2. Nomenclature

The diffraction features identified by fractional indices are referenced to the distance between the (00) platinum spot and the first order platinum diffraction features. Diffraction features

TABLE III-1.

Work Function Changes and Structural Information for Adsorption of Organic Compounds on the Pt(111) and Pt(100)-(5×1) Surfaces

		Pt(111)			Pt(100)-(5×1)			
Adsorbate	Temp °C	Work Function Change		Adsorbate Diffraction Features or Surface Structure	Work Function Change		Substrate Structure after Adsorption	Adsorbate Diffraction Features or Surface Structures
		Press (Torr)	WFC (Volts)		Press (Torr)	WFC (Volts)		
Acetylene	20°	1×10^{-8}	- 1.5	(2×2)	4×10^{-7}	- 1.65	(1×1)	$(\sqrt{2}\times\sqrt{2})R45°$
	20°	1×10^{-8} (10 min)	- 1.65	disordered				
	150°	4×10^{-7}	- 1.8	disordered	4×10^{-7}	- 1.7	(1×1)	$(\sqrt{2}\times\sqrt{2})R45°$
Aniline	20°	1×10^{-8}	- 1.8	Streaks at 1/3 order diffuse (1/2 0) features	1×10^{-8}	- 1.75	(1×1)	disordered
Benzene	20°	4×10^{-7}	- 1.8	poorly ordered	3×10^{-7}	- 1.6	(1×1)	diffuse ring-like 1/2 order streak
	20°	4×10^{-7} (5 min)	- 1.4	$\begin{vmatrix}-2 & 2\\ 4 & 4\end{vmatrix}$				
	20°	4×10^{-7} (40 min)	- .7	$\begin{vmatrix}-2 & 2\\ 5 & 5\end{vmatrix}$	3×10^{-7} (2 hrs)	- 1.3	(1×1)	diffuse 1/2 order streak
Biphenyl	20°	2×10^{-9}	- 1.85	very poorly ordered	2×10^{-9}	- 1.8	(1×1)	disordered
n-Butylbenzene	20°	8×10^{-9}	- 1.5	disordered	8×10^{-9}	- 1.5	(1×1)	disordered
t-Butylbenzene	20°	5×10^{-8}	- 1.7	disordered	5×10^{-8}	- 1.75	(1×1)	disordered
Cyanobenzene	20°	1×10^{-8}	- 1.6	diffuse (1/3 0) features	1×10^{-8}	- 1.5	faint (5×1)	disordered
1,3-Cyclohexadiene	20°	2×10^{-8}	- 1.75	poorly ordered	2×10^{-8}	- 1.7	(1×1)	diffuse 1/2 order streak
	20°C	2×10^{-8} (1 hr)	- 1.3	$\begin{vmatrix}-2 & 2\\ 4 & 4\end{vmatrix}$	2×10^{-8} (1 hr)	- 1.6	(1×1)	diffuse 1/2 order streak
	20°C	3×10^{-7} (5 hrs)	- .8	$\begin{vmatrix}-2 & 2\\ 5 & 5\end{vmatrix}$	2×10^{-8} (5 hrs)	- 1.4	(1×1)	diffuse 1/2 order streak
Cyclohexane	20°	6×10^{-9}	- 1.2	(1×1) low background	6×10^{-9}	- .75	(5×1)	low background
	20°	4×10^{-7}	- .7	very poorly ordered	4×10^{-7}	- .4	(1×1)	diffuse streaked (2×1) pattern
	150°	4×10^{-7}	- 1.1	apparent (2×2)	4×10^{-7}	- 1.2	(1×1)	streaked (2×1) pattern
	300°	4×10^{-7}	- 1.4	disordered	4×10^{-7}	- 1.5	(1×1)	disordered
Cyclohexene	20°	6×10^{-7}	- 1.7	$\begin{vmatrix}2 & 2\\ 4 & -2\end{vmatrix}$	6×10^{-7}	- 1.6	(1×1)	diffuse (1/2 0) features
	150°	6×10^{-7}	- 1.6	apparent (2×2)	6×10^{-7}	- 1.5	(1×1)	streaked (2×1) pattern
Cyclopentane	20°	7×10^{-9}	- .95	(1×1) low background	7×10^{-9}	- .4	(5×1)	low background
	20°	4×10^{-7}	- .7	disordered	4×10^{-7}	- .3	(1×1)	diffuse features at 1/2 order
Cyclopentene	20°	-	-	----	2×10^{-7}	- 1.4	(1×1)	diffuse streaked (1/2 0) features
2,6-Dimethyl-pyridine	20°	4×10^{-8}	- 1.6	diffuse 1/3.2, 2/3.2 order streaks	4×10^{-8}	- 1.5	faint (5×1)	disordered
3,5-Dimethyl-pyridine	20°	6×10^{-8}	- 2.3	diffuse 1/2 order streak	6×10^{-8}	- 2.2	(1×1)	disordered

TABLE III-1 (Cont.)

Work Function Changes and Structural Information for Adsorption of Organic Compounds on the Pt(111) and Pt(100)-(5×1) Surfaces

		Pt(111)			Pt(100)-(5×1)			
Adsorbate	Temp °C	Work Function Change		Adsorbate Diffraction Features or Surface Structure	Work Function Change		Substrate Structure after Adsorption	Adsorbate Diffraction Features or Surface Structures
		Press (Torr)	WFC (Volts)		Press (Torr)	WFC (Volts)		
Ethylene	20°	1×10^{-8}	- 1.5	diffuse (1/2 0) features	1×10^{-8}	- 1.2	(1×1)	$(\sqrt{2}\times\sqrt{2})R45°$
	250°	1×10^{-8}	- 1.7	disordered	1×10^{-8}	- 1.5	(1×1)	disordered
Graphitic Overlayer	950°		- 1.1	ringlike diffraction features		- 1.0	(1×1)	ringlike diffraction features
n-Hexane	20°	5×10^{-8}	- 1.1	disordered	5×10^{-8}	- .8	(1×1)	disordered
	20°	5×10^{-8} (5 hrs)	- .9	disordered	5×10^{-8} (5 hrs)	- .6	(1×1)	disordered
	250°	5×10^{-8}	- 1.5	disordered	5×10^{-8}	- 1.2	(1×1)	disordered
Isoquinoline	20°	6×10^{-8}	- 1.9	diffuse (1/3 0) and (2/3 0) features	6×10^{-8}	- 2.1	(1×1)	disordered
Mesitylene	20°	4×10^{-8}	- 1.7	Streaks at 1/3.4 order diffuse (2/3.4 0) features	4×10^{-8}	- 1.7	(5×1)	1/3 order streaks
	20°	4×10^{-7}	- 1.35	disordered	4×10^{-7}	- 1.2	(1×1)	disordered
2-Methyl-naphthalene	20°	6×10^{-8}	- 2.0	very poorly ordered	4×10^{-9}	- 1.6	faint (5×1)	disordered
Naphthalene	20°	9×10^{-9}	- 1.95	apparent (3×1)	9×10^{-9}	- 1.7	(1×1)	disordered
	150°	9×10^{-9}	- 2.0	(6×6)	9×10^{-9}	- 1.65	(1×1)	disordered
Nitrobenzene	20°	9×10^{-9}	- 1.5	diffuse (1/3 0) features (pattern electron beam sensitive)	9×10^{-9}	- 1.4	(1×1)	disordered
Piperidine	20°	8×10^{-8}	- 2.1	disordered	8×10^{-8}	- 2.05	faint (5×1)	disordered
Propylene	20°	2×10^{-8}	- 1.3	(2×2) (pattern electron beam sensitive)	2×10^{-8}	- 1.2	(1×1)	1/2 order streaks (pattern electron beam sensitive)
Pyridine	20°	1×10^{-8}	- 2.7	diffuse (1/2 0) features	1×10^{-8}	- 2.4	(1×1)	disordered
	250°	1×10^{-8}	- 1.7	well defined streaks at 1/3, 2/3, 3/3 order	1×10^{-8}	-	(1×1)	$(\sqrt{2}\times\sqrt{2})R45°$
Pyrrole	20°	6×10^{-8}	- 1.45	diffuse (1/2 0) features (pattern electron beam sensitive)	6×10^{-8}	- 1.6	(1×1)	diffuse (1/2 0) features
Quinoline	20°	3×10^{-8}	- 1.45	diffuse 1/3 order streaks	3×10^{-8} (6 min)	-	(5×1)	diffuse 1/3 order streaks
					3×10^{-8} (14 min)	- 1.7	(1×1)	disordered
Styrene	20°	6×10^{-8}	- 1.7	streaks at 1/3 order	6×10^{-8}	- 1.65	(1×1)	very poorly ordered
Toluene	20°	1×10^{-9}	- 1.7	streaks at 1/3 order	1×10^{-9}	- 1.55	(5×1)	streaks at 1/3 order
	150°	1×10^{-9}	- 1.65	(4×2)	1×10^{-9}	- 1.5	(1×1)	disordered
m-Xylene	20°	1×10^{-8}	- 1.8	streaks at 1/2.6 order	1×10^{-8}	- 1.65	(5×1)	streaks at 1/3 order

identified by two indices (for instance (1/2 0)) refer to a set of diffraction features which can be generated by rotating the identified diffraction features by the symmetry elements of the surface in question. For instance on the Pt(100) surface with four first order diffraction features (10), (01), $(\bar{1}0)$ and $(0\bar{1})$ the identification "(1/2 0) features" denotes four diffraction features, (1/2 0), (0 1/2), $(\overline{1/2}\ 0)$ and $(0\ \overline{1/2})$. On the Pt(111) surface with six first order diffraction features (10), (01), $(\bar{1}1)$, $(\bar{1}0)$, $(0\bar{1})$ and $(1\bar{1})$ the same name "(1/2, 0) features" refers to a set of six features (1/2 0), (0 1/2), $(\overline{1/2}\ 1/2)$, $(\overline{1/2}\ 0)$ $(0\ \overline{1/2})$ and $(1/2\ \overline{1/2})$.

The surface structures in this section are named using two systems. The first system is used to describe simple surface structures in terms of the bulk unit vectors of the substrate. For instance the notation (2×2) means that both unit vectors in the overlayer are twice as long as the unit vectors of the substrate. The unit vectors of the surface structure are $2\hat{a}$ and $2\hat{b}$ where $\hat{a}$ and $\hat{b}$ are the unit vectors of the substrate. If the surface structure unit vectors are rotated with respect to the substrate unit vectors the rotation is denoted by a postscript R. For instance the $(\sqrt{2} \times \sqrt{2})R45°$ surface structure has unit vectors $\sqrt{2}\hat{a}$, $\sqrt{2}\hat{b}$ rotated 45° with respect to $\hat{a}$ and $\hat{b}$. The second system makes use of a matrix of coefficients to describe the surface structure in terms of the substrate unit vectors. For instance the surface structure unit cell described by

$$\begin{vmatrix} -2\hat{a} & 2\hat{b} \\ 4\hat{a} & 4\hat{b} \end{vmatrix} \quad \text{or} \quad \begin{vmatrix} -2 & 2 \\ 4 & 4 \end{vmatrix}$$

has a unit cell defined by the row vectors $(-2\hat{a}, 2\hat{b})$, $(4\hat{a}, 4\hat{b})$. The underlying unit cell is described by the matrix

$$\begin{vmatrix} 1\hat{a} & 0\hat{b} \\ 0\hat{a} & 1\hat{b} \end{vmatrix} \quad \text{or} \quad \begin{vmatrix} 1 & 0 \\ 0 & 1 \end{vmatrix}$$

or the row vectors $(1\hat{a}, 0\hat{b})$, $(0\hat{a}, 1\hat{b})$.

B. Results

1. Experimental Conditions

The results presented in this section have been taken with long exposure times (typically 1 or 2 hours) with continuous monitoring of the WFC and diffraction information. The results quoted at elevated temperature were taken by heating the sample in organic vapor flux and cooling to 25°C - 40°C in vapor flux (~ 15 minutes). Thus the actual measurements were taken with the sample cooled. This procedure minimized the possibility of changes in surface coverage due to desorption at elevated temperatures. Heating experiments specified as occurring in vacuum were done in the same manner but in the absence of organic vapor flux.

2. Results

Acetylene adsorption

Acetylene adsorbed on the Pt(111) surface causes the appearance of a (2×2) surface structure. The structure is well defined at low exposures (less than 90 sec at 6×10^{-9} Torr recorded pressure or approximately 4L), but becomes less defined with increasing exposure.

The WFC accompanying the (2×2) structure is ~ -1.5 V. All evidence of a (2×2) structure disappears with 10 minutes exposure at a recorded pressure of 1×10^{-8} Torr (approximately 40L). The maximum WFC on adsorption at 20°C is -1.65 V as shown in Fig. III-1. On heating in organic vapor flux the WFC decreases and goes through a mimimum value of -1.8 V at a temperature of 150°C as shown in Fig. III-2. The magnitude of the WFC then decreases with increasing temperature. On heating the diffraction pattern remains disordered whether the sample was heated in organic vapor flux or in vacuum.

Acetylene adsorption on the Pt(100)-(5×1) surface causes the appearance of a streaked $(\sqrt{2} \times \sqrt{2})$R45° surface structure and the rapid disappearance of the (5×1) surface structure. All diffraction features are streaked along the two perpendicular (10) directions as shown in Fig. III-3. The (1/2 1/2) diffraction features are much more diffuse the the integral order diffraction features. The WFC on adsorption is -1.65 V as shown in Fig. III-4. On heating in flux the WFC decreases and goes through a minimum value of -1.7 V at 150°C; as shown in Fig. III-5 with further heating the magnitude of the WFC decreases. With heating the $(\sqrt{2} \times \sqrt{2})$R45° remains through approximately 150°C whether heated in organic vapor flux or in vacuum.

Aniline adsorption

Aniline adsorbed on the Pt(111) surface causes the formation of a complex poorly ordered surface structure. The diffraction pattern (Fig. III-6) exhibits streaks at 1/3 order along with diffuse diffraction features at the (1/2 0) positions and several broad high

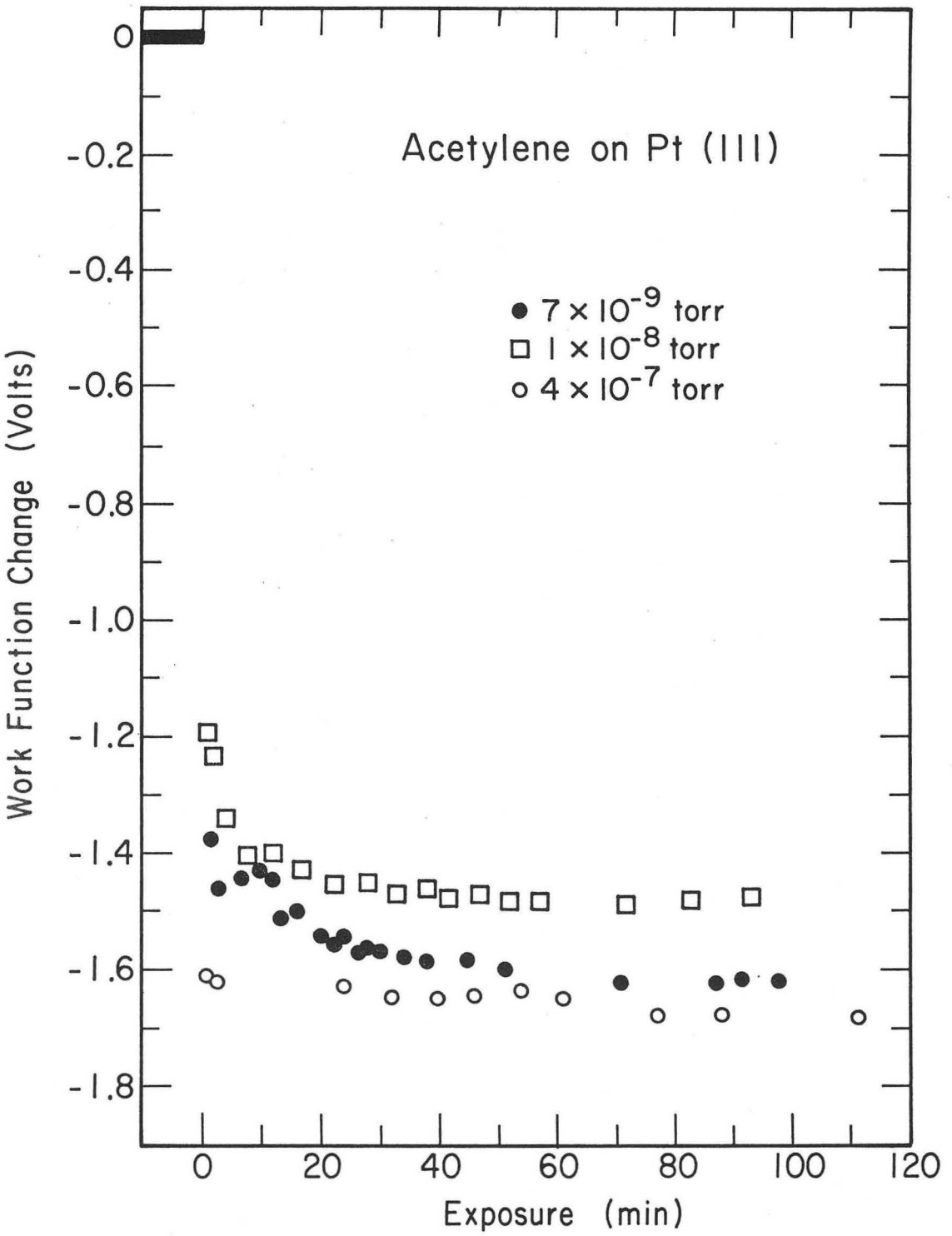

Fig. III-1. The work function change on adsorption of acetylene on the Pt(111) surface at 20°C. The indicated pressure should be multiplied by at least six to yield approximate surface pressures.

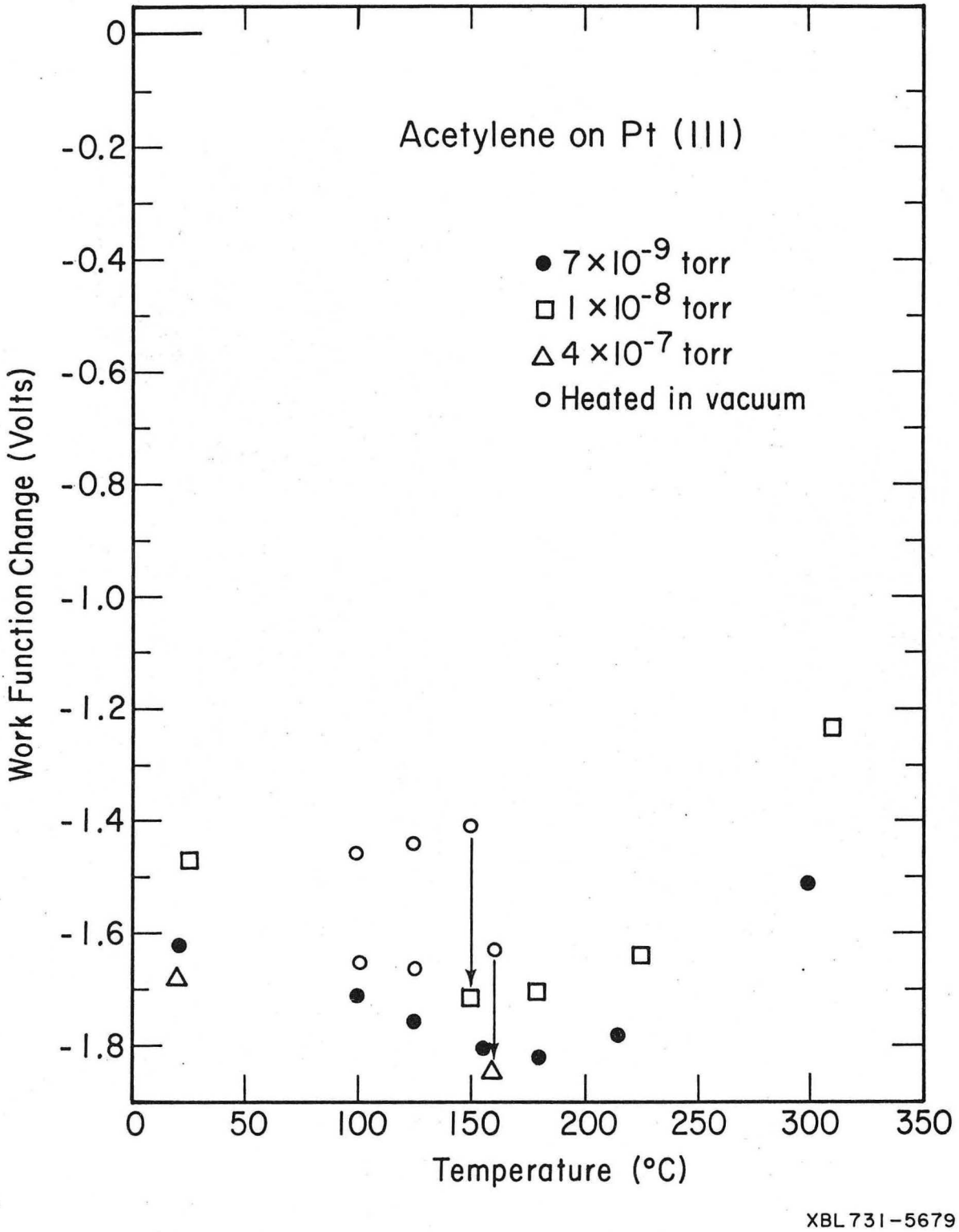

Fig. III-2. The work function change as a function of temperature for acetylene adsorbed on the Pt(111) surface. The indicated pressure should be multiplied by at least six to yield approximate surface pressures.

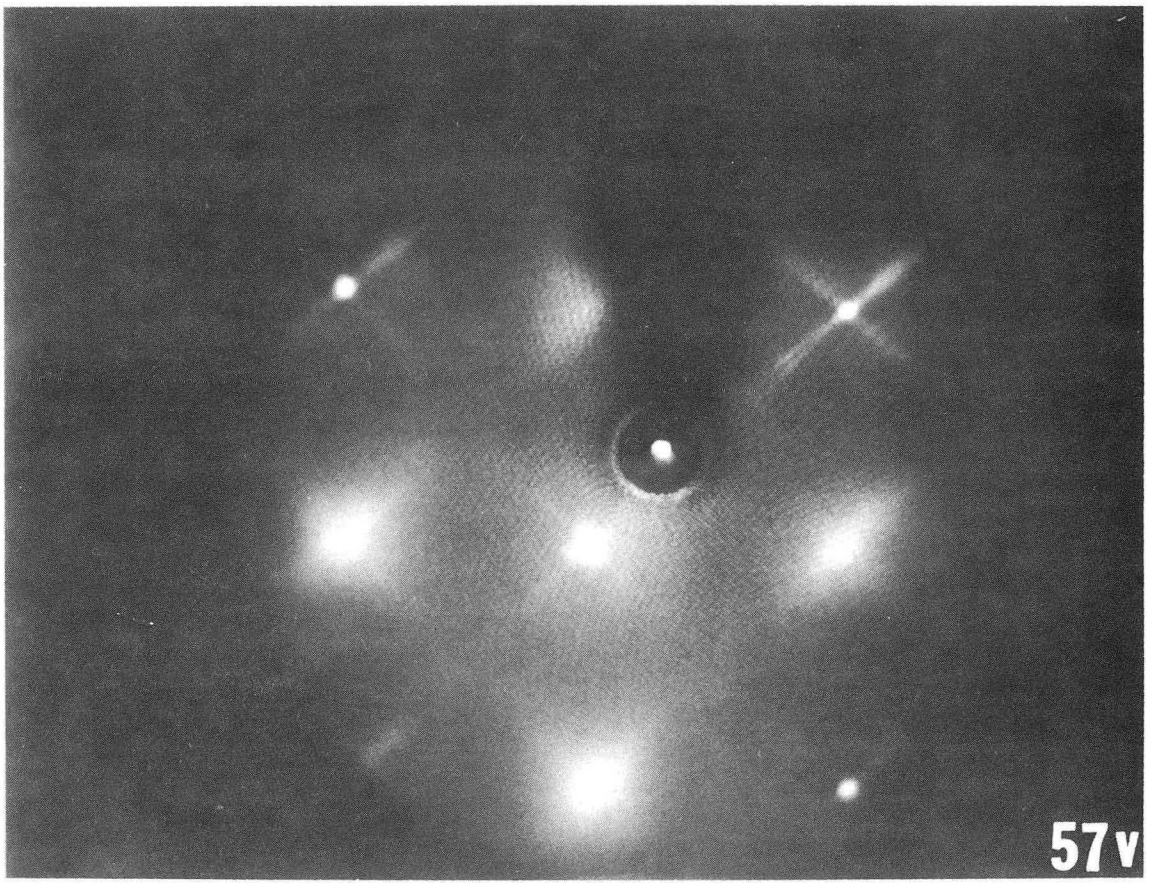

XBB 732-676

Fig. III-3. The diffraction pattern resulting from acelytene adsorption on the Pt(100)-(5×1) surface showing the first order Pt diffraction features.

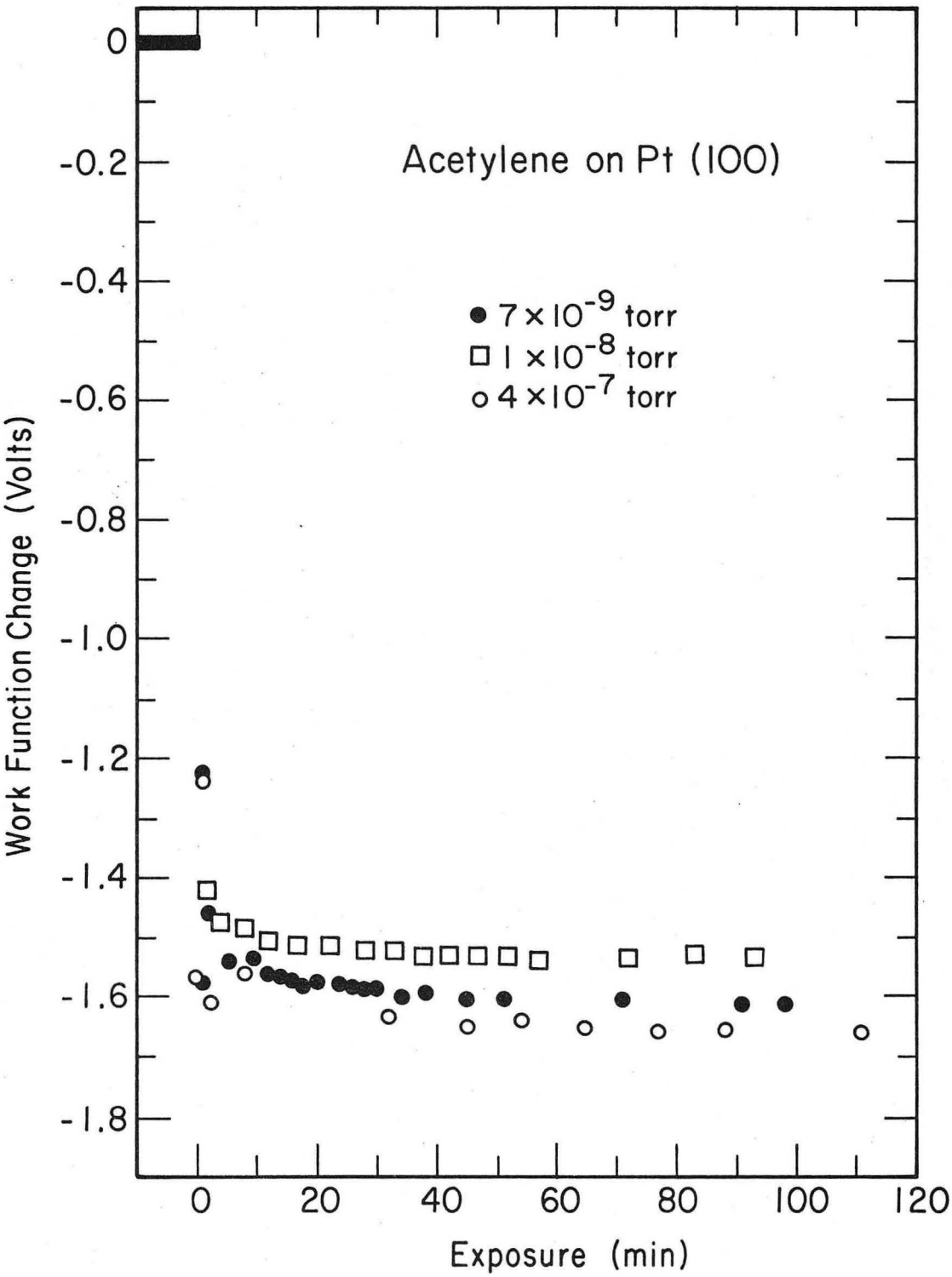

Fig. III-4. The work function change on adsorption of acetylene on the Pt(100)-(5×1) surface at 20°C. The indicated pressure should be multiplied by at least six to yield approximate surface pressures.

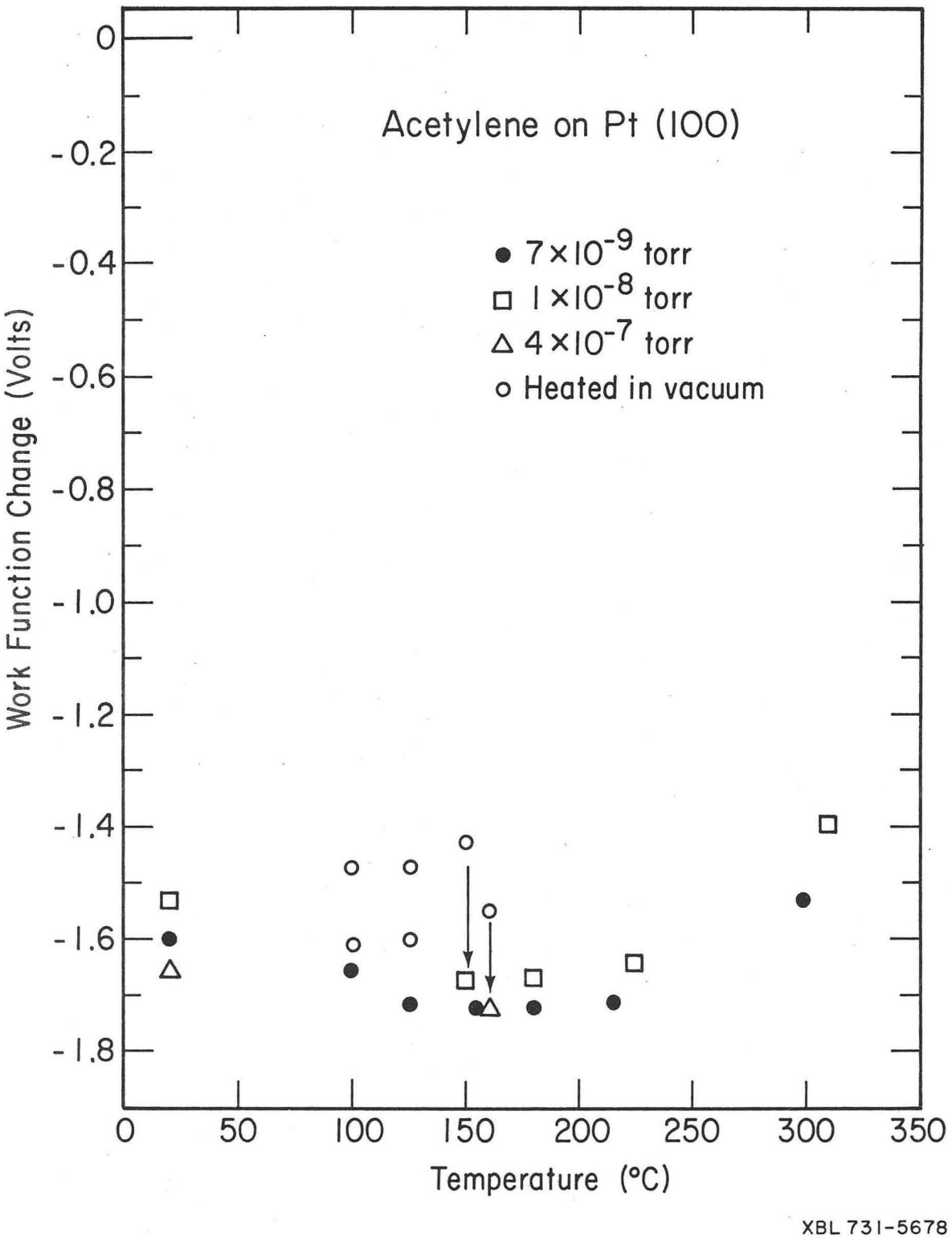

Fig. III-5. The work function change as a function of temperature for acetylene adsorbed on the Pt(100)-(5×1) surface. The indicated pressure should be multiplied by at least six to yield approximate surface pressures.

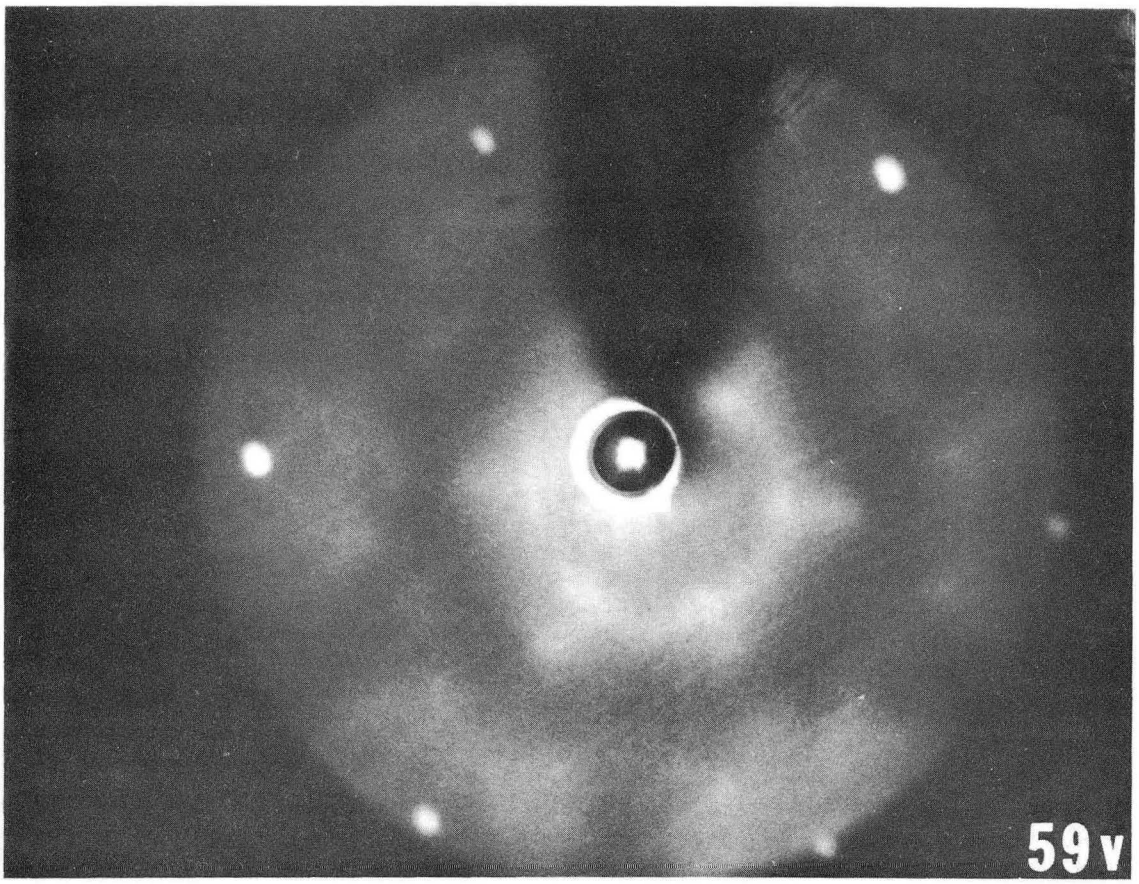

XBB 732-677

Fig. III-6. The diffraction pattern resulting from aniline adsorption on the Pt(111) surface showing the first order platinum diffraction features.

density areas centered at the (2/3 0) positions. The WFC on adsorption is -1.8 V (Fig. III-7), however, the WFC depends on the initial incident flux.

Heating the adsorbed layer in flux above 150°C causes it to become disordered. Heating the sample above 200°C causes the magnitude of the WFC to decrease as shown in Fig. III-8.

Aniline adsorption on the Pt(100)-(5×1) surface causes the diffraction features characteristic of the (5×1) structure to disappear and causes an increase in background intensity. There is no evidence for the formation of ordered structures from the diffraction pattern in the temperature range 20°C to 250°C. The WFC on adsorption is approximately -1.75 V (Fig. III-9). The magnitude of the WFC decreased above 200°C as shown in Fig. III-8.

Benzene adsorption

Benzene adsorbed on the Pt(111) surface forms a poorly ordered layer. Continued exposure to organic vapor flux causes the appearance of the diffraction pattern resulting from the Pt(111)-$\begin{vmatrix} -2 & 2 \\ 4 & 4 \end{vmatrix}$ - Benzene structure (Fig. III-10a). With continued exposure this structure changes to the Pt(111)-$\begin{vmatrix} -2 & 2 \\ 5 & 5 \end{vmatrix}$ - Benzene structure. The diffraction pattern resulting from this structure is shown in Fig. III-10b. The transformation from the $\begin{vmatrix} -2 & 2 \\ 4 & 4 \end{vmatrix}$ structure to the $\begin{vmatrix} -2 & 2 \\ 5 & 5 \end{vmatrix}$ structure occurs in absence of further exposure to organic vapor flux, but the transformation is very slow (~ 10 hours). The original transformation from a poorly ordered structure to the $\begin{vmatrix} -2 & 2 \\ 4 & 4 \end{vmatrix}$ does not occur without exposure to organic vapor flux. The apparent hexagonal symmetry of the diffraction patterns occurs because

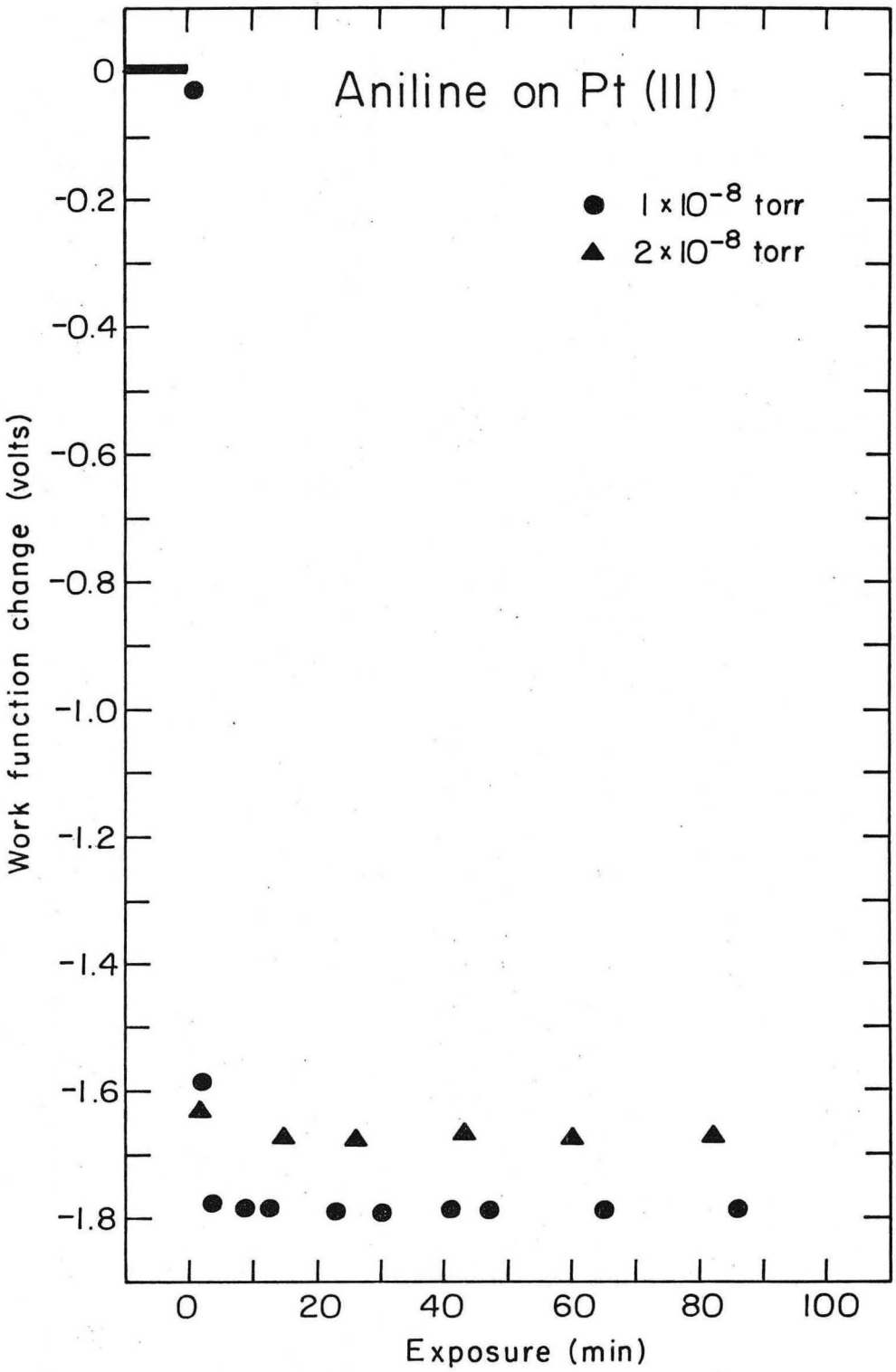

XBL 732-5743

Fig. III-7. The work function change on adsorption of aniline on the Pt(111) surface at 20°C. The indicated pressure should be multipled by at least six to yield approximate surface pressures.

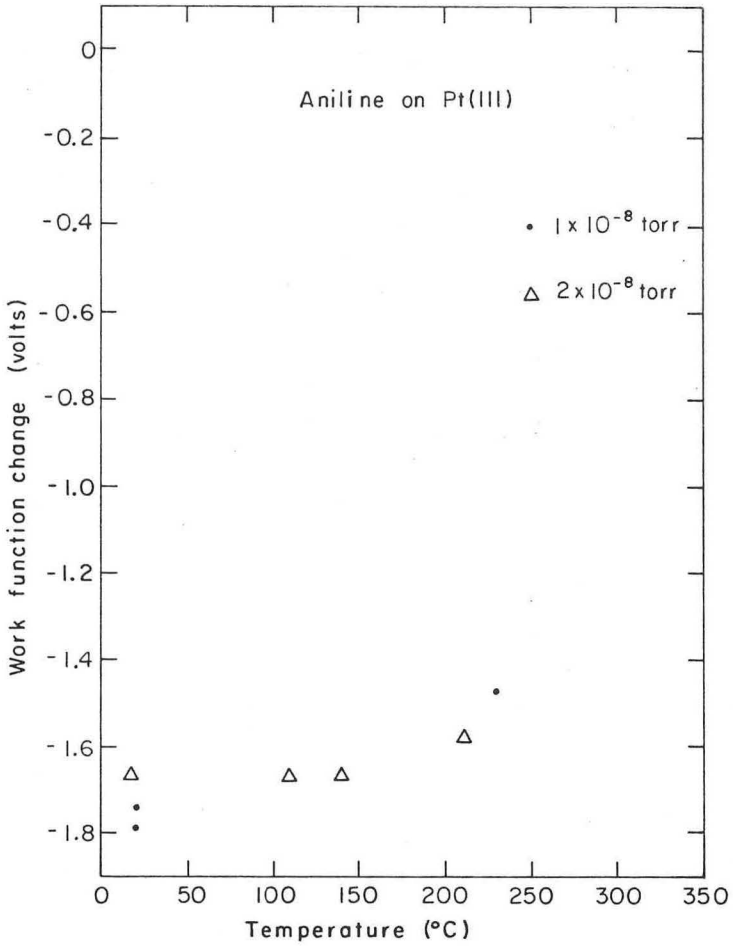

XBL734-2687

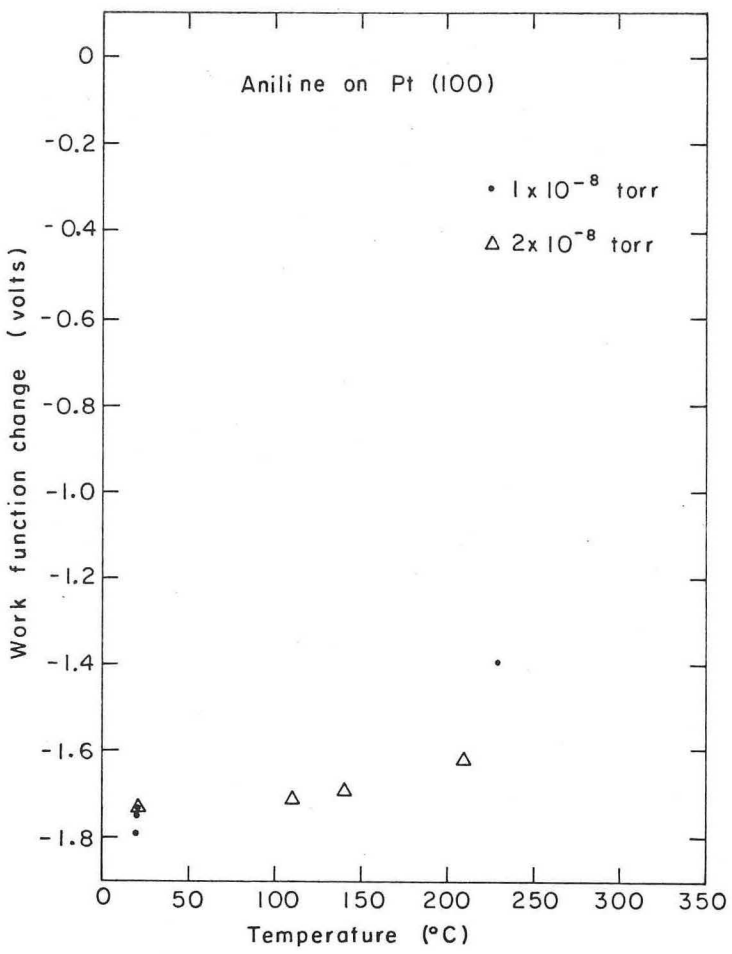

XBL734-2688

Fig. III-8. The work function change as a function of temperature for adsorption on the Pt(111) and Pt(100)-(5×1) surfaces. The indicated pressure should be multiplied by at least six to yield approximate surface pressures.

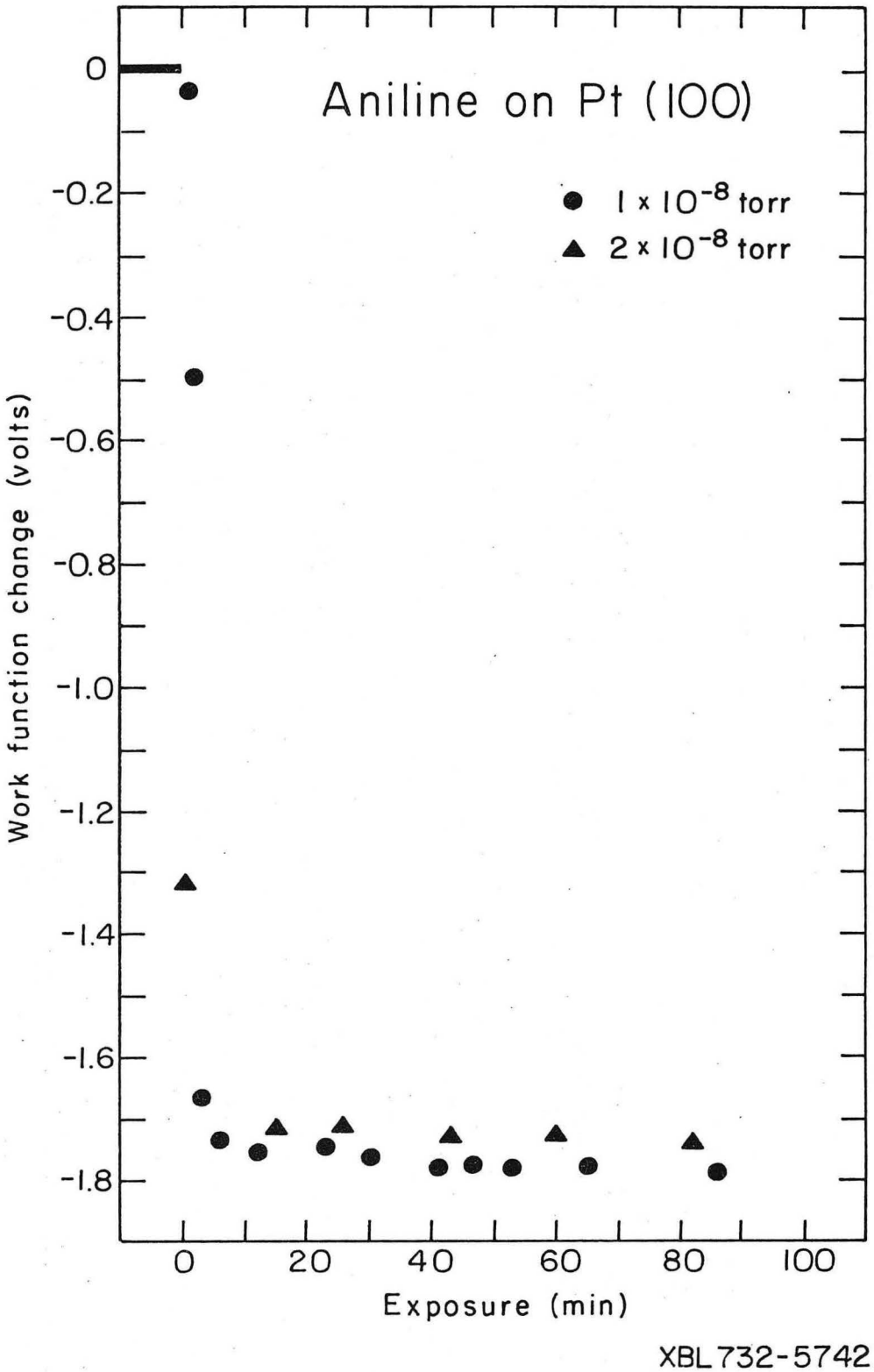

Fig. III-9. The work function change on adsorption of aniline on the Pt(100)-(5×1) surface at 20°C. The indicated pressure should be multiplied by at least six to yield approximate surface pressures.

Fig. III-10. The diffraction patterns and corresponding work function changes resulting from adsorption of benzene on the Pt(111) surface at 20°C. The indicated pressure should be multiplied by at least six to yield approximate surface pressures.

Fig. III-10a. The diffraction pattern from the Pt(111)-$\begin{vmatrix} -2 & 2 \\ 4 & 4 \end{vmatrix}$ - Benzene structure.

Fig. III-10b. The diffraction pattern from the Pt(111)-$\begin{vmatrix} -2 & 2 \\ 5 & 5 \end{vmatrix}$ - Benzene structure.

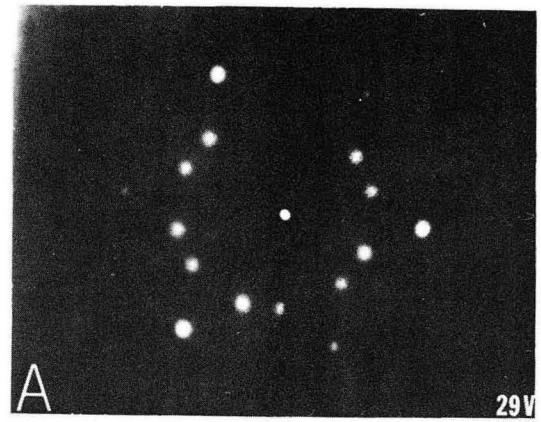

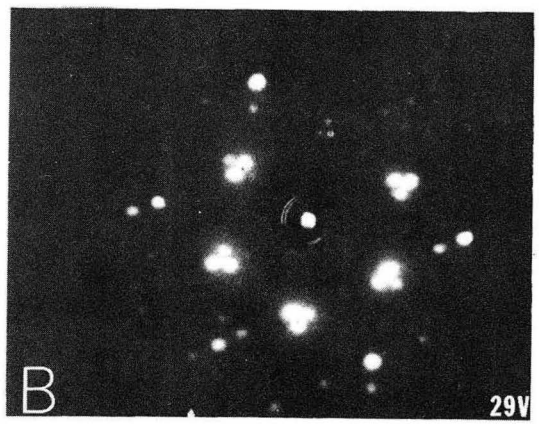

XBB 732-3814

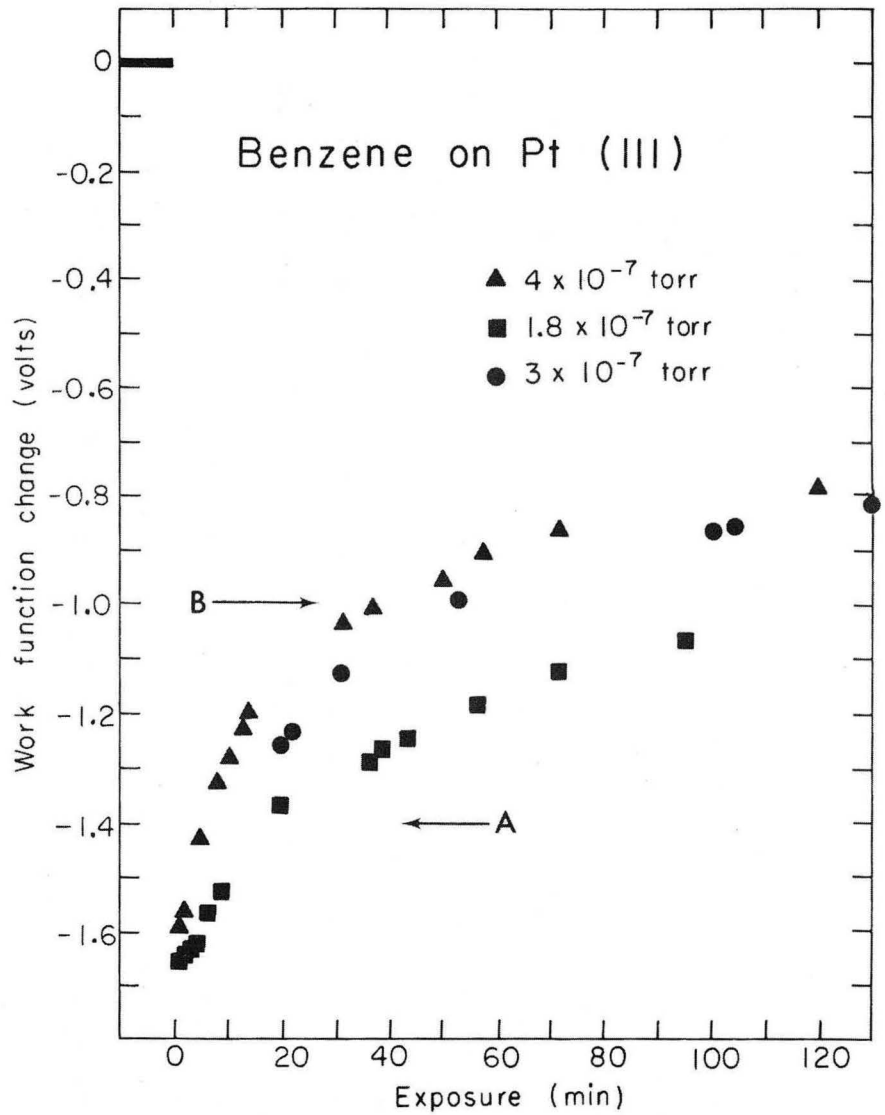

Fig. III-10, III-10a, and III-10b

three domains of these structures are possible. Observations have been made on diffraction patterns for which only two domains are predominant and the patterns did not have six fold symmetry. The work function shifts which correspond to these structural changes are shown in Fig. III-10. On initial adsorption the work function of the surface decreases very rapidly, goes through a minimum, (- 1.8 V) then increases slowly toward a higher steady state value of -.7 V. The initial ordered $\begin{vmatrix} -2 & 2 \\ 4 & 4 \end{vmatrix}$ structure appears at a WFC value of - 1.4 V slightly after the minimum work function has been reached. The second ordered $\begin{vmatrix} -2 & 2 \\ 5 & 5 \end{vmatrix}$ structure forms after the work function change has increased to ~ -1.0 V. The time required for the WFC to reach its steady state value and for the $\begin{vmatrix} -2 & 2 \\ 5 & 5 \end{vmatrix}$ structure to appear is dependent on the benzene pressure. At lower benzene fluxes, the time necessary to reach the steady state WFC and structure increases.

Heating the Pt(111)-$\begin{vmatrix} -2 & 2 \\ 5 & 5 \end{vmatrix}$ - Benzene structure in vacuum or in flux causes the adsorbed layer to become very poorly ordered. When heated to 140°C in flux the magnitude WFC increases from -.7 V to -1.6 V. The magnitude of the WFC then decreases with time either in flux or in vacuum toward the steady state value of -.7 V. If heated to 140°C in vacuum the magnitude of the WFC increases to -1.0 V and and begins to decrease toward -.7 V. However if the heated surface ($\Delta\phi$ = -1.0 V) is exposed to benzene flux the magnitude of the WFC increases to -1.6 V. With time either in vacuum or in flux the magnitude of the WFC then decreases toward a value of -.7 V.

Benzene adsorbed on the Pt(100)-(5×1) causes the (5×1) surface structure to disappear rapidly. A new diffuse ring-like diffraction feature appears at 1/2 order as shown in Fig. III-11. The WFC on adsorption (Fig. III-11) is less sensitive to benzene exposure than the Pt(111)-benzene system; however, the same type of increase in work function is observed, although there is no change in structure. When the incident benzene flux is terminated the 1/2 order diffraction features disappear while the work function increases slightly.

With heating in flux to 140°C the diffraction pattern becomes better defined and the ring-like 1/2 order feature becomes four streaked (1/2 0) features. The work function of this better defined structure is -1.2 V and it is stable to further exposure or evacuation.

Biphenyl adsorption

Biphenyl adsorbed on the Pt(111) surface causes an increase in the background intensity and extremely faint high order streaks appear. The WFC on adsorption was approximately -1.85 V and depends on the initial incident flux (Fig. III-12). A slight improvement in the high order diffraction features occurs with heating to 140°C in flux. With further stepwise heating in flux to 300°C the adsorbed layer remains disordered. The magnitude of the WFC decreases progressively with stepwise heating above 100°C.

Biphenyl adsorbed on the Pt(100)-(5×1) surface caused a slow disappearance of the (5×1) surface structure (1 hour at a recorded organic pressure of 2×10^{-9} Torr) and an increase in the background intensity. The WFC on adsorption is -1.8 V and depends on the initial

Fig. III-11. The diffraction pattern and work function change resulting from benzene adsorption on the Pt(100)-(5×1) surface at 20°C. The first order Pt diffraction features are visible in the diffraction pattern. The indicated pressure should be multiplied by at least six to yield approximate surface pressures.

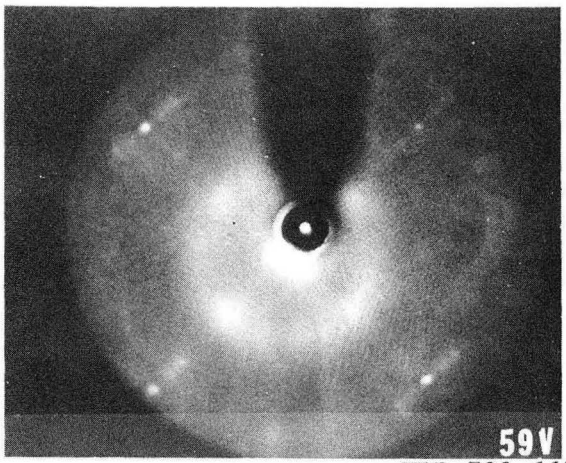

XBB 732-669

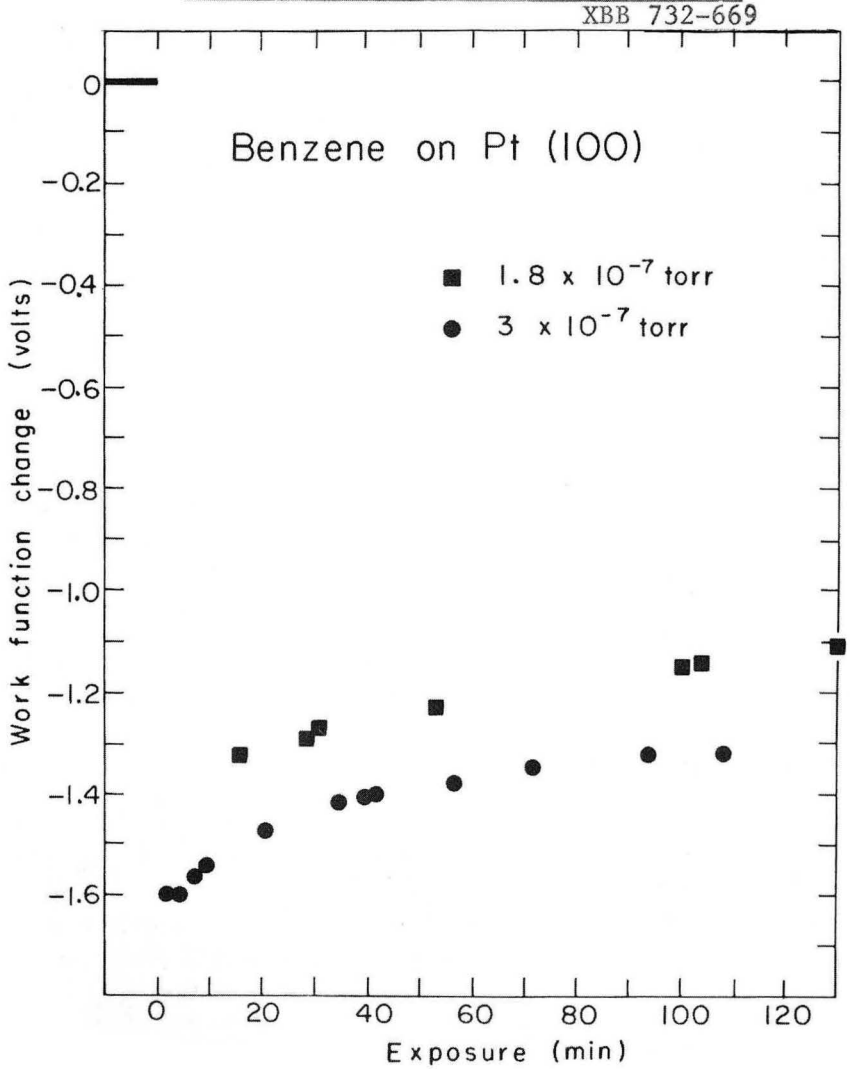

Fig. III-11.

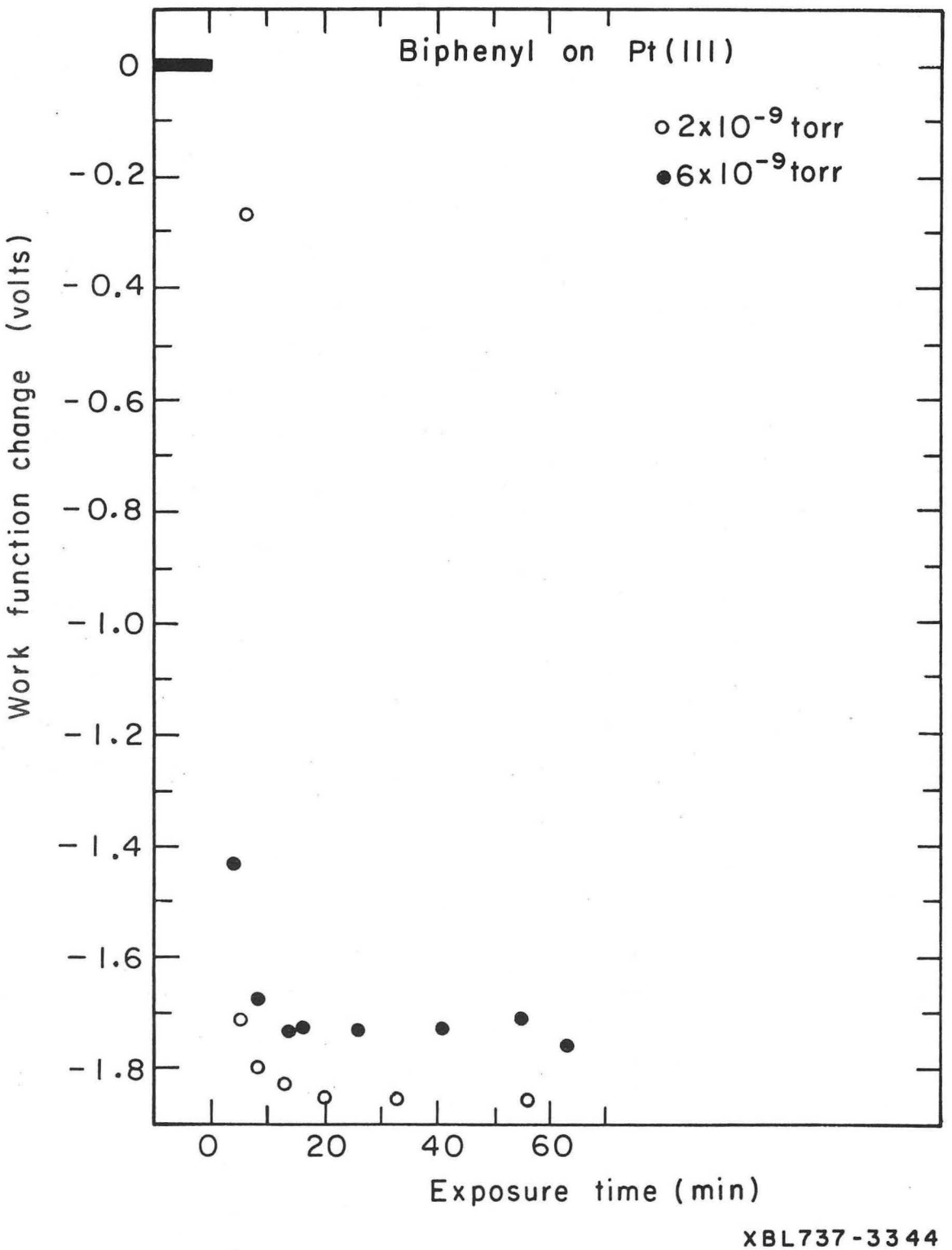

Fig. III-12. The work function change on adsorption of biphenyl on the Pt(111) surface at 20°C. The indicated pressure should be multiplied by at least six to yield approximate surface pressures.

incident flux (Fig. III-13). With stepwise heating in flux to 300°C the adsorbed layer remains disordered. The magnitude of the WFC decreases with stepwise heating above 100°C in organic vapor flux.

N-Butylbenzene adsorption

N-butylbenzene adsorbed on the Pt(111) surface forms a very poorly ordered adsorbed layer. Adsorbed layers formed at high incident fluxes (1.2×10^{-8} Torr recorded pressure) are completely disordered. A diffraction pattern taken after 6 minutes exposure at 8×10^{-9} Torr recorded pressure is shown in Fig. III-14b. There is a broad high intensity region that terminates at 1/2 order. The extra diffraction features disappear after approximately 20 minutes of exposure at a recorded pressure of 8×10^{-9} Torr. That is, the WFC on adsorption is -1.5 V (Fig. III-15) the WFC depends markedly on the initial incident vapor flux.

With stepwise heating to 400°C in flux the adsorbed layer remains disordered. The WFC remains constant until the sample is heated above 250°C, the magnitude of the WFC then decreases with increasing temperature (Fig. III-16).

Adsorption of n-butylbenzene on the Pt(100)-(5×1) surface causes the appearance of very faint high order streaks which disappear with continued exposure. The (5×1) diffraction features disappear at a slightly slower rate than the extra diffraction features due to the adsorbate. Figure III-14 a shows the diffraction pattern after 12 minutes exposure at 8×10^{-9} Torr recorded pressure. The WFC on adsorption is -1.5 V (Fig. III-17); the value of the WFC is strongly

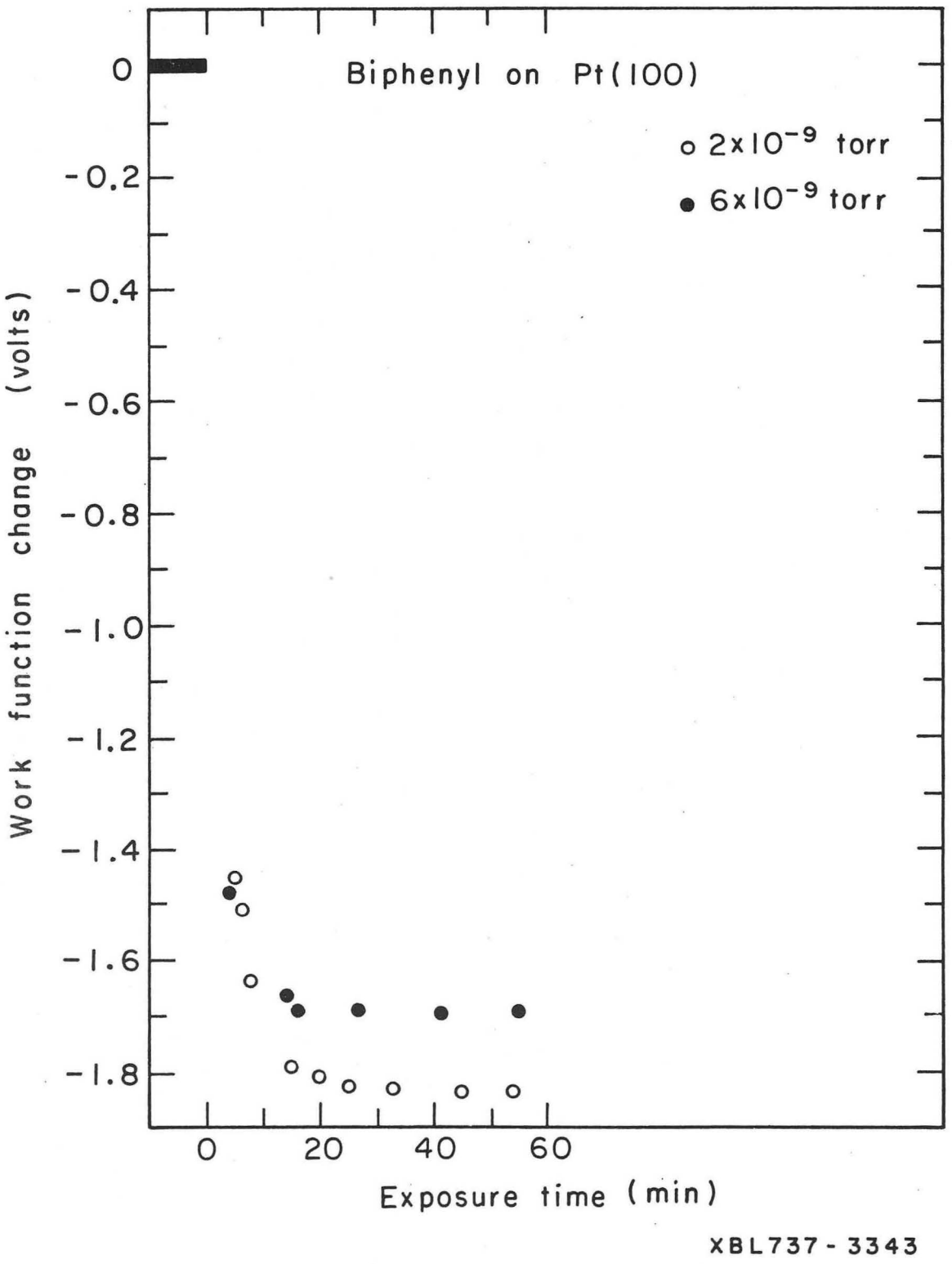

Fig. III-13. The work function change on adsorption of biphenyl on the Pt(100)-(5×1) surface. The indicated pressure should be multiplied by at least six to yield approximate surface pressures.

Fig. III-14a. The diffraction pattern resulting from n-butylbenzene adsorption on the Pt(100)-(5×1) surface.

Fig. III-14b. The diffraction pattern resulting from n-butylbenzene adsorption on the Pt(111) surface. (6 minutes at a recorded pressure of 1.2×10^{-8} Torr)

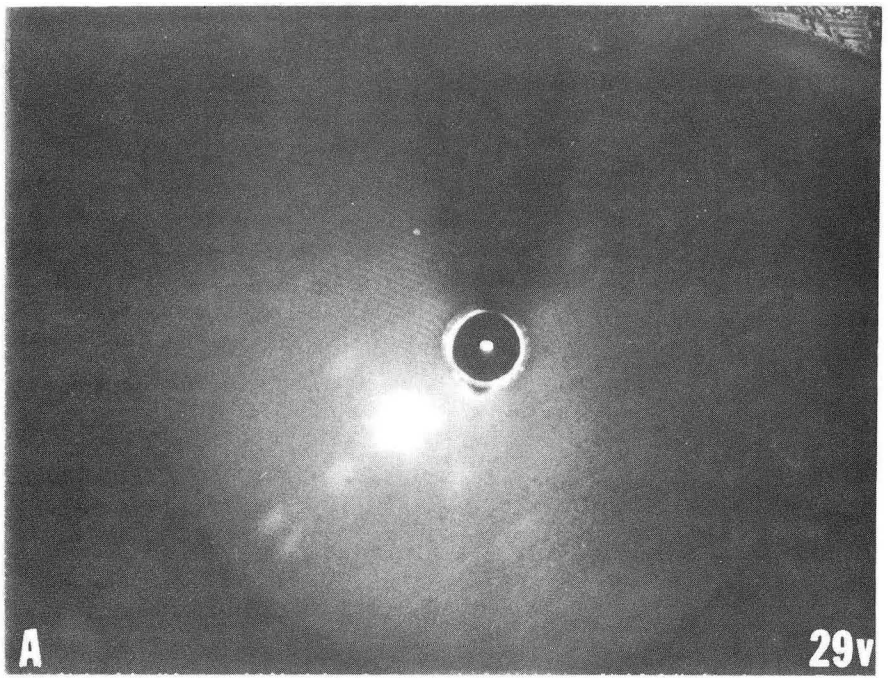

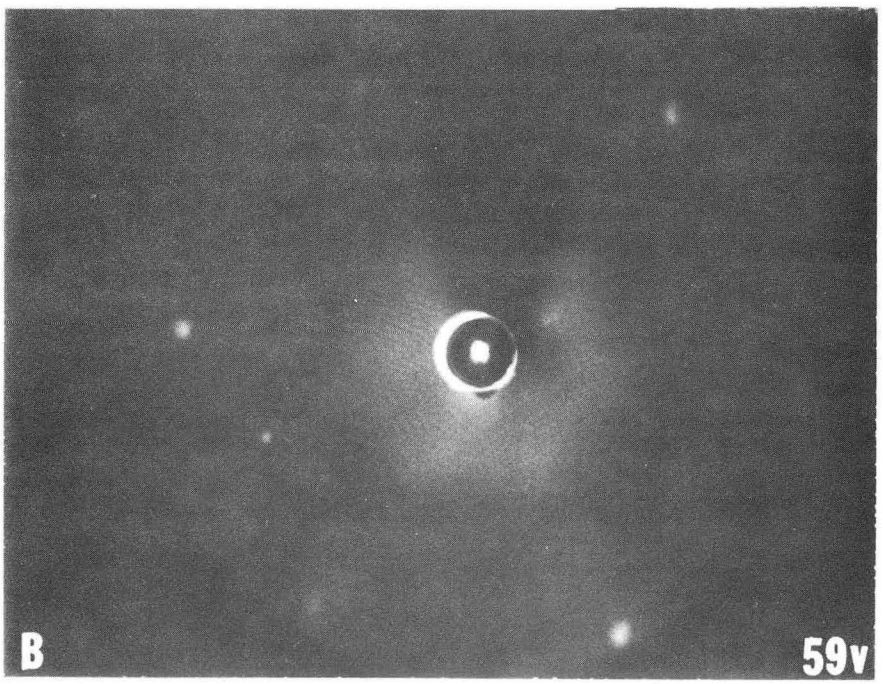

XBB 732-683

Fig. III-14a & III-14b.

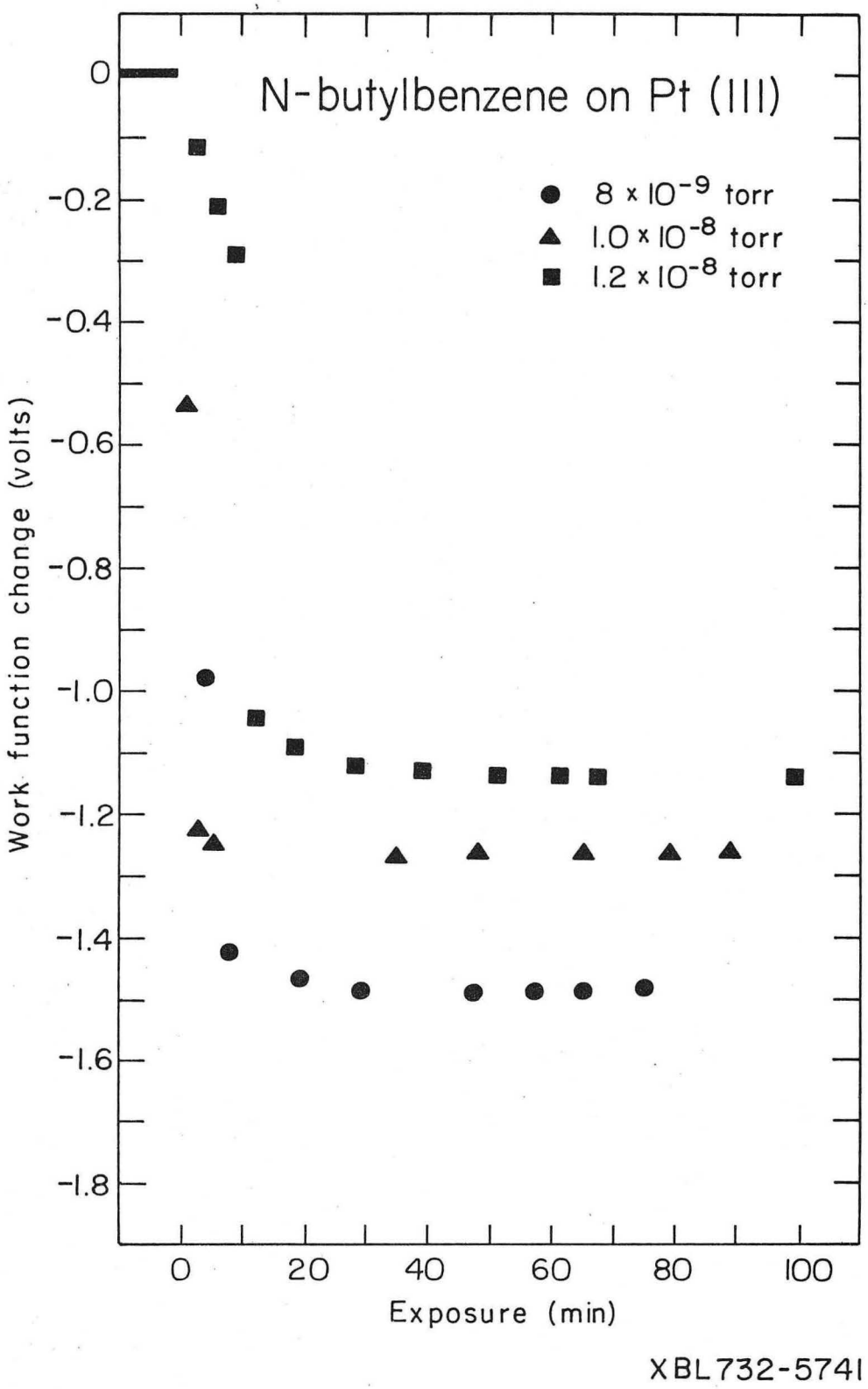

Fig. III-15. The work function change on adsorption of n-butylbenzene on the Pt(111) surface at 20°C. The indicated pressure should be multiplied by at least six to yield approximate surface pressures.

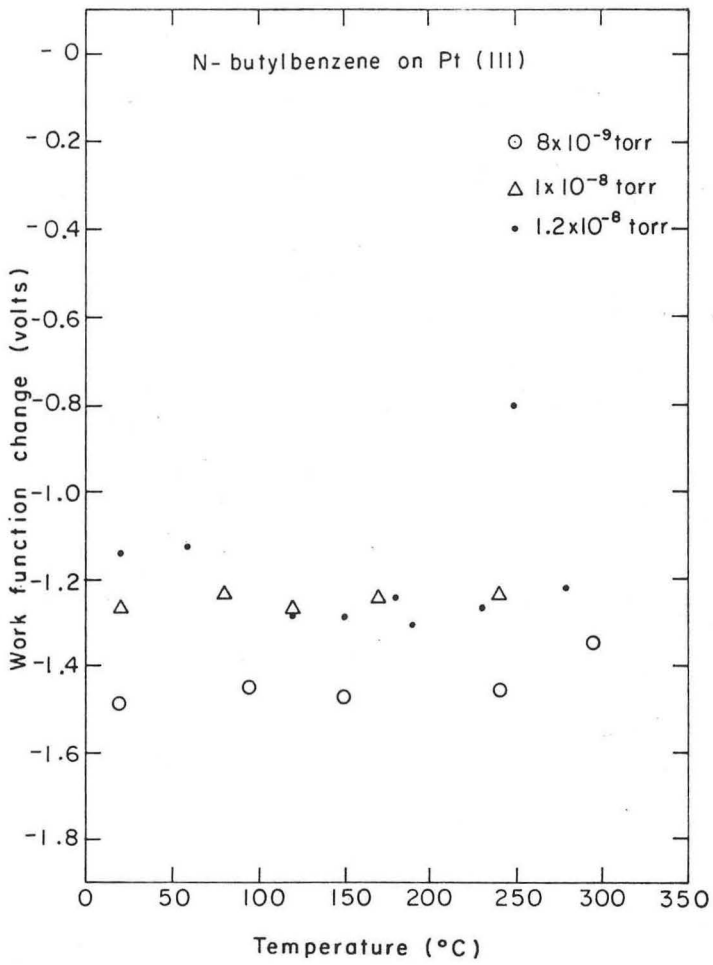

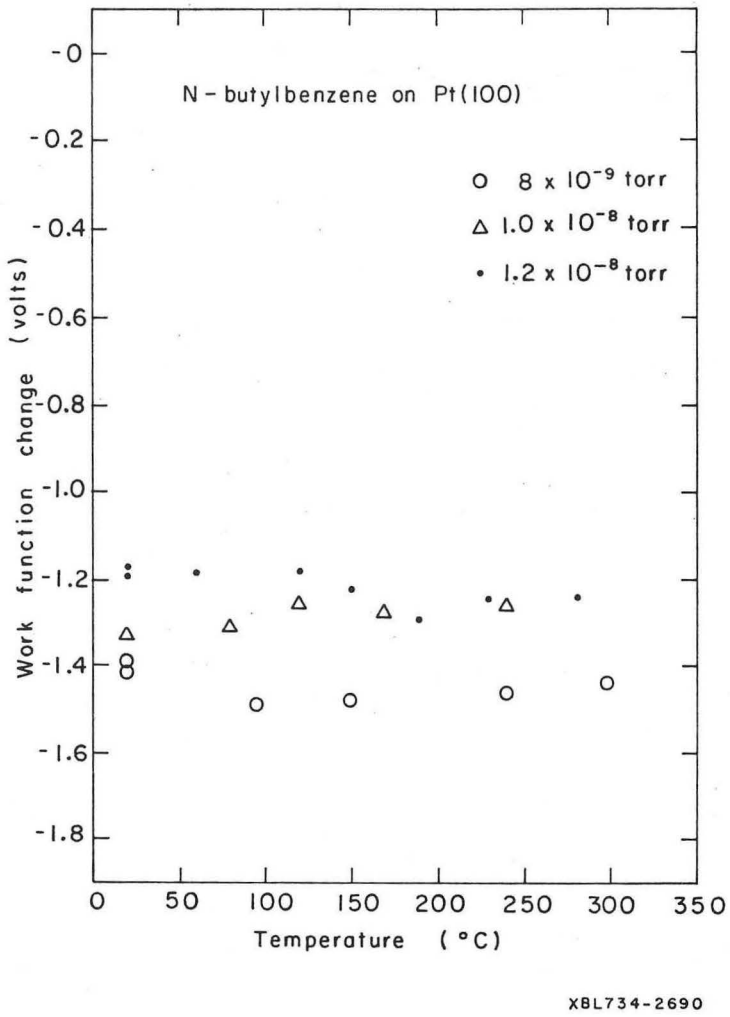

Fig. III-16. The work function change as a function of temperature for n-butylbenzene adsorption on the Pt(111) and Pt(100)-(5×1) surfaces. The indicated pressure should be multiplied by at least six to yield approximate surface pressures.

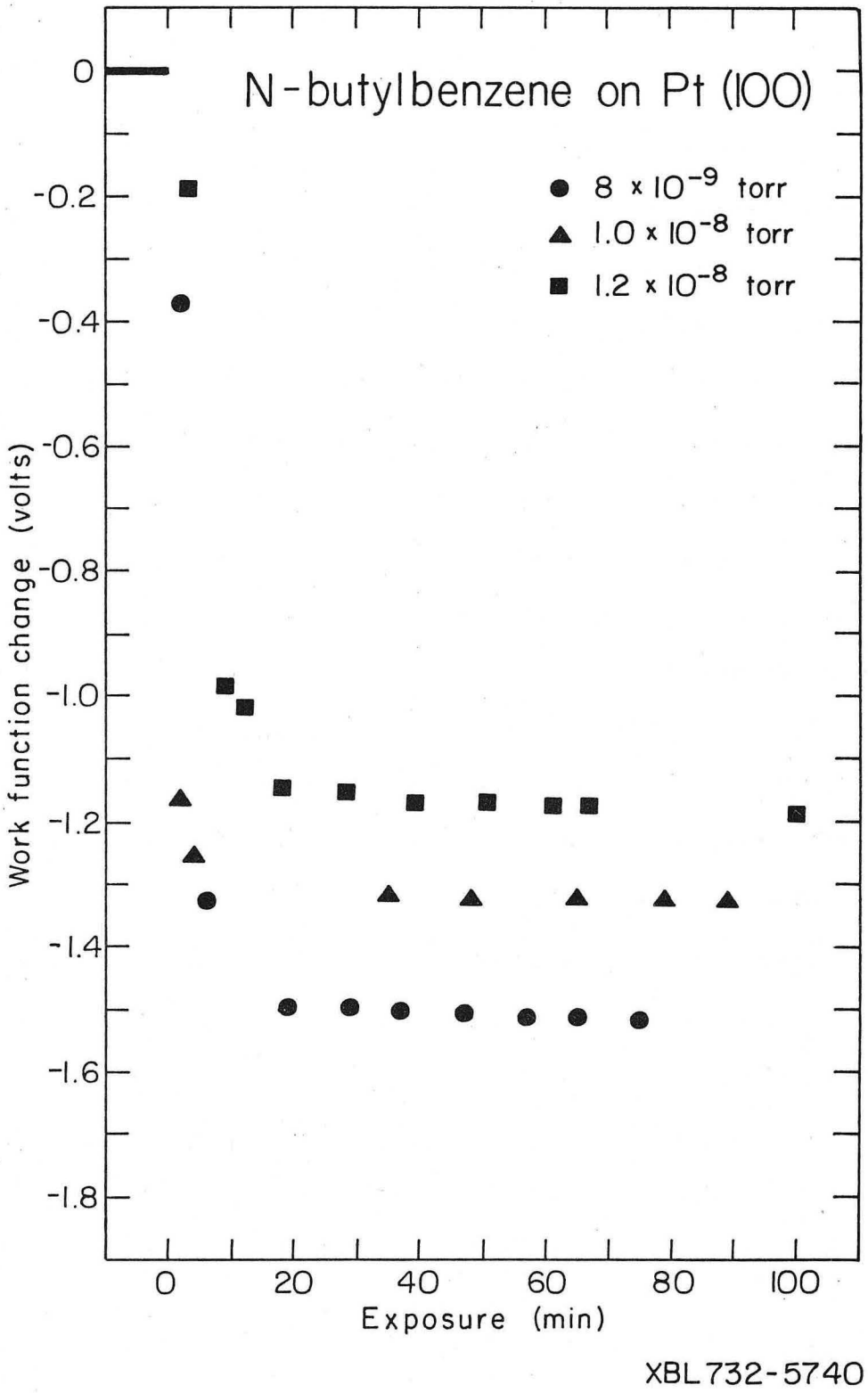

Fig. III-17. The work function change on adsorption of n-butylbenzene on the Pt(100)-(5×1) surface. The indicated pressure should be multiplied by at least six to yield approximate surface pressures.

dependent on the initial incident vapor flux.

With stepwise heating to 400°c in flux the adsorbed layer remains disordered. The WFC remains constant up to a sample temperature of 300°C as shown in Fig. III-16.

T-Butylbenzene adsorption

The adsorption of t-butylbenzene on the Pt(111) surface causes the formation of a largely disordered surface layer. Faint streaked high order features are visible for a time after initial exposure but their intensity decreases slowly with time. Finally, only diffraction features characteristic of a (1×1) surface structure with high background intensity are observed (after 4 hours at a recorded pressure of 5×10^{-8}). The WFC on adsorption is approximately -1.7 V as shown in Fig. III-18; however, it depends on the initial incident flux. Adsorption experiments have been run at a pressure of 4×10^{-7}; no unexpected WFC's were observed and the diffraction patterns observed were simply less ordered than those observed for low pressure adsorption.

With stepwise heating to 350°C in flux or in vacuum the adsorbed layer remains disordered or becomes disordered if the adsorbed layer had not previously become disordered. The WFC with heating in flux shows little variation until the sample is heated above 250°C (Fig. III-19), the magnitude of the WFC then decreases with increasing temperature. Heating in vacuum causes the magnitude of the WFC to decrease above 80°C.

The adsorption of t-butylbenzene on the Pt(100)-(5×1) causes the disappearance of the (5×1) substrate structure and an increase in the background intensity (20 minutes at a recorded pressure of 6×10^{-8}).

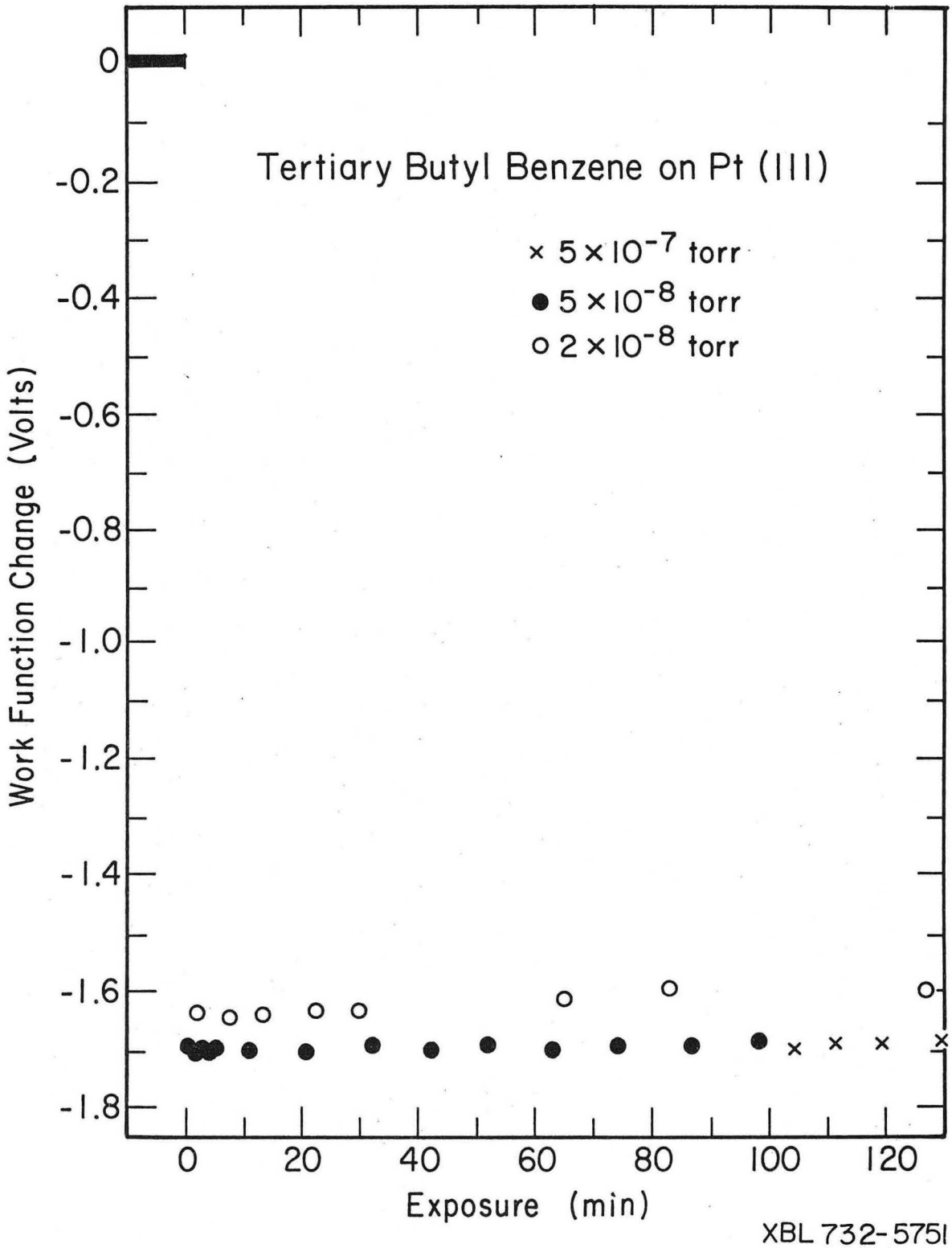

Fig. III-18. The work function change on adsorption of t-butylbenzene on the Pt(111) surface at 20°C. The indicated pressure should be multiplied by at least six to yield approximate surface pressures.

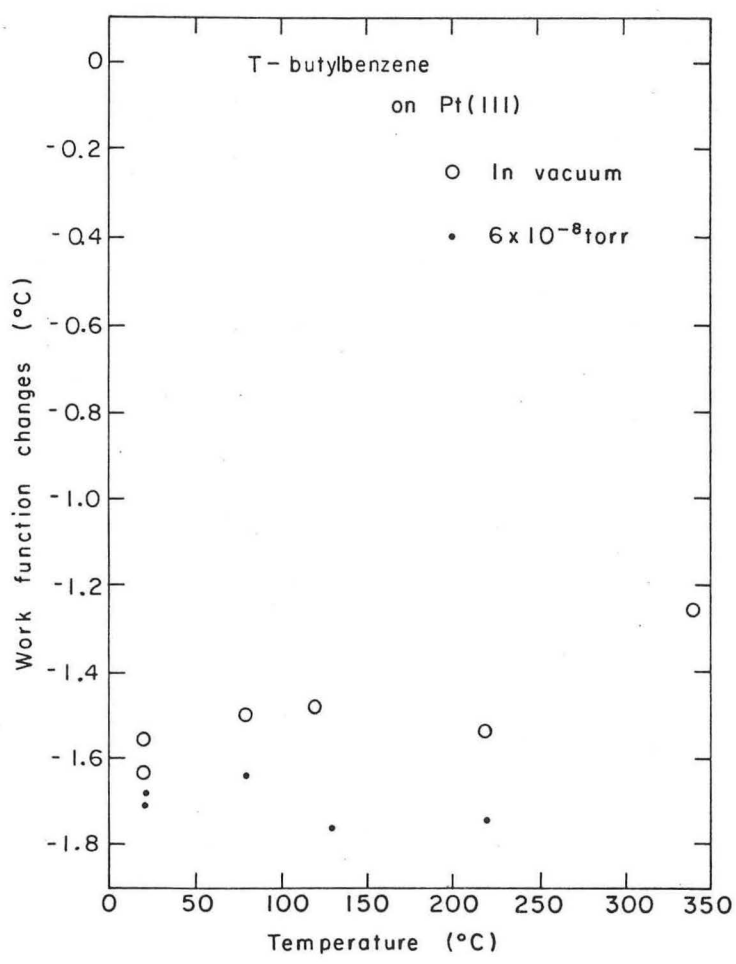

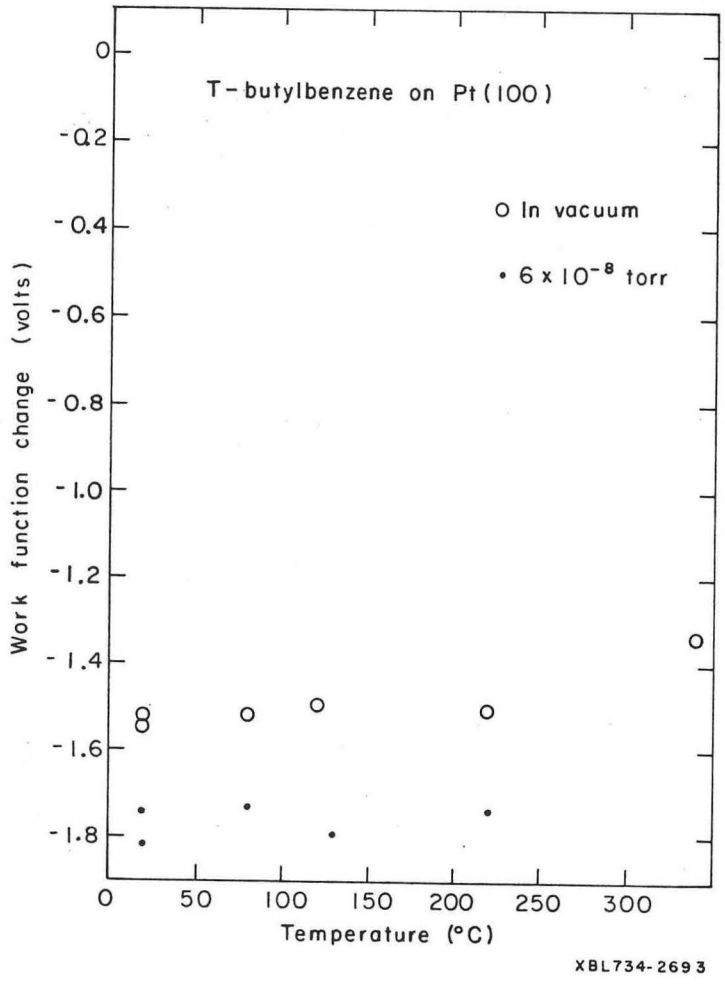

Fig. III-19. The work function change as a function of temperature for t-butylbenzene adsorbed on the Pt(111) and Pt(100)-(5×1) surfaces. The indicated pressure should be multiplied by at least six to yield approximate surface pressures.

The WFC on adsorption is -1.75 V (Fig. III-20); however, the WFC on adsorption depends on the initial incident vapor flux. Adsorption experiments have been run at pressures up to 4×10^{-7} Torr; no unexpected behavior was observed for either the WFC or diffraction results. With stepwise heating to 350°C in vacuum or in flux, the adsorbed layer remains disordered. The WFC shows little variation with heating in flux or in vacuum until heated above 250°C; the magnitude of the WFC then decreases with increasing temperature as shown in Fig. III-19.

Cyanobenzene adsorption

Adsorption of cyanobenzene on the Pt(111) surface causes the appearance of diffuse (1/2 0) diffraction features (Fig. III-21). The extra diffraction features slowly become less prominent during continued exposure (gone in 2 hours at 2×10^{-8} Torr). The WFC on adsorption is approximately -1.6 V (Fig. III-22).

With heating to 100°C in flux the adsorbed layer remains disordered or becomes disordered in cases where it had previously been ordered. The magnitude of the WFC decreases with heating above 100°C (Fig. III-23) and the adsorbed layer remains disordered.

Adsorption of cyanobenzene on the Pt(100)-(5×1) surface causes an increase in the background intensity and a slow decrease in the intensity of the (5×1) diffraction features (gone after 90 min. 2×10^{-8} Torr). The WFC on adsorption is -1.5 V (Fig. III-24).

With stepwise heating to 250° in flux the adsorbed layer remains disordered. The WFC remains constant with heating in flux to 100°C; with further heating the magnitude of the WFC decreases as shown in Fig. III-23.

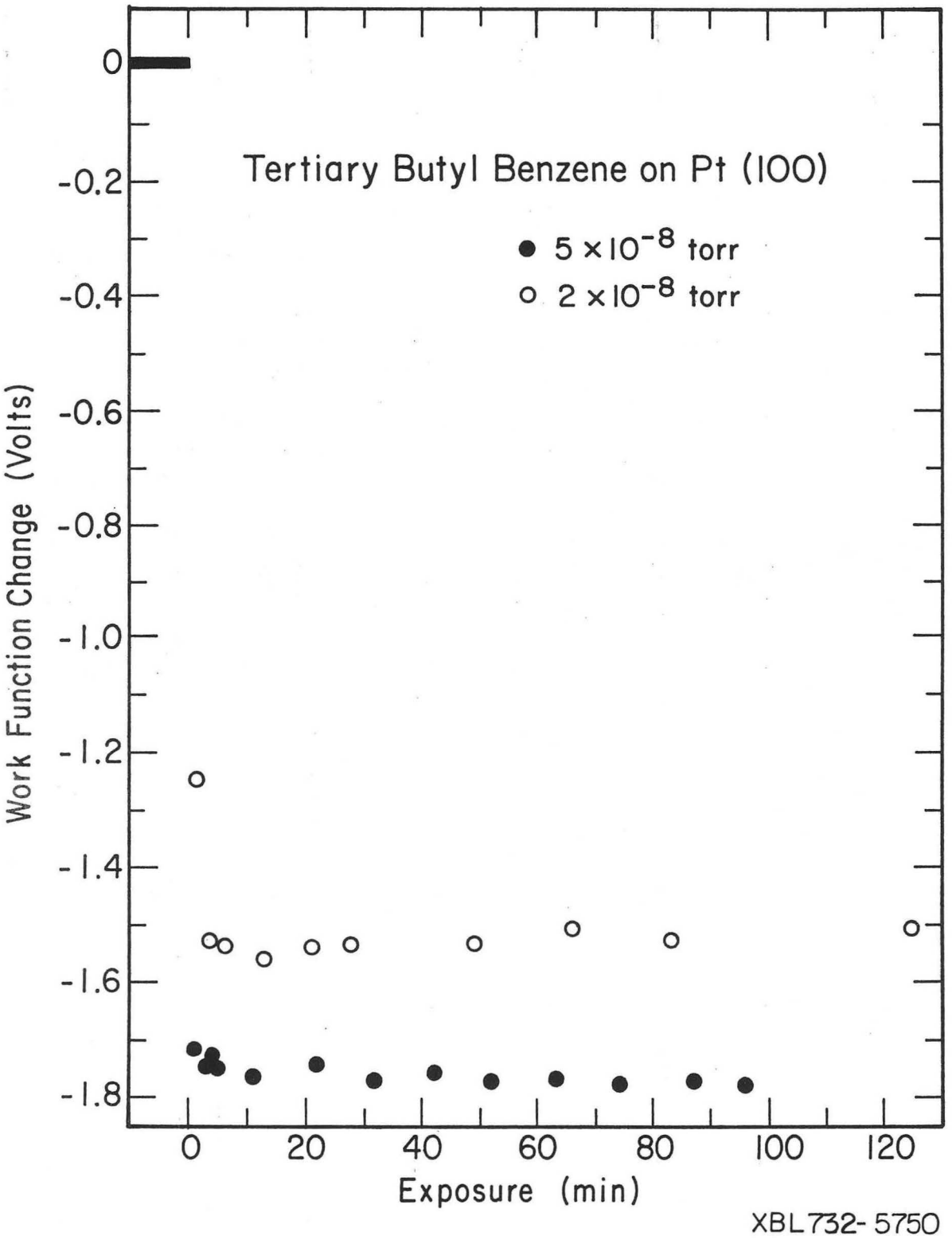

Fig. III-20. The work function change as a function of temperature for t-butylbenzene adsorbed on the Pt(100)-(5×1) surface at 20°C. The indicated pressure should be multiplied by at least six to yield approximate surface pressures.

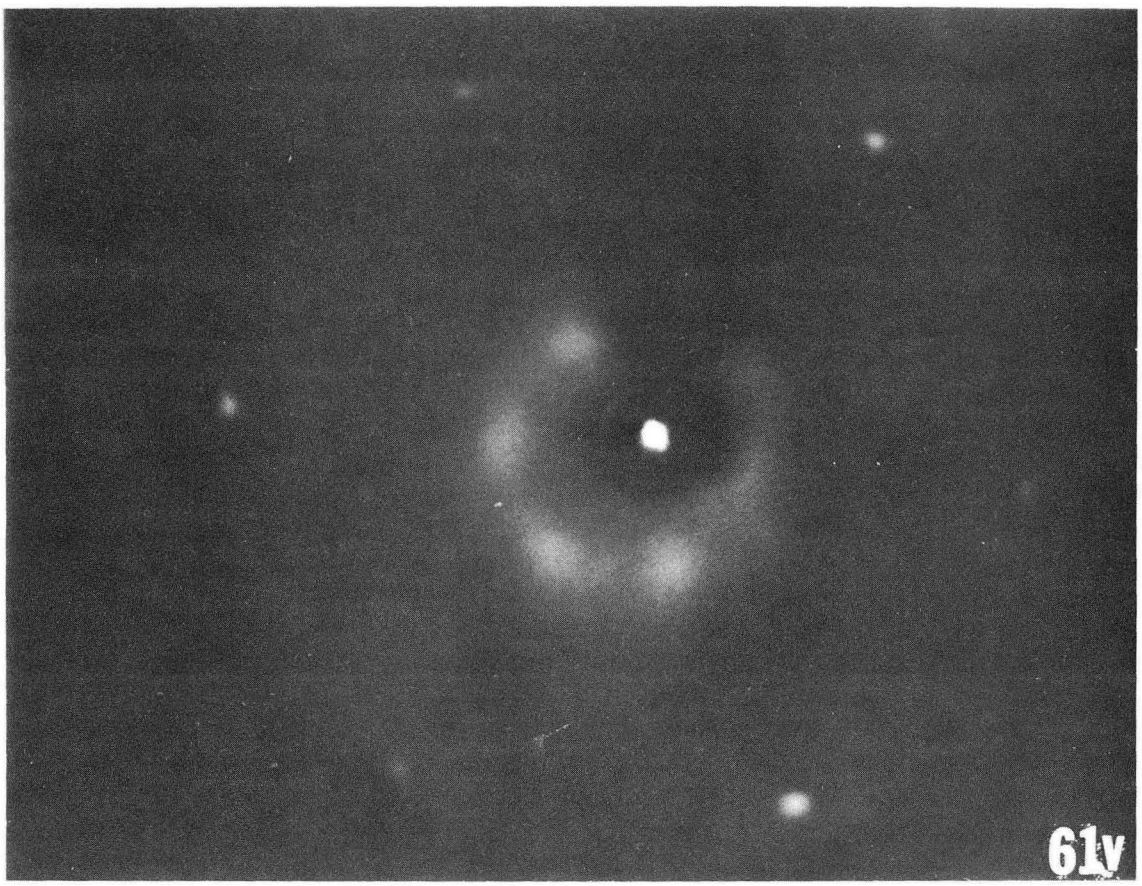

XBB 732-673

Fig. III-21. The diffraction pattern resulting from cyanobenzene adsorption on the Pt(111) surface showing the first order Pt diffraction features.

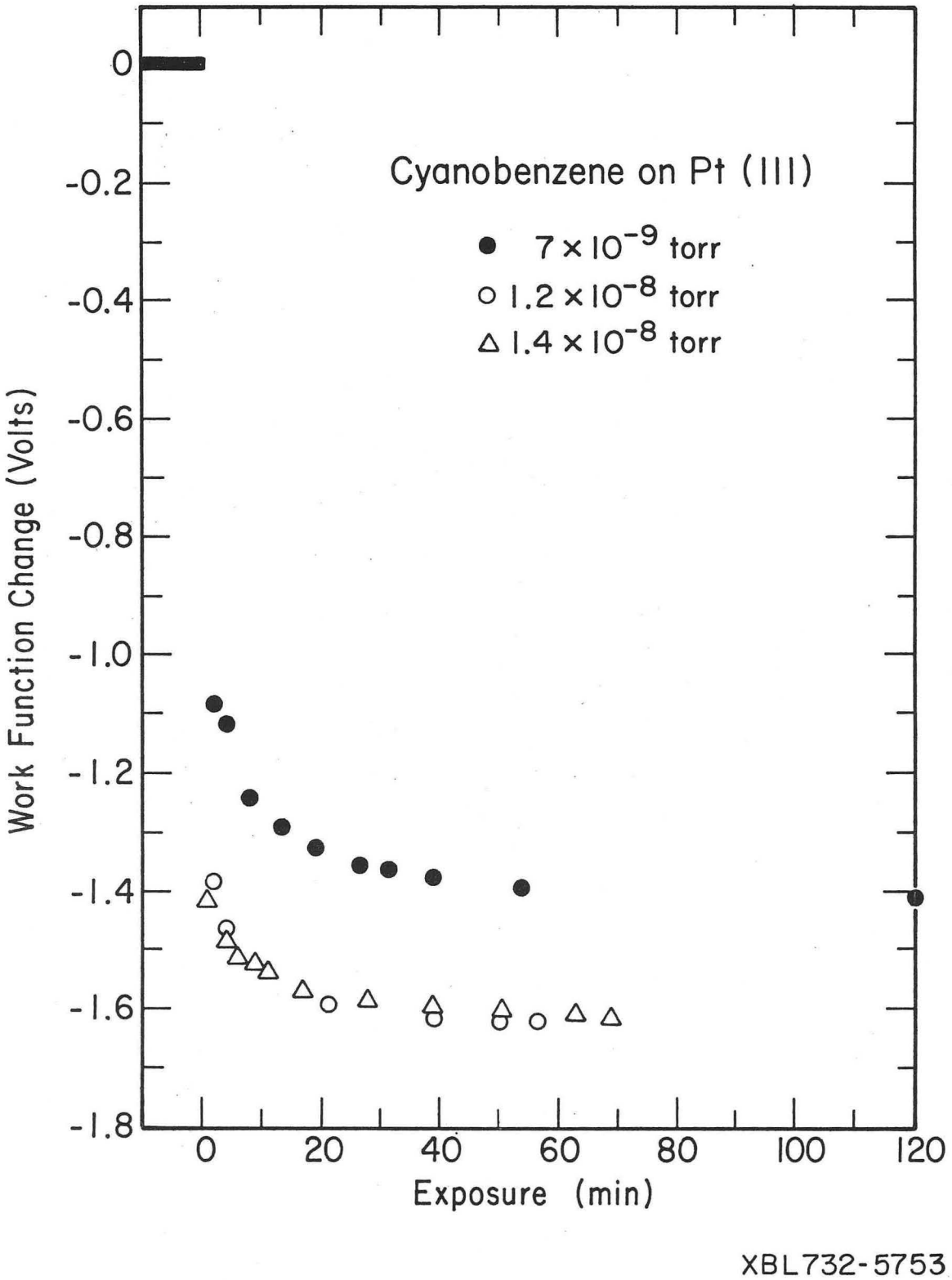

Fig. III-22. The work function change on adsorption of cyanobenzene on the Pt(111) surface at 20°C.

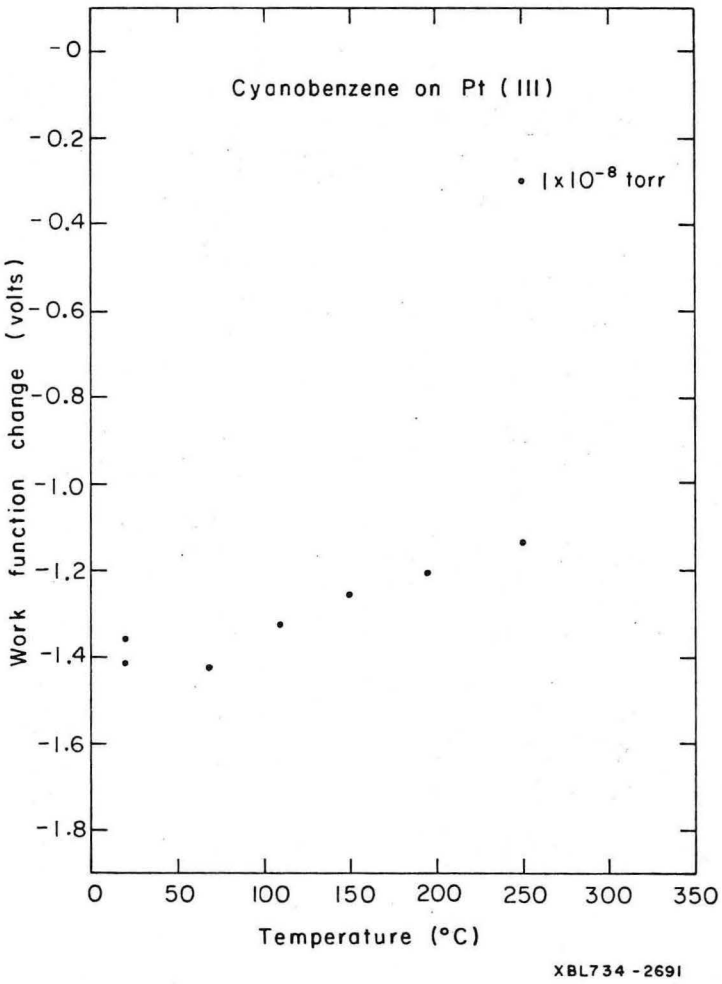

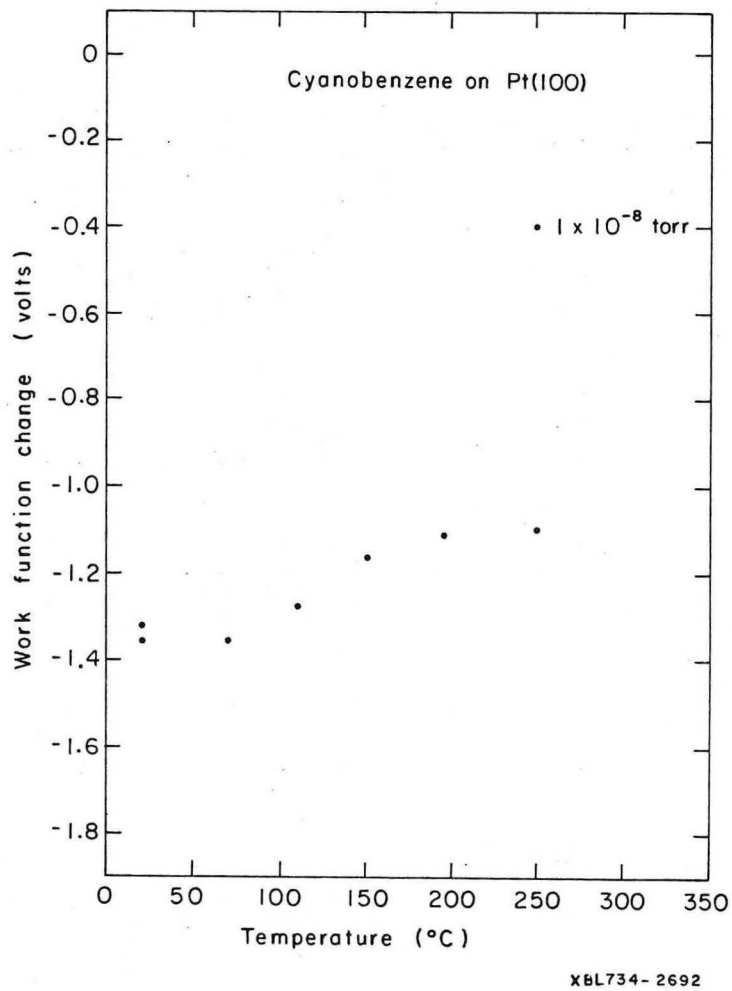

Fig. III-23. The work function change as a function of temperature for cyanobenzene adsorbed on the Pt(111) and Pt(100)-(5×1) surfaces. The indicated pressure should be multiplied by at least six to yield approximate surface pressures.

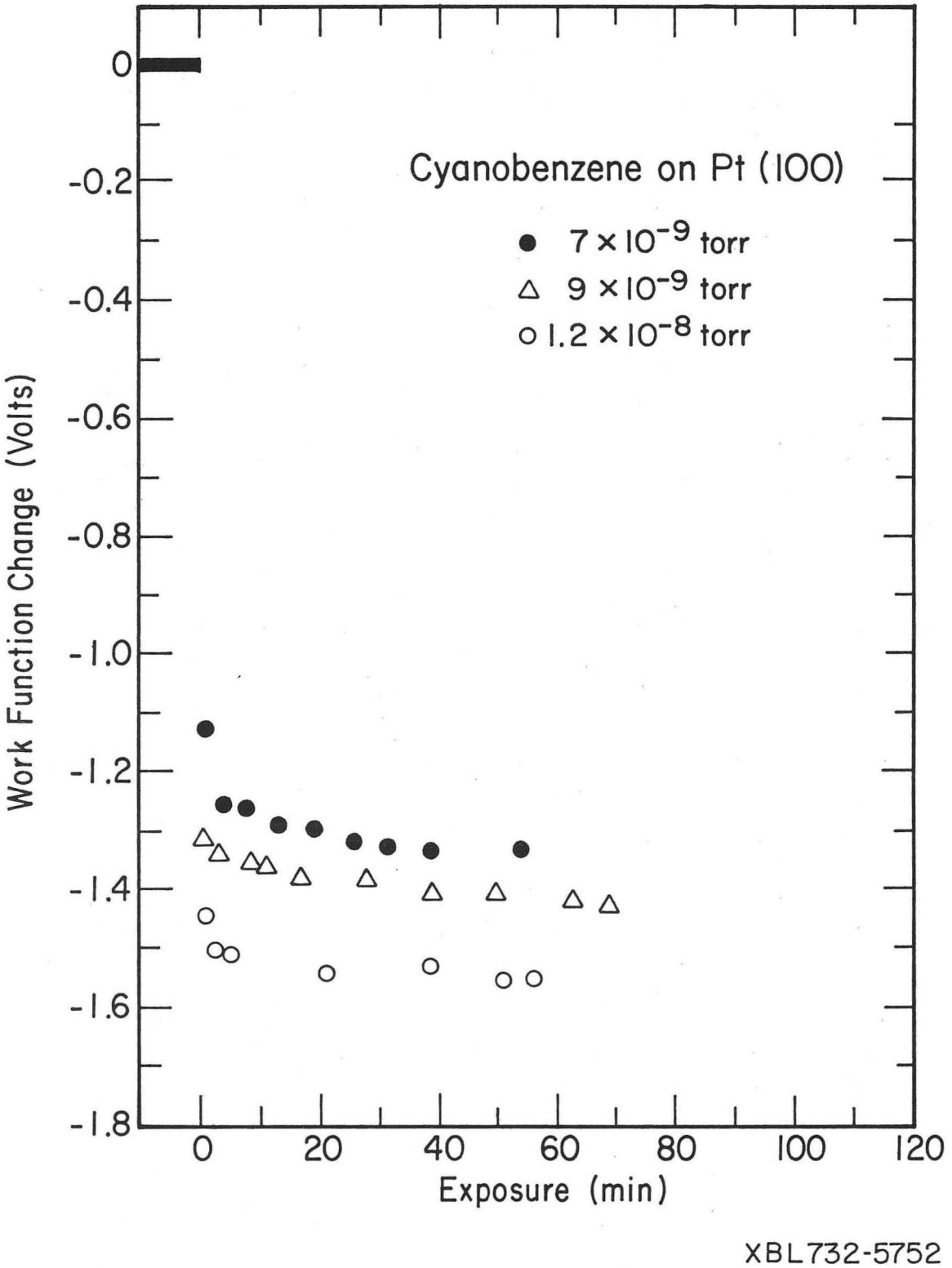

Fig. III-24. The work function change on adsorption of cyanobenzene on the Pt(100)-(5×1) surface at 20°C. The indicated pressure should be multiplied by at least six to yield approximate surface pressures.

1,3-Cyclohexadiene adsorption

1,3-Cyclohexadiene adsorbed on the Pt(111) initially forms a poorly ordered layer. Continued exposure causes the appearance of the $\begin{vmatrix} -2 & 2 \\ 4 & 4 \end{vmatrix}$ structure as shown in Figs. III-25a and III-25b. With continued exposure this structure slowly changes to the $\begin{vmatrix} -2 & 2 \\ 5 & 5 \end{vmatrix}$ structure shown in Figs. III-25c and III-25d. The work function shifts which accompany these changes in structure are shown in Fig. III-26. On initial adsorption the work function change goes through a minimum ($\sim$ -1.75 V) then increases slowly toward a higher steady state value ($\sim$ -.8 V). The initial ordered $\begin{vmatrix} -2 & 2 \\ 4 & 4 \end{vmatrix}$ structure appears at a WFC value of $\sim$ -1.3 V after the minimum work function has been passed. The second ordered structure $\begin{vmatrix} -2 & 2 \\ 5 & 5 \end{vmatrix}$ forms after the work function has increased further.

1,3-Cyclohexadiene adsorbed on the Pt(100)-(5×1) surface causes the (5×1) structure to disappear rapidly. A new diffraction pattern with a diffuse ring-like 1/2 order streak appears as shown in Fig. III-27. The work function change on adsorption is approximately -1.7 V as shown in Fig. III-28. The magnitude of the WFC decreases with exposure to organic vapor flux.

The results for 1,3-cyclohexadiene adsorption on the Pt(111) and Pt(100)-(5×1) surfaces are very similar to the distinctive results obtained for benzene adsorption on the same surfaces. Because of these results mass spectra were taken of this organic sample immediately after the adsorption experiment to check for benzene contamination. Total contamination of the sample was less than 1% and benzene was significantly lower than 1%.

Fig. III-25a. The diffraction pattern resulting from the 1,3-cyclohexadiene $\begin{vmatrix} -2 & 2 \\ 4 & 4 \end{vmatrix}$ structure on the Pt(111) surface.

Fig. III-25b. The diffraction pattern resulting from the 1,3 cyclohexadiene $\begin{vmatrix} -2 & 2 \\ 4 & 4 \end{vmatrix}$ structure on the Pt(111) surface showing the first order Pt diffraction features..

Fig. III-25c. The diffraction pattern resulting from the 1,3-cyclohexadiene $\begin{vmatrix} -2 & 2 \\ 5 & 5 \end{vmatrix}$ structure on the Pt(111) surface.

Fig. III-25d. The diffraction pattern resulting from the 1,3-cyclohexadiene $\begin{vmatrix} -2 & 2 \\ 5 & 5 \end{vmatrix}$ structure on the Pt(111) surface showing the first order Pt diffraction features.

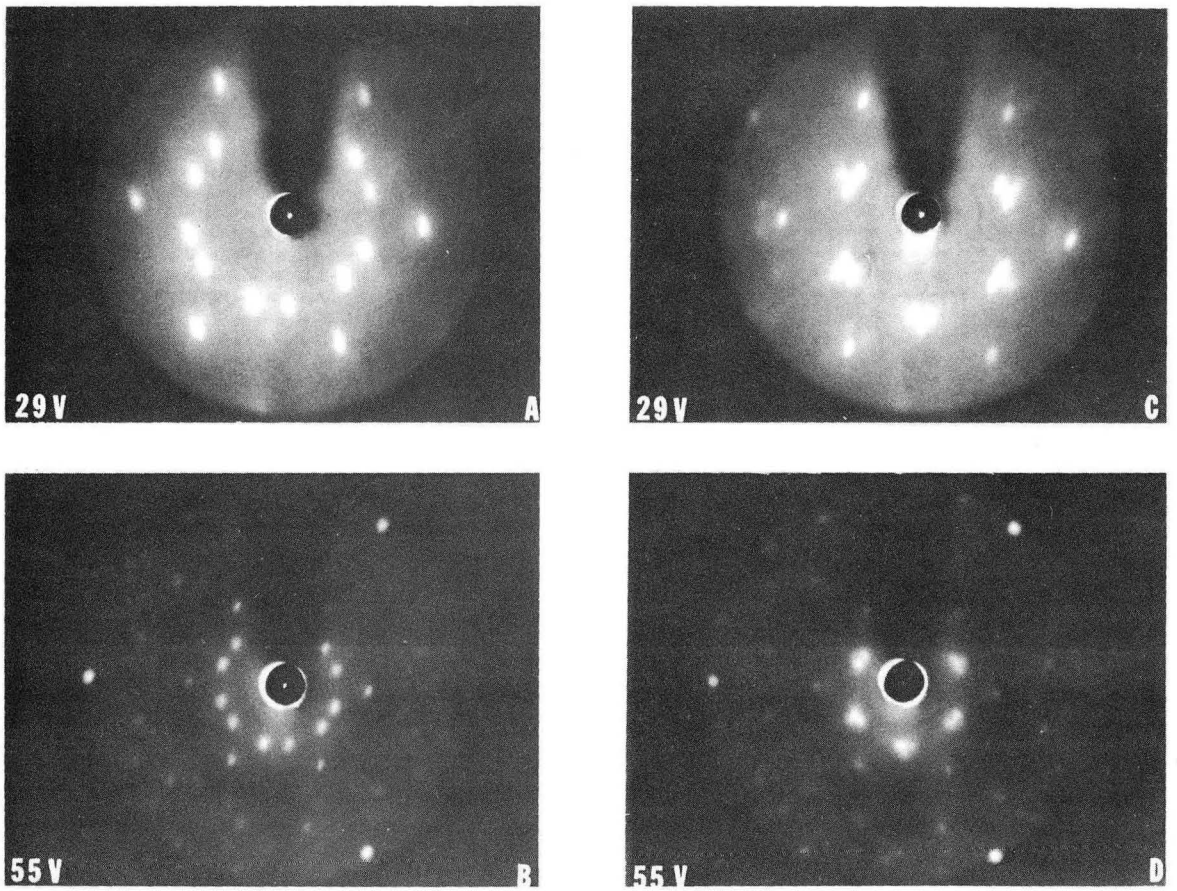

XBB 737-4300

Fig. III-25 (a, b, c, & d).

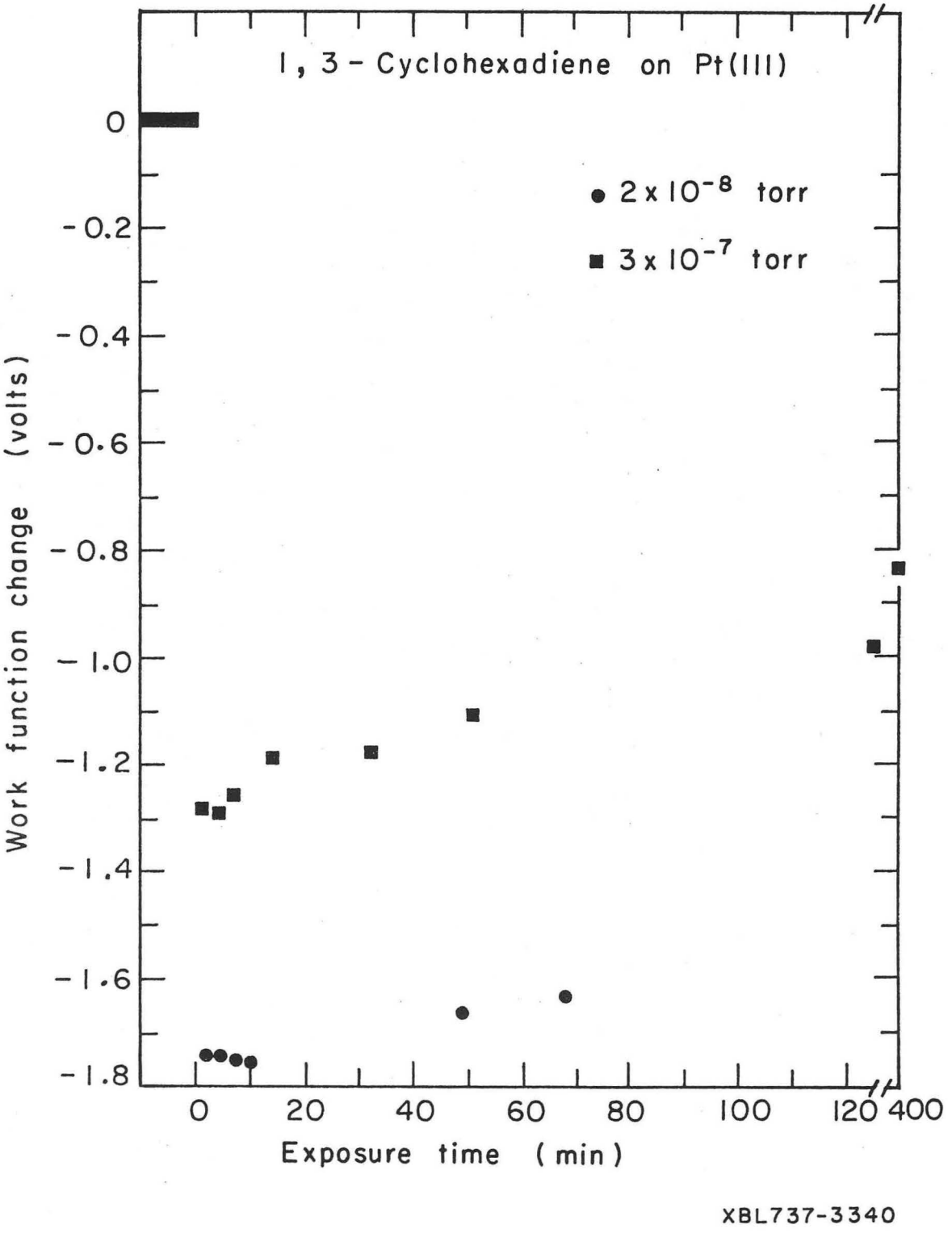

Fig. III-26. The work function change on adsorption of 1,3-cyclohexadiene on the Pt(111) surface. The indicated pressure should be multiplied by at least six to yield approximate surface pressures.

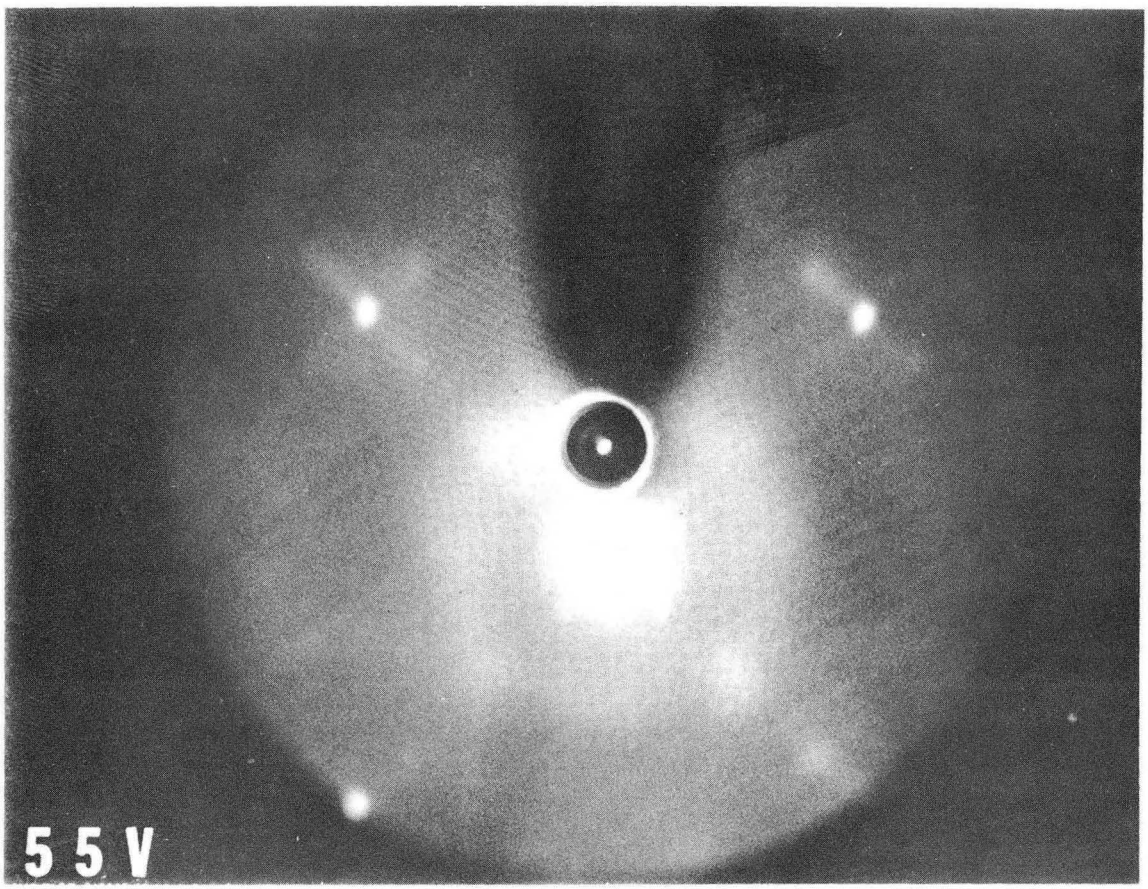

XBB 737-4297

Fig. III-27. The diffraction pattern resulting from 1,3-cyclohexadiene adsorption on the Pt(100)-(5×1) surface showing the first order Pt diffraction features.

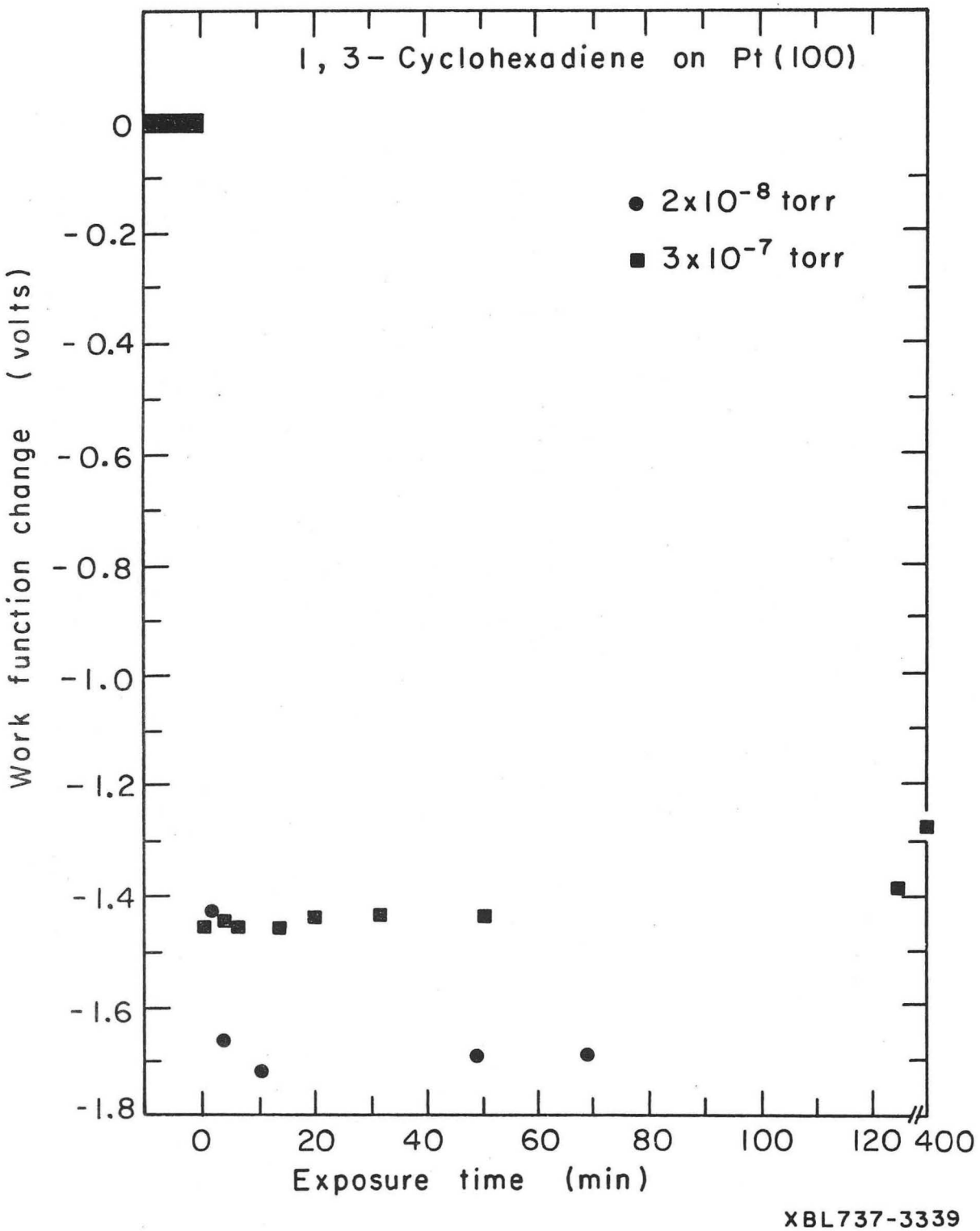

Fig. III-28. The work function change on adsorption of 1,3-cyclohexadiene on the Pt(100) surface at 20°C. The indicated pressure should be multiplied by at least six to yield approximate surface pressures.

Cyclohexane adsorption

Cyclohexane adsorption on the Pt(111) surface at 20°C and with low incident vapor flux (6×10^{-9} Torr recorded pressure) causes little change in the diffraction pattern observed. The WFC on adsorption is -1.2 V as shown in Fig. III-29. With increased organic vapor flux the WFC becomes -.7 V and the adsorbed layer begins to order. The diffraction pattern shows two faint diffuse high order features. The WFC for cyclohexane as a function of exposure is shown in Fig. III-29. With gentle heating to 150°C the adsorbed layer forms an apparent (2×2) structure as shown in Fig. III-30. With further heating the adsorbed layer becomes disordered and the magnitude of the WFC increases to -1.4 V at 300°C as shown in Fig. III-31. With further stepwise heating to 600°C the magnitude of the WFC decreases. For cyclohexane adsorbed on the Pt(100)-(5×1) surface at 20°C at low incident organic vapor flux (6×10^{-9} Torr recorded pressure) the (5×1) surface structure remains and the WFC is -.75 V (Fig. III-32). With increased organic vapor flux (4×10^{-7} Torr recorded pressure) the (5×1) surface structure relaxes and the diffraction pattern displays diffuse streaked (1/2 0) diffraction features with gentle heating to 150°C the streaks become narrow and well defined, centering on the positions expected from a (2×1) surface structure as shown in Fig. III-30b. The magnitude of the WFC increases with heating in flux up to a temperature of 300°C ($\Delta\phi$ = -1.5 V) as shown in Fig. III-33. Further heating in flux to 600°C causes the magnitude of the WFC to decrease progressively.

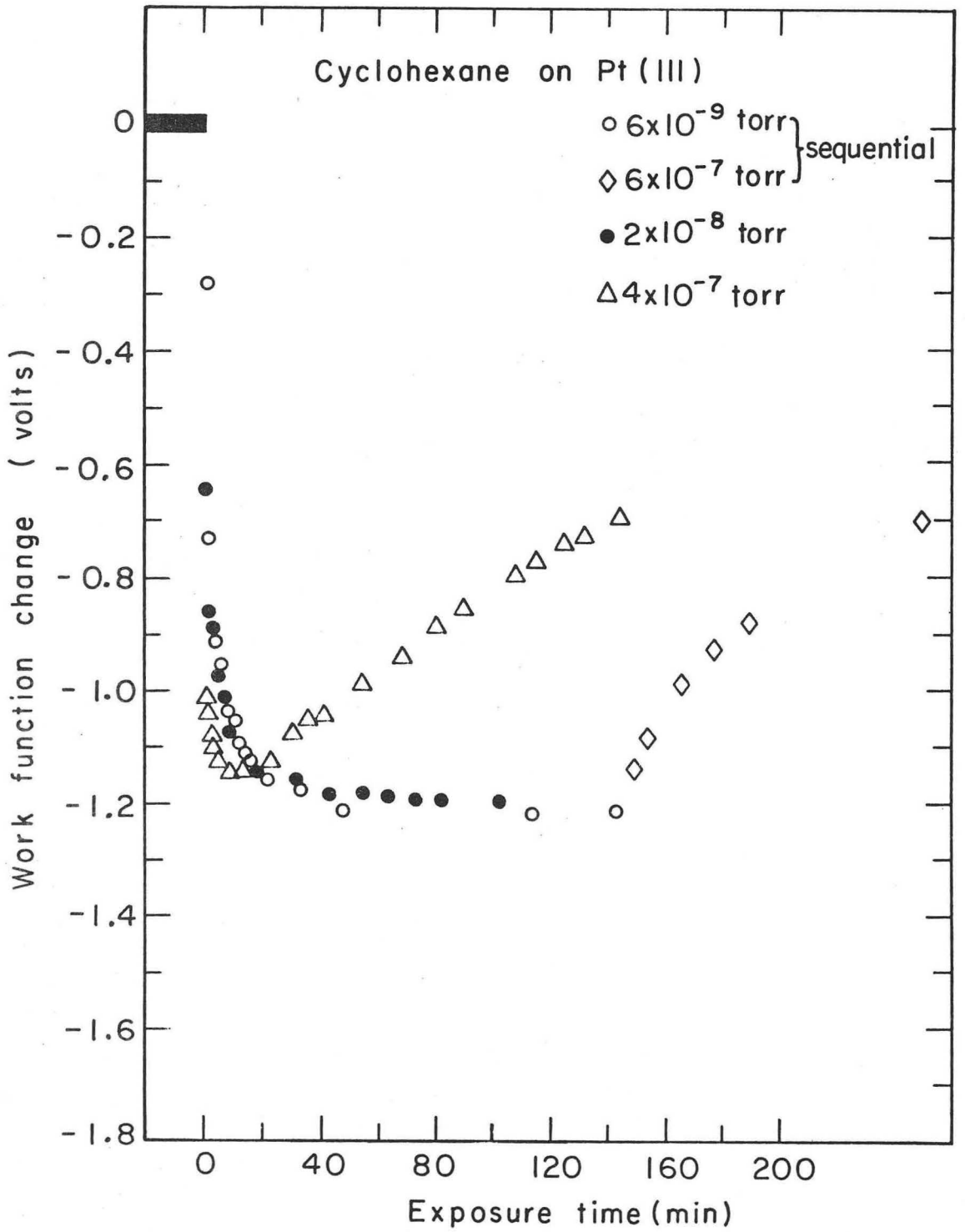

XBL737-3348

Fig. III-29. The work function change on adsorption of cyclohexane on the Pt(111) surface at 20°C. The indicated pressure should be multiplied by at least six to yield approximate surface pressures.

Fig. III-30a. The diffraction pattern resulting from an adsorbed layer of cyclohexane on the Pt(111) surface after heating to 150°C.

Fig. III-30b. The diffraction pattern resulting from an adsorbed layer of cyclohexane on the Pt(100)-(5×1) surface after heating to 150°C.

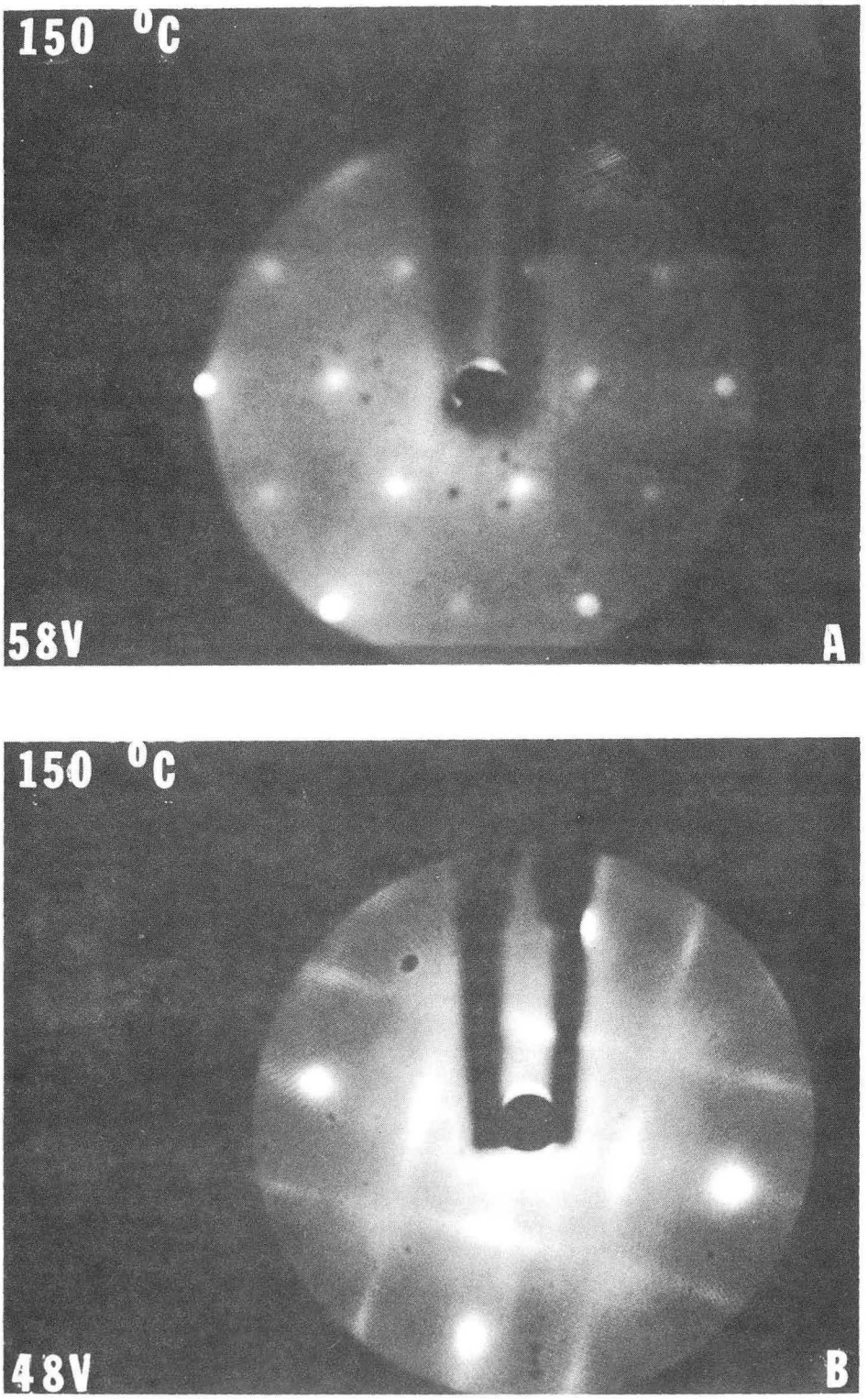

XBB 737-4301

Fig. III-30 (a & b).

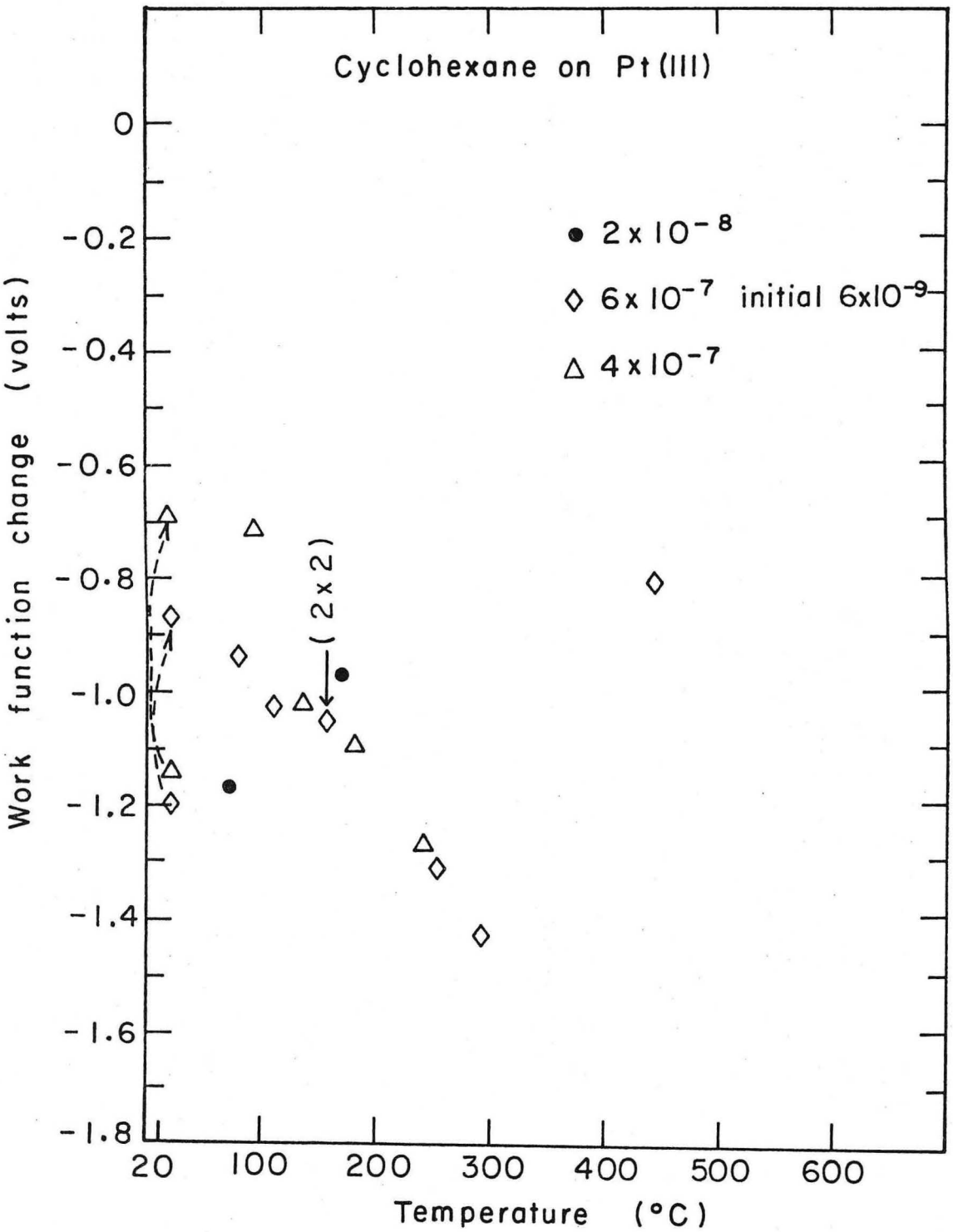

XBL737-3338

Fig. III-31. The work function change as a function of temperature for cyclohexane adsorbed on the Pt(111) surface. The indicated pressure should be multiplied by at least six to yield approximate surface pressures.

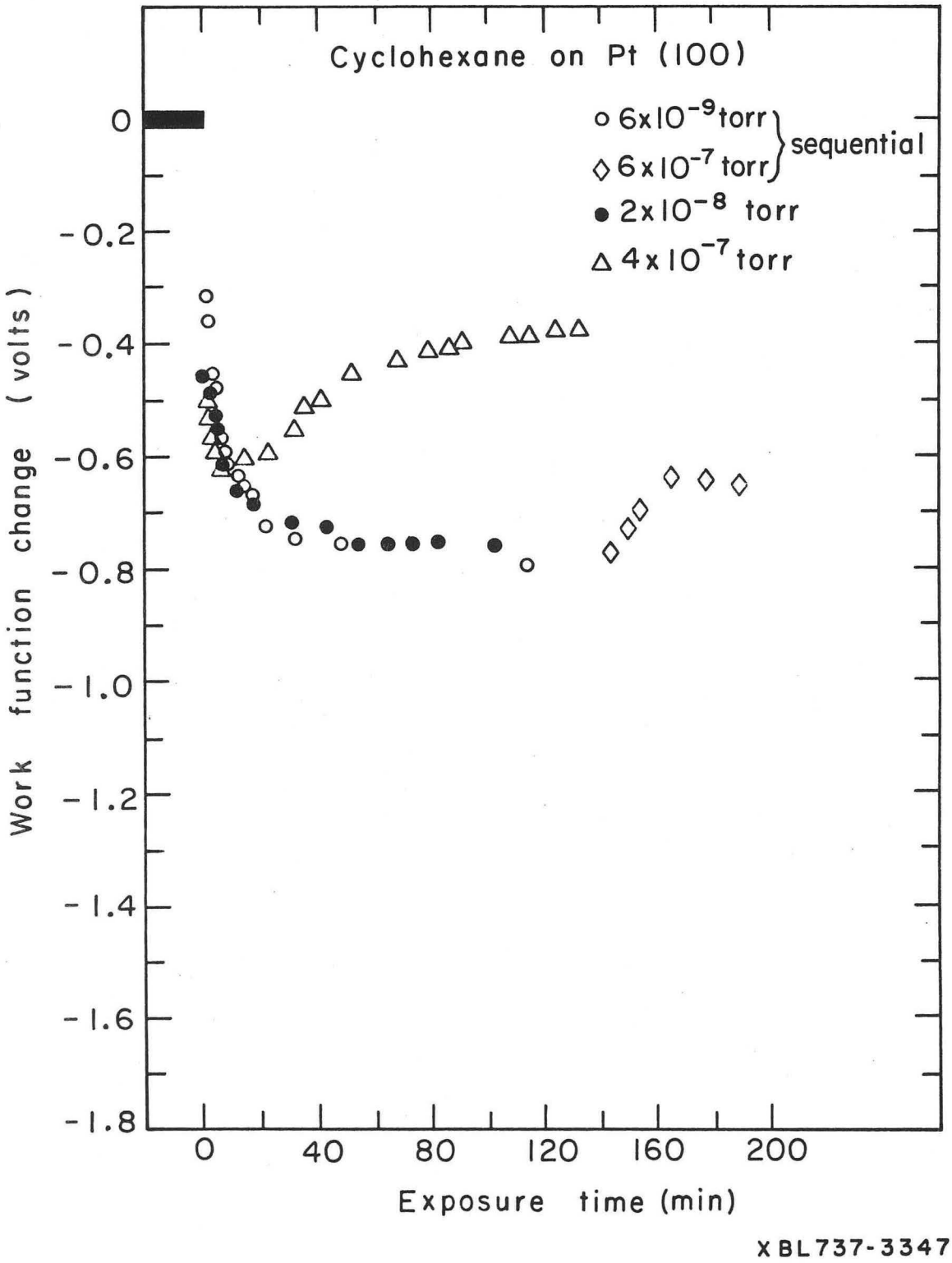

Fig. III-32. The work function change on adsorption of cyclohexane on the Pt(100)-(5×1) surface at 20°C. The indicated pressure should be multiplied by at least six to yield approximate surface pressures.

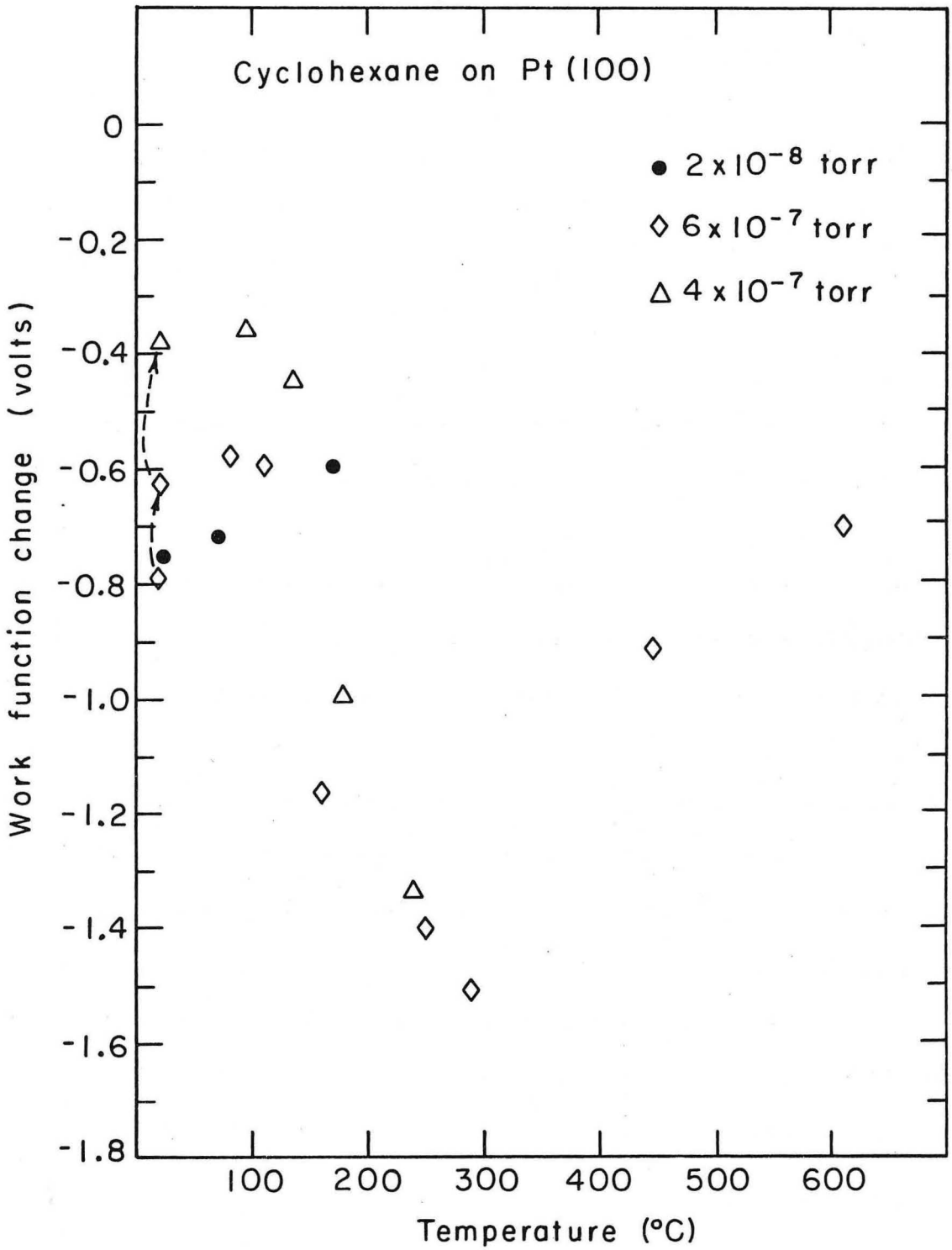

XBL737-3337

Fig. III-33. The work function change as a function of temperature for cyclohexane on the Pt(100)-(5×1) surface. The indicated pressure should be multiplied by at least six to yield approximate surface pressures.

Cyclohexene adsorption

Cyclohexene adsorption on the Pt(111) surface causes the formation of the ordered Pt(111)- $\begin{vmatrix} 2 & 2 \\ 4 & -2 \end{vmatrix}$ - Cyclohexene structure as shown in Figs. III-34a and b. The WFC on adsorption is approximately -1.7 V as shown in Fig. III-35. With heating to 150°C and subsequent cooling the diffraction features become more diffuse and the diffraction pattern becomes that due to a (2×2) structure. The magnitude of the WFC decreases with heating in flux above a sample temperature of 200°C. The dependence of the WFC on temperature is shown in Fig. III-36. Cyclohexene adsorption on the Pt(100)-(5×1) surface causes the rapid disappearance of the (5×1) structure. The pattern which appears has diffuse extra order diffraction features at the (1/2 0) position as shown in Fig. III-37. This pattern is beam sensitive; that is, exposure to the electron beam causes the poorly ordered structure to become completely disordered. The WFC on adsorption is approximately -1.6 V as shown in Fig. III-38. With heating to 200°C the adsorbed layer becomes more ordered and a streaked (2×1) pattern appears. The streaks in the diffraction pattern are perpendicular to the (10) direction. The magnitude of the WFC decreases with heating in flux above a sample temperature of 300°C. The dependence of the WFC on temperature is shown in Fig. III-39.

Fig. III-34a. The diffraction pattern resulting from cyclohexene adsorption on the Pt(111) surface at 20°C.

Fig. III-34b. The diffraction pattern resulting from cyclohexene adsorption on the Pt(111) surface at 20°C showing the first order platinum diffraction features.

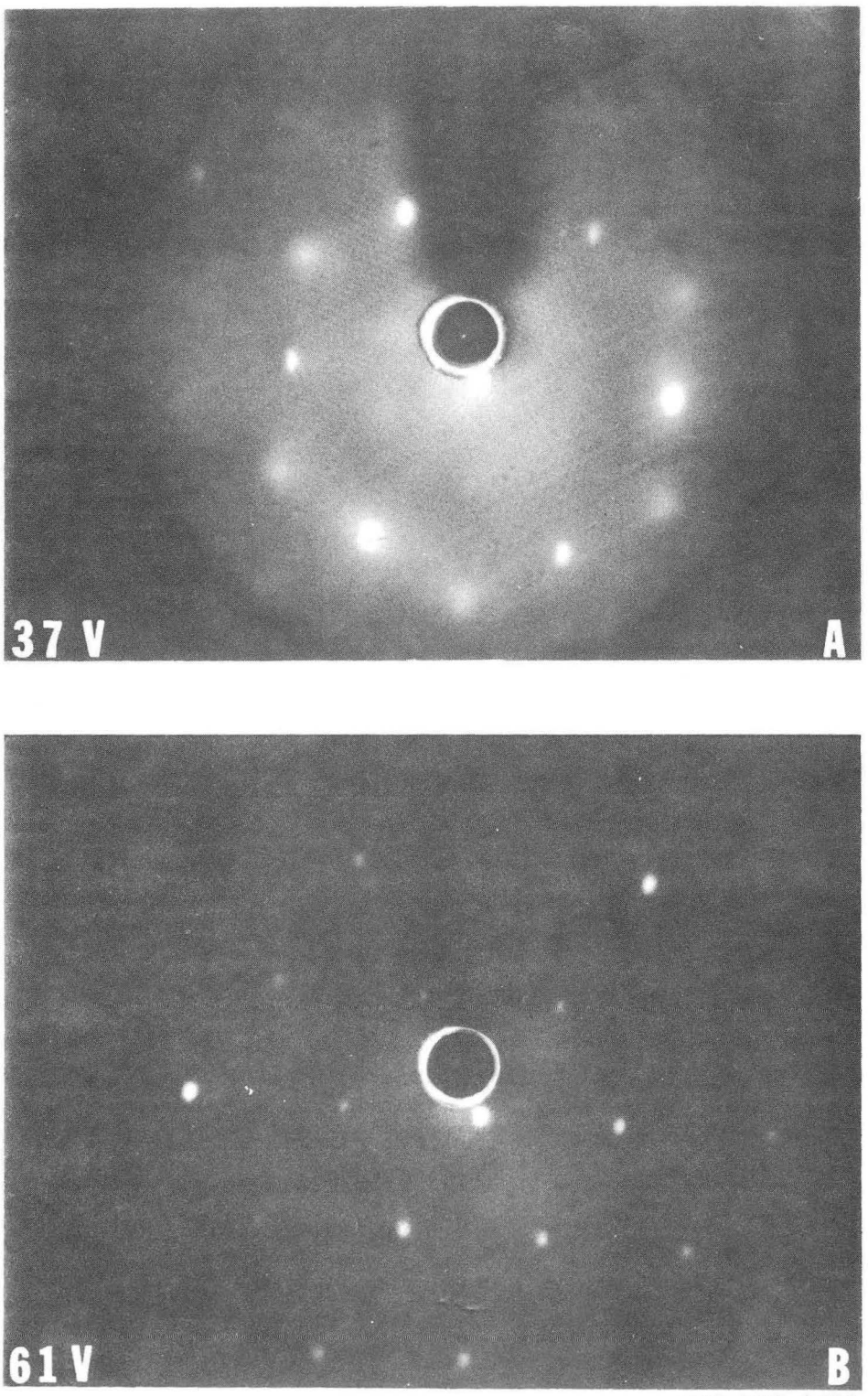

XBB 737-4302

Fig. III-34 (a & b).

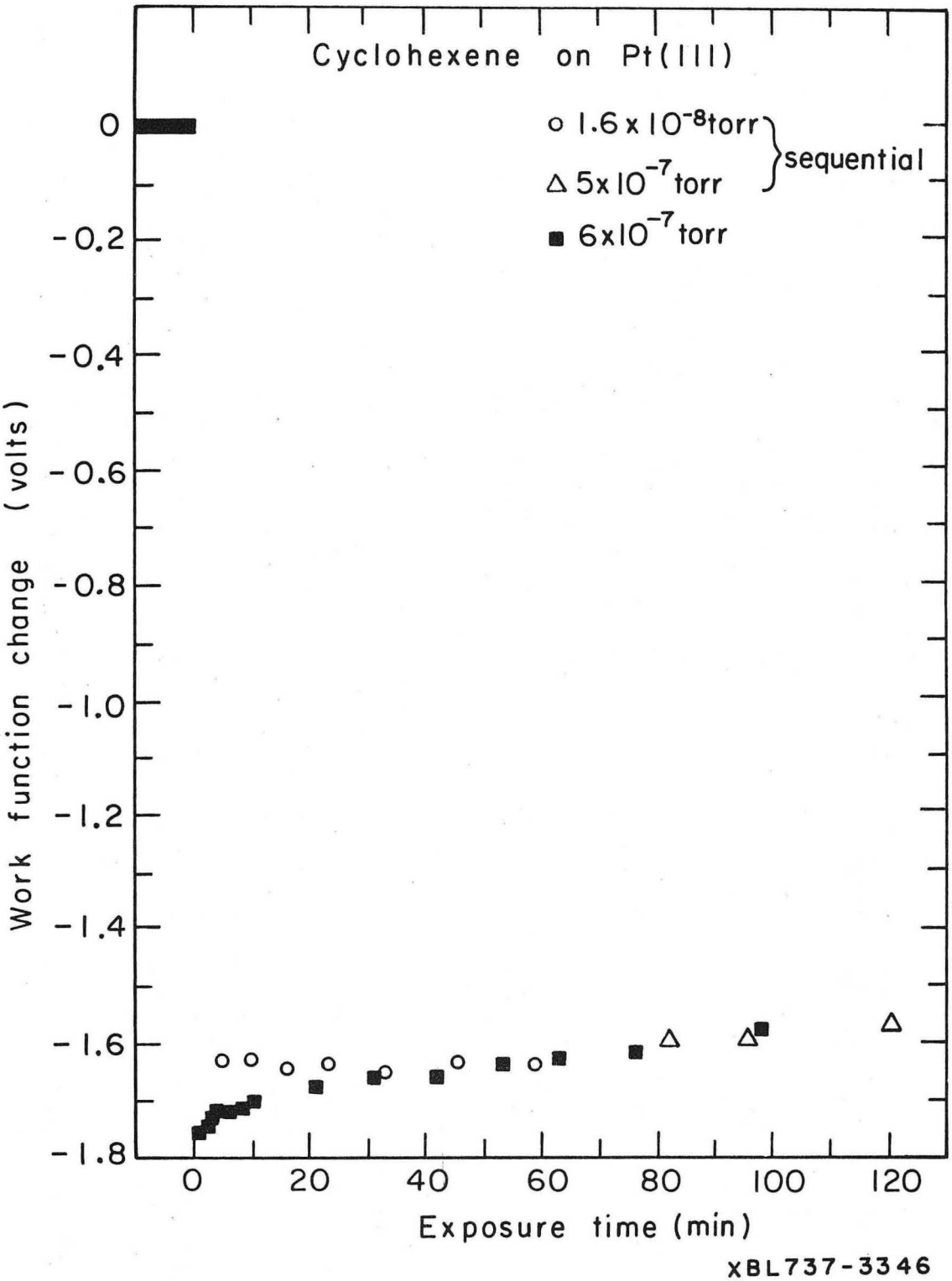

Fig. III-35. The work function change observed on adsorption of cyclohexene on the Pt(111) surface at 20°C. The indicated pressure should be multiplied by at least six to yield approximate surface pressures.

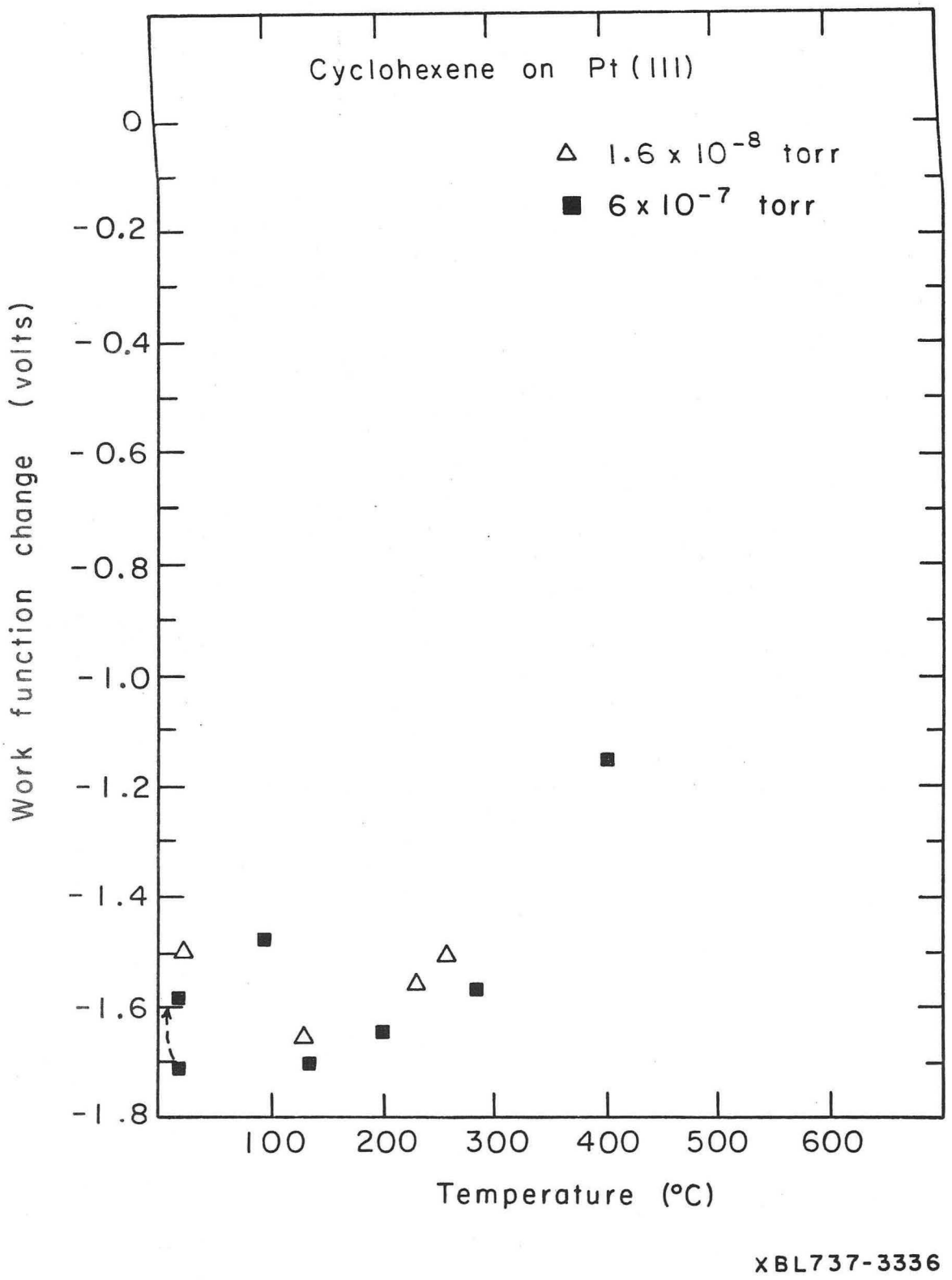

Fig. III-36. The work function change as a function of temperature for cyclohexene adsorption on the Pt(111) surface. The indicated pressure should be multiplied by at least six to yield approximate surface pressures.

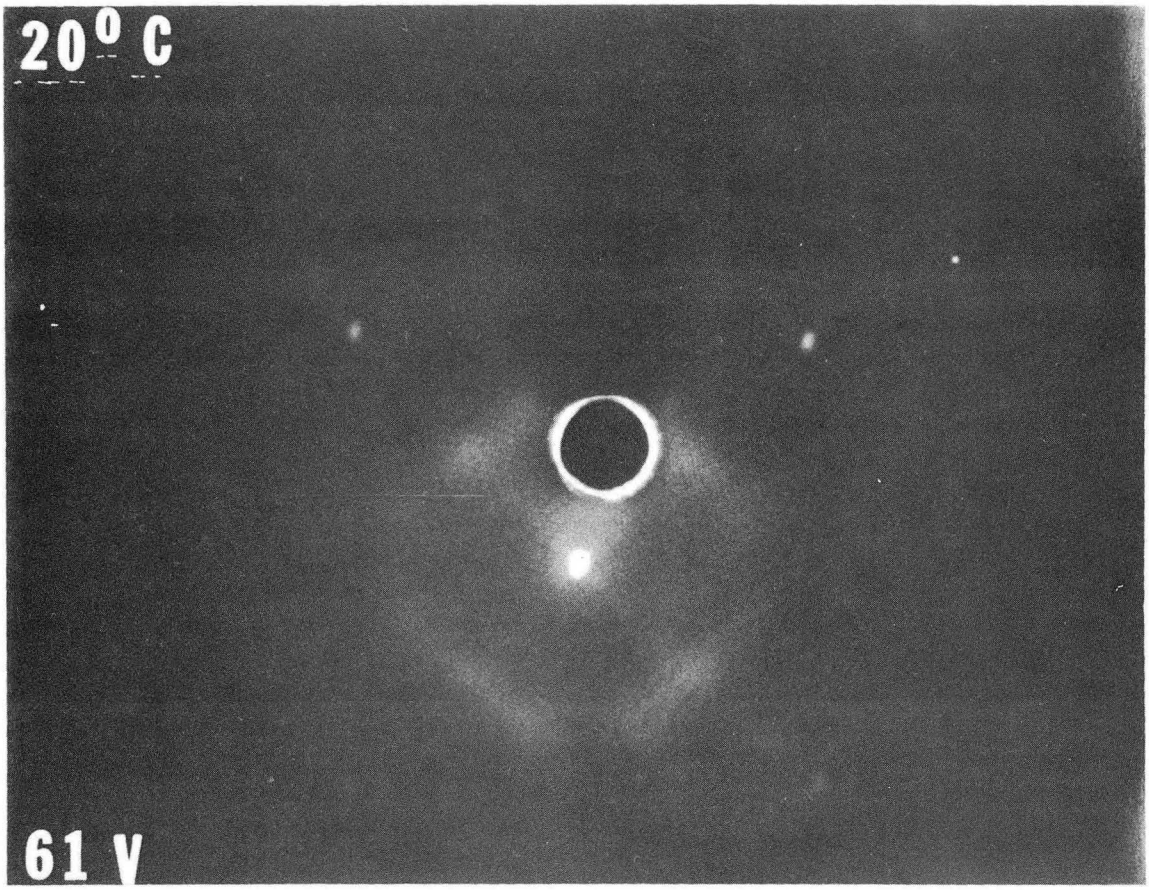

XBB 737-4298

Fig. III-37. The diffraction pattern resulting from cyclohexene adsorption on the Pt(100)-(5×1) surface at 20°C showing the first order Pt diffraction features.

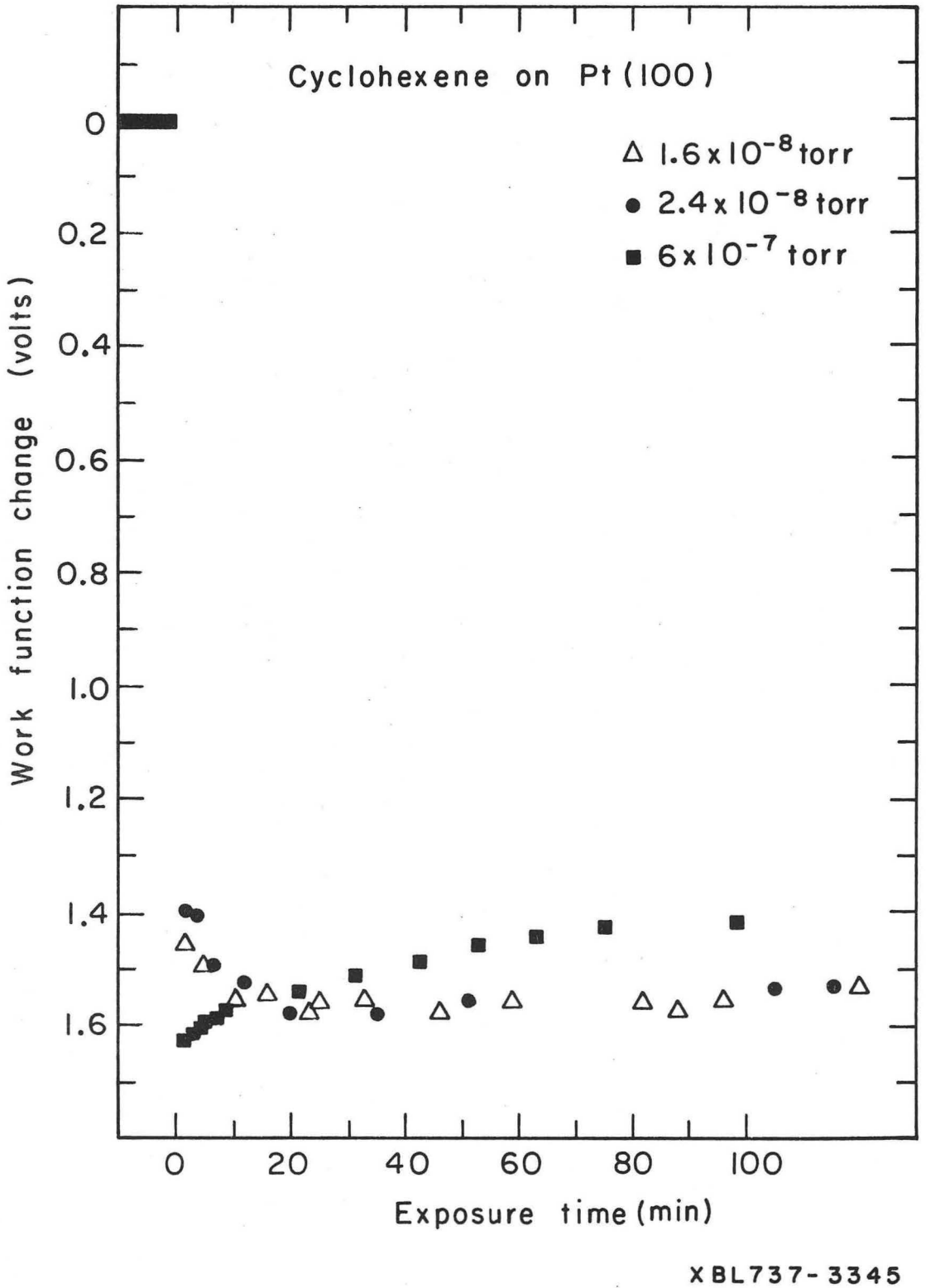

Fig. III-38. The work function change on adsorption of cyclohexene on the Pt(100)-(5×1) surface at 20°C. The indicated pressure should be multiplied by at least six to yield approximate surface pressures.

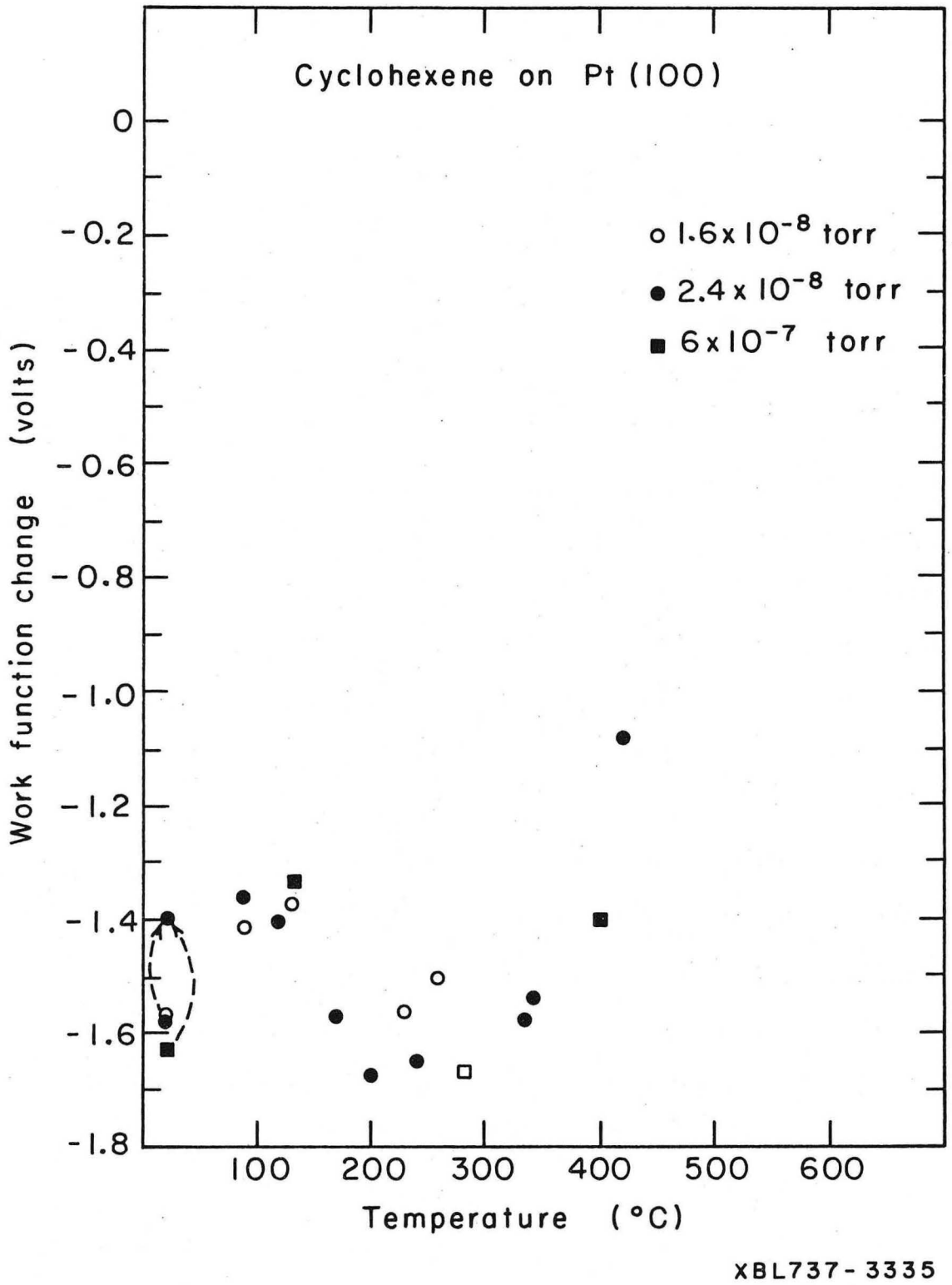

Fig. III-39. The work function change as a function of temperature for cyclohexene adsorption on the Pt(100)-(5×1) surface. The indicated pressure should be multiplied by at least six to yield approximate surface pressures.

Cyclopentane adsorption

Cyclopentane adsorbed on the Pt(111) surface at 7×10^{-9} Torr causes little change in the diffraction pattern; the WFC on adsorption is -.95 V. With increasing organic vapor pressure (recorded pressure 4×10^{-7} Torr) the WFC observed increases to -.7 V as shown in Fig. III-40. The background intensity observed in the diffraction pattern increases markedly with this increase in pressure.

Cyclopentane adsorbed on the Pt(100)-(5×1) at low organic vapor flux (recorded pressure 7×10^{-9} Torr) causes little change in the diffraction pattern. The WFC observed is -.4 V. With increased pressure (4×10^{-7} Torr) the magnitude of the WFC decreases to -.3 V as shown in Fig. III-41. With increased pressure new diffuse diffraction features appear at 1/2 order. With increased temperature the extra diffraction features become better defined. At 150°C the pattern has well defined streaks at positions centering on the positions expected from a (2×1) structure. The streaks run perpendicular to the (10) direction as shown in Fig. III-42.

Ethylene adsorption

Ethylene adsorbed on the Pt(111) surface causes the appearance of diffuse features at the (1/2 0) positions. These diffraction features become better ordered with time. The WFC on adsorption is -1.5 V as shown in Fig. III-43. With heating in flux the WFC decreases and goes through a minimum value of -1.7 V at 225°C as shown in Fig. III-44. With heating in vacuum the magnitude of the WFC decreases with progressive heating above 100°C Fig. III-44. The

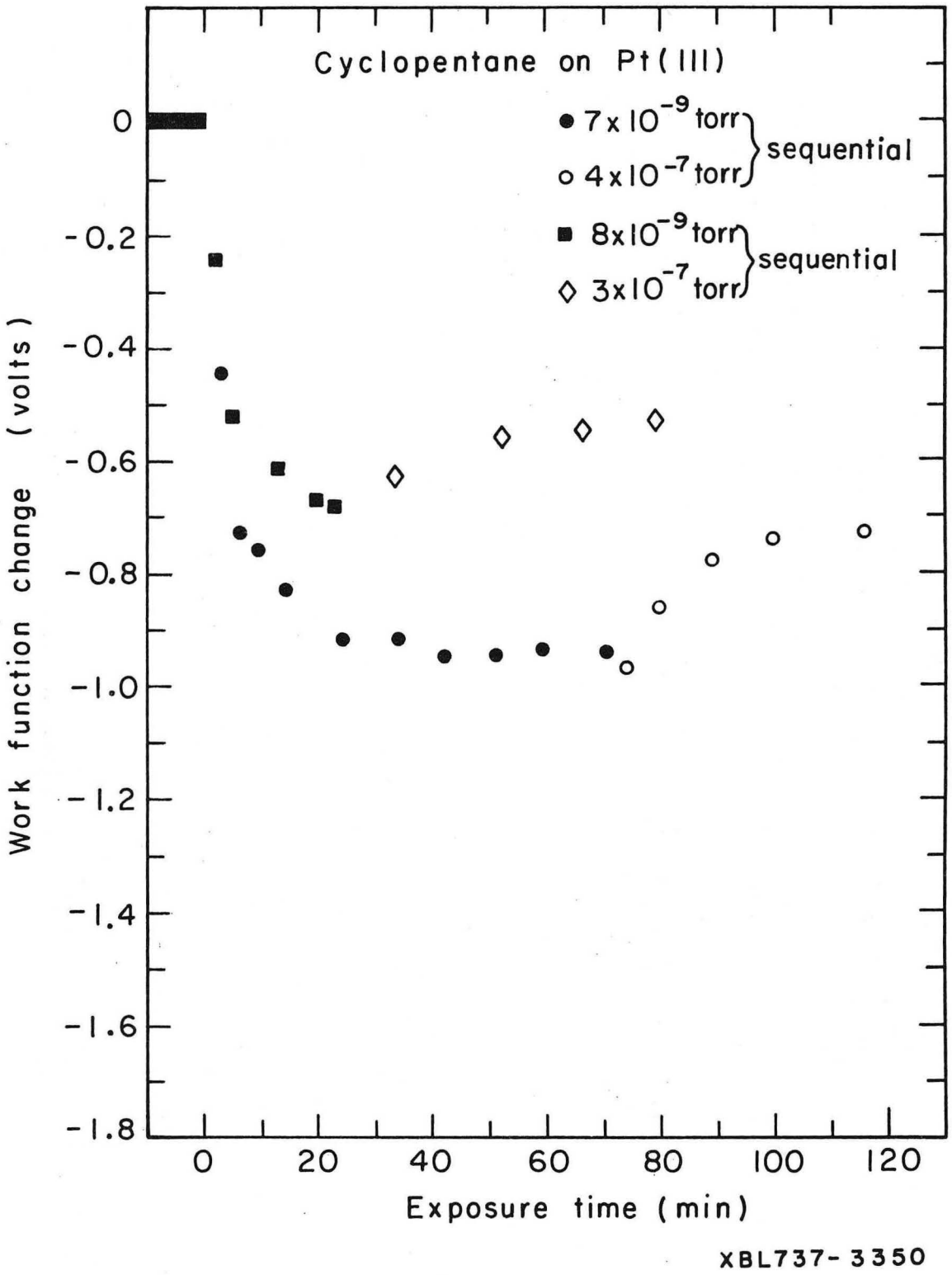

Fig. III-40. The work function change on adsorption of cyclopentane on the Pt(111) surface at 20°C. The indicated pressure should be multiplied by at least six to yield approximate surface pressures.

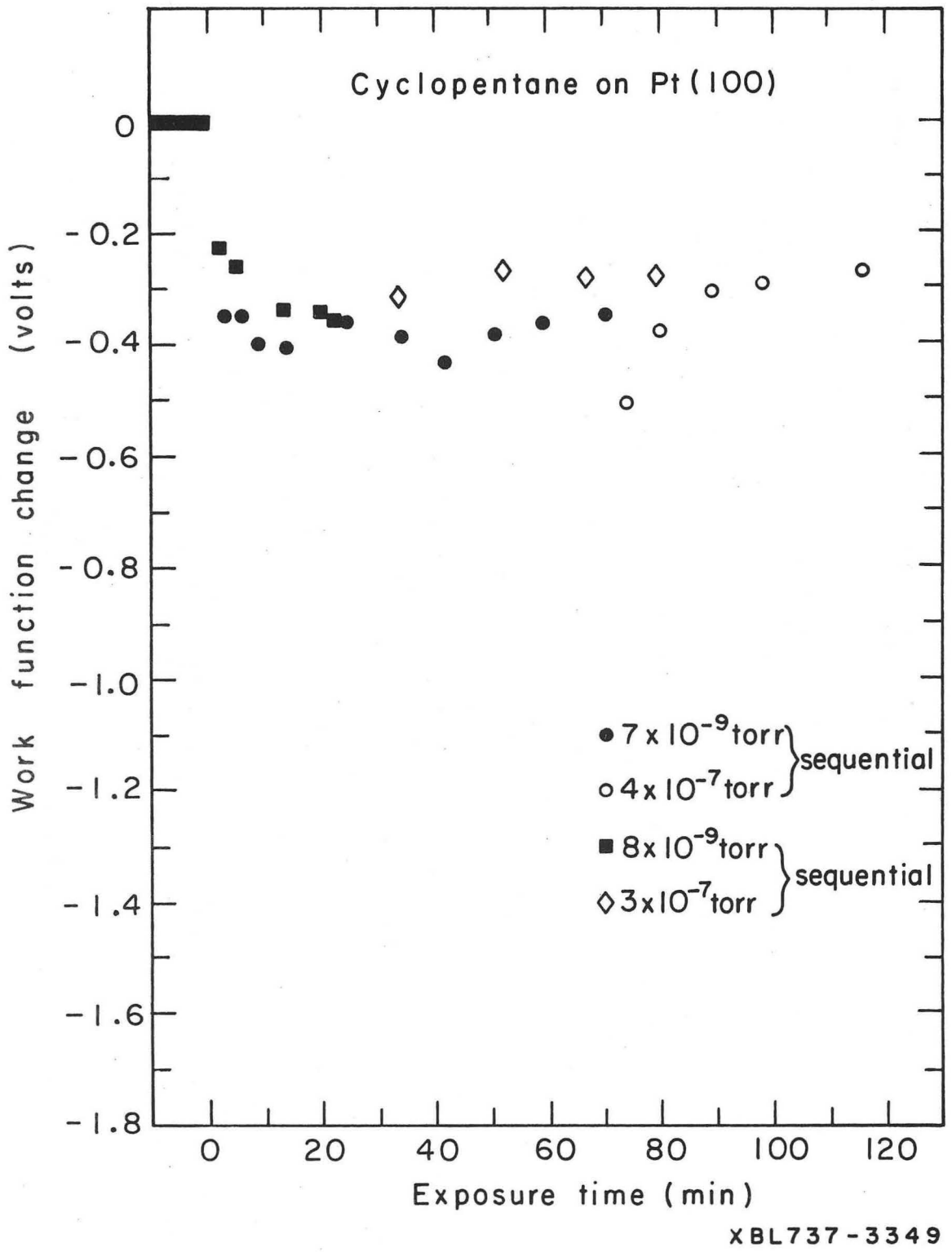

Fig. III-41. The work function change on adsorption of cyclopentane on the Pt(100)-(5×1) surface at 20°C. The indicated pressure should be multiplied by at least six to yield approximate surface pressures.

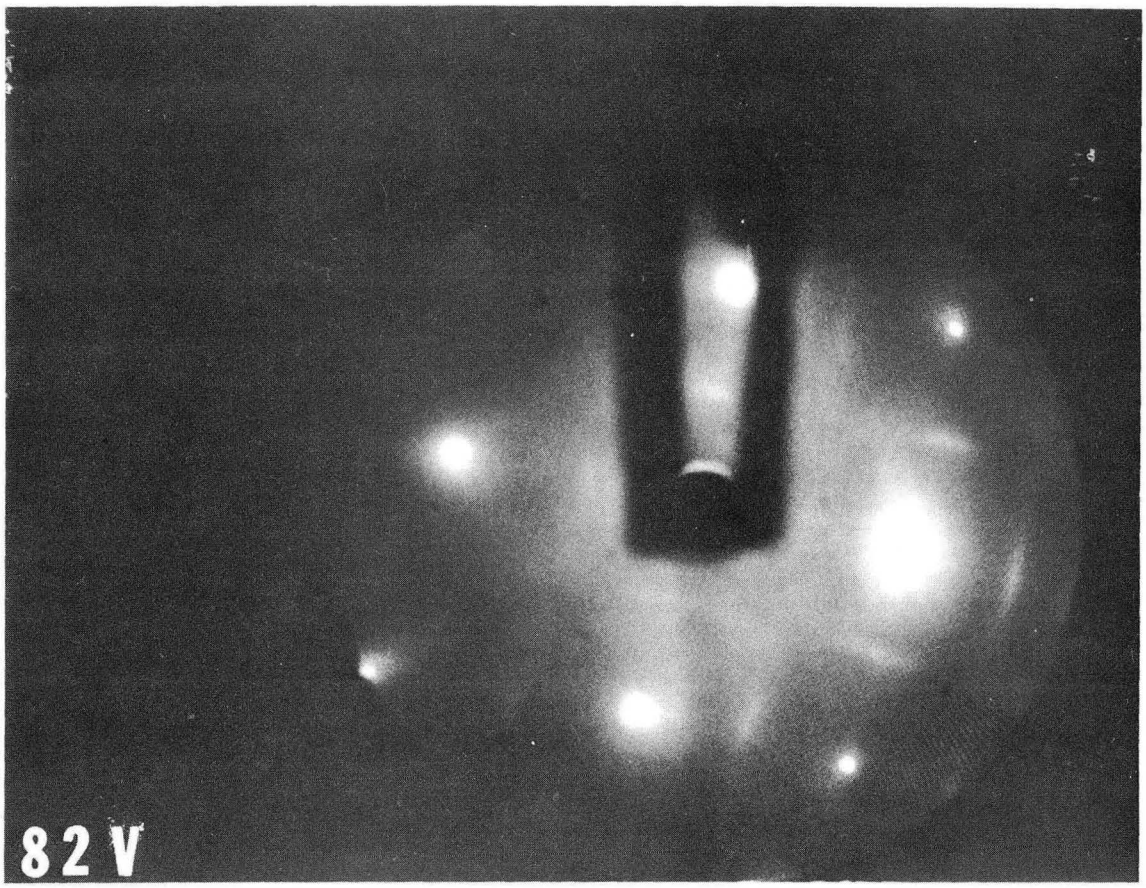

XBB 737-4296

Fig. III-42. The diffraction pattern resulting from an adsorbed layer of cyclopentane being heated to 150°C showing the first two sets of platinum diffraction features.

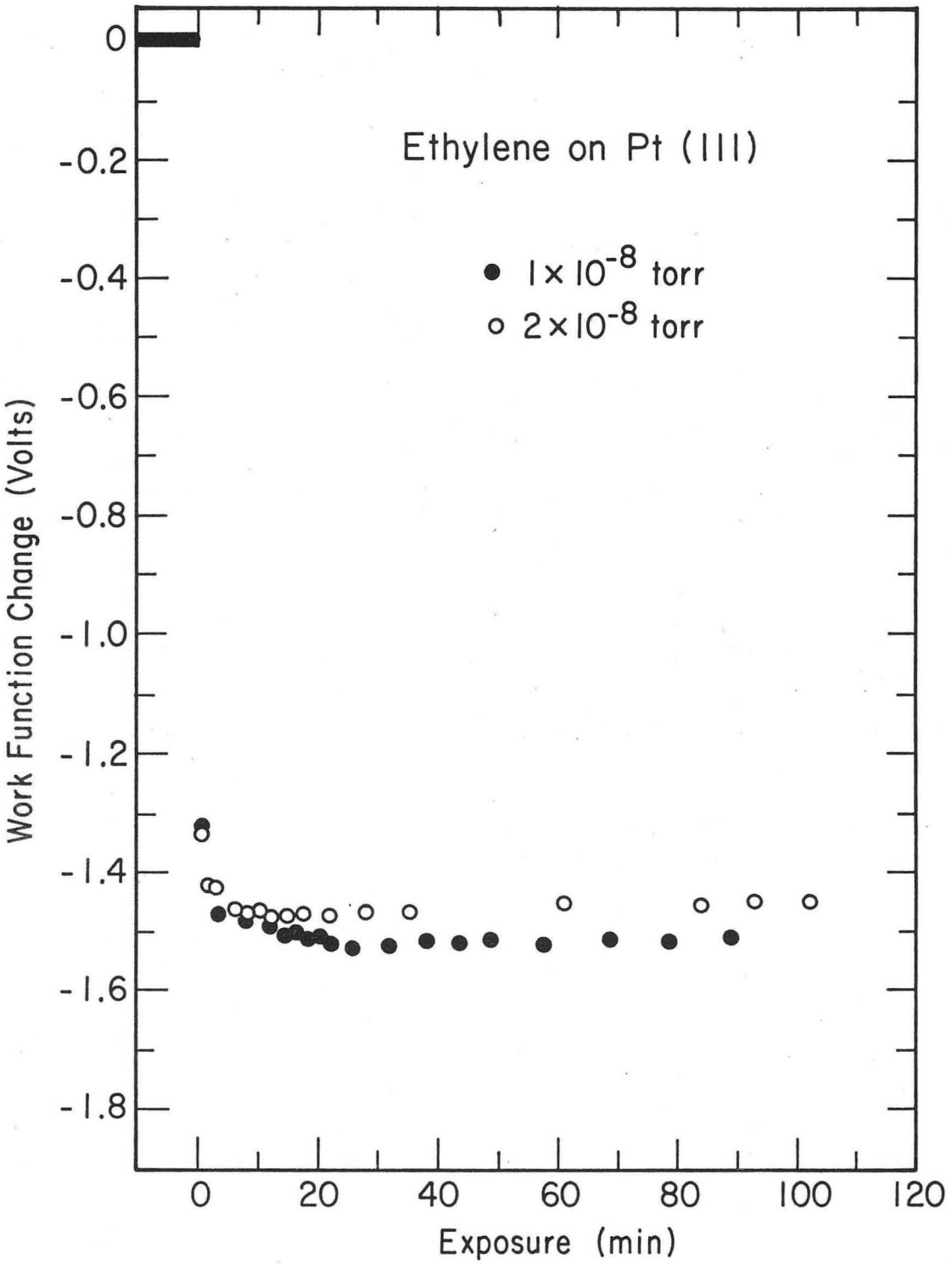

Fig. III-43. The work function change on adsorption of ethylene on the Pt(111) surface at 20°C. The indicated pressure should be multiplied by at least six to yield approximate surface pressures.

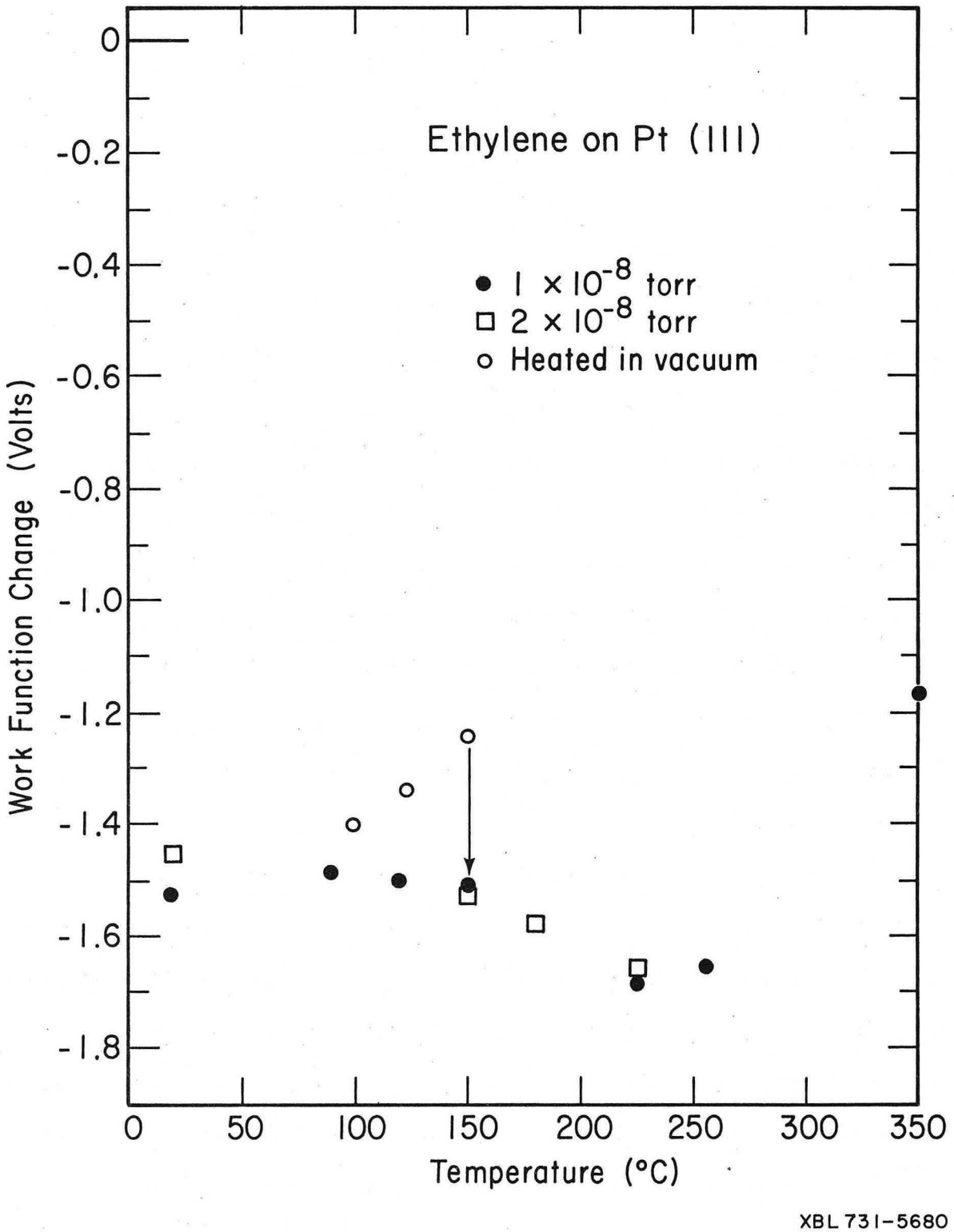

Fig. III-44. The work function change as a function of temperature for ethylene adsorbed on the Pt(111) surface. The indicated pressure should be multiplied by at least six to yield approximate surface pressures.

extra diffraction features become less intense with heating in flux. The extra features are gone with heating in flux to 200°C; subsequent stepwise heating to 350°C causes an increase in background intensity.

Ethlylene adsorbed on the Pt(100)-(5×1) surface causes the appearance of streaked diffraction features at half order. With time the extra features become better defined and the pattern becomes that expected of a $(\sqrt{2} \times \sqrt{2})R45°$ surface structure. The diffraction pattern resulting from the (5×1) surface structure disappears during this ordering process. The WFC on adsorption is -1.2 V as shown in Fig. III-45. With heating in flux the WFC goes through a minimum value of -1.5 V at 250°C as shown in Fig. III-46. With heating in vacuum the work function decreases (Fig. III-46). The C(2×2) diffraction features disappear with heating to 200°C in flux and subsequent step wise heat treatment to 350°C increases the background intensity.

n-Hexane adsorption

The adsorption of n-hexane on the Pt(111) surface causes the formation of a disordered adsorbed layer. The WFC on adsorption is -1.1 V with initial adsorption at a recorded pressure of 5×10^{-8} Torr (Fig. III-47). With continued exposure to organic vapor flux the magnitude of the WFC decreases to -.9 V (5 hours at a recorded pressure of 5×10^{-8}). With heating by steps in flux to 250°C the WFC becomes -1.5 V; however, the adsorbed layer remains disordered.

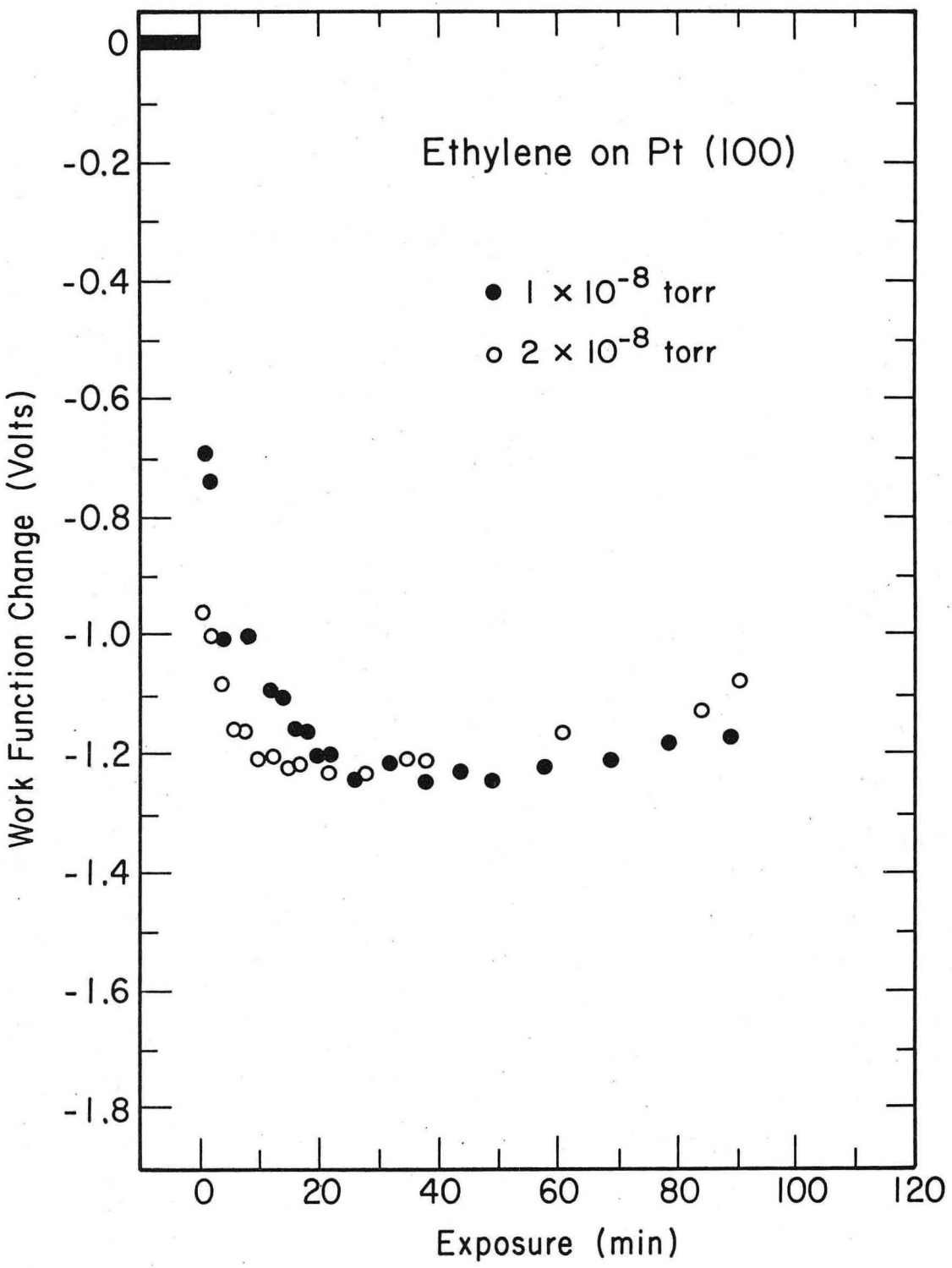

XBL731-5674

Fig. III-45. The work function change on adsorption of ethylene on the Pt(100)-(5×1) surface at 20°C. The indicated pressure should be multiplied by at least six to yield approximate surface pressures.

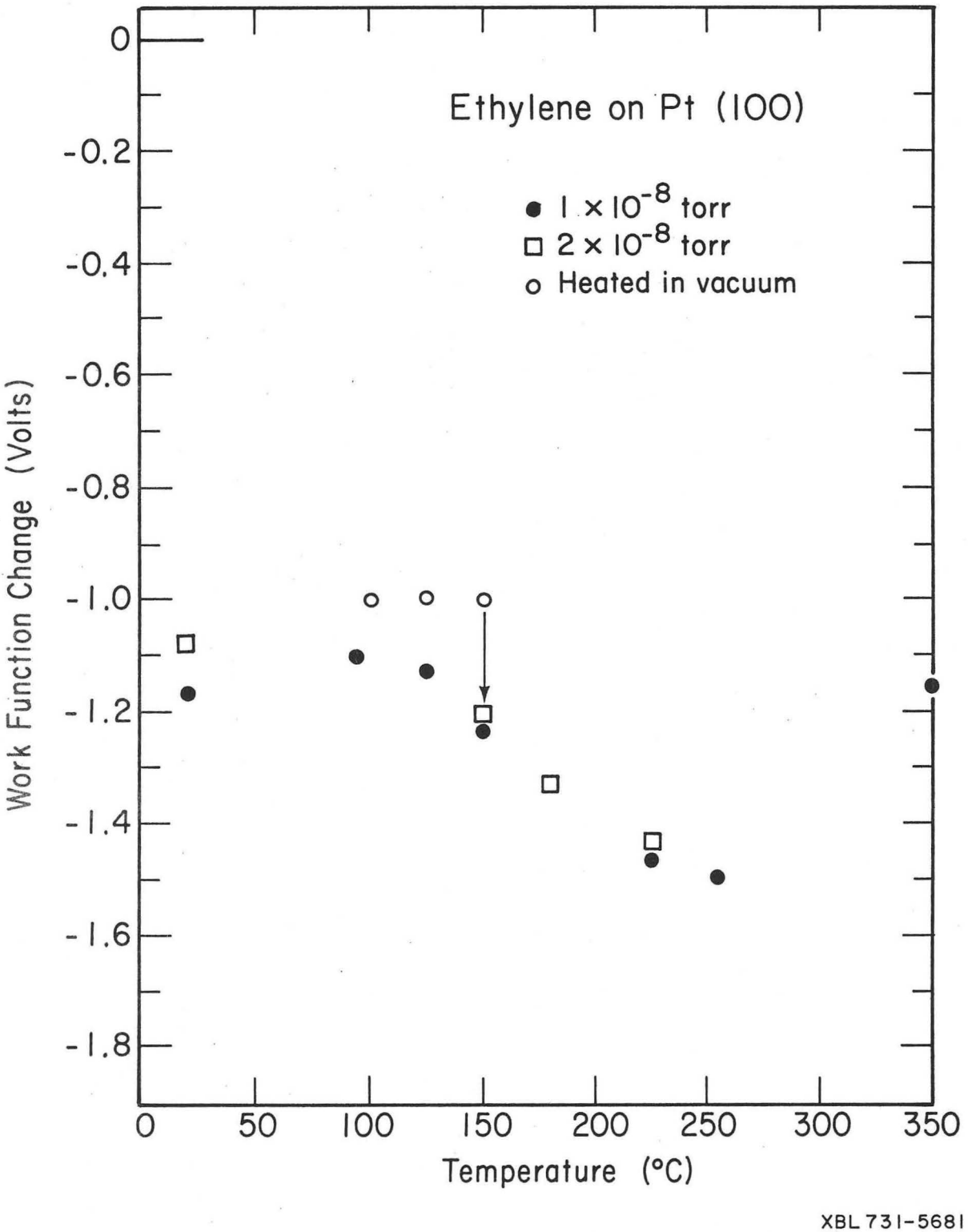

Fig. III-46. The work function change as a function of temperature for ethylene adsorption on the Pt(100)-(5×1) surface. The indicated pressure should be multiplied by at least six to yield approximate surface pressures.

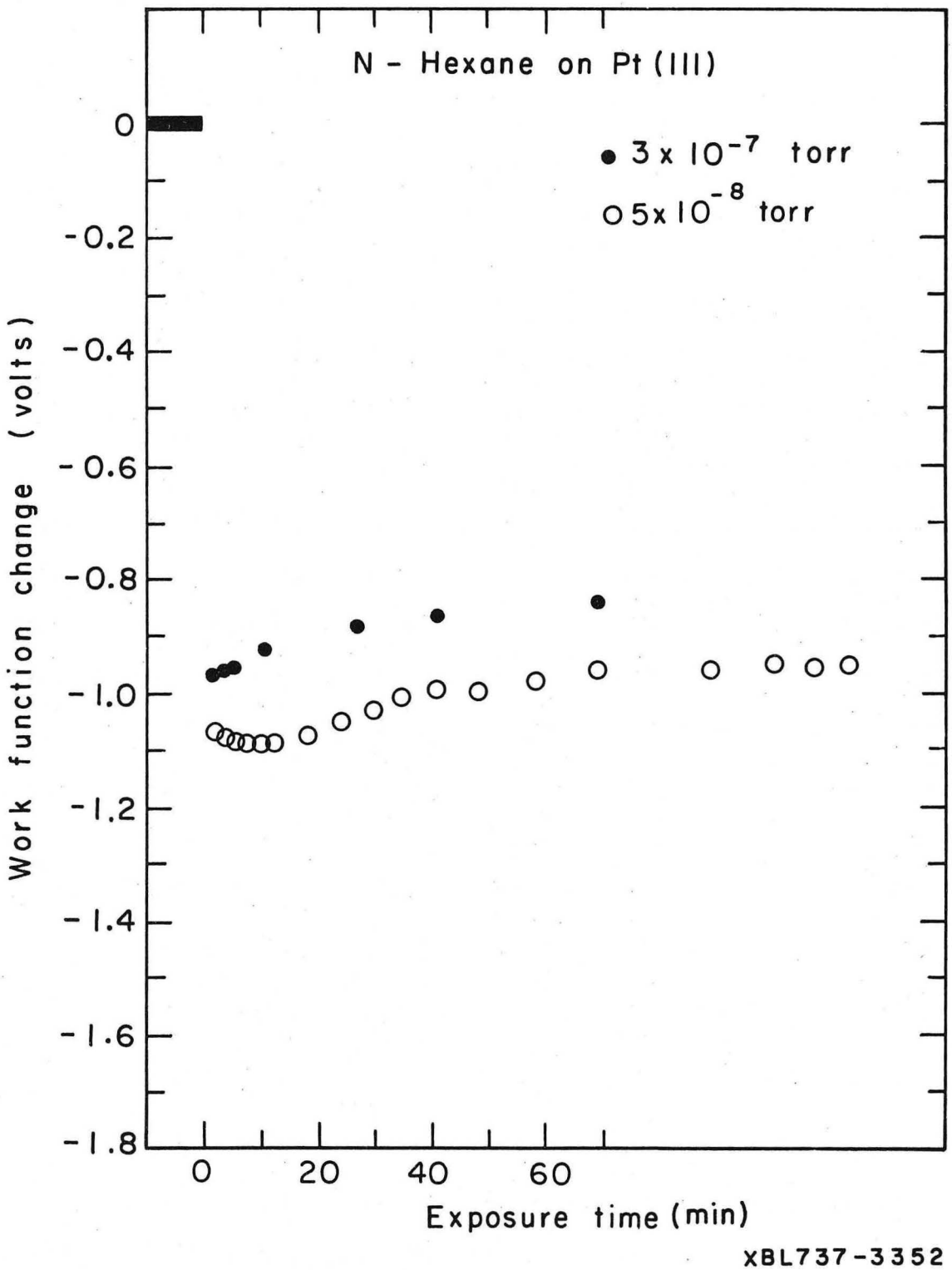

Fig. III-47. The work function change on adsorption of n-hexane on the Pt(111) surface at 20°C. The indicated pressure should be multiplied by at least six to yield approximate surface pressures.

Adsorption of n-hexane on the Pt(100)-(5×1) surface causes the slow disappearance of the (5×1) (70 minutes at a recorded pressure of 3×10^{-7}) surface structure and an increase in the background intensity. The WFC on initial adsorption at a recorded pressure of 5×10^{-8} is -.8 V as shown in Fig. III-48, with further exposure (5 hours) the magnitude of the WFC decreases to -.6 V. With stepwise heating to 250°C in flux the WFC becomes -1.2 V, however the adsorbed layer remains disordered.

Mesitylene adsorption

Mesitylene adsorbed on the Pt(111) surface causes the appearance of a streaked diffraction feature at 1/3.4 order and diffuse diffraction features centered at the (2/3.4 0) positions as shown in Fig. III-49. The WFC on adsorption is -1.7 V (Fig. III-50); however, the WFC and degree of order of the surface structure depend on the initial incident vapor flux. Adsorption at high initial fluxes ($\sim 4\times10^{-7}$ Torr recorded pressure) causes the formation of a disordered adsorbed layer and the magnitude of the WFC (-1.35 V) is smaller than the WFC observed during low pressure adsorption.

Heating above 150°C in flux causes the extra diffraction features to disappear. The magnitude of the WFC decreases with heating above 250°C, as shown in Fig. III-51.

Mesitylene adsorbed on the Pt(100)-(5×1) surface causes the appearance of streaked diffraction features at 1/3 order while the diffraction pattern resulting from the (5×1) surface structure remains

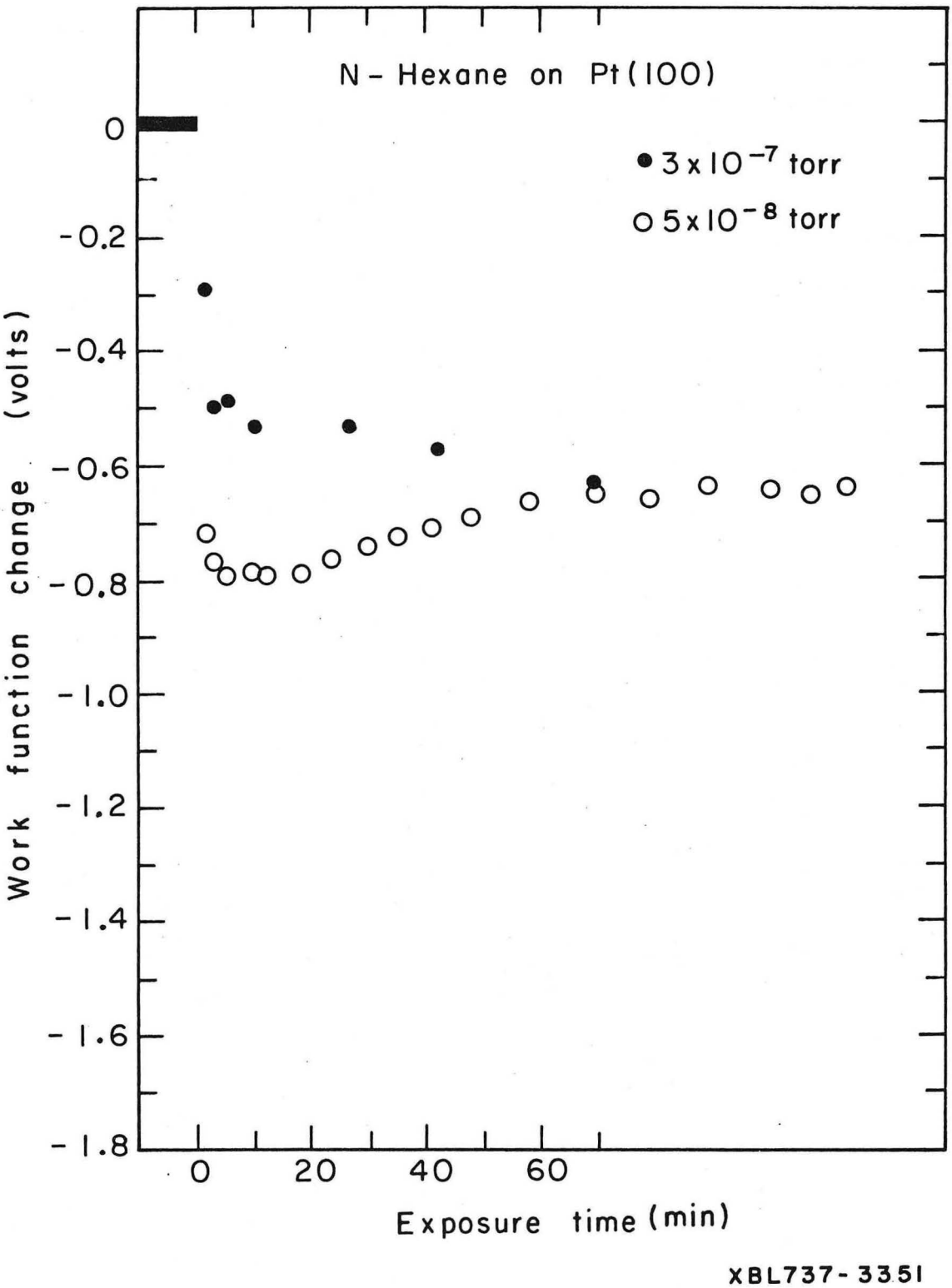

Fig. III-48. The work function change on adsorption of n-hexane on the Pt(100)-(5×1) surface at 20°C. The indicated pressure should be multiplied by at least six to yield approximate surface pressures.

Fig. III-49a. The diffraction pattern resulting from mesitylene adsorption on the Pt(111) surface at 20°C.

Fig. III-49b. The diffraction pattern resulting from mesitylene adsorption on the Pt(111) surface at 20°C showing the first order Pt diffraction features.

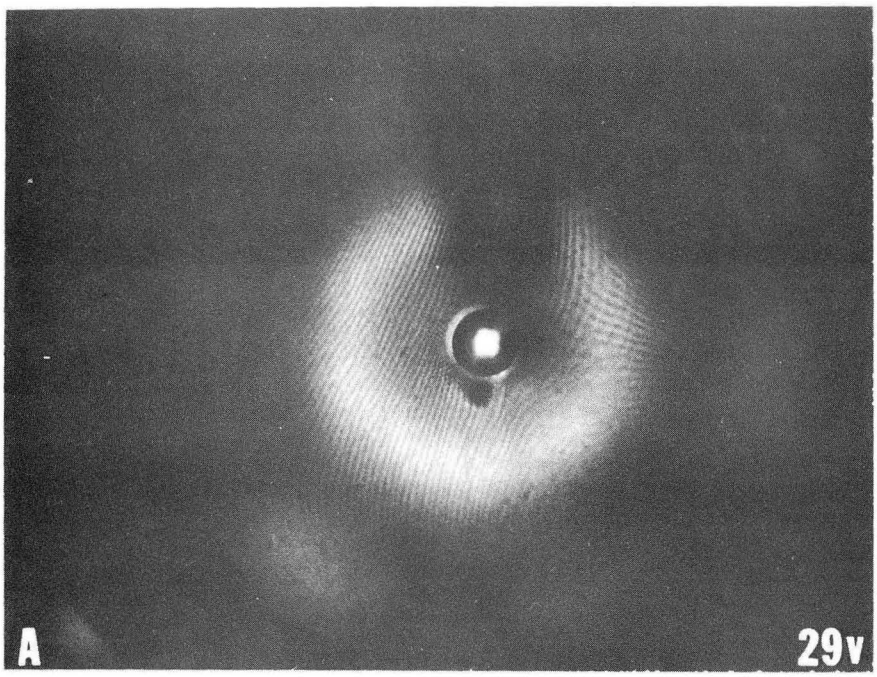

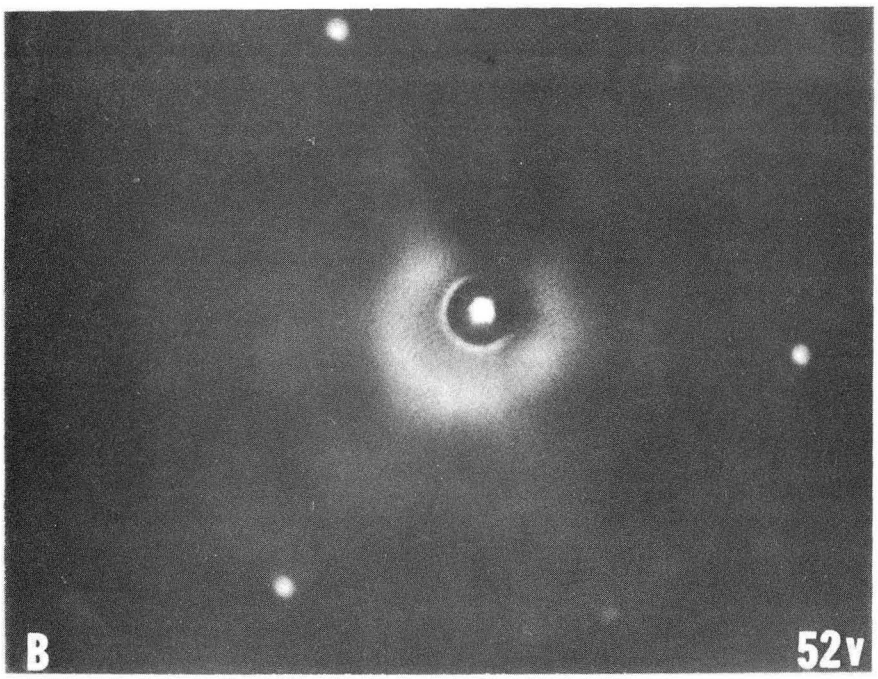

XBB 732-685

Fig. III-49 (a & b).

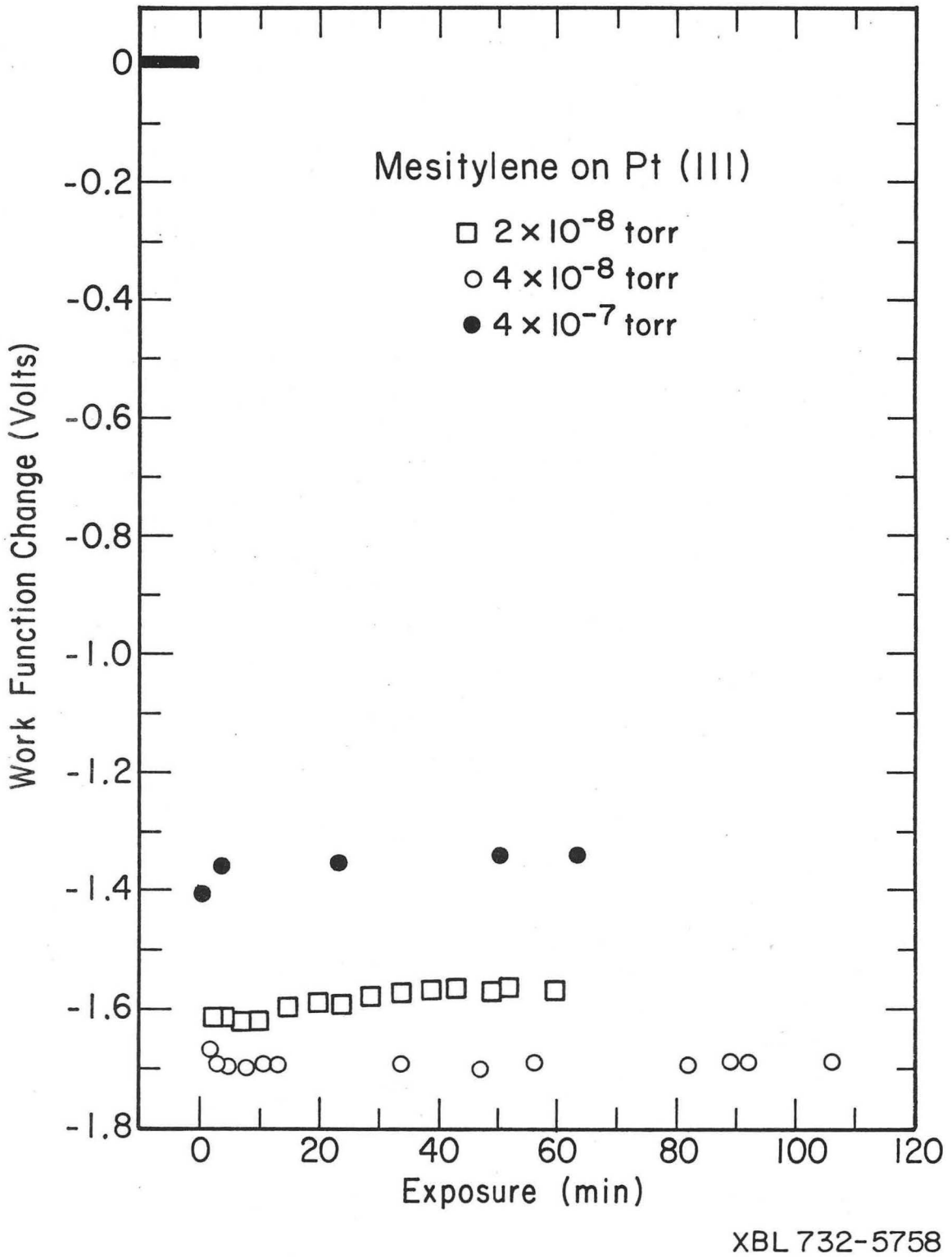

Fig. III-50. The work function change on adsorption of mesitylene on the Pt(111) surface at 20°C. The indicated pressure should be multiplied by at least six to yield approximate surface pressures.

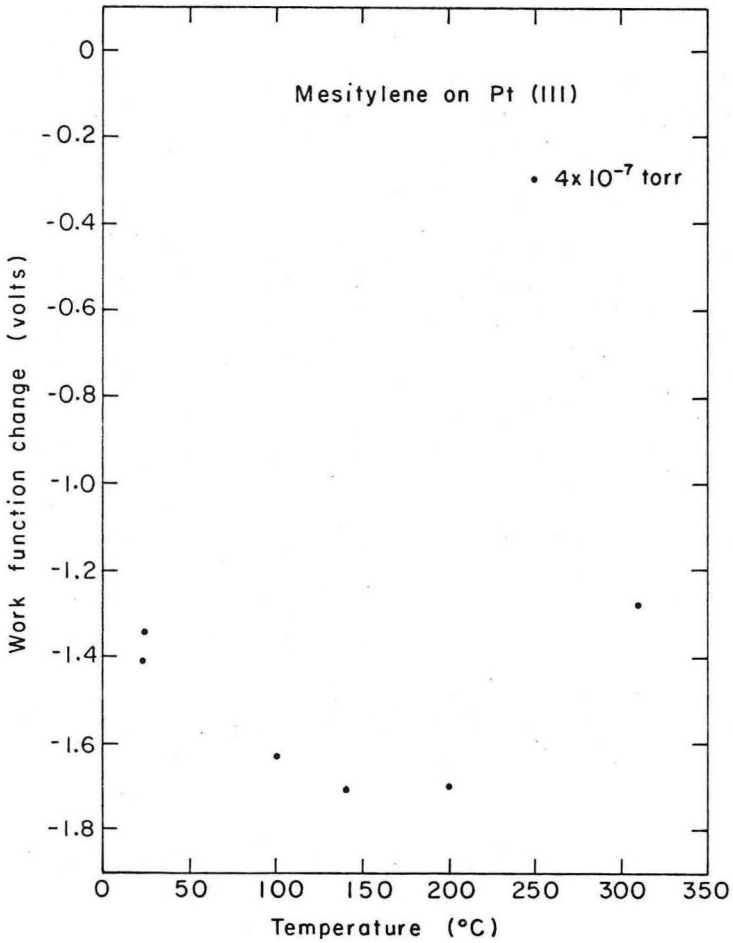

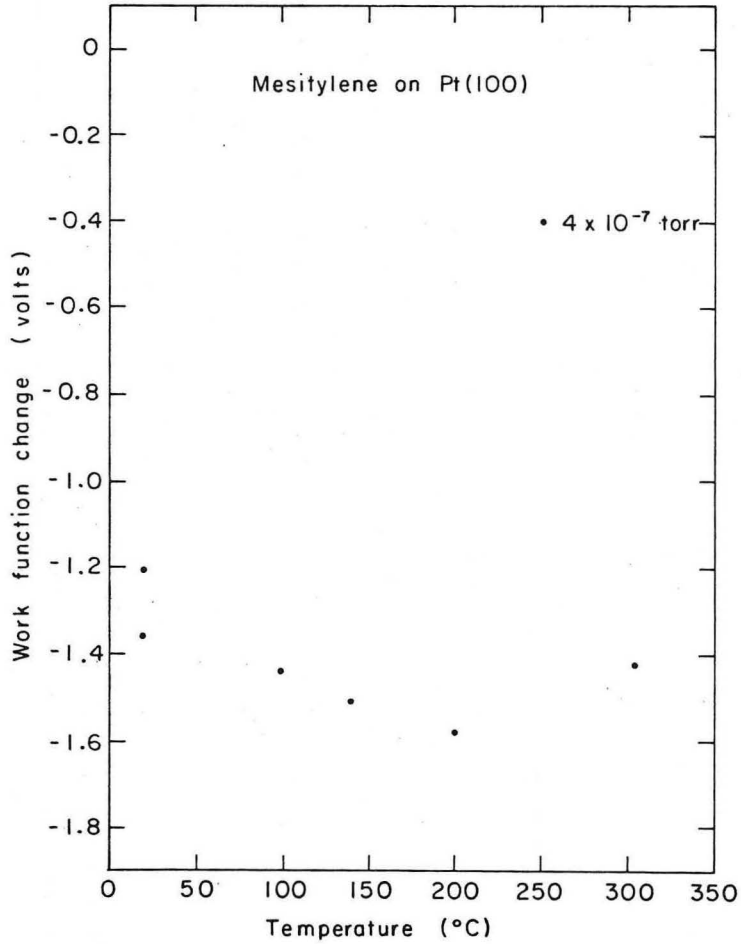

Fig. III-51. The work function change as a function of temperature for mesitylene adsorbed on the Pt(111) and Pt(100)-(5×1) surfaces. The indicated pressure should be multiplied by at least six to yield approximate surface pressures.

as shown in Fig. III-52. The (5×1) surface structure and streaked features are stable to exposures longer than 2 hours at a recorded pressure of 2×10^{-8} Torr. The WFC on adsorption is -1.5 V as shown in Fig. III-53. Adsorption at higher pressures (4×10^{-7}) causes the formation of a disordered adsorbed layer, the (5×1) surface structure disappears and the WFC (-1.2 V) is less than that observed with low pressure adsorption. Heating above 150°C in flux causes the extra diffraction features and the (5×1) structure to disappear. The magnitude of the WFC decreases with heating above 250°C as shown in Fig. III-51.

2-Methylnaphthalene adsorption

2-Methylnaphthalene adsorbed on the Pt(111) surface causes the formation of a poorly ordered adsorbed layer. On adsorption the background intensity increases markedly and diffuse low intensity high order streaked diffraction features appear. These diffuse extra features disappear with gentle heating to 100°C. The WFC on adsorption is approximately -2.0 V and depends on the initial incident flux as shown in Fig. III-54. With stepwise heating in flux above 100°C (done up to 400°C) the magnitude of the WFC decreases progressively with heating.

Adsorption of 2-methylnaphthalene on the Pt(100)-(5×1) surface causes an increase in the background intensity and a decrease in the intensity of the diffraction pattern caused by the (5×1) surface structure. The (5×1) structure disappears with heating of the surface to 100°C. The WFC on adsorption is approximately -1.6 V and depends

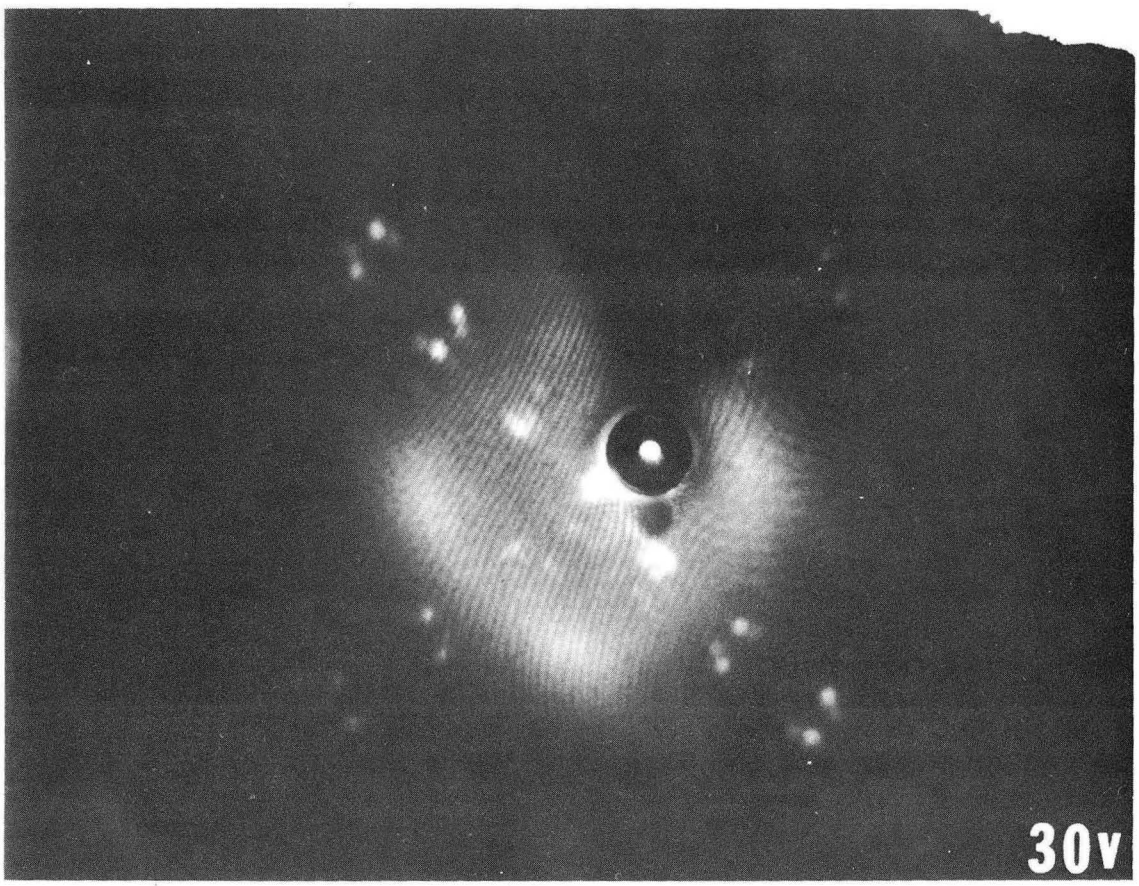

XBB 732-678

Fig. III-52. The diffraction pattern resulting from mesitylene adsorption at low pressure on the Pt(100)-(5×1) surface.

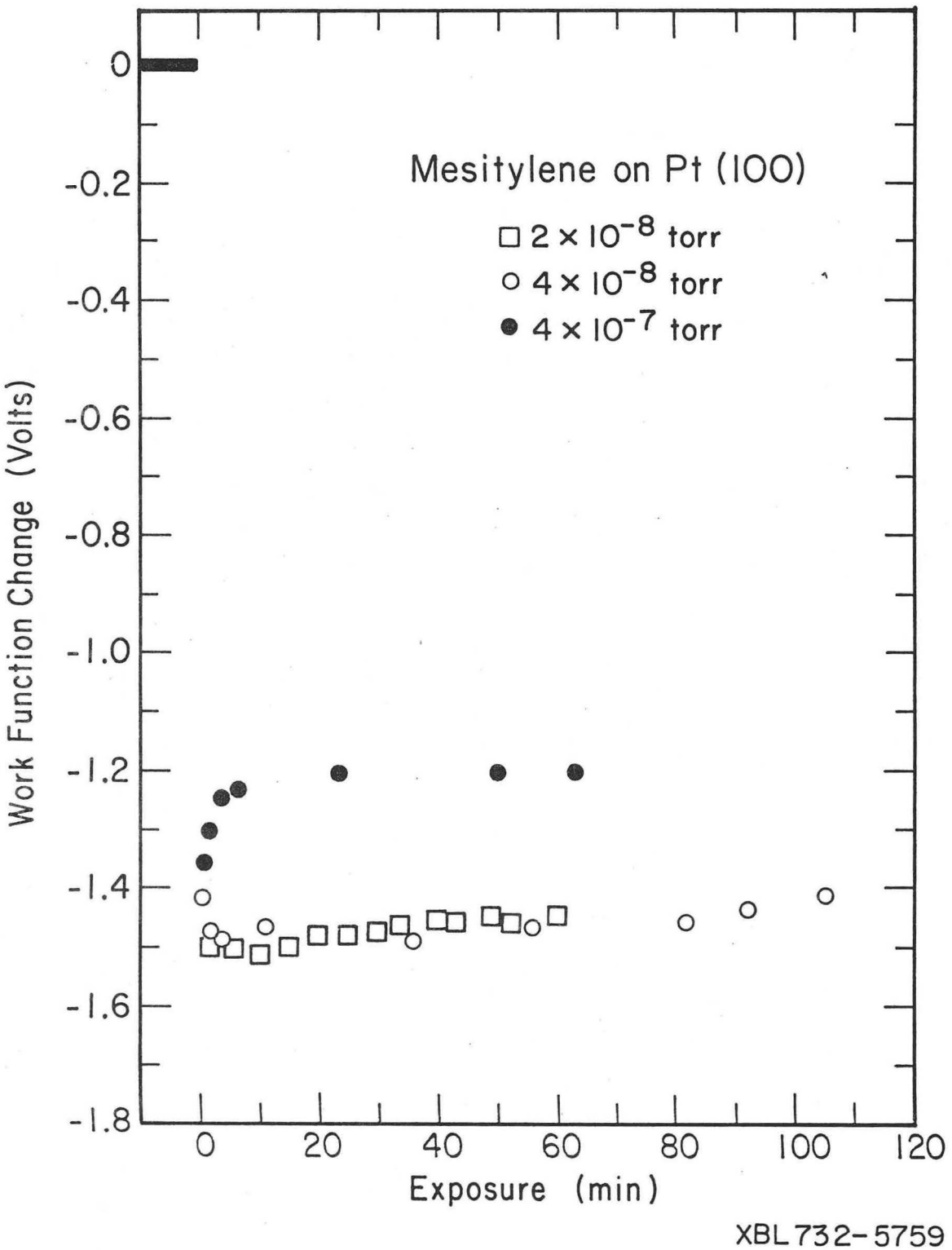

Fig. III-53. The work function change on adsorption of mesitylene on the Pt(100)-(5×1) surface at 20°C. The indicated pressure should be multiplied by at least six to yield approximate surface pressures.

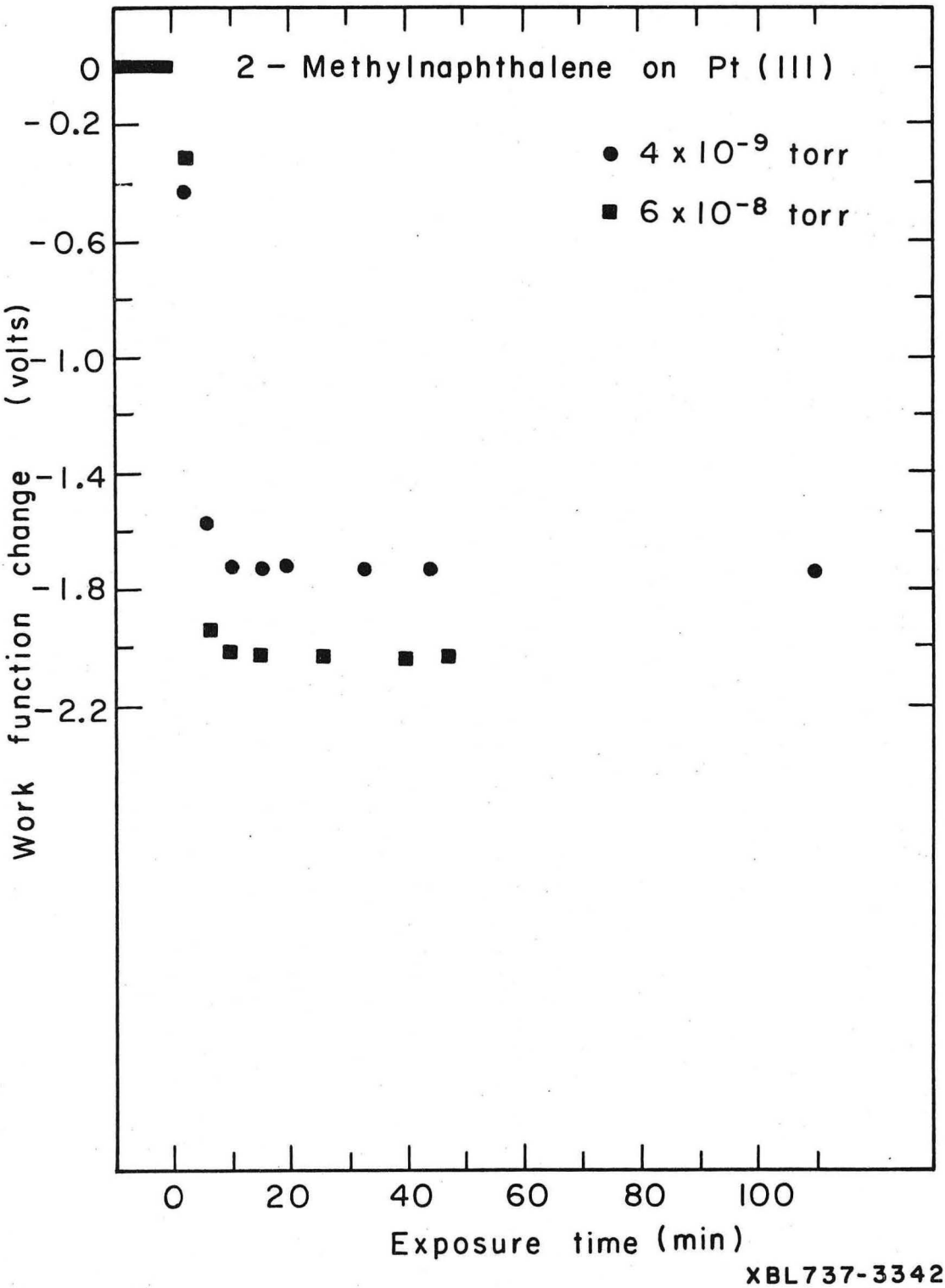

Fig. III-54. The work function change on adsorption of 2-methylnaphthalene on the Pt(111) surface at 20°C. The indicated pressure should be multiplied by at least six to yield approximate surface pressures.

on the initial incident flux as shown in Fig. III-55. With stepwise heating in flux above 100°C (done up to 400°C) the magnitude of the WFC decreases progressively with heating.

Naphthalene adsorption

Naphthalene adsorbed at 150°C forms a (6×6) structure as shown in Fig. III-56b. The WFC which accompanies this ordered adsorption is -2.0 V. The initial value of the WFC does not change with continued exposure. When adsorbed at room temperature naphthalene forms an apparent (3×1) surface structure with diffuse diffraction features as shown in Fig. 56a. With room temperature adsorption the degree of ordering and the work function change depend on the exposure rate. Large exposure rates (.4L/sec) lead to poor order and smaller WFC's on adsorption. With heating to 150°C in flux or in vacuum the diffraction pattern becomes that expected from a (6×6) surface structure (Fig. III-56b). With heat treatment the magnitude of the WFC increases slightly. Further heating (above 150°C) in flux or in vacuum causes the adsorbed layer to become disordered and the magnitude of the WFC to decrease as shown in Fig. 56.

Adsorption of naphthalene on the Pt(100)-(5×1) surface causes the rapid disappearance of the (5×1) surface structure and an increase in the background intensity. The WFC on adsorption is -1.75 V but is sensitive to the initial exposure rates as shown in Fig. III-57. The magnitude of the WFC remains constant with heating to 250°C and then begins to decrease as shown in Fig. III-58. With heating in flux or in vacuum the adsorbed layer remains disordered.

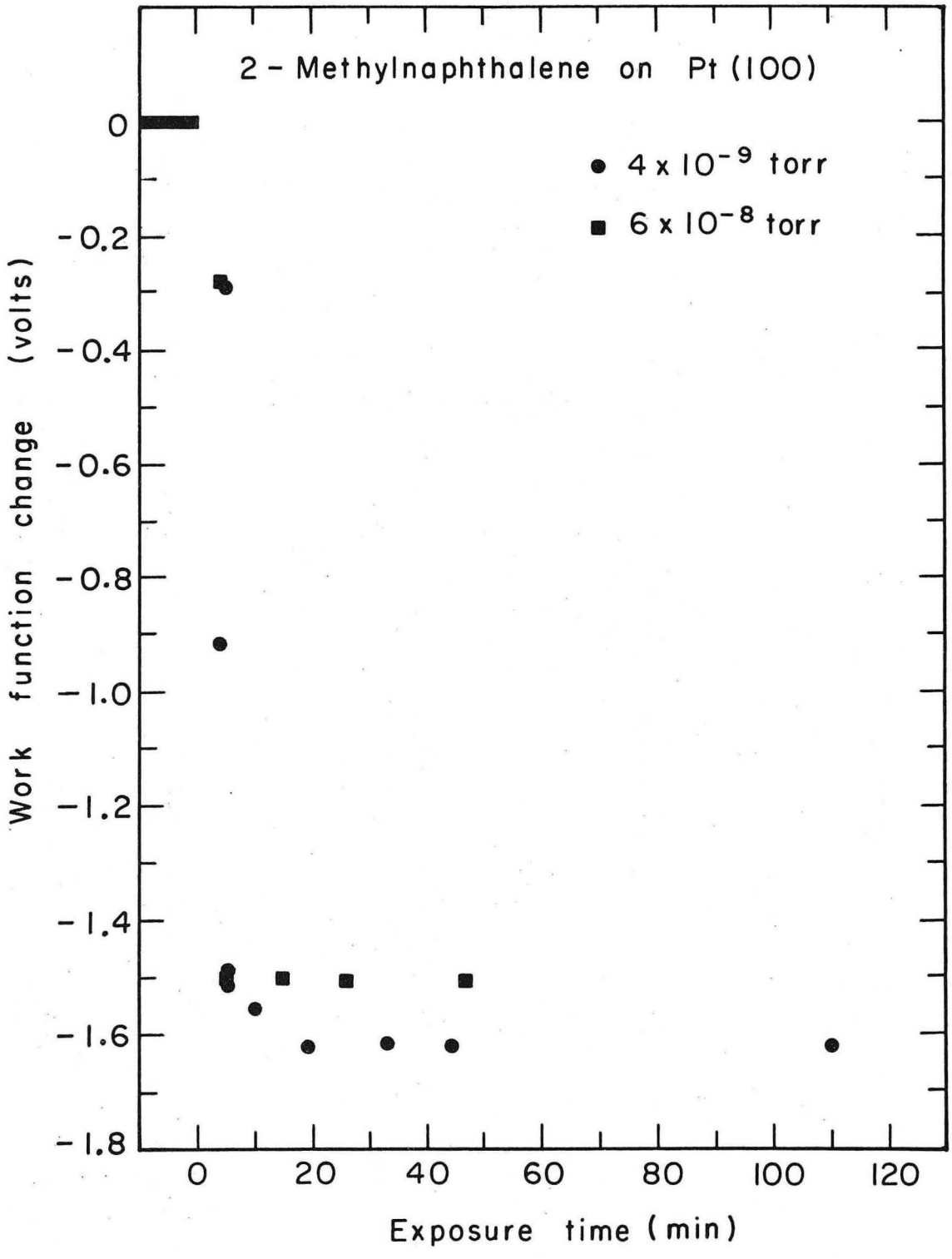

XBL737-3341

Fig. III-55. The work function change on adsorption of 2-methylnaphthalene on the Pt(100)-(5×1) surface at 20°C. The indicated pressure should be multiplied by at least six to yield approximate surface pressures.

Fig. III-56. The diffraction patterns and corresponding work function changes as a function of temperature resulting from adsorption of napthalene on the Pt(111) surface. The indicated pressure should be multiplied by at least six to yield approximate surface pressures.

Fig. III-56a. The diffraction pattern resulting from naphthalene adsorption at 20°C on the Pt(111) surface showing the first order Pt diffraction features.

Fig. III-56b. The diffraction pattern resulting from heating an adsorbed naphthalene layer to 150°C or by adsorption at 150°C on the Pt(111) surface. The first order Pt diffraction features are visible.

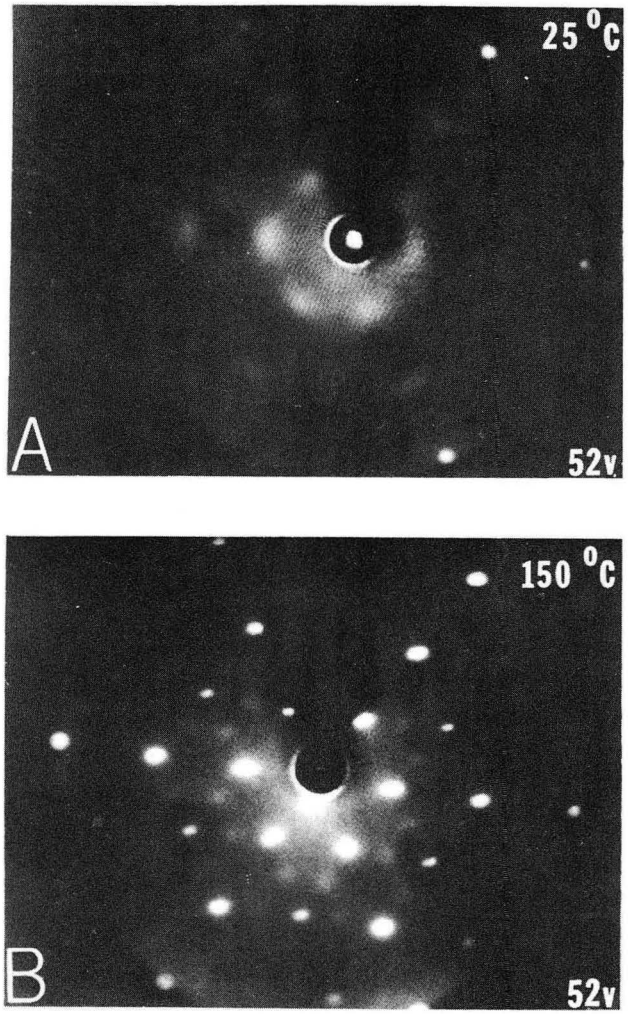

XBB 732-605

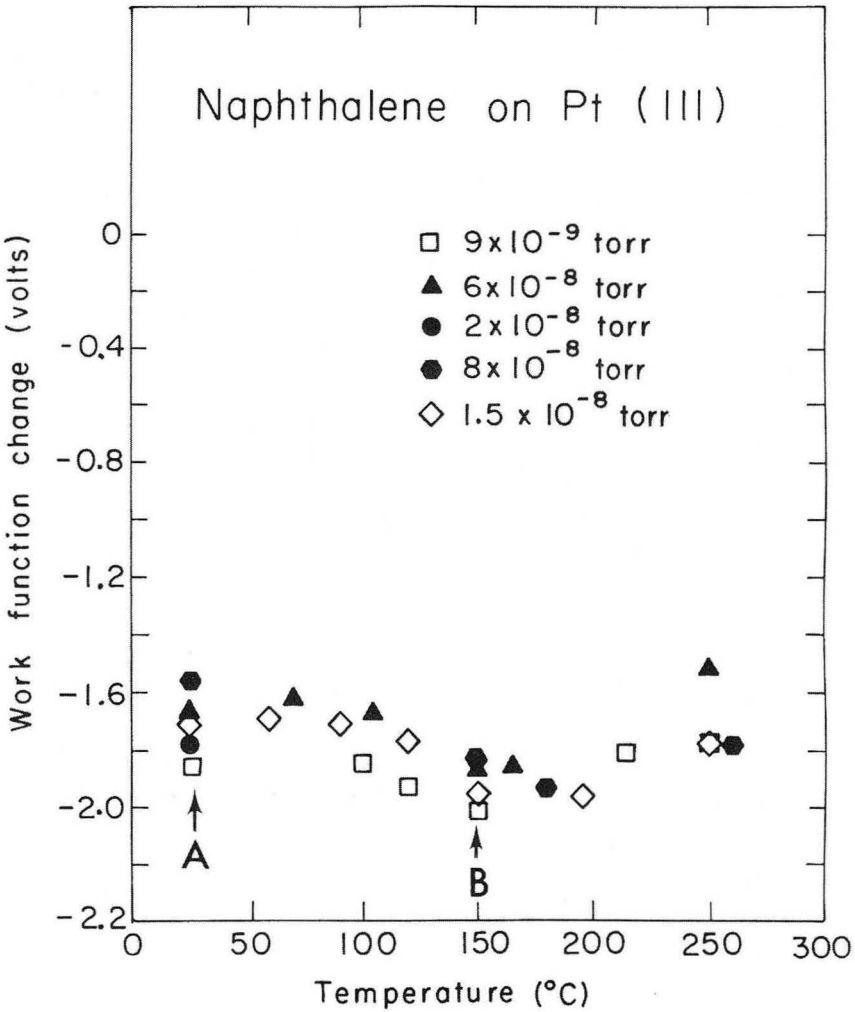

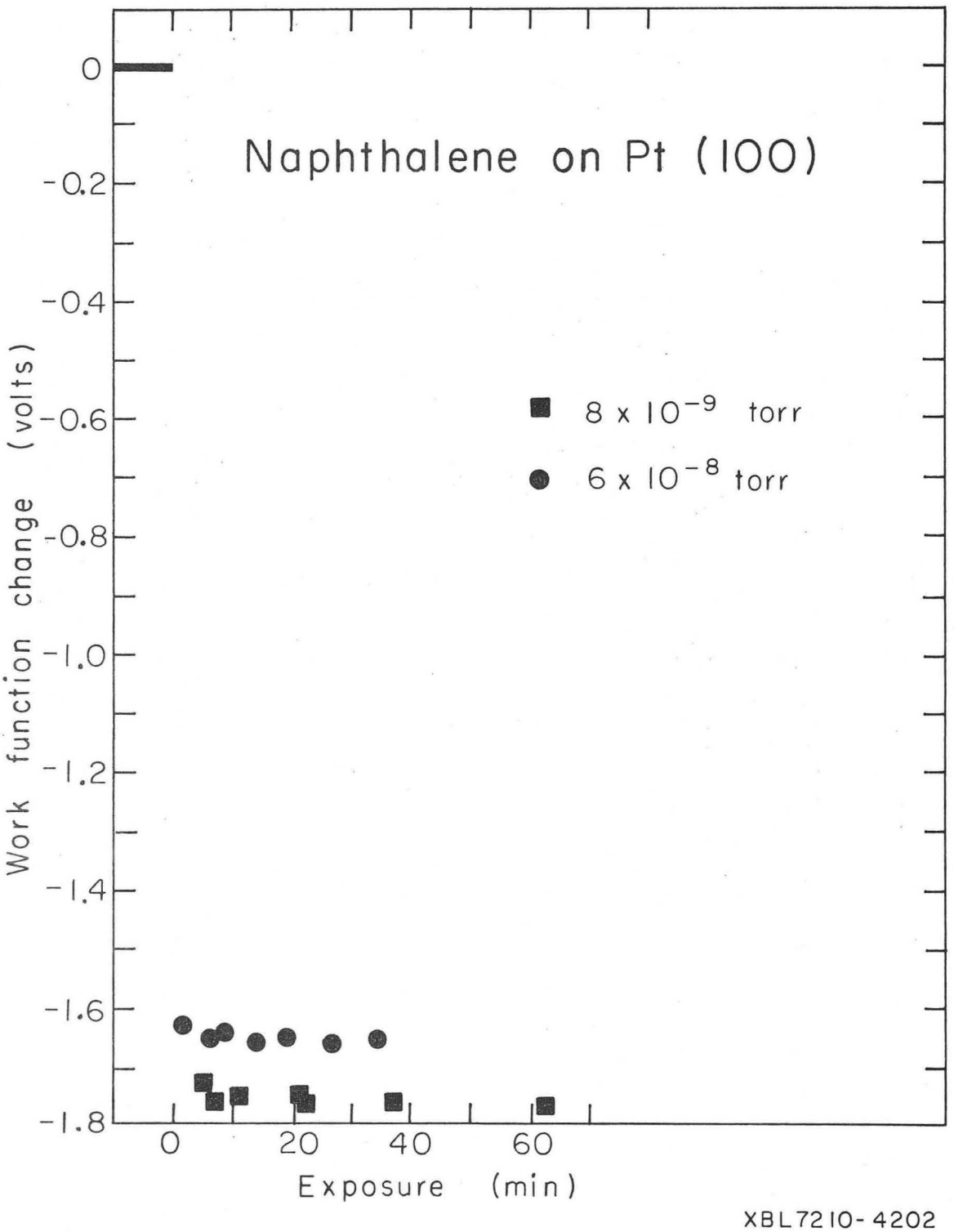

Fig. III-57. The work function change on adsorption of napthalene on the Pt(100)-(5×1) surface at 20°C. The indicated pressure should be multiplied by at least six to yield approximate surface pressures.

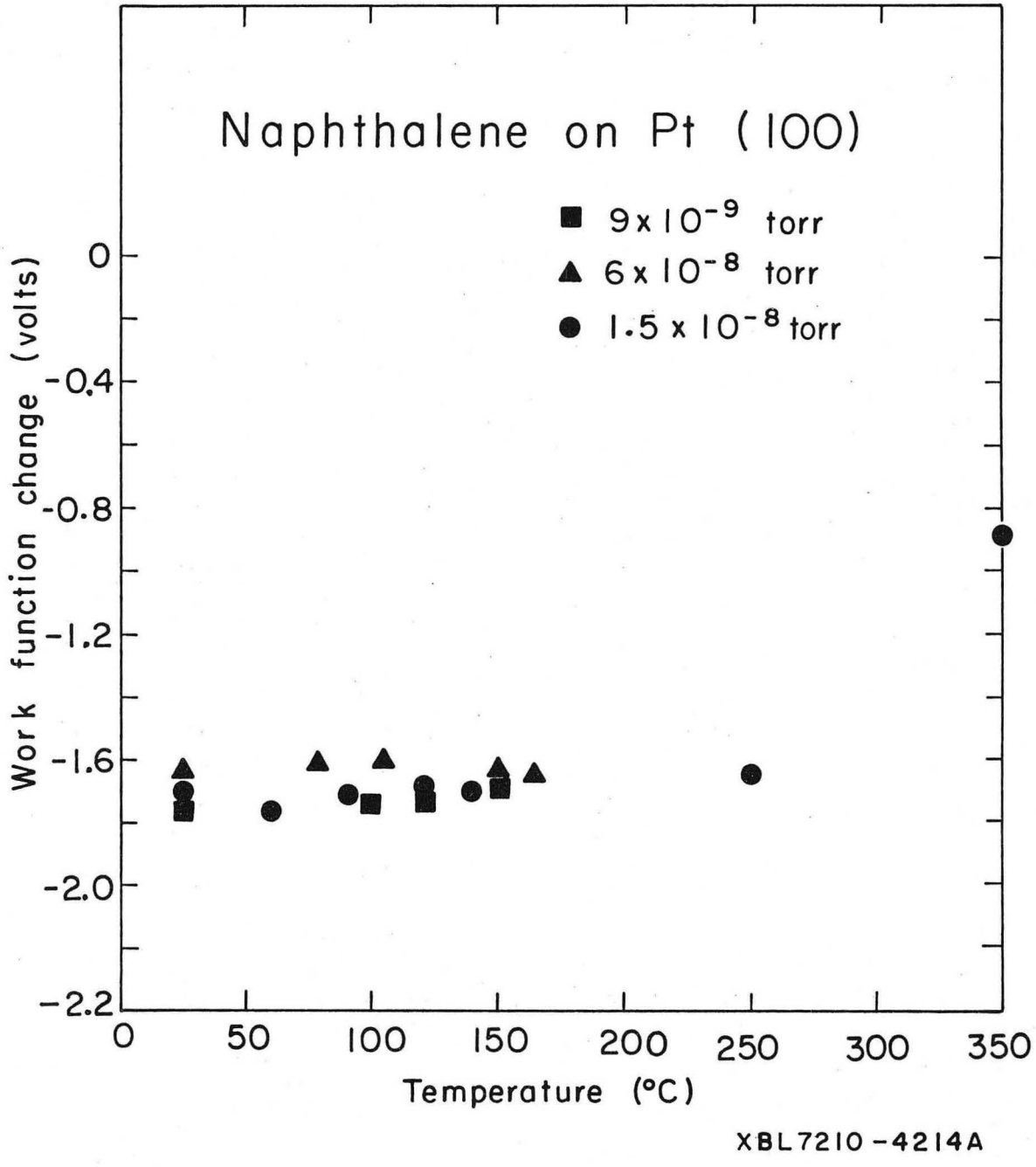

Fig. III-58. The work function change as a function of temperature for naphthalene adsorbed on the Pt(100)-(5×1) surface. The indicated pressure should be multiplied by at least six to yield approximate surface pressures.

Nitrobenzene adsorption

Adsorption of nitrobenzene on the Pt(111) surface causes the formation of diffraction features at (1/3 0) order (Fig. III-59). The WFC on adsorption is approximately -1.5 V (Fig. III-60); however, the degree of ordering and the WFC depend on the total amount of electron bombardment which has occurred. The initially ordered layer becomes disordered during approximately 7 minutes of exposure to a 30 V electron beam at 2×10^{-6} amps.

With stepwise heating in flux through 250°C the diffraction pattern remains largely disordered. (In the temperature range 80°C to 100°C very faint diffuse features appear near the (1/2 0) positions). The WFC remains essentially constant with stepwise heating in vacuum or in flux until 150°C as shown in Fig. III-61. Above 150°C the magnitude of the WFC decreases with increasing temperature.

Nitrobenzene adsorbed on the Pt(100)-(5×1) surface causes the (5×1) diffraction features to disappear and very faint high order features to appear for a short time. The WFC on adsorption is -1.4 V (Fig. III-62).

With stepwise heating in vacuum or in flux to 250°C the adsorbed layer remains disordered. The WFC on heating in flux reamins constant until 150°C; above 150°C the magnitude of the WFC decreases with increasing temperature as shown in Fig. III-61. With heating in vacuum the magnitude of the WFC decreases with heating above 90°C.

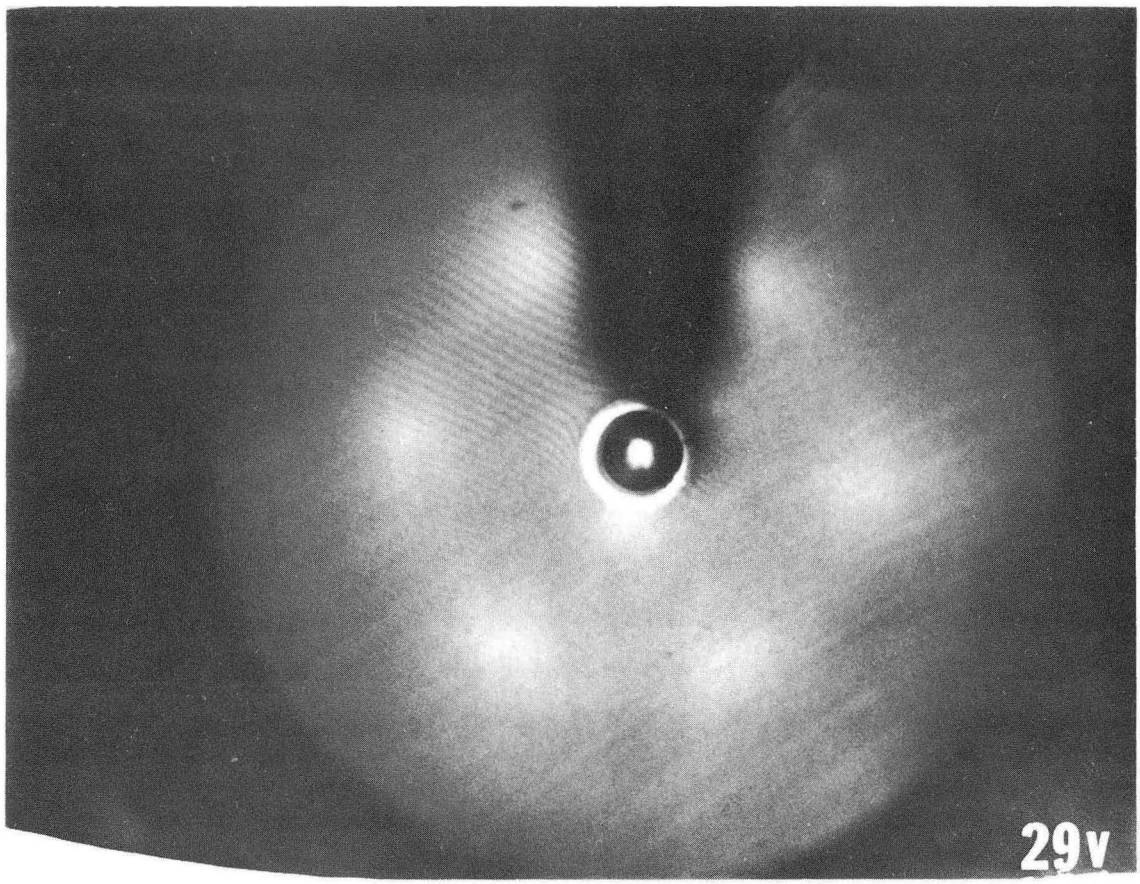

XBB 732-674

Fig. III-59. The diffraction pattern resulting from adsorption of nitrobenzene on the Pt(111) surface at 20°C.

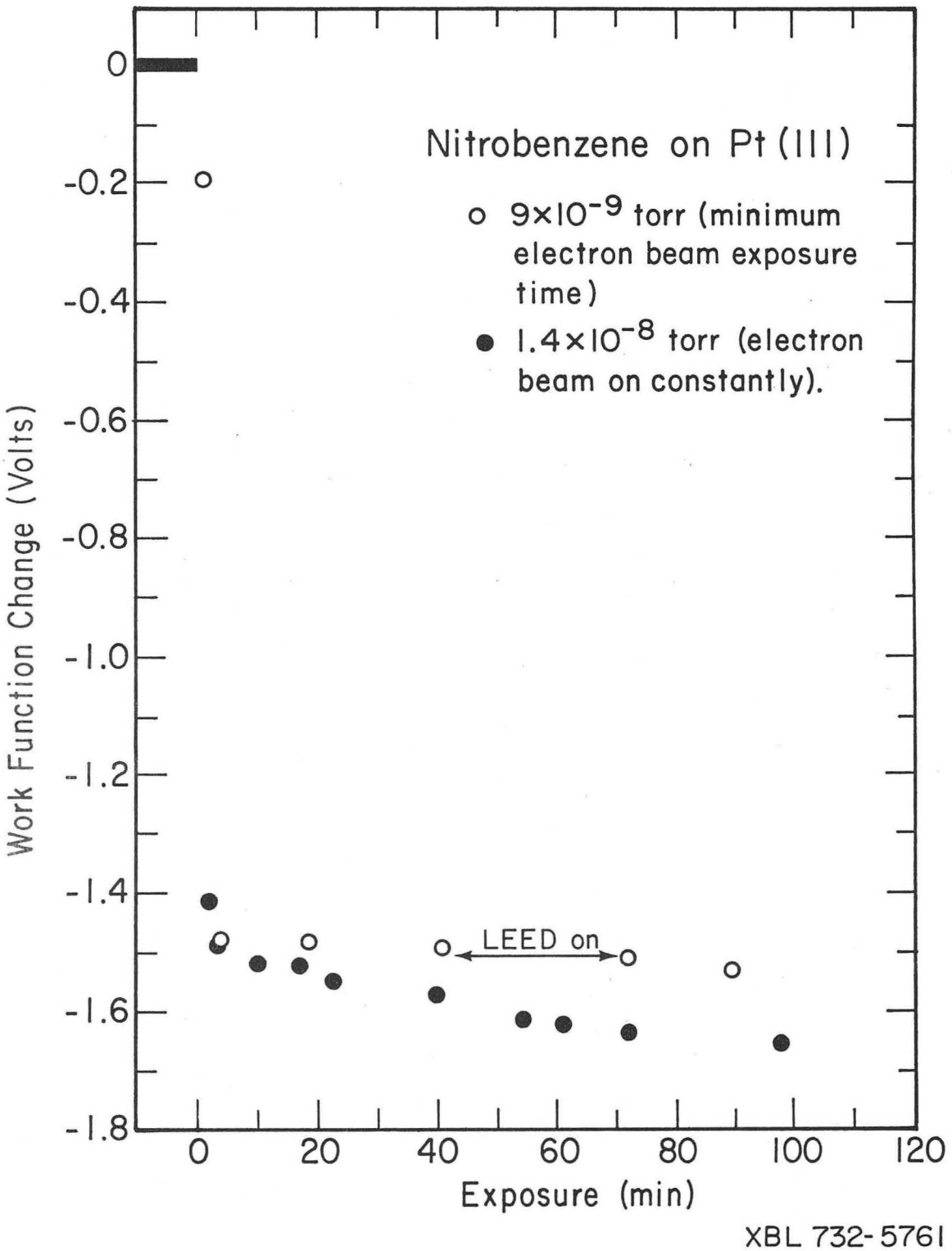

Fig. III-60. The work function change on adsorption of nitrobenzene on the Pt(111) surface at 20°C. The indicated pressure should be multiplied by at least six to yield approximate surface pressures.

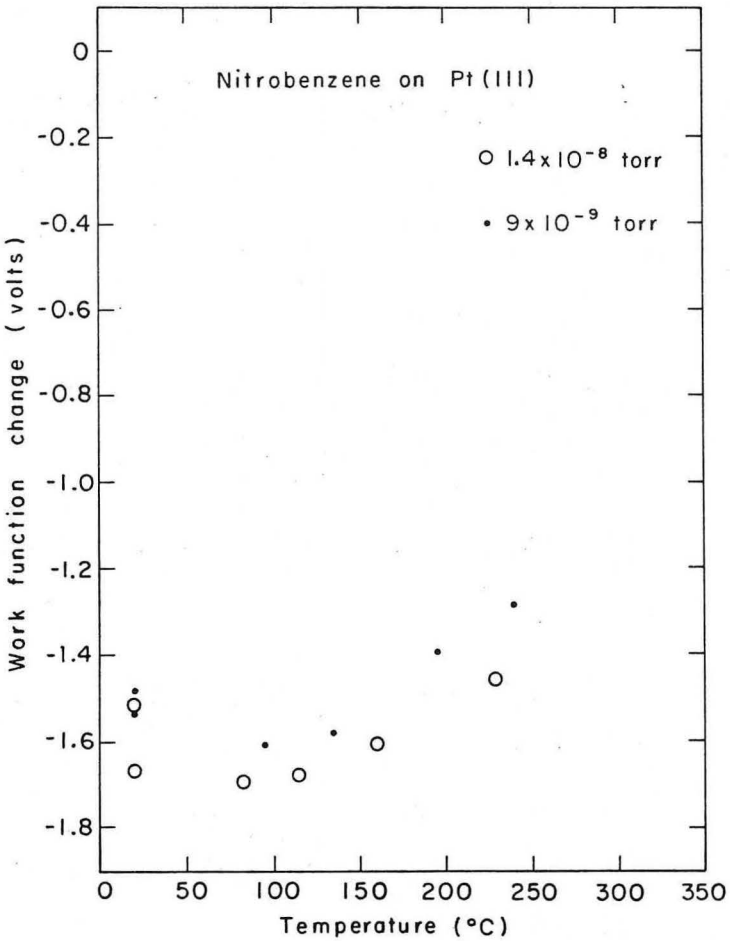

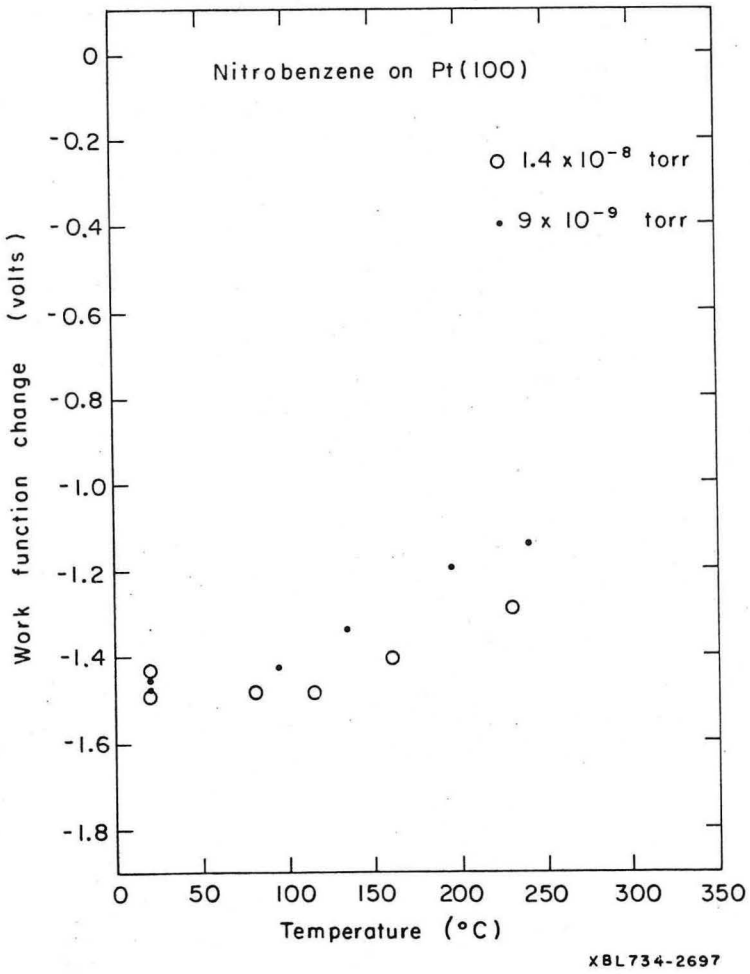

Fig. III-61. The work function change as a function temperature for nitrobenzene adsorbed on the Pt(111) and Pt(100)-(5×1) surfaces. The indicated pressure should be multiplied by at least six to yield approximate surface pressures.

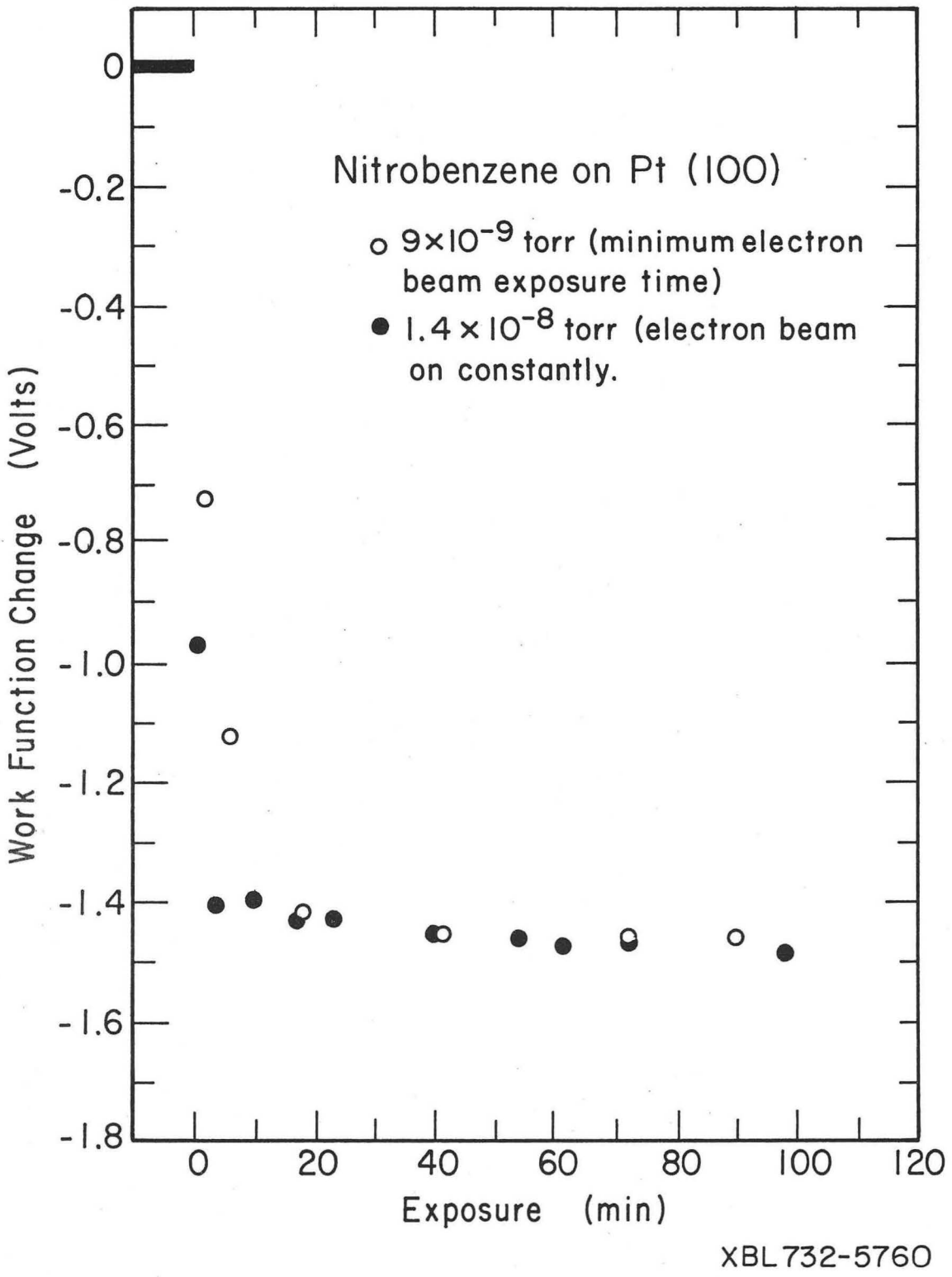

Fig. III-62. The work function change on adsorption of nitrobenzene on the Pt(100)-(5×1) surface at 20°C.

Propylene adsorption

Prolylene adsorption on the Pt(111) surface causes the appearance of a (2×2) surface structure as shown in Fig. III-63. The (2×2) structure becomes disordered with prolonged exposure (3 hours) to the electron beam or by standing for extended time periods (8 hours). The WFC on adsorption is -1.3 V as shown in Fig. III-64. The WFC does not appear to depend on the degree of ordering of the overlayer.

Propylene adsorbed on the Pt(100)-(5×1) surface causes the slow disappearance of the (5×1) structure (1 hour at 6×10^{-9} Torr recorded pressure). The diffraction pattern after relaxation of the (5×1) surface structure contains diffuse 1/2 order streaks. The WFC on adsorption is -1.2 V as shown in Fig. III-65. The WFC does not depend on the degree of ordering of the adsorbed overlayer.

Pyridine adsorption

Pyridine adsorbed on the Pt(111) surface produces diffuse diffraction features centered at the (1/2 0) positions as shown in Fig. III-66. The WFC on adsorption is -2.7 V (Fig. III-67); however both the WFC and the degree of ordering are sensitive to initial exposure rates. With lower pyridine fluxes the adsorbed layer is more ordered and the magnitude of the WFC is larger.

By heating the adsorbed layer to 250° a new surface structure is formed. The diffraction pattern corresponds to an overlayer with one-dimensional order and a spacing three times the size of the underlying lattice. This pattern is shown in Fig. III-66. Accompanying this change in structure is a decrease in the magnitude of the WFC

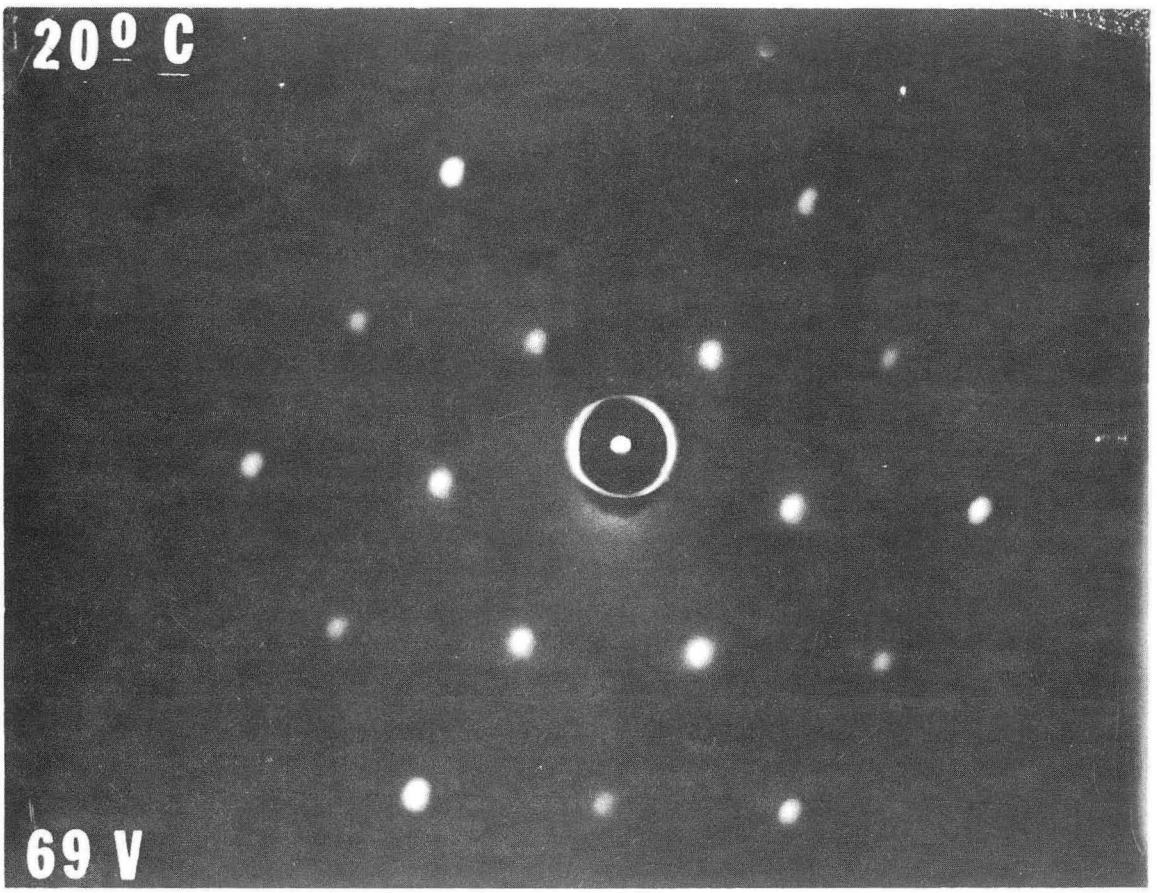

XBB 737-4295

Fig. III-63. The diffraction pattern resulting from propylene adsorption on the Pt(111) surface at 20°C showing the first order Pt diffraction features.

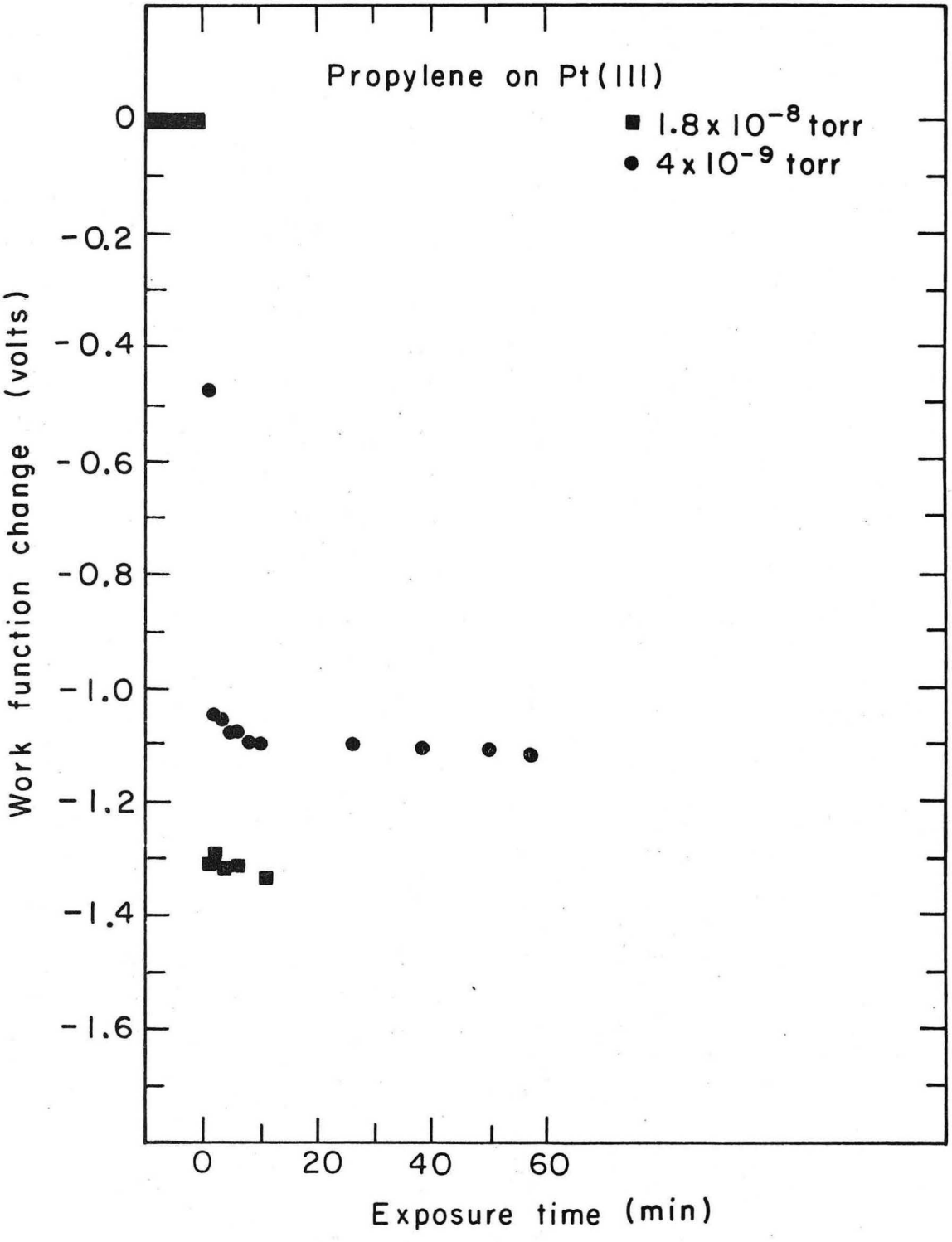

XBL737-3354

Fig. III-64. The work function change on adsorption of propylene on the Pt(111) surface at 20°C. The indicated pressure should be multiplied by at least six to yield approximate surface pressures.

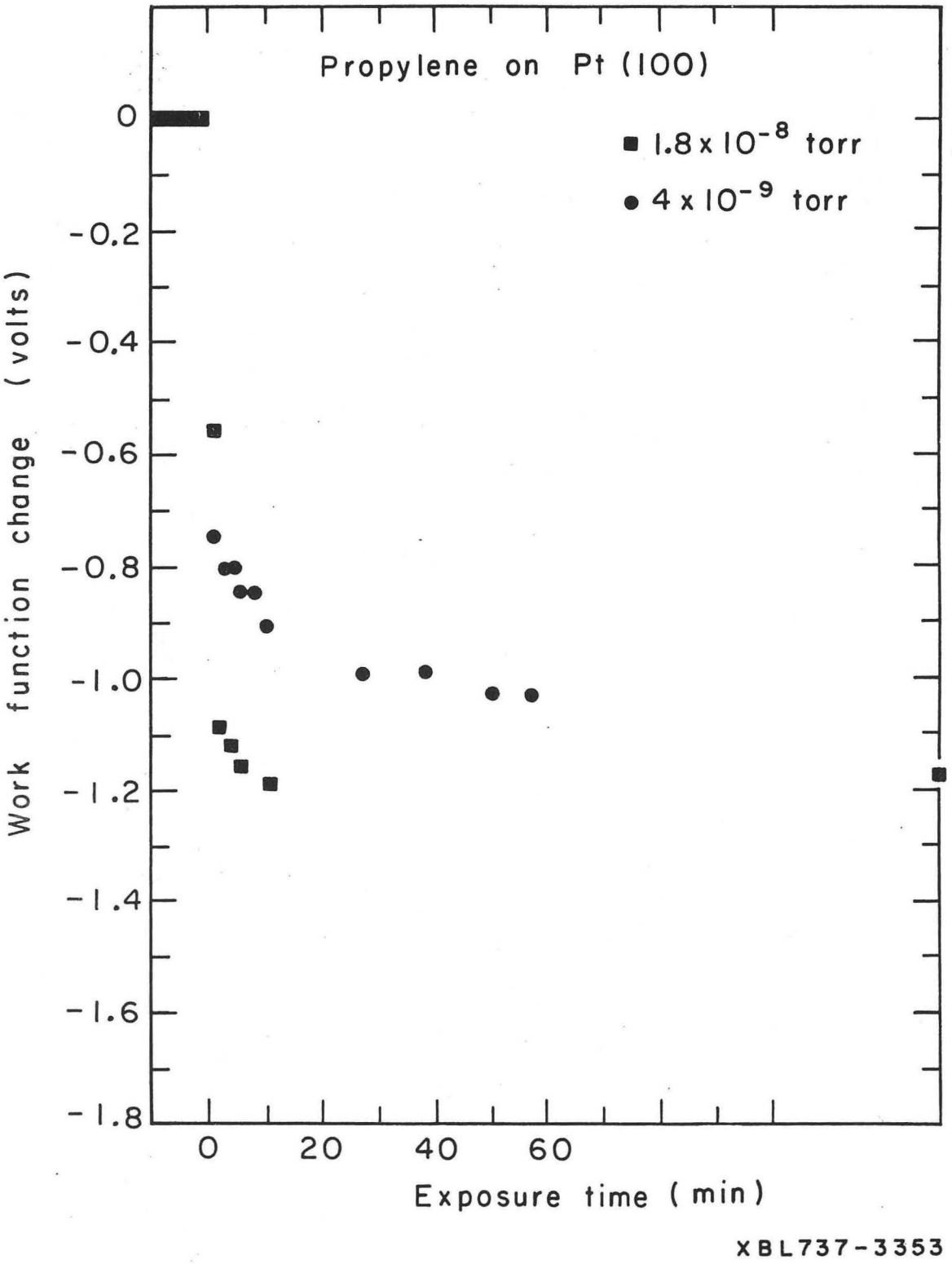

Fig. III-65. The work function change on adsorption of propylene on the Pt(100) surface at 20°C. The indicated pressure should be multiplied by at least six to yield approximate surface pressures.

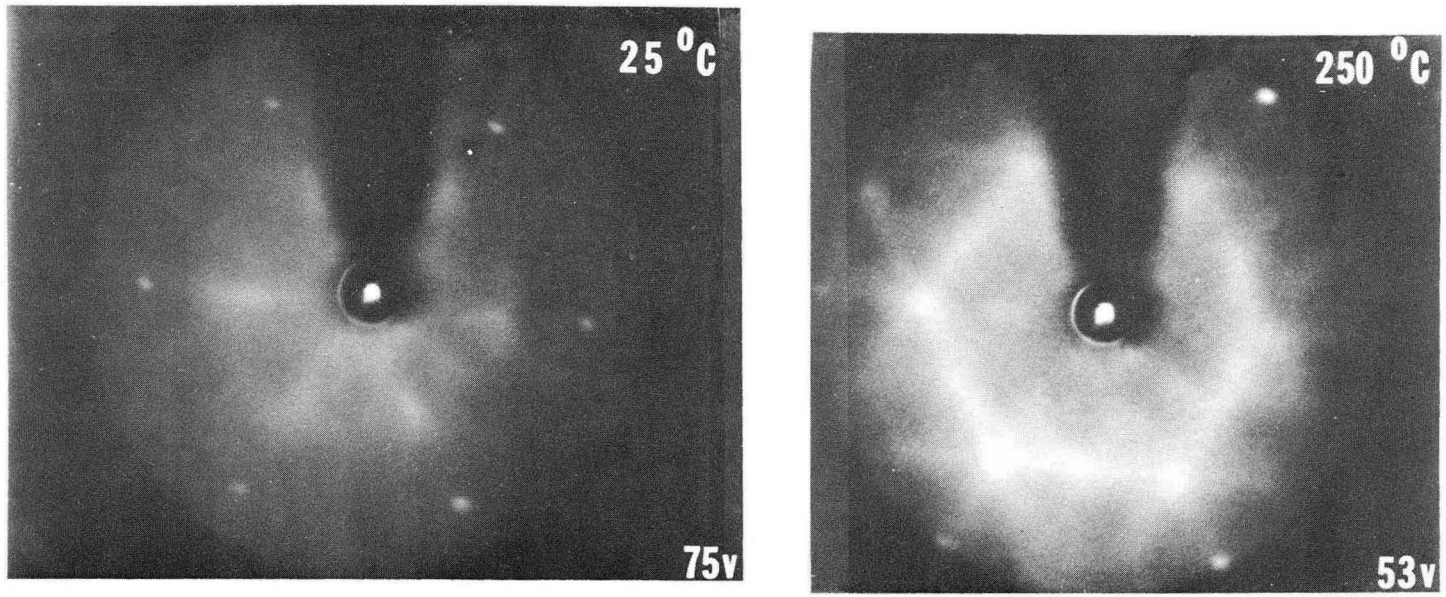

XBB 732-668

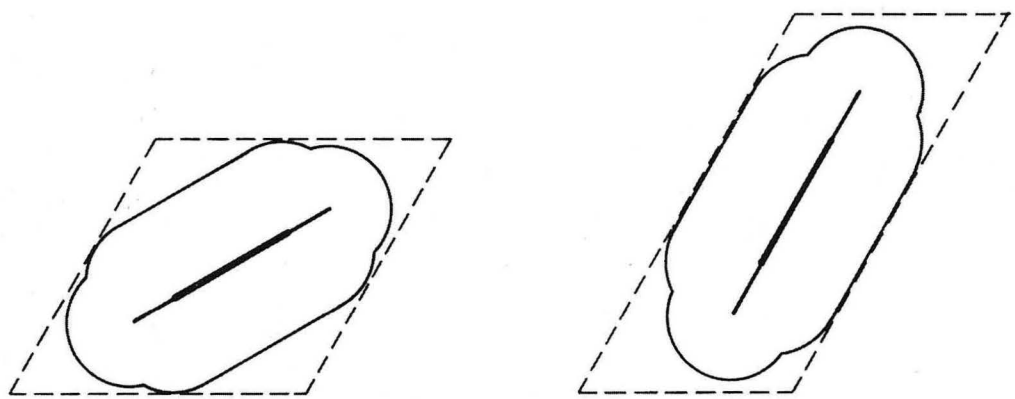

Pt(111)-2×2 Pt(111)-3×1.5

Fig. III-66. The diffraction patterns resulting from pyridine adsorption on the Pt(111) surface. Two possible pyridine orientations on the Pt(111) surface are shown below the corresponding diffraction patterns.

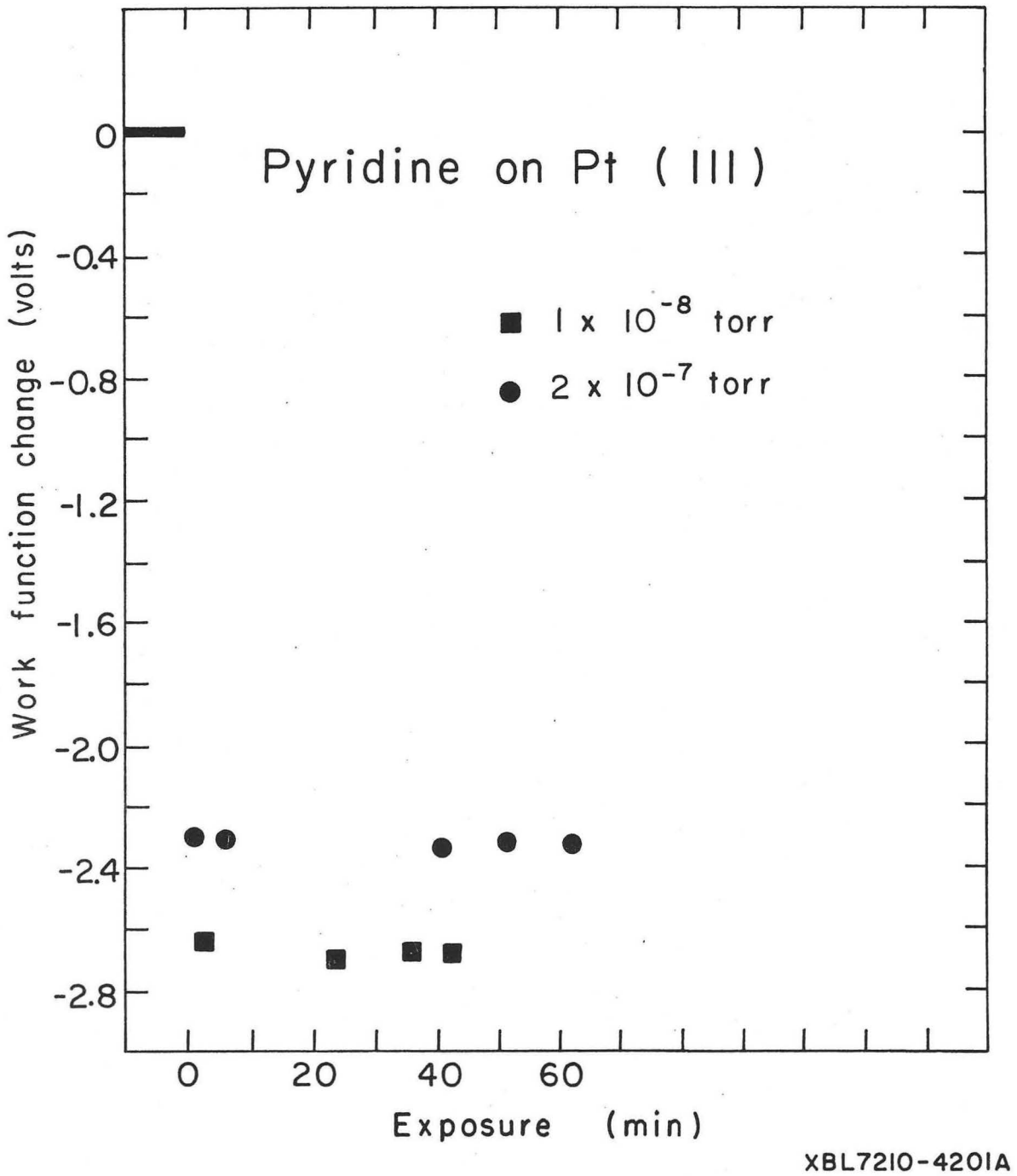

Fig. III-67. The work function change on adsorption of pyridine on the Pt(111) surface at 20°C. The indicated pressure should be multiplied by at least six to yield approximate surface pressures.

from -2.7 V to -1.7 V. This structure and WFC can also be obtained by exposing a clean Pt(111) surface to pyridine at 250°C.

Pyridine adsorbed on the Pt(100)-(5×1) surface causes a rapid disappearance of the (5×1) surface structure and an increase in background intensity. The WFC on adsorption is -2.4 V (Fig. III-68); however, this value depends on the initial rate of adsorption. Higher initial exposure rates give smaller work function changes. Heating to 250°C in organic vapor flux causes the appearance of a poorly ordered $(\sqrt{2} \times \sqrt{2})R45°$ diffraction pattern.

Toluene adsorption

Toluene adsorbed on the Pt(111) surface causes the appearance of streaked diffraction features at 1/3 order as shown in Figs. III-69a and b. The WFC on adsorption is -1.7 V (Fig. III-70); however, the WFC depends on the initial incident vapor flux. Adsorption experiments have been carried out at recorded pressures up to 3×10^{-7} with no evidence for any unexpected modifications of WFC or diffraction pattern.

If the poorly ordered adsorbed layer is heated to 150°C in organic vapor flux, ordering is greatly improved and the Pt(111)-(4×2)-toluene structure forms. The diffraction patterns observed are shown in Fig. III-69c and d. The WFC does not appear to be effected by reordering of the adsorbate layer as shown in Fig. III-71. Further stepwise heating in flux causes the adsorbed layer to become disordered and the magnitude of the WFC to decrease. All traces of extra diffraction features are gone by 250°C and the background intensity increases.

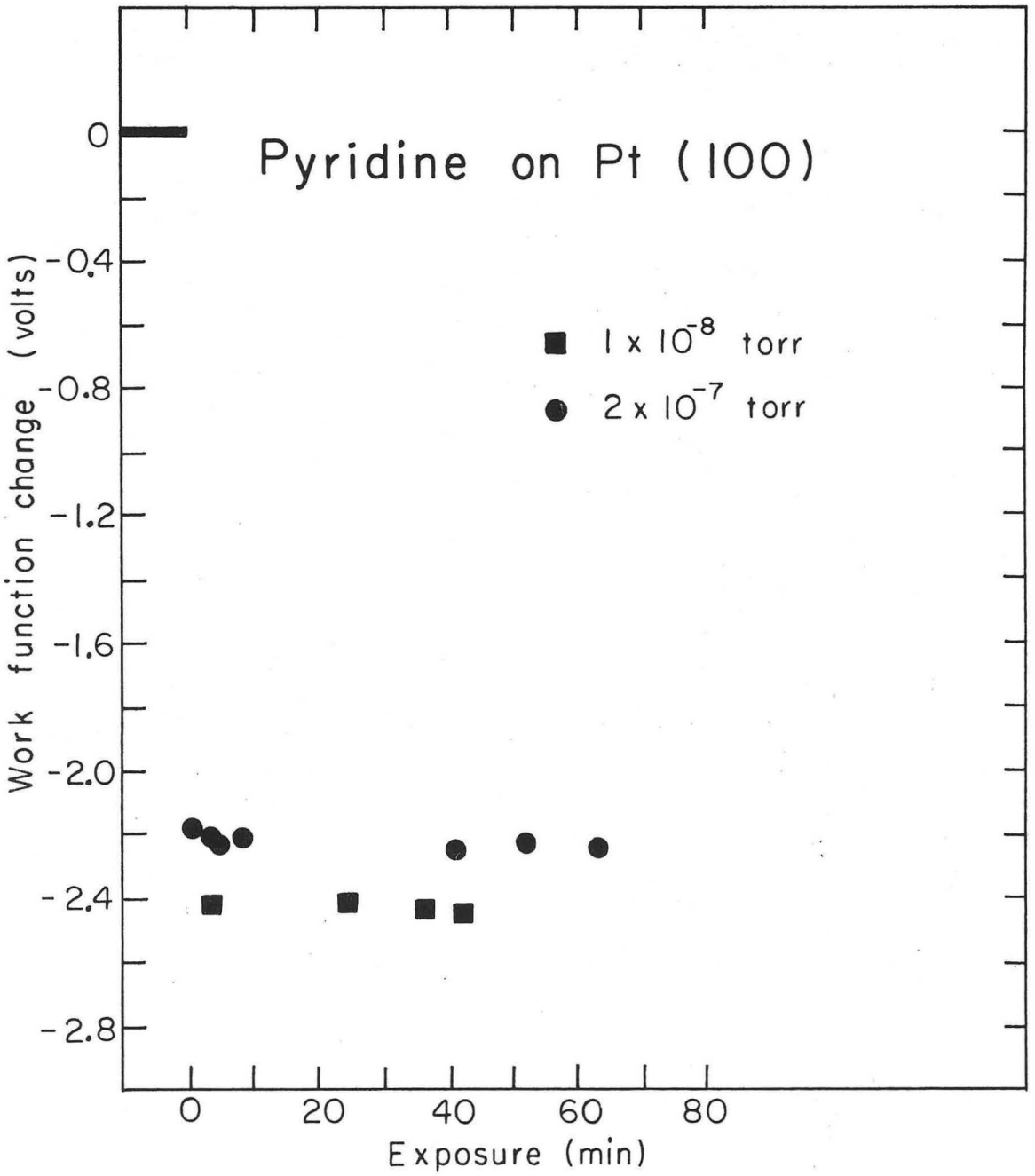

XBL7210 - 4203A

Fig. III-68. The work function change on adsorption of pyridine on the Pt(100)-(5×1) surface at 20°C. The indicated pressure should be multiplied by at least six to yield approximate surface pressures.

Fig. III-69a. The diffraction pattern resulting from toluene adsorption on the Pt(111) surface at 25°C.

Fig. III-69b. The diffraction pattern resulting from toluene adsorption on the Pt(111) surface at 25°C showing the first order Pt diffraction features.

Fig. III-69c. The diffraction pattern resulting from 160°C heat treatment of the surface and adsorbed toluene.

Fig. III-69d. The diffraction pattern resulting from 160° heat treatment of the surface and adsorbed toluene. The first order Pt diffraction features are also visible.

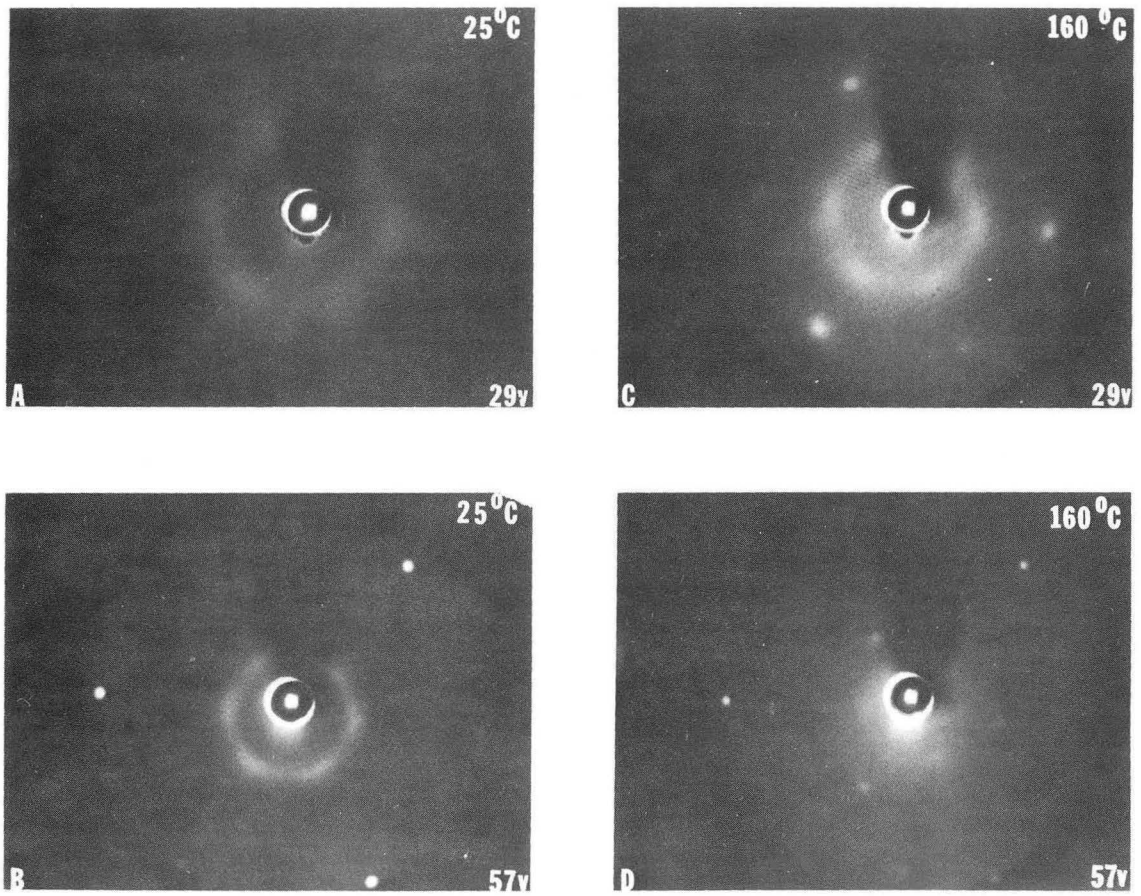

XBB 732-680

Fig. III-69 (a,b,c, & d).

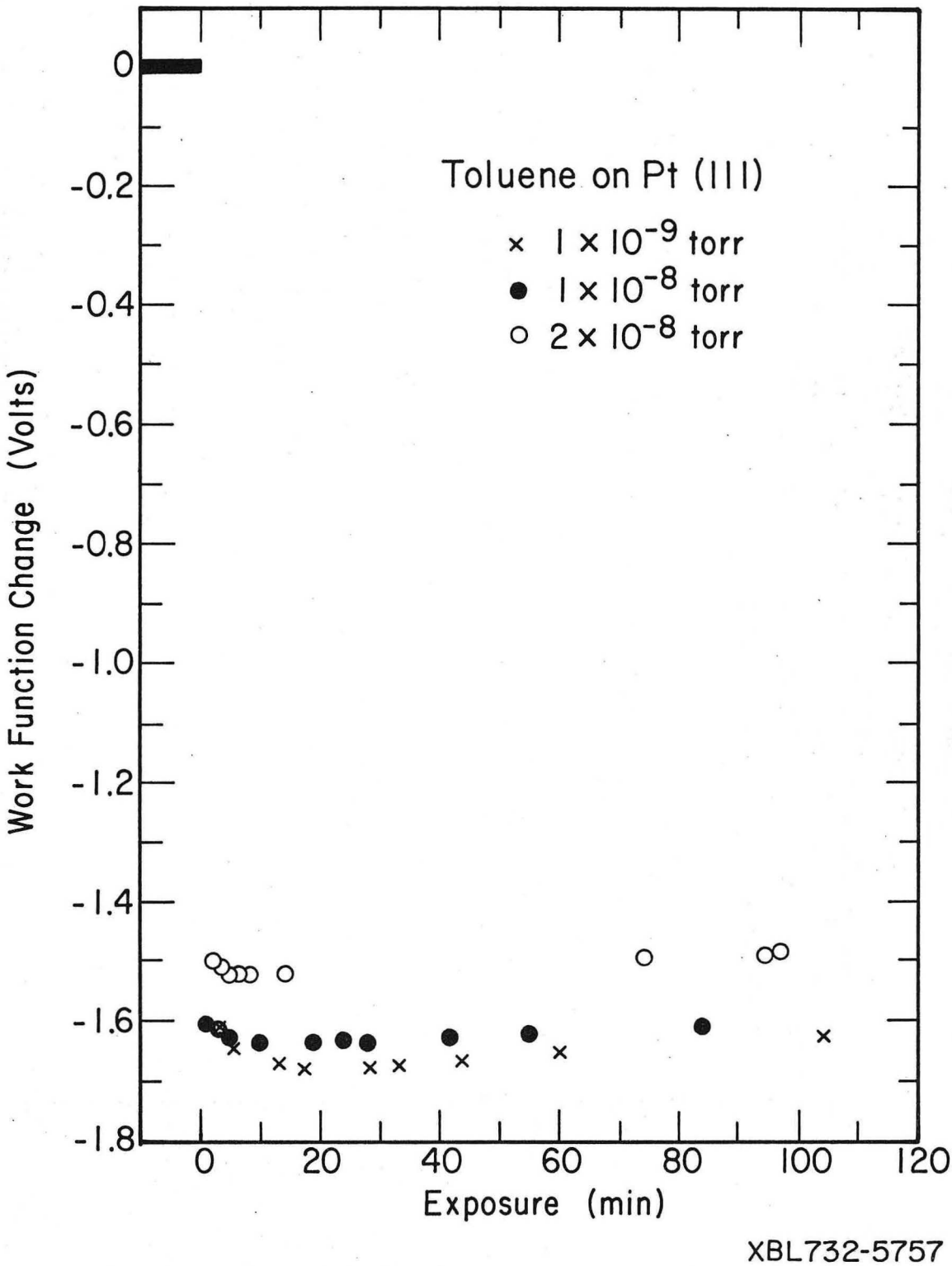

Fig. III-70. The work function change on adsorption of toluene on the Pt(111) surface at 20°C. The indicated pressure should be multiplied by at least six to yield approximate surface pressures.

Toluene adsorbed on the Pt(100)-(5×1) causes the appearance of 1/3 order streaks in the diffraction pattern while the (5×1) diffraction features remain. The diffraction pattern observed is shown in Fig. III-72. The same diffraction pattern is observed for toluene, m-xylene and mesitylene. The diffraction pattern indicates the presence of two domains of the surface structure at right angles to each other since observations have been made on a single domain. The domains of the adsorbed layer are coincident with the domains of the (5×1) structure. When viewing a single domain, the 1/3 order streaks are always parallel with the direction of the 1/5 order diffraction features. Both diffraction features resulting from the (5×1) surface structure and the 1/3 order streaks fade slowly until the pattern becomes a(1×1) with high background intensity (90 min at 1×10^{-8} Torr recorded pressure) during this transformation the WFC remains -1.55 V (Fig. III-73). The WFC on adsorption depends on the initial incident flux.

On heating to 150°C during continued exposure to organic vapor flux, the adsorbed layer remains disordered or becomes disordered if the structure mentioned above had not previously become disordered. The WFC after heating to 150°C is -1.5 V as shown in Fig. III-74. Heating in flux above 250°C causes progressive decreases in the magnitude of the WFC.

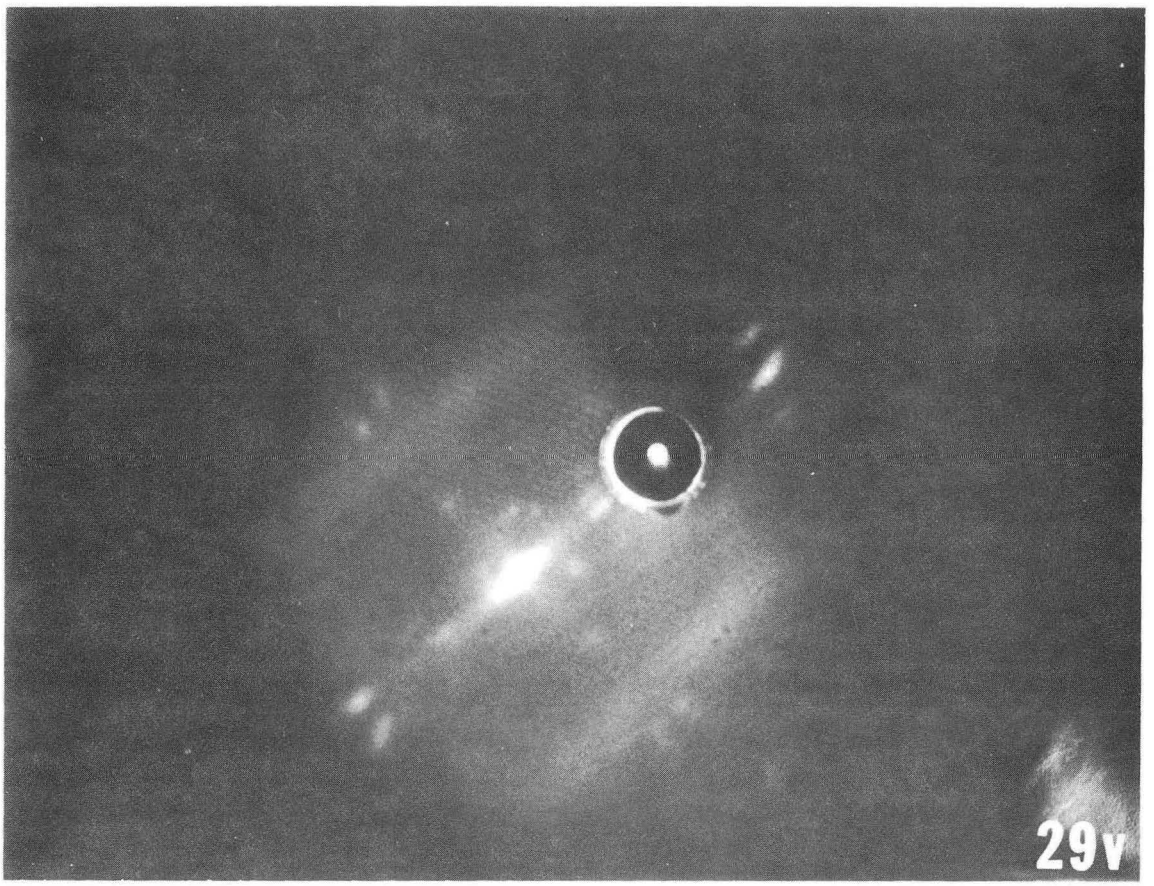

XBB 732-675

Fig. III-72. The diffraction pattern resulting from toluene adsorption on the Pt(100)-(5×1) at 20°C.

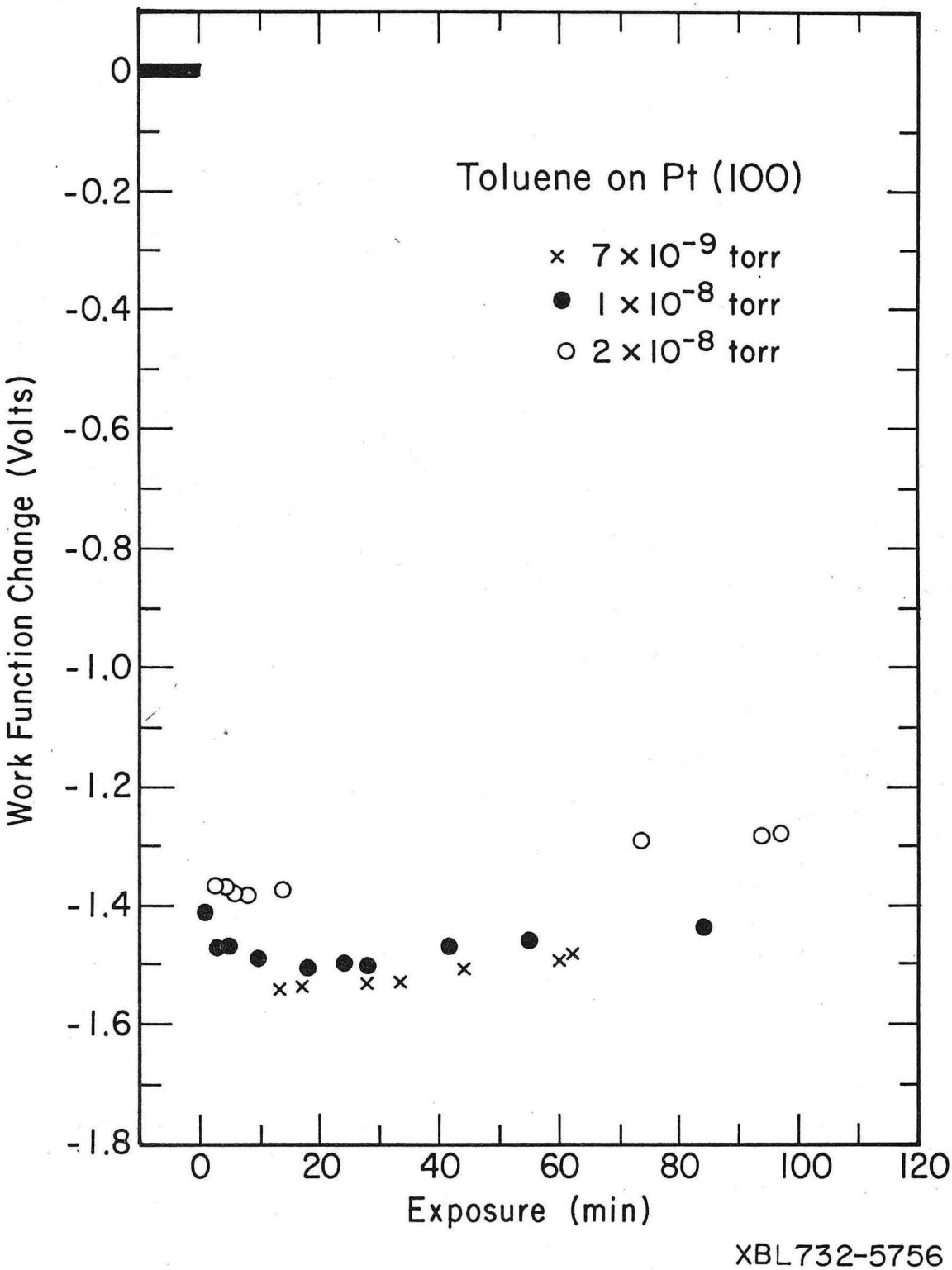

Fig. III-73. The work function change on adsorption of toluene on the Pt(100)-(5×1) surface at 20°C. The indicated pressure should be multiplied by at least six to yield approximate surface pressures.

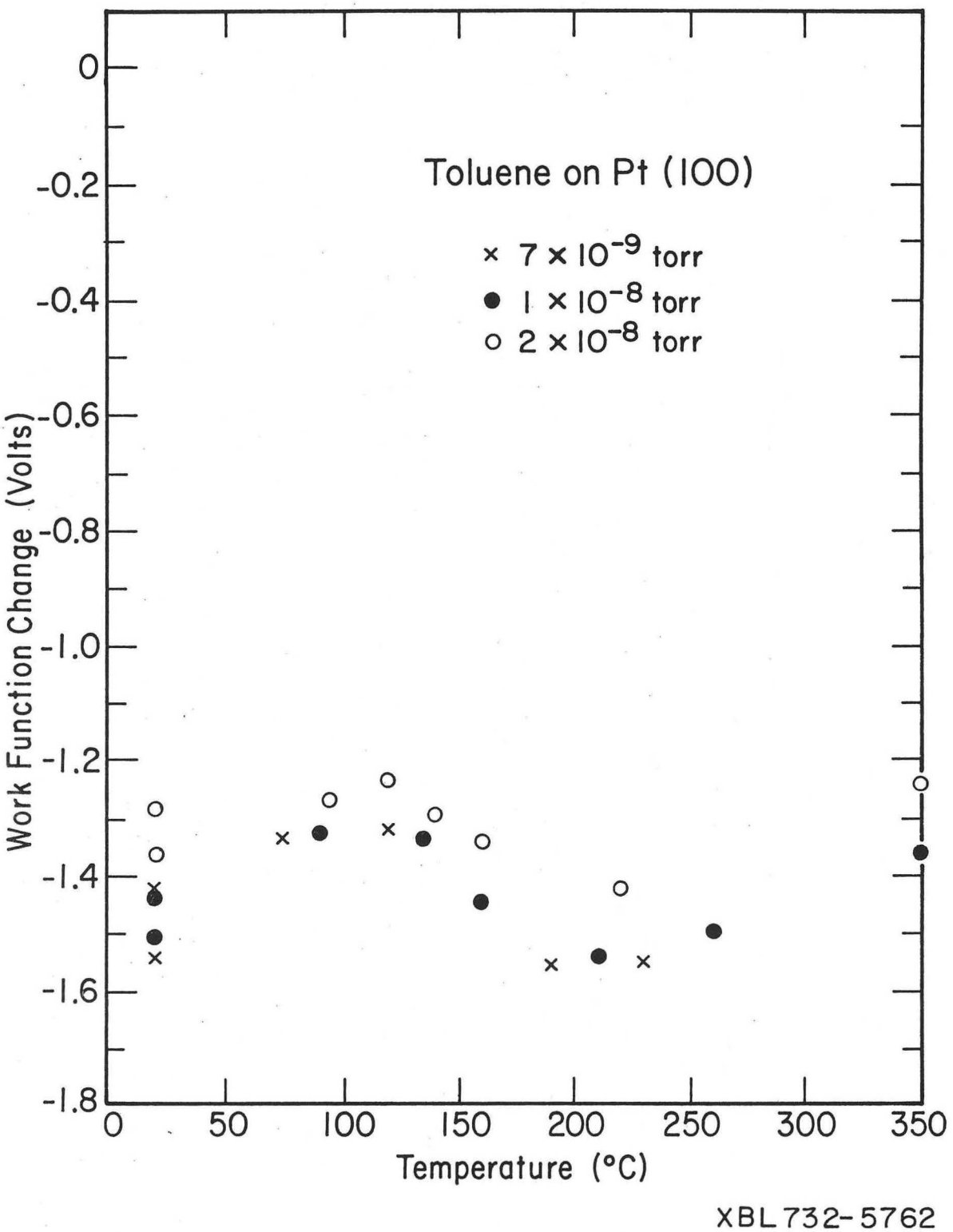

Fig. III-74. The work function change as a function of temperature for toluene adsorption on the Pt(100)-(5×1) surface. The indicated pressure should be multiplied by at least six to yield approximate surface pressures.

Metaxylene adsorption

Adsorption of m-xylene on the Pt(111) surface causes the formation of streaked diffraction features at 1/2.6 and 2/2.6 order as shown in Fig. III-75a. The WFC on adsorption is -1.8 V (Fig. III-76), and depends on the initial incident vapor flux.

With heating to 150°C in organic vapor flux the diffraction pattern becomes slightly more ordered than the diffraction pattern resulting from 20°C adsorption. With heating to 150°C the WFC is essentially unchanged as shown in Fig. III-77. Further heating causes the adsorbed layer to become disordered. Heating above 250°C causes a decrease in the magnitude of the WFC.

M-xylene adsorbed on the Pt(100)-(5×1) surface causes the appearance of 1/3 order streaks while the (5×1) structure remains as shown in Fig. III-75b. The WFC on adsorption is -1.65 V (Fig. III-78); and depends on the initial incident vapor flux. The diffraction patterns which result from m-xylene, toluene, and mesitylene adsorption are the same. The domains of the adsorbed structure are parallel to the domains of the (5×1) structure. Both the diffraction features resulting from the (5×1) surface structure and the 1/3 order streaks fade slowly until the pattern becomes a (1×1) with high background intensity (90 min. at a recorded pressure of 1×10^{-8} Torr). During this transformation the WFC remains -1.65 V (Fig. III-78).

On heating to 150°C during continued exposure to vapor flux, the adsorbed layer remains disordered or becomes disordered if the structure mentioned above had not previously become disordered. The magnitude of the WFC increases to -1.75 V with heating in flux to

Fig. III-75a. The diffraction pattern resulting from m-xylene adsorption on the Pt(111) surface at 20°C showing the first order Pt diffraction features.

Fig. III-75b. The diffraction pattern resulting from m-xylene adsorption on the Pt(100)-(5×1) surface at 20°C.

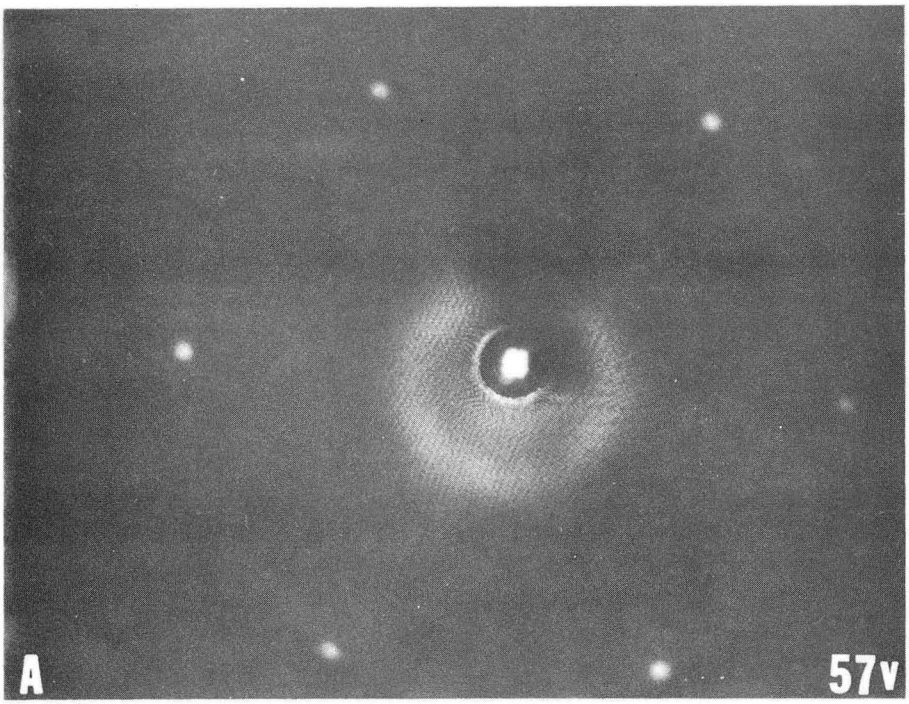

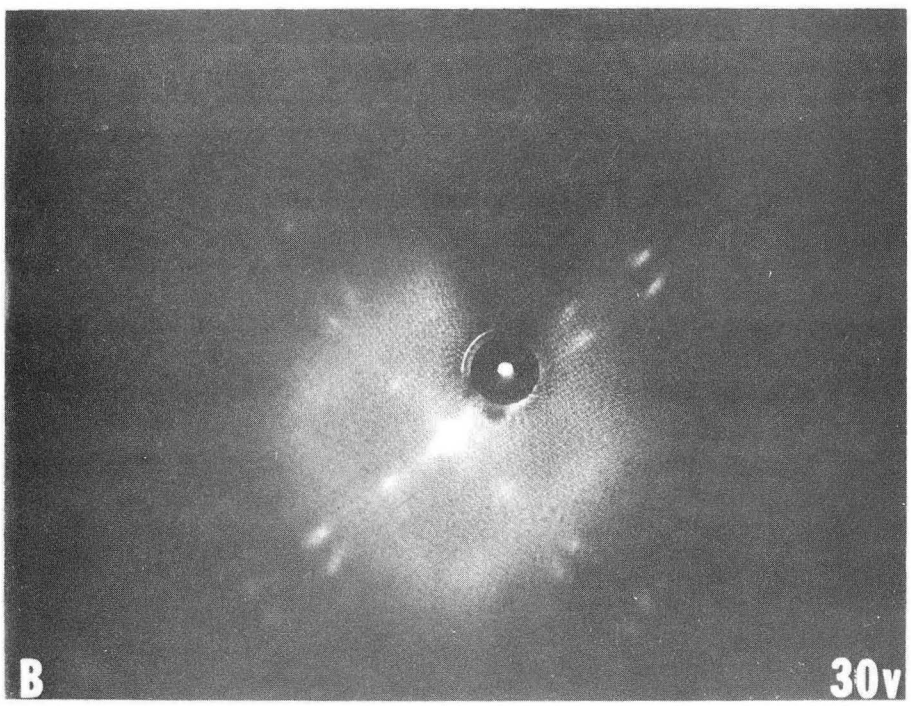

XBB 732-682

Fig. III-75 (a & b).

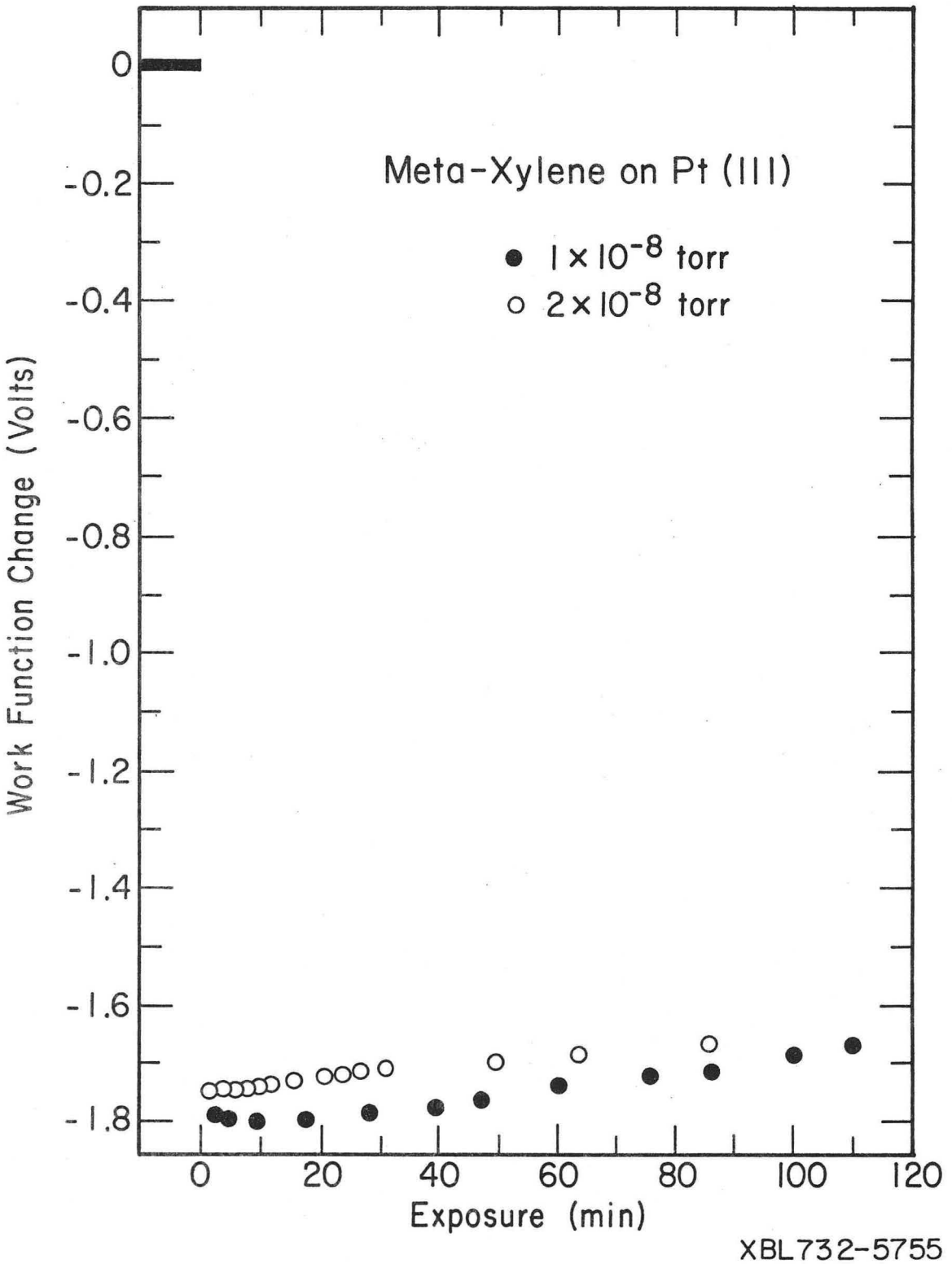

Fig. III-76. The work function change on adsorption of m-xylene on the Pt(111) surface at 20°C. The indicated pressure should be multiplied by at least six to yield approximate surface pressures.

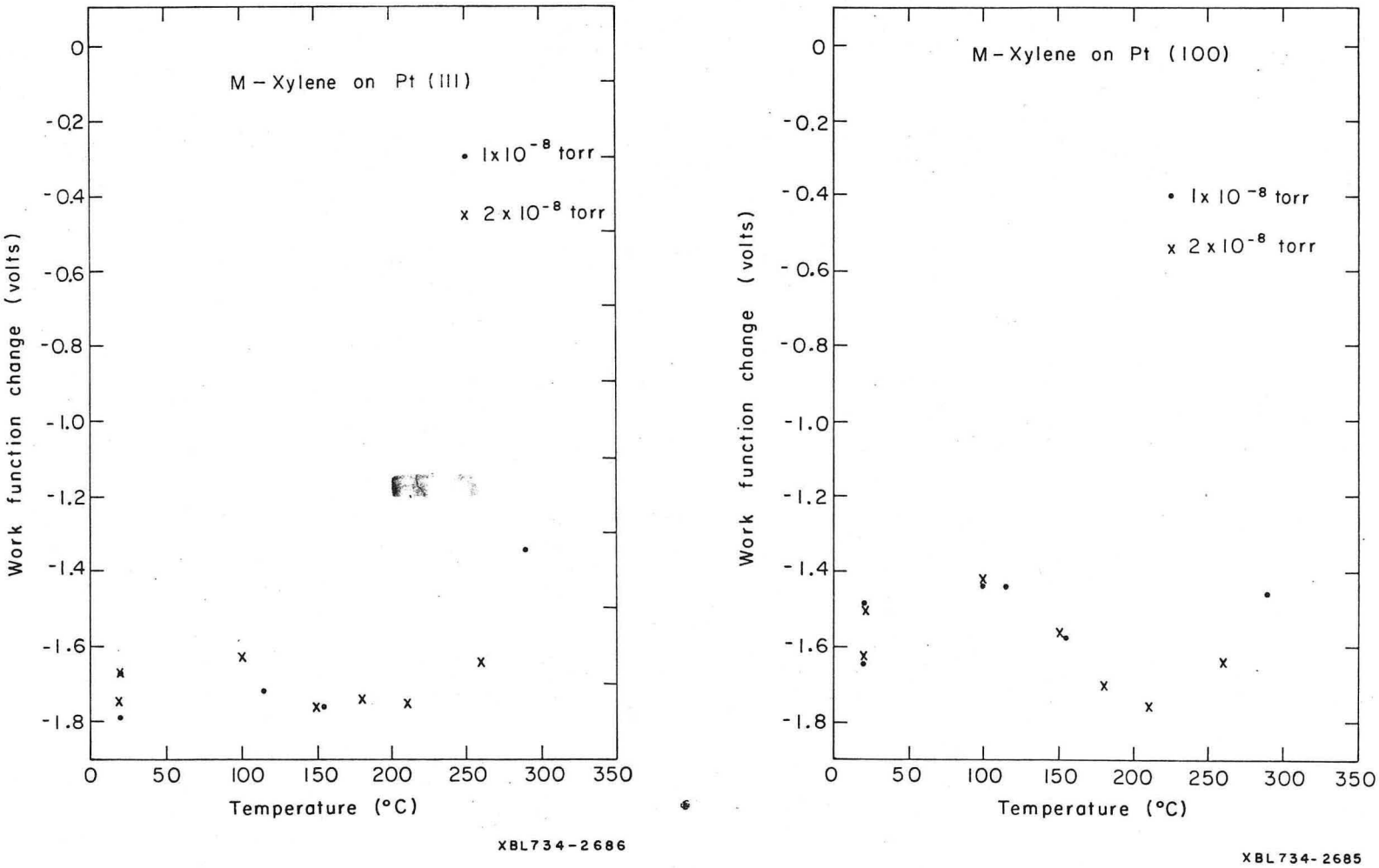

Fig. III-77. The work function change as a function of temperature for m-xylene adsorbed on the Pt(111) and Pt(100)-(5×1) surfaces. The indicated pressure should be multiplied by at least six to yield approximate surface pressures.

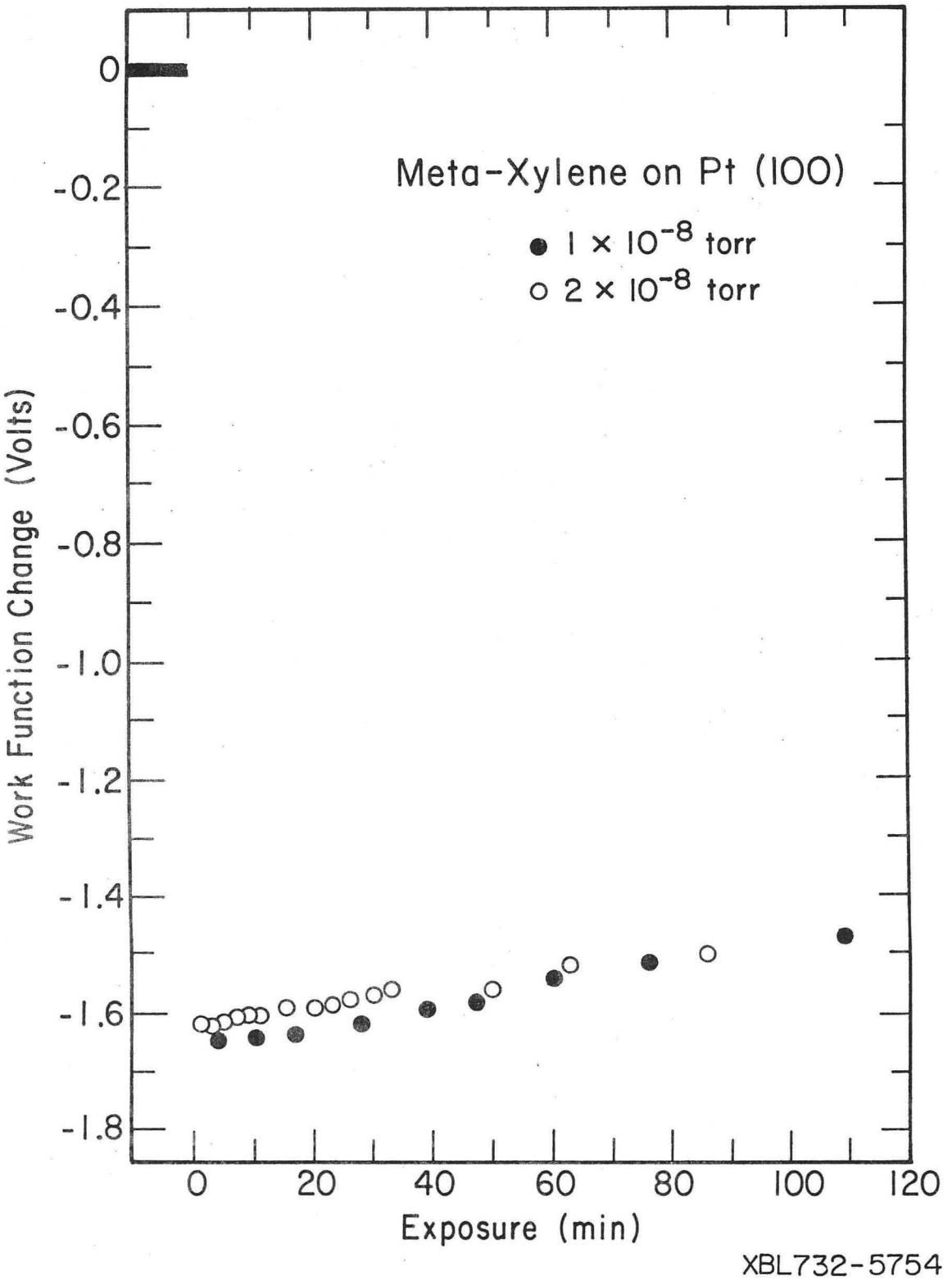

Fig. III-78. The work function change on adsorption of m-xylene on the Pt(100)-(5×1) surface at 20°C. The indicated pressure should be multiplied by at least six to yield approximate surface pressures.

150°C (Fig. III-77). Heating above 250°C causes a decrease in the magnitude of the WFC.

C. Results

1. Experimental Conditions

The results presented in this section have been taken in the following manner. During the 12-15 minute exposure period the diffraction information was monitored continuously. The WFC was measured near the end of the exposure period. The samples were heated in vacuum; however, the samples were cooled to 20-40°C before WFC measurements were made or diffraction information taken.

2. Results

Cyclopentene adsorption

The adsorption of cyclopentene on the Pt(100)-(5×1) surface causes the (5×1) surface structure to disappear rapidly. Diffuse streaked (1/2 0) diffraction features appear in the diffraction pattern. The streaks are perpendicular to the (10) directions. The WFC on adsorption is -1.4 V. With stepwise heating in vacuum to 300°C the magnitude of the WFC decreases. The adsorbed layer is disordered above 100°C.

No experiments were performed on the Pt(111) surface.

2,6-Dimethylpyridine adsorption

Adsorption of 2,6-dimethylpyridine on the Pt(111) surface causes the appearance of diffuse streaks at 1/3.2 and 2/3.2 order. The uncertainty for this measurement is ±10% since the diffraction features are very diffuse. The WFC on adsorption is -1.6 V. With heating

to 100°C the adsorbate produces some unknown substance which poisons the electron emitting surface severely so further experimentation at high temperature was terminated.

Adsorption of 2,6-dimethylpyridine on the Pt(100)-(5×1) surface causes an increase in the background intensity along with a decrease in the intensity of the diffraction features caused by the (5×1) surface. The WFC on adsorption is -1.5 V. Experiments at elevated temperature caused severe electron gun poisoning.

3,5-Dimethylpyridine adsorption

Adsorption of 3,5-dimethylpyridine on the Pt(111) surface causes the appearance of a diffuse streak at 1/2 order. The WFC on adsorption is -2.3 V. With gentle heating to 100°C the adsorbate produces some unknown substance which poisons the electron gun severely even though the pressure was 2×10^{-9} Torr.

Adsorption of 3,5-dimethylpyridine on the Pt(100)-(5×1) surface causes the slow disappearance of the (5×1) surface structure (4 minutes at 4×10^{-7} Torr recorded pressure). The work function change on adsorption is -2.2 V. Experiments at elevated temperature cause severe electron gun poisoning.

Isoquinoline adsorption

Isoquinoline adsorbed on the Pt(111) surface causes the appearance of new diffraction features at 1/3 and 2/3 order. The diffuse (1/3 0) diffraction features overlap. At 2/3 order the diffraction features are separate but diffuse regions of high intensity centered at the (2/3 0) positions. The WFC on adsorption is -1.9 V. On heating

in vacuum by steps to 200°C the magnitude of the WFC decreases with increased temperature. The extra features in the diffraction pattern disappear on heating to 90°C and are replaced by uniform high background intensity.

Isoquinoline adsorbed on the Pt(100)-(5×1) surface causes the slow disappearance of the (5×1) surface structure (6 minutes at 6×10^{-8}). While the (5×1) remains, faint high order streaks are visible in the diffraction pattern parallel to features produced by the (5×1) surface structure. After disappearance of the (5×1) surface structure (and the diffuse extra feature) the pattern has a uniform high background intensity. On heating in vacuum by steps to 300°C the magnitude of the WFC decreases and the overlayer remains disordered.

Piperidine adsorption

Piperidine adsorbed on the Pt(111) surface causes an increase in the background intensity. The WFC on adsorption is -2.1 V. With heating in steps to 300°C in vacuum the background intensity increases and the magnitude of the WFC decreases.

Piperidine adsorbed on the Pt(100)-(5×1) surface causes a decrease in the intensity of the diffraction pattern and an increase in the background intensity. The WFC on adsorption is approximately -2.05 V. With heating in steps to 300°C in vacuum the (5×1) diffraction pattern becomes less intense ((5×1) gone at 150°C) and the background intensity becomes progressively more intense. With heating the magnitude of the WFC decreases.

Pyrrole adsorption

Pyrrole adsorbed on the Pt(111) surface causes the appearance of diffuse new diffraction features at the (1/2 0) positions. The WFC on adsorption is -1.45 V. With heating by steps to 200°C in vacuum the diffraction pattern has a uniform high background intensity indicative of a disordered overlayer.

Pyrrole adsorbed on the Pt(100)-(5×1) surface causes the rapid disappearance of the diffraction pattern due to the (5×1) surface structure. New diffuse diffraction features appear at the (1/2 0) positions. The WFC on adsorption is -1.6 V. With heating by steps to 200°C in vacuum the diffraction pattern has a uniform high background intensity indicative of a disordered overlayer.

Quinoline adsorption

Quinoline adsorbed on the Pt(111) surface causes the appearance of a diffuse streak at 1/3 the distance between the (00) and (10) platinum features. The WFC on adsorption is -1.45 V. With heating in vacuum the extra diffraction features are gone after 120°C heat treatment; as the extra features disappear the background intensity increases. With heating by steps to 200°C in vacuum the WFC decreases with increasing temperature.

Quinoline adsorbed on the Pt(100)-(5×1) surface causes the slow disappearance of the (5×1) surface structure (14 minutes at a recorded pressure of 3×10^{-8} Torr). While the (5×1) persists diffuse streaks appear at 1/3 order; the streaking is parallel to the direction of the diffraction features which occur because of the (5×1) surface

structure. As the (5×1) surface structure and 1/3 order streaks disappear the background intensity of the adsorbed layer increases. The WFC on adsorption is -1.7 V. With heating by steps to 200°C the magnitude of the WFC decreases and the background intensity increases in the diffraction pattern.

Styrene adsorption

Styrene adsorbed on the Pt(111) surface causes the appearance of streaked diffraction features at 1/3 and 2/3 order with respect to the (10) platinum diffraction features. The WFC on adsorption is -1.7 V. With heating in vacuum by steps to 200°C the magnitude of the WFC observed decreases and the diffraction pattern has uniform high background intensity indicative of disorder in the adsorbed overlayer.

Styrene adsorbed on the Pt(100)-(5×1) surface causes the slow disappearance of the (5×1) surface structure (10 minutes at 6×10^{-8}). The diffraction pattern observed after relaxation of the (5×1) surface structure displays very weak diffuse high order features along with high background intensity. With heating by steps to 200°C in vacuum the magnitude of the WFC decreases and the diffraction pattern has a uniform high background intensity indicative of disorder in the adsorbed layer.

IV. DISCUSSION

A. Generalizations

1. Conclusions

All the organic molecules studied adsorb on both the Pt(111) and Pt(100)-(5×1) surface. Ordering in the adsorbed layer was more pronounced on the Pt(111) surface than on the Pt(100)-(5×1) surface. The work function decreases with adsorption for all the organic molecules studied. This implies that the adsorbed molecules are acting as electron donors to the metal surface. In fact this might be expected since the metal surface has a high work function ($\sim$ 5.7 V)[1,2] and all of the molecules studied are polarizable.[3] The work function change on adsorption for most of the molecules studied varies approximately inversely with the first ionization potential of the adsorbate as shown in Fig. IV-1 and IV-2. The data for these figures are shown in Table IV-1. The data are scattered, however there are many different types of molecules represented, many of which have sizable permanent dipole moments. Several of the compounds which do not fit this correlation have basic nitrogens which are known to be involved in the bonding between substrate and adsorbate. The basic nitrogens may cause the permanent dipole moment of the molecule to line up with respect to the surface and cause unexpected work function changes on adsorption. The correlation between polarizability[3] and work function change on adsorption is much worse than the correlation shown between ionization potential and work function change.

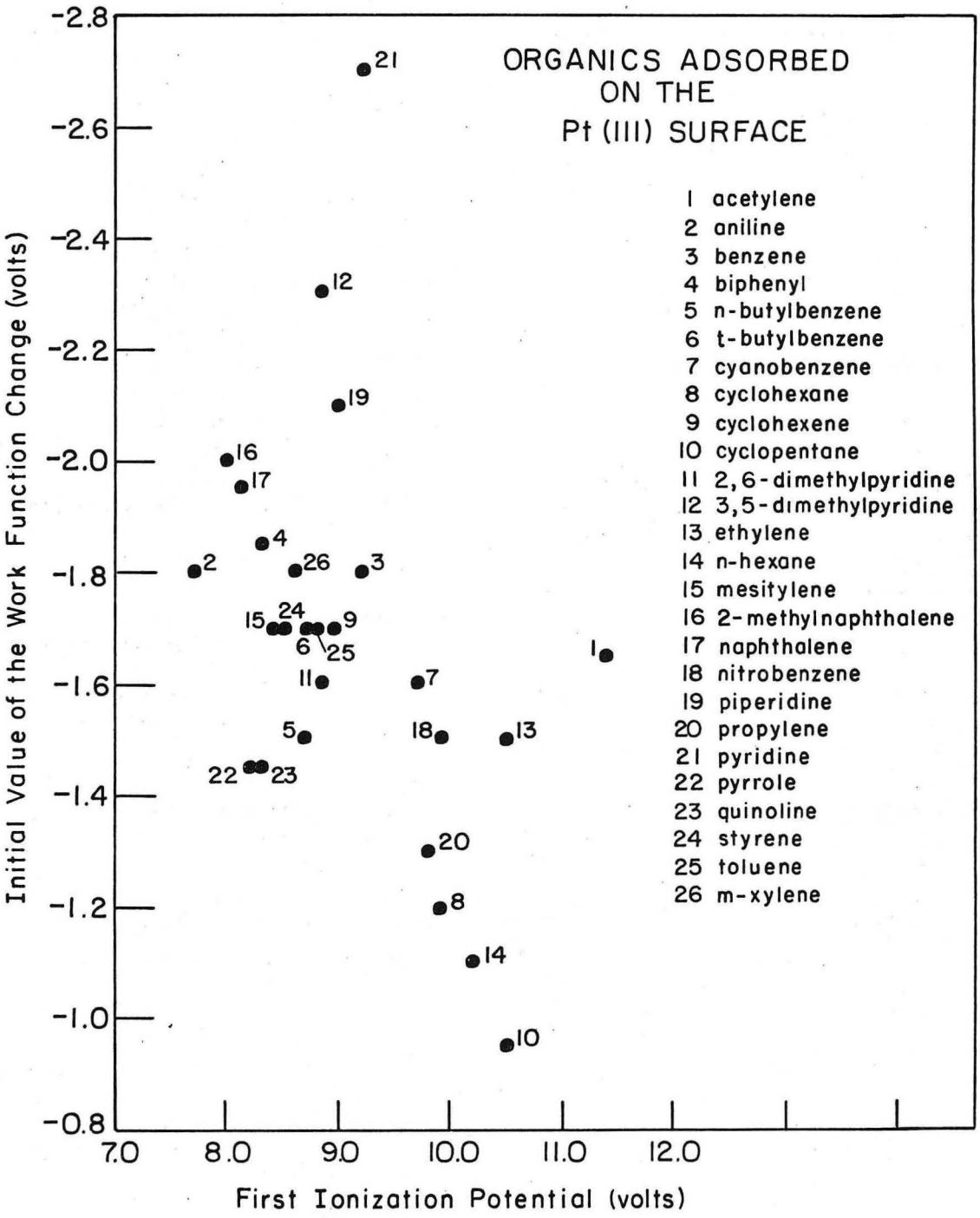

Fig. IV-1. The maximum work function change on adsorption versus the first ionization potential of organic molecules adsorbed on the Pt(111) surface.

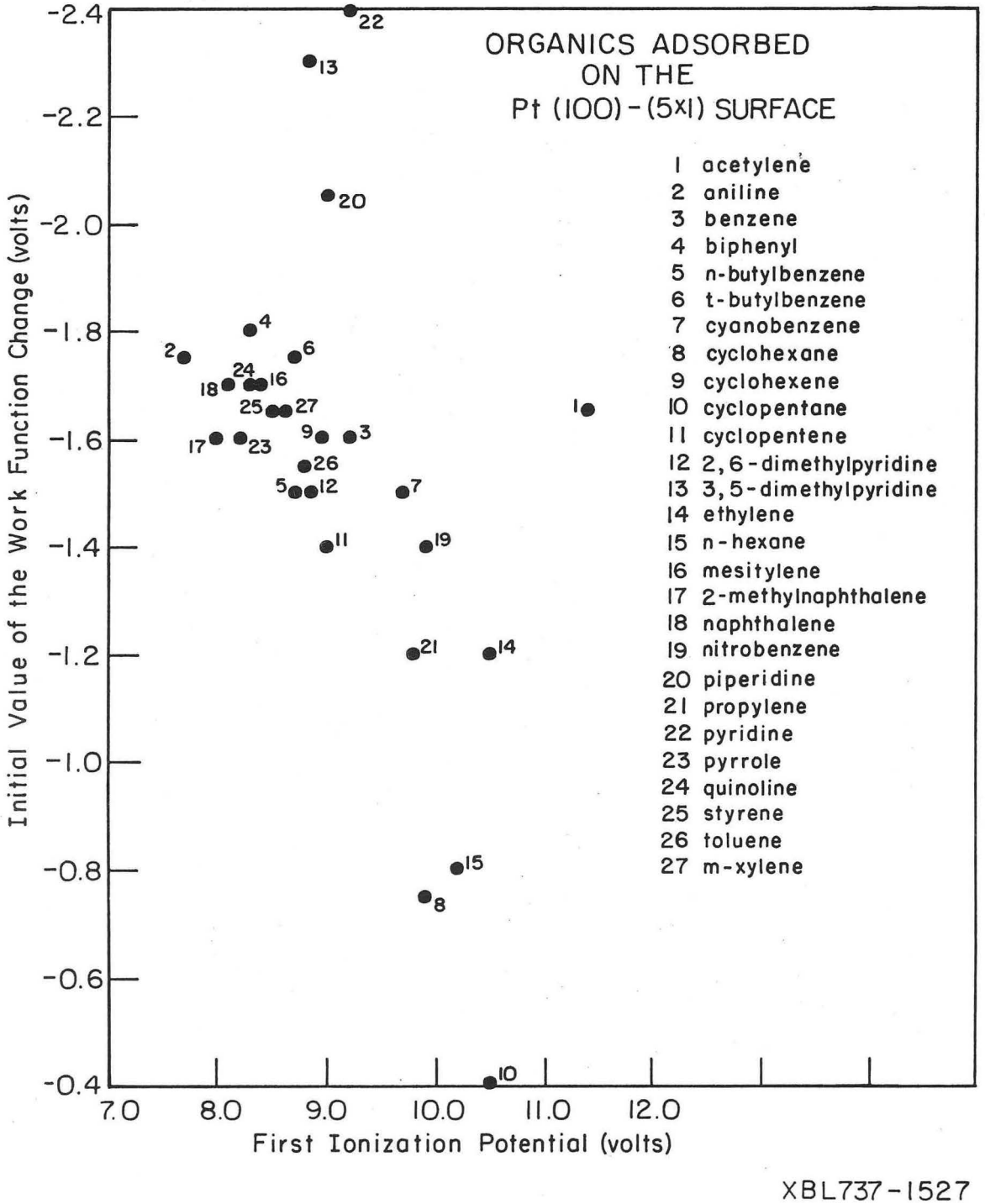

Fig. IV-2. The maximum work function change an adsorption versus the first ionization potential of organic molecules adsorbed on the Pt(111) surface.

Table IV-1. Ionization Potential and maximum work function changes for Organic molecules adsorbed on the Pt(100)-(5×1) and Pt(111) surfaces.

Name	Formula	Ionization Potential† (Volts)	Maximum Work Function Change Observed (Volts)	
			Pt(111)	Pt(100)
Acetylene	C_2H_2	11.4	-1.65	-1.65
Aniline	C_6H_7N	7.7	-1.8	-1.75
Benzene	C_6H_6	9.2	-1.8	-1.6
Biphenyl	$C_{12}H_{10}$	8.3	-1.85	-1.8
n-Butylbenzene	$C_{10}H_{14}$	8.7	-1.5	-1.5
t-Butylbenzene	$C_{10}H_{14}$	8.7	-1.7	-1.75
Cyanobenzene	C_7H_5N	9.7	-1.6	-1.5
Cyclohexane	C_6H_{12}	9.9	-1.2	- .75
Cyclohexene	C_6H_{10}	8.95	-1.7	-1.6
Cyclopentane	C_5H_{10}	10.5	- .95	- .4
Cyclopentene	C_5H_8	9.0	---	-1.4
2,6-Dimethylpyridine	C_7H_9N	8.85	-1.6	-1.5
3,5-Dimethylpyridine	C_7H_9N	*8.85	-2.3	-2.2
Ethylene	C_2H_4	10.5	-1.5	-1.2
n-Hexane	C_6H_{14}	10.2	-1.1	- .8
Mesitylene	C_9H_{12}	8.4	-1.7	-1.7
2-Methylnapthalene	$C_{11}H_{10}$	8.0	-2.0	-1.6
Naphthalene	$C_{10}H_8$	8.1	-1.95	-1.7
Nitrobenzene	$C_6H_5NO_2$	9.9	-1.5	-1.4
Piperidine	$C_5H_{11}N$	9.0	-2.1	-2.05
Propylene	C_3H_6	9.8	-1.3	-1.2
Pyridine	C_5H_5N	9.2	-2.7	-2.4
Pyrrole	C_4H_5N	8.2	-1.45	-1.6

Name	Formula	Ionization Potential (Volts)	Maximum Work Function Change Observed (Volts) Pt(111)	Pt(100)
Quinoline	C_9H_7N	8.3	-1.45	-1.7
Styrene	C_8H_8	8.5	-1.7	-1.65
Toluene	C_7H_8	8.8	-1.7	-1.55
m-Xylene	C_8H_{10}	8.6	-1.8	-1.65

(*assumed to be the same as 2,6-dimethylpyridine)

†from J. L. Franklin, J. G. Dillard, H. M. Rosenstock, J. T. Herron, K. Draxl, and F. H. Field, Ionization Potentials, Appearance Potentials and Heats of Formation of Gaseous Positive Ions, Nat. Sland. Ref. Data Series--National Bureau of Standards (U.S.) 26, 1969 (U.S. Government Printing Office, Washington D.C.)

During several experiments the Pt(100)-(5×1) surface structure relaxed to the (1×1) surface structure after adsorption was complete. The relaxation of the (5×1) surface structure had no apparent cause, usually it occurred slowly with exposure at some constant pressure or more rapidly with gentle heating (100°C). During relaxation of the (5×1) surface structure no change occurred in the work function of the surface. It appears that no marked change in the charge transfer occurred with relaxation. Thus the binding between substrate and adsorbate remains largely unchanged with relaxation of the (5×1) surface structure. For cycloyexane and cyclopentane, increased organic flux caused the (5×1) to relax rapidly and caused a decrease in the magnitude of the WFC; however, it seems that in this case both effects were caused by increased organic vapor pressure.

2. Criteria Used for the Determination of Surface Structures from the Diffraction Information

Analysis of the diffraction information yields only the translational unit vectors of the adsorbed surface layer. The position of the unit vectors in the adsorbed layer relative to the underlying unit vectors has not been determined uniquely; likewise the number of adsorbate molecules per unit cell has not been uniquely determined. Rigorous answers for both of these questions await the development of structure analysis techniques utilizing LEED intensity data.

The number of adsorbate molecules per unit cell has been determined by using the crystallographic information available for the system. This includes the size of the clean substrate unit cell, the size of

the adsorbate-induced unit cell, the symmetry of the adsorbate-induced unit cell, and the size and symmetry of the adsorbate molecules. Three additional criteria have been employed. The first is that the number of equivalent adsorbate molecules per unit cell should not lead to a reduction in the unit cell size. For instance, if the $\begin{vmatrix} -2 & 2 \\ 4 & 4 \end{vmatrix}$ unit cell could accommodate two benzenes in equivalent positions the unit cell might be reduced to $\begin{vmatrix} -2 & 2 \\ 2 & 2 \end{vmatrix}$. The second criterion is that the adsorbed layer must be close packed over the surface. In particular the surface should not contain large unoccupied areas. The third criteria is that the adsorbed layer be homogeneous. Thus in determining surface structures we have assumed that the adsorbed species is of predominantly one adsorption type, that is, that the adsorbed layer is not made up of patches with varying composition and/or binding between substrate and adsorbate. This assumption seems reasonable but is not necessarily true.

B. Benzene Adsorption

1. Benzene Adsorption on the Pt(111) Surface

With adsorption on the Pt(111) surface, benzene forms a poorly ordered adsorbed layer; the WFC on adsorption is -1.8 V. With further exposure the Pt(111)-$\begin{vmatrix} -2 & 2 \\ 4 & 4 \end{vmatrix}$-Benzene structure forms and the magnitude of the WFC decreases (-1.4 V). With further exposure the $\begin{vmatrix} -2 & 2 \\ 5 & 5 \end{vmatrix}$ structure forms and the magnitude of the WFC decreases unit it reaches a steady state value of -.7 V. The $\begin{vmatrix} -2 & 2 \\ 5 & 5 \end{vmatrix}$ structure forms when the WFC is approximately -1.1 V.

This correlation between the transformation of the benzene surface structure and the change in work function suggests that the orientation of the adsorbed benzene molecules is changing markedly as a function of increased exposure. Another possibility for such a correlated change in work function and structure might involve adsorption of a second layer of benzene. However for the case of ethylene adsorption where second layer adsorption has been reported previously[4] we find the magnitude of the WFC increases with addition of a second layer (Section IV-G). Since the change in the WF measured here is in the opposite direction, it seems unlikely that double layer adsorption is occurring.

The diffraction information indicates a change in the packing of the adsorbed benzene layer. A decrease in the density (number of benzenes per unit surface area) of the adsorbed layer during the transformation is not possible because of the high flux (.5L/sec) incident on the crystal throughout some of these experiments. In fact the observation that higher incident benzene fluxes cause the transformation to occur more rapidly indicates that the density of the adsorbed layer is increasing. The work function change during the transformation indicates that there is a decrease in the magnitude of the charge transfer occurring as the density of the adsorbed layer increases. If the adsorbed species retained the same bonding characteristics during the transformation and the coverage increased, the magnitude of the WFC would increase. Thus, the increased density accompanied by a decrease in the magnitude of the WFC can only be

explained by assuming the area per adsorbed molecule must be decreasing. The criteria for the transition are then:

1) the area of the adsorbed species must decrease, and

2) the charge transfer must decrease.

Keeping these criteria in mind a comparison of the WFC observed for benzene with other WFC data is valuable. With initial adsorption of benzene a WFC of -1.8 V occurs. This WFC is slightly larger than the WFC on adsorption of mesitylene (-1.7 V)(Section IV-F) a compound which is sterically hindered from interaction in any manner other than π-bonding. Indeed the WFC on adsorption for benzene is similar to the WFC observed on adsorbtion of most of the simple substituted aromatics studied. (Table III-1, Fig. IV-1) These facts support the contention that π-bonding is occurring between benzene and the platinum surface in the initial disordered adsorbed state. That is, the aromatic π electrons are extensively involved in the transfer of charge between the substrate and adsorbate.

The final value of the WFC, -.7 V corresponds with the WFC observed at the same pressure for cyclohexane and cyclopentane (-.7 V) adsorption. This indicates that the binding for these two cases (benzene in its final adsorbed state and cyclohexane or cyclopentane) is similar. For cyclopentane or cyclohexane adsorbed on platinum the binding appears to involve single dehydrogentation and subsequent binding of the adsorbate to the substrate through the dehydrogerated site (Section IV-E).

A likely model consistent with the criteria [1) the area of the adsorbed species must decrease and 2) the charge transfer must decrease] and the comparisons made with the WFC observed on adsorption of other similar compounds. [The initial adsorbed state involve π-bonding and the final adsorbed state involves dehydrogenation and σ-bonding] is that the initial adsorbed state involves a benzene adsorbed with its ring at some small angle or parallel to the surface. The final adsorbed state with a $\begin{vmatrix} -2 & 2 \\ 5 & 5 \end{vmatrix}$ surface structure involves reoriented benzene molecules adsorbed with their rings at some large angle or perpendicular to the surface.

The initial adsorbed species would be held on the surface by a π-bond through the aromatic ring similar to the bonds in the so called "sandwich compounds".[4] Since the metal surface is highly electron deficient ($\phi_{Pt} \cong 5.7$ V) a large induced dipole would be expected in the adsorbed layer. The final adsorbed state with a $\begin{vmatrix} -2 & 2 \\ 5 & 5 \end{vmatrix}$ surface structure involves benzene molecules covalently bonded to the surface with their rings perpendicular or nearly perpendicular to the surface. For this type of adsorption to occur, the benzene must either lose a hydrogen or its aromaticity. Recent exchange studies between perdeuterobenzene and benzene on Pt films have shown rapid exchange of hydrogen and deuterium between these species. These workers postulate a dissociation of the benzene (without loss of aromaticity) and loss of hydrogen atoms to form a singly bonded intermediate.[5] Thus the adsorbed specie which gives the $\begin{vmatrix} -2 & 2 \\ 5 & 5 \end{vmatrix}$ structure is most likely a singly dehydrogenated benzene molecule covalently bonded to

the surface through its dehydrogenated site.

This type of reorientation satisfies all the criteria for the transformation. That is, the initial adsorbed state involves π-bonding. The surface area occupied by the adsorbed species decreases and the charge transfer decreases through the transformation. The final adsorbed benzene specie interacts with the surface in a manner similar to interaction postulated for cyclohexane and cyclopentane i.e., σ-bonding. Using the criteria mentioned in section IV-A2 and the fact that the area per benzene molecule should decrease through the transition we postulate the benzene structures shown in Figs. IV-3 and IV-4. The $\begin{vmatrix} -2 & 2 \\ 4 & 4 \end{vmatrix}$ structure contains three benzene molecules per unit cell (approximately 35.6 $Å^2$ per benzene molecule). The $\begin{vmatrix} -2 & 2 \\ 5 & 5 \end{vmatrix}$ structure contains four benzene molecules per unit cell (approximately 33.3 $Å^2$ per benzene molecule). The position of the adsorbate unit cell relative to the substrate unit cell is uncertain. However, there is sufficient evidence to indicate that the postulated number of benzene molecules per unit cell is correct.

The intermediate $\begin{vmatrix} -2 & 2 \\ 4 & 4 \end{vmatrix}$ structure shown in Fig. IV-3 may involve either a homogeneous intermediate layer as shown with the benzene rings at some angle to the surface and partially dehydrogenated. However the apparent $\begin{vmatrix} -2 & 2 \\ 4 & 4 \end{vmatrix}$ diffraction pattern may also be due to a mixture of patches of the $\begin{vmatrix} -2 & 2 \\ 5 & 5 \end{vmatrix}$ structure and some other unknown structure.

With gentle heating in flux the benzene structures and the WFC results suggest that the transformation from π to σ bonding may be

Fig. IV-3. A diffraction pattern resulting from the Pt(111)-$\begin{vmatrix} -2 & 2 \\ 4 & 4 \end{vmatrix}$-benzene structure with a schematic diagram of the unit cell divided into areas containing a single benzene molecule. The relative position of the adsorbate and substrate unit cell is uncertain. The benzene is shown parallel to the surface for convience; it may be rotated by some angle relative to the surface. All dimensions are in angstroms.

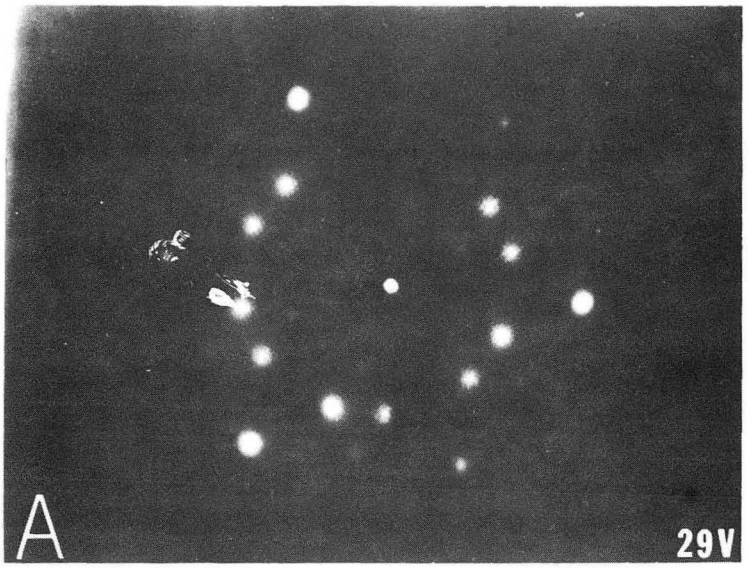

XBB 732-667

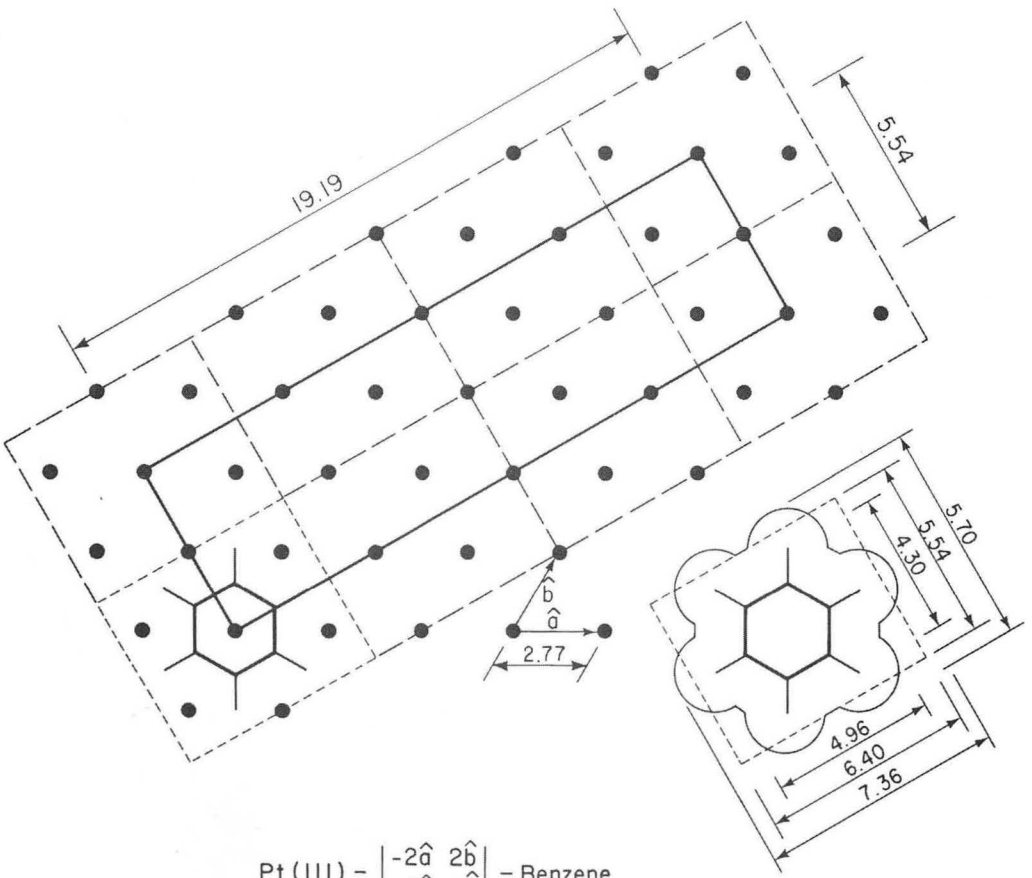

Pt (111) - $\begin{vmatrix} -2\hat{a} & 2\hat{b} \\ 4\hat{a} & 4\hat{b} \end{vmatrix}$ - Benzene

Fig. IV-3.

Fig. IV-4. Diffraction patterns taken at several voltages for the Pt(111) - $\begin{vmatrix} -2 & 2 \\ 5 & 5 \end{vmatrix}$ - benzene structure (Pattern A contains the first order platinum diffraction features) and a schematic diagram of the unit cell divided into areas which contain a single benzene molecule. The benzene is shown in several orientations; the most likely is shown in the top left corner. The position of the unit cell relative to the substrate unit cell is uncertain. All dimensions are in angstroms.

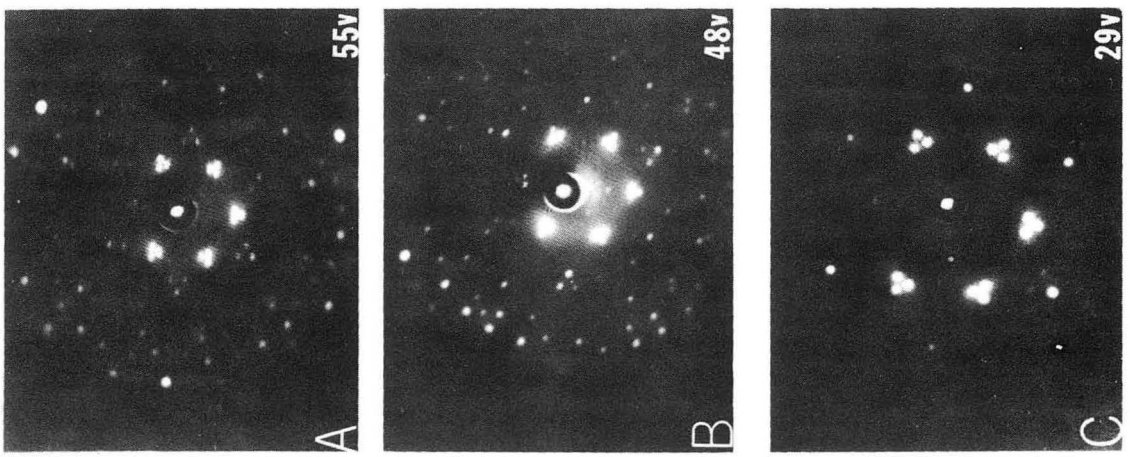
A
55v
B
48v
C
29v

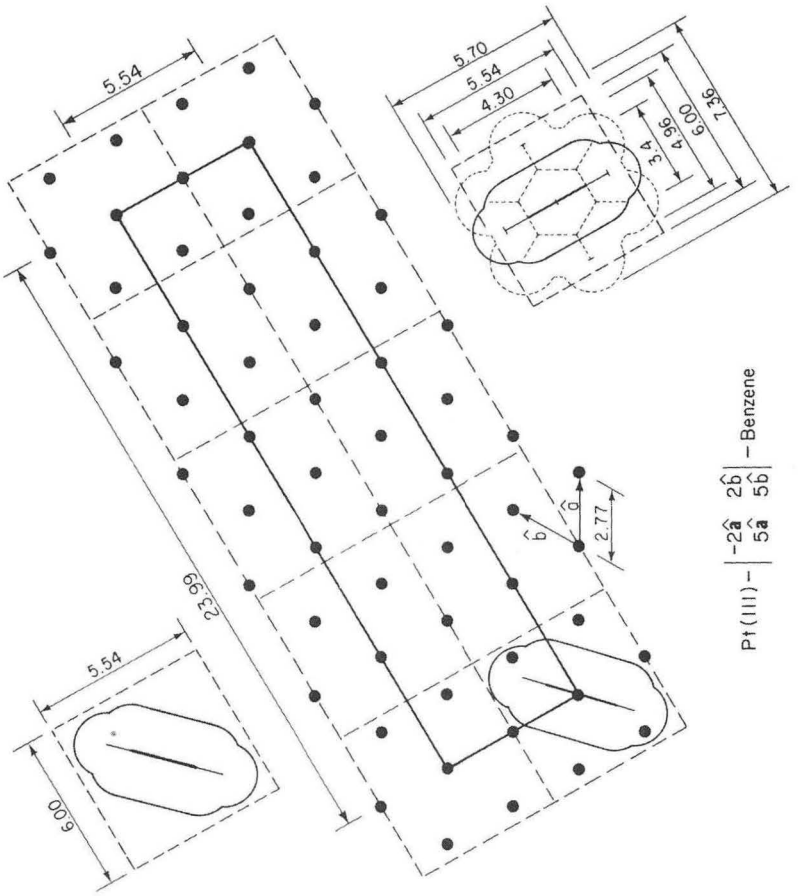
5.54
6.00
5.54
23.99
2.77
5.70
5.54
4.30
3.4
4.96
6.00
7.36
Pt(111) - $\begin{vmatrix} -2\hat{a} & 2\hat{b} \\ 5\hat{a} & 5\hat{b} \end{vmatrix}$ - Benzene

XBB 732-663

reversible; however, the adsorbed layer becomes disordered so that structural corroboration of this result by LEED is not possible.

2. Benzene Adsorbed on the Pt(100)-(5×1) Surface

Benzene adsorbed on the Pt(100)-(5×1) surface causes a WFC of -1.6 V and diffuse 1/2 order ring-like diffraction features to appear. With exposure the magnitude of the WFC decreases (-1.3 V), however, the diffraction pattern remains largely unchanged. The initial WFC suggests π-bonding. The value of the WFC is only slightly lower than the WFC on adsorption for several other simple substituted aromatics on the(100)surface. Initial adsorption may involve π-bonding between the aromatic ring and the surface while the final state may involve dehydrogenation and σ-bonding in combination with some π-bonding. The LEED results suggest that benzene may be singly dehydrogentated since a singly dehydrogenated specie adsorbed via the dehydrogenated site has a size which correlates well with the formation of 1/2 order diffraction feature. The apparent contradiction between these results is probably caused by incomplete diffraction information since the diffraction information is diffuse and higher order features may be missing. However, the WFC data indicates that some sort of transition is occurring on the (100) surface similar to the transition on the (111) surface. Detailed interpretation must await further experimentation.

C. Naphthalene Adsorption

1. Naphthalene Adsorption on the Pt(111) Surface

The adsorption of naphthalene on the Pt(111) surface at 150°C causes the formation of a(6×6) structure. The large WFC on adsorption (-2.0 V) indicates that a large amount of charge transfer occurs between substrate and adsorbate. It seems likely that the naphthalene ring system is involved in the formation of a π-bond, that is the ring system is parallel or nearly parallel to the metal surface. Adsorption of naphthalene at 25°C causes the formation of a poorly ordered structure (WFC = -1.8 V ± .1 V). The degree of ordering and WFC depend on the exposure rate; the lower the exposure rate the better the order and the larger the magnitude of the WFC. However, heating any of these poorly ordered structures to 150°C causes the appearance of the (6×6) structure and causes the WFC to approach -2.0 V. These phenomena seem to indicate that naphthalene has low mobility on the surface. The adsorbed layer may order on heating to 150° because the mobility of the adsorbed species increases; that is, the poorly ordered surface structure may be annealed at higher temperatures. The fact that better order results from low initial exposure rates seems to indicate that better ordering on the surface is also aided by slow crystallite growth, e.g., the growth of ordered domains of naphthalene. The transition required for the formation of a(6×6) diffraction pattern may be either an increase in domain size or an actual change in the adsorbed structure involving reorientation of the naphthalenes on the surface. The structure shown in Fig. IV-5 was

Fig. IV-5. A diffraction pattern and schematic diagram of the Pt(111)-(6×6)-naphthalene structure with a probable arrangement of naphthalene molecules in the unit cell. The angle of rotation of one set of parallel naphthalene molecules with respect to the other set is uncertain. The position of the unit cell relative to the substrate unit cell is also uncertain. All dimensions are in angstroms.

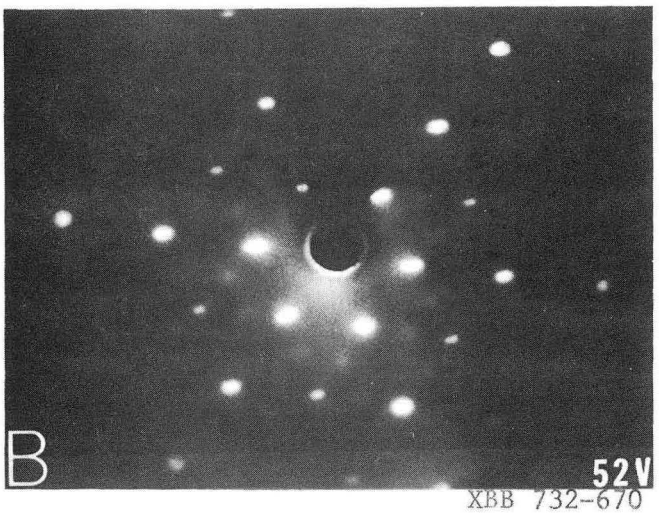

XBB 732-670

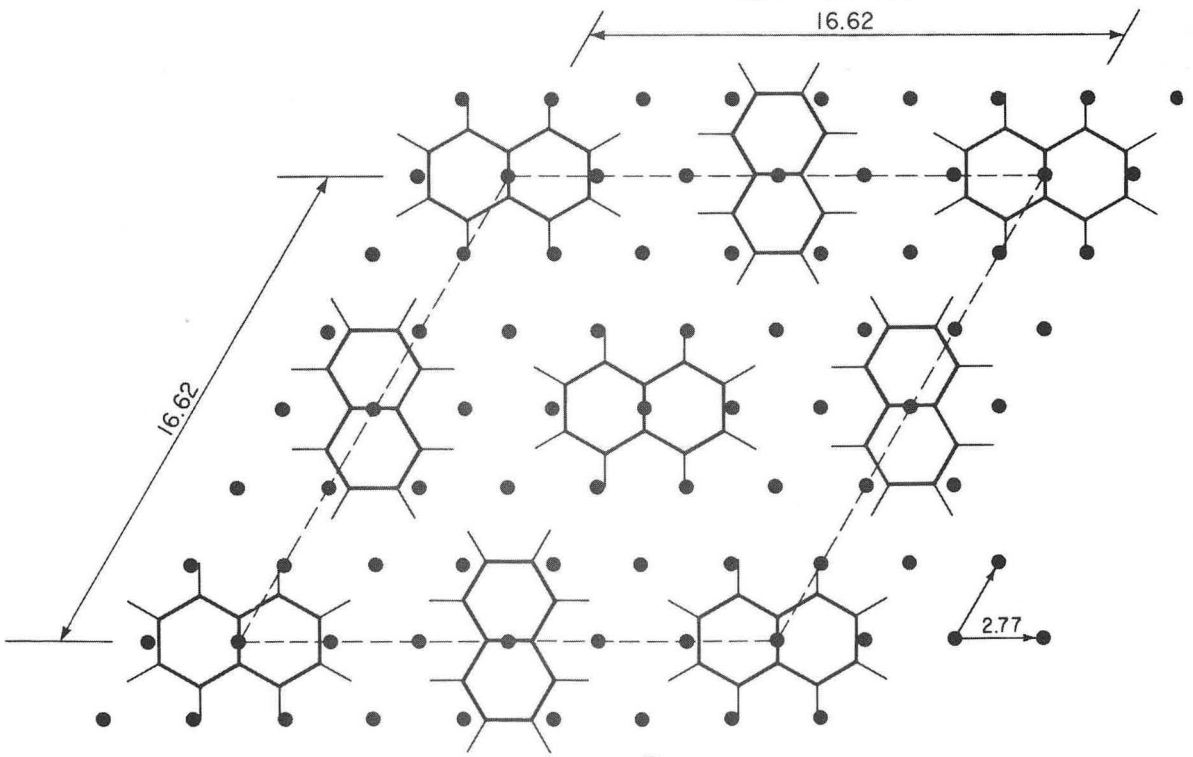

Pt(111) - (6×6) - Naphthalene

Fig. IV-5

constructed with half of the naphthalenes arbitrarily rotated by 90°. In fact we are certain only that the two scattering centers per unit cell cannot be equivalent. The structure proposed in Fig. IV-5 is based on our best estimate of the number of naphthalenes per unit cell. The position of the adsorbed unit cell relative to the substrate is uncertain.

The adsorption of 2-methylnaphthalene was carried out to test the hypothesis that naphthalene was adsorbed parallel to the surface. If 2-methylnaphthalene gave the same structure as naphthalene, adsorption parallel to the surface would have been ruled out. However, 2-methylnaphthalene gave a disordered adsorbed layer on adsorption therefore the parallel adsorption model was not disproved. The WFC on adsorption of 2-methylnaphthalene (-2.0 V) indicates that this substance is bound to the surface in a manner similar to naphthalene.

2. Naphthalene Adsorbed on the Pt(100)-(5×1) Surface

Naphthalene adsorbed on the Pt(100) surface causes a WFC on adsorption of -1.7 V. Adsorption of 2-methylnaphthalene causes a WFC of -1.6 V. Apparently both of the compounds interact primarily by forming π-bonds with the surface. Diffraction information is completely lacking so that this interpretation is largely speculative.

D. Pyridine and Dimethylpyridine Adsorption

1. Pyridine and Dimethylpyride Adsorption on the Pt(111) Surface

Pyridine adsorbed on the Pt(111) surface at 25°C forms a poorly ordered structure with a characteristic distance two times the size of the underlying lattice. The proposed structure is shown in Fig. IV-6.

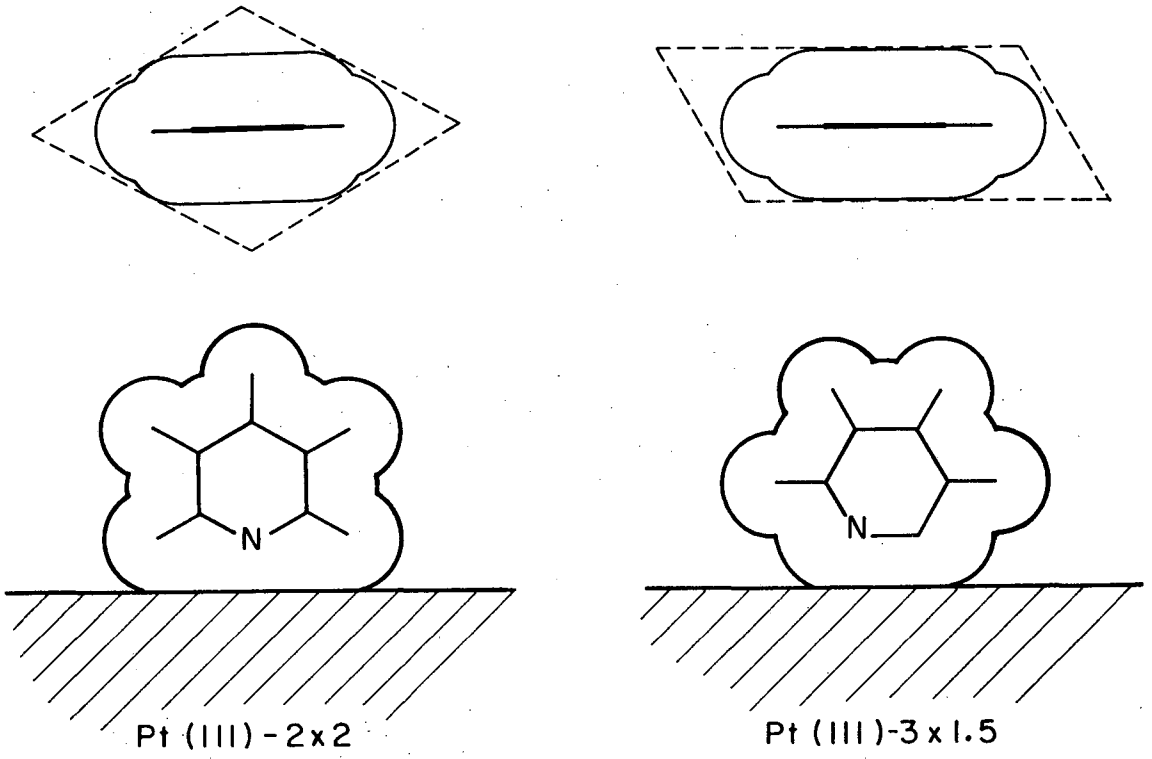

XBL737-3431

Fig. IV-6. A schematic diagram indicating the orientation of adsorbed pyridine on the Pt(111) surface. The orientation shown for the Pt(111)-(2×2) structure correlates with the adsorption data at 20°C. The orientation shown for the Pt(111)-(3×1.5) structure correlates with the adsorption data at 250°C and corresponds to a singly dehydrogenated pyridine adsorbed through both its nitrogen and the dehydrogenated ortho site.

The large WFC on adsorption (-2.7 V) indicates that the nitrogen lone electron pair must be involved in the bonding. Pyridine adsorbed through its nitrogen with the aromatic ring perpendicular to the metal surface fits nicely into a Pt(111)-(2×2) unit cell as shown in Fig. IV-6.

With this adsorption geometry the WFC would be expected to be large since the molecule has a 2.2 D permanant dipole which would be aligned with its positive end away from the substrate. That is, the large WFC may be due to actual electron transfer from the adsorbate to the substrate and/or alignment of the permanent dipoles of the adsorbate with their positive end away from the surface.

The hypothesis that the nitrogen lone electron pair was extensively involved in bonding between pyridine and the metal surface was tested by adsorbing 2,6-dimethylpyridine and 3,5-dimethylpyridine. The nitorgen lone electron pair is sterically hindered from interaction with the surface in 2,6-dimethypyridine;[6,7] 3,5-dimethylpyridine was used to check for the influence of other effects of dimethyl substitution such as the increased size of the molecule and electron density changes with methyl substitution.

Adsorption of 3,5-dimethylpyridine on the Pt(111) surface causes a WFC of -2.3 V. This value imples involvement of the nitrogen lone electron pair in the bonding. 3,5-Dimethylpyridine causes the appearance of diffuse 1/2 order diffraction features; however, the molecule is too large to fit in a Pt(111)-(2×2) unit cell, thus the diffraction information appears to be incomplete because of poor ordering.

Adsorption of 2,6-dimethylpyridine causes a WFC of -1.6 V on the Pt(111) surface. This value of the WFC is significantly smaller than the WFC on adsorption of 3,5-dimethylpyridine and is similar to the WFC observed for most of the simple substituted aromatics (Section IV-F). This imples that the nitrogen lone electron pair is not extensively involved in bonding and that π-bonding is the primary type of interaction which is occurring. The diffraction pattern which is caused by the adsorption of 2,6-dimethylpyridine has streaked diffraction features at 1/3.2 order and 2/3.2 order. This type of diffraction pattern was observed for toluene, m-xylene and mesitylene compounds which are approximately the same size and which form π-bonds with the surface.

The adsorption of these two dimethylpyridines has shown that if a pyridine type nitrogen is not sterically hindered it interacts strongly with the surface and causes adsorption of the aromatic ring perpendicular to the substrate surface. This evidence supports the hypothesis that pyridine interacts with the surface through its basic nitrogen.

If the adsorbed pyridine is heated to 250°C, a new structure forms characterized by one dimensional order with the unit vector in the overlayer being three times as long as the unit vectors in the substrate lattice. The diffraction pattern and proposed structure is shown in Fig. IV-6. The diffraction information seems to indicate an increase in the area per molecule since the unit cell size increases. The magnitude of the WFC decreases with heating (-1.7 V) indicating a less favorable geometry for the nitrogen lone electron pair interaction

or less favorable orientation of the permanent dipole. Exchange studies with pyridine have indicated that the ortho position (next to the nitrogen) is very susceptible to exchange.[8] Therefore it is probable that pyridine at high temperature is singly dehydrogenated and is doubly adsorbed on the surface through the nitrogen an a dehydrogenated ortho-carbon as shown in Fig. IV-6. The cross section of such a species is three by one and one half in terms of the Pt(111) unit vectors and thus this adsorbed orientation of pyridine could give rise to the observed diffraction pattern. The decrease in the magnitude of the WFC is easily explained using this pyridine orientation since the nitrogen has a less favorable geometry for interaction with the surface and the permanent dipole is no longer aligned perpendicular to the substrate surface.

2. Pyridine and Dimethypyridine Adsorption on the Pt(100)-(5×1) Surface

Adsorption of pyridine on the Pt(100)-(5×1) surface causes a WFC of -2.4 V indicating that the nitrogen's lone electron pair is extensively involved in the interaction between substrate and adsorbate. This hypothesis is confirmed by experiments done with 2,6-dimethylpyridine and 3,5-dimethylpyridine. The nitrogen lone pair is sterically hindered from interaction with the surface in 2,6-dimethylpyridine. The WFC on adsorption of 3,5-dimethylpyridine was -2.2 V. The WFC on adsorption of 2,6-dimethylpyridine is -1.5 V indicating little involvement of the nitrogen lone electron pair. Thus it appears that pyridine on the Pt(100) is adsorbed with its ring perpendicular or nearly perpendicular to the surface.

With heating the disordered pyridine layer forms a very poorly ordered $(\sqrt{2} \times \sqrt{2})R45°$ structure. Pyridine is too large to fit in this unit cell, therefore it appears that the diffraction information is incomplete because of poor order.

E. Cyclohexane, Cyclohexene, 1,3-Cyclohexadiene and Benzene Adsorption

1. Cyclohexane and Cyclohexene Adsorbed on the Pt(111) Surface

Cyclohexane adsorbed on the Pt(111) surface at low pressure (6×10^{-9} Torr recorded pressure) causes a WFC of -1.2 V. With increased pressure (4×10^{-7} Torr recorded pressure) the magnitude of WFC decreases to -.7 V and a disordered adsorbed layer forms. Cyclohexene adsorbed on the Pt(111) surface causes a WFC of -1.7 V and forms a $\begin{vmatrix} -2 & 2 \\ 4 & 4 \end{vmatrix}$ structure. Thus it seems apparent that cyclohexane is not adsorbed in the same manner as cyclohexene. That is, cyclohexane is not doubly dehydrogenated and adsorbed as an olefin at 20°C. Single dehydrogenation followed by interaction with the surface through the dehydrogenated site seems to be the most likely possibility. Using this type of bonding the transition which occurs at high pressure can be easily explained by examining the availability of several ring orientations relative to the surface. It appears that with increased pressure the adsorbed cyclohexanes "stand up" with respect to the surface. This transition may be caused by the repulsive interaction of the adsorbate molecules as the number of adsorbate molecules per unit surface area increases with increased organic vapor pressure. Cyclohexene forms a $\begin{vmatrix} -2 & 2 \\ 4 & 4 \end{vmatrix}$ structure and causes a WFC of -1.7 V on adsorption. The large WFC on

adsorption indicates interaction of the π-electrons with the metal surface. A possible configuration for the $\begin{vmatrix} -2 & 2 \\ 4 & 4 \end{vmatrix}$ structure is shown in Fig. IV-7. The structure has been constructed using the criteria and assumptions discussed in Section IV-A-2. Note that cyclohexene has several possible ring conformations; we have used the one with the smallest projected area without allowing dehydrogenation. The structure allows fairly close approach of the unsaturated carbon-carbon bond to the metal surface. However, it may be possible for double dehydrogenation of the cyclohexene to occur and allow even closer approach of the unsaturated bond to the surface. This would allow further reorientation and even smaller surface area per adsorbate molecule. It would also allow σ-bonding between substrate and adsorbate. (In this case the formation of an acetylenic π-bonded surface species seems unlikely without ring rupture since a six-membered ring cannot remain intact with four linear carbon atoms.) The behavior of the WFC with exposure (a slight slow decrease in magnitude of the WFC at high pressure) indicates that slight reorientation of the ring system is occurring without major chemical changes. Ethylene, a case for which dehydrogenation on adsorption at 20°C seems likely, displays a slow increase in magnitude of the WFC with exposure. However, it may be possible for double dehydrogenation of the cyclohexene to occur and allow even closer approach of the double bond to the surface as well as allowing σ-bonding between substrate and adsorbate.

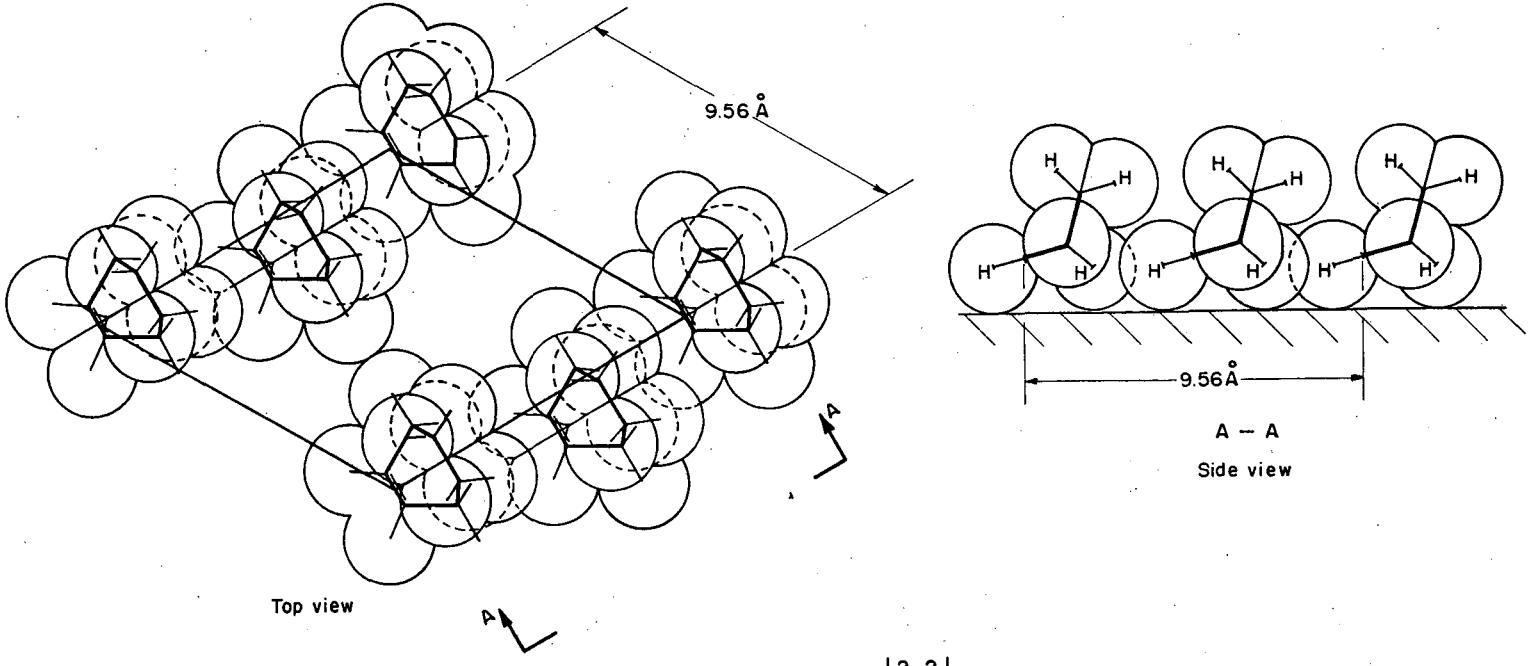

Fig. IV-7. A schematic diagram indicating a possible orientation of cyclohexene on the Pt(111) surface. The carbon-carbon double bond is near the surface.

With heating to 150°C in flux, cyclohexane and cyclohexene both cause an apparent (2×2) surface structure with diffuse diffraction features. The magnitude of the WFC increases to -1.1 V for cyclohexane and decreases for cyclohexene to -1.6 V. With further heating to 300°C the magnitude of the WFC increases to -1.4 V for cyclohexane and decreases for cyclohexene to -1.5 V. Both adsorbed layers are disordered at 300°C.

The marked increase in the magnitude of the WFC for cyclohexane from -.7 V at 20° to -1.4 V at 300°C indicates that dehydrogenation is occurring with heating. The fact that the magnitude of the WFC does not increase even more is probably caused by partial decomposition of the adsorbed layer to small fragments or amorphous carbon with heating. The identical diffraction patterns at 150°C are further evidence that dehydrogenation of the cyclohexane is occurring with heating. The small change in WFC value for cyclohexene with heating from 20°C to 150°C implies that little change is occurring in the bonding between the adsorbed layer and the substrate for cyclohexene. Thus it appears that the apparent (2×2) cyclohexene structure may be a disordered $\begin{vmatrix} -2 & 2 \\ 4 & 4 \end{vmatrix}$ surface structure or a $\begin{vmatrix} -2 & 2 \\ 4 & 4 \end{vmatrix}$ surface structure which is unresolved by LEED because of small domain size. The apparent (2×2) cyclohexane structure may be due to the same sort of disordered structure. The difference in WFC values observed at 150° could be explained by assuming that the cyclohexane structure is made up of approximately one half cyclohexane (high pressure form) and one half cyclohexene; that is, at 150°C the dehydrogenation was not complete.

2. 1,3-Cyclohexadiene and Benzene Adsorbed on the Pt(111) Surface

1,3-Cyclohexadiene on the Pt(111) surface apparently loses two hydrogens and is converted to benzene on the surface. 1,3-Cyclohexadiene causes the same sequence of surface structures as benzene. Initially the adsorbed layer is disordered, then the $\begin{vmatrix} -2 & 2 \\ 4 & 4 \end{vmatrix}$ forms and with further exposure the $\begin{vmatrix} -2 & 2 \\ 5 & 5 \end{vmatrix}$ structure forms. The WFC values for these three structures are similar to those observed for benzene adsorption (± .1 V). The deviations in the WFC value can be easily explained by considering that part of the surface may be covered with hydrogen from the dehydrogenation of 1,3-cyclohexadiene. In fact the transformation takes a significantly longer time for 1,3-cyclohexadiene than for benzene. This may also be a result of increased surface hydrogen concentration for the 1,3-cyclohexadiene case. For a detailed explanation of the benzene structures see Section IV-B-1. In brief the benzene first forms a π-bond with the surface (disordered surface structure, WFC = -1.8 V) and the final adsorbed state involves a singly dehydrogenated benzene σ-bonded to the surface ($\begin{vmatrix} -2 & 2 \\ 5 & 5 \end{vmatrix}$ surface structure, WFC = -.7 V)

3. The Pt(111) Surface and Cyclohexane Conversion to Benzene

The Pt(111) surface seems capable of catalyzing the conversion of cyclohexane to cyclohexene at elevated temperatures but not cyclohexane or cyclohexene to benzene. However, 1,3-cyclohexadiene converts to benzene at room temperature. The primary difference between cyclohexane, cyclohexene and 1,3-cyclohexadiene is adsorption geometry. Both cyclohexane and cyclohexene adsorbed on the Pt(111)

surface may have little "contact" with the surface since they may adsorb in a "standing up" position. That is, several of the carbons are far removed spatially from the metal surface because of the conformations of the ring systems. Cyclohexadiene on the other hand is locked in a planar configuration so that all carbons are in intimate contact with the surface. In essence the activation barrier for dehydrogenation is reduced dramatically for 1,3-cyclohexadiene because the metal can interact with the portions of the molecule where dehydrogenation must occur. This comes about because the ring system is rigid and the molecule is π-bonded parallel to the surface. For cyclohexane and cyclohexene the activation barrier is increased at high pressure (10^{-6} Torr surface pressure) since the molecules "stand up" on the surface because of repulsive interaction between adsorbate molecules.

4. Cyclohexane and Cyclohexene on the Pt(100)-(5×1) Surface

Cyclohexane adsorbed on the Pt(100) surface goes through a transition with increasing organic pressure similar to that observed on the Pt(111) surface. Adsorption at low pressure (6×10^{-9} Torr recorded pressure) causes a WFC of -.75 V while the (5×1) surface structure remains. Increasing the cyclohexane pressure (to 4×10^{-7} Torr recorded pressure) causes the magnitude of the WFC to decrease and also causes the (5×1) surface structure to disappear and a diffuse (2×1) diffraction pattern to form. Cyclohexene adsorbed on the Pt(100)-(5×1) surface causes the disappearance of the (5×1) and the appearance of a diffuse (2×1) surface structure; the WFC on adsorption is -1.6 V.

Even though the diffraction patterns are similar, the large difference in the WFC indicates a marked difference in the bonding characteristics between substrate and adsorbate for the two cases. The similar diffraction patterns may indicate similar geometries of adsorption for the two adsorbates, however, cyclohexane is not adsorbed as a doubly dehydrogenated olefinic species at room temperature. Single dehydrogenation followed by interaction with the surface through the dehydrogenated site seems to be the most likely possibility. The transition which occurs with cyclohexane adsorption may be rationalized by considering possible ring orientations relative to the metal surface. It appears that with increased pressure the adsorbed cyclohexane molecules "stand up" with respect to the metal surface. This transition may be caused by repulsive interaction between adsorbates as the density (number of adsorbates per unit surface area) in the adsorbed layer increases with increasing organic vapor pressure. The large WFC on adsorption (-1.6 V) of cyclohexene imples that π-bonding is occurring between substrate and adsorbate.

With heating in flux to 150°C both cyclohexane and cyclohexene cause the formation of a streaked (2×1) diffraction pattern. The magnitude of the WFC increases to -1.2 V (from -.4 V) for cyclohexane and decreases slightly for cyclohexene to -1.5 V. With further heating to 300°C the magnitude of the WFC increases slightly for both cyclohexane (-1.5 V) and cyclohexene (-1.6 V).

The marked increase in the magnitude of the WFC for cyclohexane from -.4 V to -1.5 V at 300°C indicates that dehydrogenation is occurring with heating. The fact that the WFC values are very similar

at 300°C indicates that a large portion of the adsorbed cyclohexane layer is adsorbed in the same manner as cyclohexene at 300°C. In fact the identical ordered structures observed at 150°C indicate that the adsorption geometry is similar for these two compounds at 150°C. Thus it seems that at elevated temperatures cyclohexane may be converted to cyclohexene.

5. Adsorption of 1,3-Cyclohexadiene and Benzene on the Pt(100)-(5×1) Surface

Adsorption of 1,3-Cyclohexadiene on the Pt(100)-(5×1) surface causes a WFC and diffraction pattern very similar to those caused by benzene adsorption on this surface. Benzene causes an initial WFC of -1.6 V which decreases to -1.3 V with exposure. 1,3-Cyclohexadiene causes an initial WFC of -1.7 V which decreases to -1.4 V with exposure. Both adsorbates cause surface structures with a periodicity twice the underlying lattice. Thus it appears that 1,3-cyclohexadiene is converted to benzene on the Pt(100)-(5×1) although the evidence is certainly not as detailed as the data on the Pt(111) surface.

6. The Pt(100) Surface and the Conversion of Cyclohexane to Benzene

The Pt(100) surface seems capable of catalyzing the conversion of cyclohexane to cyclohexene at elevated temperature but not the conversion of cyclohexane or cyclohexene to benzene. However, 1,3-cyclohexadiene is converted to benzene at room temperature. The primary difference between cyclohexane, cyclohexene and 1,3-cyclohexadiene appears to be adsorption geometry. 1,3 Cyclohexadiene adsorbs parallel to the surface because the ring is rigid and π-bonding occurs. The

ease with which conversion of 1,3-cyclohexadiene to benzene takes place may be explained because the portion of the molecule which must be dehydrogenated is in close proximity of the metal surface. The activation barrier for cyclohexane and cyclohexane appears to be high because the molecules "stand up" with high pressure (10^{-6} Torr surface pressure) and the part of the molecule which must be dehydrogenated is some distance from the surface.

Judging solely from WFC results it appears that the Pt(100) surface is a better catalyst for the reaction cyclohexane → cyclohexene than the Pt(111) surface. The (111) surface may be less selective and more reactive (leading to decomposition of the reactant) or simply less reactive since the WFC results indicate only that the Pt(100) surface is covered by a larger portion of cyclohexene than the Pt(111) surface at 150°C and 300°C.

F. Adsorption of Substituted Aromatic Molecules

1. Generalizations

The aromatic molecules which have small substituent groups or high rotational symmetry form more ordered overlayers under the experimental conditions employed. Thus, the shape of the adsorbate molecules and the rotational symmetry of the substrate determines the degree of ordering which occurs in the adsorbed layer.

We have also found that the WFC on adsorption and the degree of ordering in the overlayer varies with the initial rate of growth of the adsorbed layer which can be varied by changing the incident vapor flux.

The slower the rate of growth (smaller the incident flux), the larger the WFC change and the more ordered the overlayer for substituted aromatics. These observations seem to indicate that with low incident vapor flux the density of the adsorbed layer may be increased because of more efficient packing in the ordered overlayer. With slow growth rates, the size of the ordered domains is being increased in the adsorbed layer, leading to an increase in the density of surface sites occupied by the adsorbate.

Both of these observations (1. High symmetry promotes ordered surface structure formation. 2. Slow growth of the adsorbed layer promotes ordered structure formation.) can be explained by a simple model of ordering for adsorbed aromatic systems on Pt surfaces. Ordered adsorption for these large molecules may proceed by a two-step mechanism. Initially the aromatic molecules may adsorb on the surface in a disordered fashion. The second step involves ordering of the adsorbed layer and indicates the importance of surface diffusion (either translational or rotational) in this ordering process. If the adsorbate has a shape which approximates a circular cross section, reorientation into ordered layers is less difficult than reorientation of adsorbates with bulky side groups. Slow deposition of the overlayer allows adsorbed molecules more reorientation time before they become locked into place by a large number of neighbors. This type of ordering should be distinguished from ordering caused by site adsorption. Site adsorption involves adsorption into a specific surface site in a specific orientation. Ordering results because the surface sites are ordered. During site adsorption, adsorption and ordering occur

simultaneously.

The WFC observed on adsorption ranges from -1.4 V for nitrobenzene to -1.8 V for aniline. Charge transfer of such magnitude indicates extensive interactions of the aromatic π systems with the substrate.

The interpretation of the diffraction information in these studies has been complicated by the absence of well-defined diffraction features. The diffraction features may be characteristic of the size and orientation of the unit cell in the ordered adsorbed layer or they may be characteristic of a coincidence distance between the adsorbed lattice and the substrate lattice. Studies involving ordered adsorption of organic molecules on single crystal platinum surfaces have indicated that either situation may occur. Specifically, benzene forms coincidence lattices on the Pt(111) surface while naphthalene forms a structure for which molecular size is easily related to the unit mesh determined from the diffraction pattern. With these facts in mind, we have used the available chemical information, molecular dimensions, the observed WFC and the diffraction information to analyze the nature of the interaction between adsorbate and substrate.

2. Toluene m-xylene, Mesitylene, t-butylbenzene, and n-butylbenzene Adsorption on the Pt(111) Surface

a. Work function change. The maximum WFC observed on adsorption for these compounds range from -1.5 V for n-butylbenzene to -1.8 V for m-xylene. This large electron transfer from the adsorbed molecules to the metal substrate implies that the polarizable π electrons are involved extensively in the interaction between adsorbate and substrate. The similarity of the WFC on adsorption for this family of compounds

also indicates that the primary interaction occurs between the aromatic π system and the substrate surface since the benzene ring is the only structural entity common to all molecules in the series. If the aromatic π system is the primary interaction center, it follows that the adsorption geometry should be similar for this family of compounds. In the absence of dehydrogenation the aromatic systems would be expected to adsorb parallel or nearly parallel to the substrate surface so that the aromatic π system could efficiently interact with the substrate surface.

That these aromatic systems are adsorbed parallel or nearly parallel to the surface is further supported by the results of the mesitylene adsorption studies carried out at low pressure (10^{-9} Torr). Each aromatic hydrogen in mesitylene has adjacent methyl groups. Since methyl groups are known to deactivate the exchange of adjacent hydrogens in hydrogen-deuterium exchange studies, there should be little chance for dehydrogenation of the aromatic hydrogens and for subsequent interaction of the dehydrogenated site with the surface to form σ (electron pair) bonds. Excluding demethylation, the only alternative for interaction appears to be π-bonding with the substrate surface. That is, mesitylene should be fairly inactive toward any type of interaction except π-bonding. The fact that its WFC on adsorption is similar to the WFC of other aromatic adsorbates supports our contention that the primary interaction occurs via π-bonding.

N-butylbenzene induces the smallest WFC on adsorption; the WFC on adsorption also depends markedly on the growth rate of the adsorbed layer. Both of these effects are caused by the presence of the long side chain which makes efficient packing in the surface plane difficult.

b. Diffraction studies. The diffraction patterns observed for this family of compounds indicate poor ordering of the adsorbed layer. For the series toluene, m-xylene, mesitylene adsorbed at room temperature, streaked diffraction features appear at 1/3, 1/2.6, 1/3.4 of the distance between the (00) beam and the first order platinum features. The unit cell size impled by these streaked features does not correlate with the molecular size of the adsorbed species since they are listed in order of increasing size above (the distance to the first order diffraction should vary inversely with the size of the unit cell). However, the diffraction patterns become better ordered in the series toluene, m-xylene, mesitylene. T-butylbenzene and n-butylbenzene on the other hand form disordered adsorbed layers. Thus, it appears that large π-bonded adsorbed molecules of the same rotational multiplicity order more easily in the absence of long side-chains.

Detailed information concerning molecular orientation cannot be extracted from the diffraction patterns since poorly ordered layers are formed. However, it seems worthwhile to point out that toluene adsorbed parallel to the surface fits into the (3×3) unit cell observed while m-xylene and mesitylene do not fit into the (2.6×2.6) and (3.4×3.4) unit cells, respectively, which can be deduced from the diffraction features. The Pt(111)-(4×2)-toluene structure which forms at 150°C does not have a large enough unit cell to accommodate toluene

adsorbed parallel to the surface even though the WFC observed seems to support this adsorption geometry. However, for all cases mentioned above the diffraction features are diffuse since the layers were poorly ordered; therefore, caution must be exercised in attempting to deduce much structural information.

3. Toluene, b-Xylene, Mesitylene, t-Butylbenzene, and n-Butylbenzene Adsorption on the Pt(100)-(5×1) Surface

a. Work function change. The maximum WFC observed on adsorption for these compounds range from -1.5 V for n-butylbenzene and mesitylene to -1.75 V for t-butylbenzene. Again, the large amount of electron transfer, the similarity of the WFC on adsorption for the entire series, and the fact that the WFC for mesitylene adsorbed at low pressures is similar to the WFC observed for the other compounds in the series indicates that the interaction occurs predominantly between the metal and the π electron cloud of the adsorbate.

The WFC on adsorption of n-butylbenzene depends markedly on the growth rate of the adsorbed overlayer. It appears that this is due to the long side chain which makes reorientation of the adsorbed molecules difficult.

b. Diffraction studies. Ordered adsorption on the Pt(100)-(5×1) surface seems to be correlated with the persistance of the (5×1) surface structure for these large π-bonded adsorbates. That is, if the (5×1) surface structure remains detectable after adsorption the adsorbed layer will be fairly well-ordered. On adsorption of toluene, m-xylene, and mesitylene, streaked 1/3 order diffraction features appear which co-exist with the diffraction features due to the (5×1)

surface structure. Upon gentle heat treatment, both the (5×1) surface structure and 1/3 order streaks disappear leaving a (1×1) pattern with increased background intensity. On adsorption n-butylbenzene initially causes the appearance of diffuse streaked 1/3 order features along with a decrease in the intensity of the diffraction beams due to the presence of the (5×1) surface structure. With continued exposure both the (5×1) surface structure and the 1/3 order streaks are replaced by a (1×1) pattern with increased background intensity indicating disordered adsorption. T-butylbenzene forms a disordered overlayer on adsorption and the (5×1) surface structure reverts to a (1×1) sturcture with high background intensity. During this order-disorder transformation in the adsorbed layer while the substrate surface structure is also changing from (5×1) to (1×1), no significant work function change takes place.

The (5×1) surface structure may be due to the formation of a hexagonal platinum overlayer on top of the square surface unit cell expected by projecting the bulk structure onto the surface plane.[9,10,11] This model explains the observed order-disorder transformation upon changes of substrate structure since a hexagonal surface (even one formed by reconstruction) might be expected to yield more ordered overlayers. It should be noted that several ordered surface structures have been observed on the Pt(100)-(1×1) surface even though the (5×1) structure has relaxed. We have observed structures for CO, ethylene acetylene, benzene, and pyridine on the Pt(100)-(1×1) surface structure. These molecules appear to order via the one-step site mechanism. That

is, the adsorption occurs with the molecules in a specific orientation at a specific surface site. The bonding arguments made for CO, ethylene and acetylene by other authors[12,13,14] supports this contention. Benzene and pyridine appear to interact with the (100) via the formation of an electron pair bond to the Pt(100) surface.

During the adsorption of mesitylene at high pressure (4×10^{-7} Torr), a pressure induced transition occurs on both low index platinum surfaces. The WFC decreases, and the LEED pattern becomes markedly different (on the Pt(111) a disordered layer forms; on the (100) surface the (5×1) structure converts to the (1×1)). A change in the nature of interaction between the substrate and adsorbate is occurring which depends on the incident vapor flux. A comparison with the results obtained for benzene seems to indicate that a $\pi \rightarrow \sigma$ bond transition may be occurring. This may be due to demethylation of the aromatic ring and subsequent interaction with the surface through the demethylated carbon site or dehydrogenation of a methyl group and interaction of the substrate with the dehydrogenated site.

4. Aniline, Nitrobenzene and Cyanobenzene Adsorption on the Pt(111) Surface

a. Work function change. The WFC observed on adsorption of aniline, nitrobenzene, and cyanobenzene are -1.8 V, -1.5 V and -1.6 V, respectively. The similarity of WFC within the series and also the similarity to the WFC on adsorption of the other hydrocarbons studied supports the contention that these molecules also interact primarily by forming a π bond with the substrate surface. That is, they adsorb with the benzene ring parallel or nearly parallel to the surface.

Nitrobenzene appears to decompose in the electron beam when adsorbed on the Pt(111) surface since the WFC and diffraction pattern both change with electron beam exposure at moderate voltages (30 V).

b. Diffraction studies. The diffraction patterns observed on adsorption are poorly ordered for this group of compounds. All three molecules cause the appearance of 1/3 order features in the diffraction pattern. Aniline adsorption gives rise to streaked diffraction features at 1/3 order along with streaks extending radially to (1/2 0) positions. This diffraction pattern seems to be the result of a poorly ordered complex structure. Adsorption of nitrobenzene and cyanobenzene cause the formation of diffuse 1/3 order diffraction features. Both of these molecules, adsorbed with their benzene ring parallel to the metal surface, fit into a (3×3) unit cell. However, the diffraction patterns indicate a great deal of disorder in the adsorbed layer and the diffuse diffraction features might obscure much information necessary to interpret the surface structures.

5. Aniline, Nitrobenzene and Cyanobenzene Adsorption on the Pt(100)-(5×1) Surface

a. Work function change. The WFC's on adsorption of aniline, nitrobenzene and cyanobenzene are -1.75 V, -1.4 V and -1.5 V, respectively. The similarity of the WFC within the series and the similarity to the WFC on adsorption of the other hydrocarbons studied supports the contention that these molecules also interact primarily by forming a π bond with the substrate surface. We expect the molecules to be adsorbed with their benzene ring parallel or nearly parallel to the substrate surface. Nitrobenzene adsorbed on the Pt(100)-(5×1)

surface is not as sensitive to electron beam exposure as the overlayer on the Pt(111) surface. Apparently small changes in the interaction between substrate and adsorbate can markedly affect the electron beam sensitivity of the adsorbed layer.

b. Diffraction studies. These compounds form disordered overlayers on adsorption.

G. Acetylene, Ethylene, and Propylene Adsorption

1. Acetylene, Ethylene and Proplyene Adsorbed on the Pt(111) Surface

A substantial body of experimental data exists concerning ethylene and acetylene adsorption on the Pt(111) surface.[12,13,14] A recent paper by Weinberg, Deans and Merril[13] reviews the relevant data and proposes a detailed adsorption model for ethylene and acetylene on the Pt(111) surface. In short they conclude that ethylene is adsorbed dissociatively, while acetylene remains intact on adsorption and that both form a (2×2) surface structure. There is a second layer of reversibly adsorbed ethylene on top of the dissociatively adsorbed first layer. This reversibly adsorbed ethylene desorbs at 100°C. The hydrogen resulting from ethylene dissociation desorbs at 200°C and the adsorbed layer of acetylenic residue consolidates above this temperature. They also conclude that the adsorbed acetylene (2×2) structure is not stable with respect to acetylene exposure since more acetylene may adsorb in vacant interstitial sites and cause the adsorbed layer to become disordered. However the ethylene (2×2) structure is stable to acetylene exposure since the dissociated

hydrogens block the interstitial sites.

The results of the present experiments do not contradict any of the above conclusions. In fact several new experimental facts support various conclusions made above.

The adsorption of ethylene and acetylene on the Pt(111) surface induces the formation of a (2×2) surface structure. The acetylene (2×2) structure rapidly becomes disordered with further exposure to acetylene flux (completely disordered with ~ 40L). The ethylene (2×2) surface structure was not affected by further exposure to ethylene flux. The WFC observed for the acetylene (2×2) structure is -1.5 V and the WFC observed with ethylene adsorption is -1.5 V. The similarity of the WFC on adsorption is a strong indication that in the adsorbed state these molecules are very similar. That is, on adsorption ethylene dissociates into acetylene and two adsorbed hydrogens while acetylene adsorbs associatively. The two adsorbed structures may behave in a different manner with exposure to flux because the hydrogen on the surface from dissociation of the ethylene may inhibit further adsorption of ethylene which might cause the adsorbed layer to become disordered. This hypothesis is born out by the WFC results. As the (2×2) acetylene structure is exposed to further acetylene flux, the pattern becomes that expected from a disordered layer and the magnitude of the WFC slowly increases to -1.65 V indicating an increase in the density of adsorbed species on the surface. Further exposure of the ethylene structure to ethylene flux results in no change in the work function indicating no change in the density of the adsorbed layer.

With heating in vacuum the density of the adsorbed acetylene layer remains essentially constant up to 150°C (the highest temperature used) as indicated by no variation of the WFC. However, the density of the adsorbed ethylene layer decreases markedly with heating in vacuum above 100°C as indicated by a marked decrease in the magnitude of the WFC. Weinberg, Deans and Merril[13] attribute this low temperature desorption to a second layer of reversibly adsorbed ethylene which is adsorbed on top of the acetylenic first layer.

Heating the adsorbed acetylene layer in flux up to approximately 150°C causes a maximum to occur in the magnitude of the WFC (-1.8 V) indicating an increase in density of the adsorbed layer. Heating the adsorbed ethylene layer in flux causes a maximum in the magnitude of the WFC of -1.7 V at approximately 250°C indicating an increase in the density of the adsorbed layer. These increases in density may be caused by increased surface mobility which may result in increased packing efficiency. Hydrogen is known to desorb from ethylene covered Pt(111) surfaces at approximately 200°C.[12,13] Thus the presence of surface hydrogen for the adsorbed ethylene case appears to limit the adsorbate surface density until substantial hydrogen disorption has occurred. Propylene adsorbed on the Pt(111) surface causes the formation of a (2×2) structure; the WFC on adsorption is -1.3 V. These results suggest that propylene may not become dissociated on adsorption at 20°C. Propyne and two atomic hydrogens take up an area larger than the (2×2) unit cell. The magnitude of the WFC is smaller than that observed for ethylene while the density of the adsorbed layer is the

same (one molecule per (2×2) unit cell). In fact propylene just fits into a (2×2) unit cell (using 1.2 Å for the Van der Waals radius of H and 2.0 Å for the Van der Waals radius of CH_3). Thus it appears that propylene may adsorb intact on the Pt(111) surface at 20°C.

The discrepancy between the WFC results found by Morgan and Somorjai[12] and those found in the current study can be explained by considering the differences in experimental procedures and equipment used. The work of Morgan and Somorjai was often preformed on samples which were cleaned only by heating between adsorption experiments. This procedure produces carbon contaminated surfaces which do not adsorb as much gas as clean surfaces therefore the magnitude of the WFC observed on adsorption would be expected to be smaller than the WFC observed with adsorption on a clean surface. The system used had a high CO background since Ti sublimation pumping was not employed. Carbon monoxide is known to displace adsorbed olefins,[12] displacement would also lead to a reduction in the WFC observed.

2. Acetylene, Ethylene and Propylene Adsorbed on the Pt(100)-(5×1) Surface

The adsorption of ethylene or acetylene on the Pt(100)-(5×1) surface causes the formation of a $(\sqrt{2} \times \sqrt{2})R45°$ surface structure. The WFC on adsorption is -1.65 V for acetylene and -1.2 V for ethylene. The WFC values seem to indicate that these molecules adsorb as distinct chemical species. That is, it appears that ethylene adsorbs associatively at 20°C on the Pt(100)-(5×1) surface.

The diffraction pattern resulting from the $(\sqrt{2} \times \sqrt{2})R45°$ surface structures have diffuse (1/2 1/2) diffraction features but well defined (10) features. The broadening of diffraction features results from the existence of adsorbate domain boundaries.[15] The structure of certain types of antiphase domain boundaries can be simply related to the symmetry of the adsorption sites occupied by adsorbate molecules on the surface.[15] The type of broadening observed for ethylene and acetylene implies that adsorption is occurring in a four-fold symmetric site. An analysis for $(\sqrt{2} \times \sqrt{2})R45°$ structures on square symmetric substrate unit cells has been done by R. L. Park.[15]

Heating the adsorbed acetylene layer in flux to approximately 150°C causes a slight maximum to occur in the magnitude of the WFC (-1.7 V) indicating a slight increase in the density of the adsorbed layer. Heating the adsorbed ethylene layer in flux to 250°C causes a maximum to occur in the magnitude of the WFC (-1.5 V) indicating an increase in the density of the adsorbed layer and/or partial dehydrogenation of the adsorbed layer. Hydrogen is known to desorb from ethylene covered Pt(100)-(5×1) surfaces at approximately 200°C;[12] the desorption of hydrogen implies partial dehydrogenation of the adsorbed ethylene. Since desorption of hydrogen is occurring, an increase in the density of the adsorbed layer could be easily accomplished by further ethylene adsorption from the gas phase. The similarity of the WFC values at 250°C (-1.65 for acetylene and -1.5 V for ethylene) seems to indicate that the adsorbed layers are similar after heat treatment.

Propylene adsorbed on the Pt(100)-(5×1) surface causes the appearance of diffuse 1/2 order streaks and a WFC of -1.2 V. This seems to imply associate adsorption for propylene since the WFC results are identical with those observed for ethylene adsorption.

The discrepancy between the WFC reported here and those reported by Morgan and Somorjai[12] may be due to the fact that in earlier work cleaning was carried out between adsorption runs by heating the surface in vacuum, which is now known to produce carbon contaminated surfaces. Carbon monoxide displacement of adsorbed olefins may also have occurred.

H. Adsorption of Nitrogen Containing Heterocycles

1. Generalization Resulting from Work Function Changes for Nitrogen Heterocycles Adsorbed on the Pt(111) and Pt(100)-(5×1) Surfaces

The compounds studied fall into two groups when viewed in terms of work function change observed on adsorption. The first group appears to interact with the Pt surfaces primarily by forming a π bond; these compounds cause a WFC on adsorption approximately inversely proportioned to their respective first ionization potential. Pyrrole, quinoline, isoquinoline, and 2,6-dimethylpyridine are members of this group. Therefore these compounds appear to be adsorbed parallel or nearly parallel to the metal surface. These compounds have permanent dipoles ranging from 1.6 D to 2.8 D which if aligned perpendicular to the surface might cause unexpected work function changes.

The remaining compounds pyridine, piperidine, and 3,5-dimethylpyridine apparently interact with the surface via their basic nitrogen since they cause large work function changes on adsorption. That is, these compounds are better electron donors than expected from the magnitude of their ionization potential. As mentioned in the pyridine section (IV-D) the large WFC may be due to actual electron transfer from the adsorbate to substrate and/or alignment of the permanent dipoles of the adsorbate with the positive end away from the surface. In either case the adsorption geometry involves adsorption through the basic nitrogen with the ring system aligned perpendicular or nearly perpendicular to the metal surface.

2. Nitrogen Heterocycles Adsorbed on the Pt(111) Surface

Pyridine and the dimethylpyridines adsorbed on the Pt(111) surface have been discussed in detail in Section IV-D. In brief, the results for 20°C adsorption, show that pyridine and 3,5-dimethylpyridine adsorb perpendicular or nearly perpendicular to the metal surface and interact with the metal surface primarily through their basic nitrogens. Interaction of 2,6-dimethylpyridine occurs through the formation of a π bond with the metal surface since the basic nitrogen is sterically hindered from interaction with the metal surface by two adjacent methyl groups.

The diffraction patterns resulting from adsorption of quinoline and isoquinoline on the Pt(111) surface at 20°C are similar to the diffraction pattern resulting from naphthalene adsorption at 20°C. The WFC on adsorption of isoquinoline (-1.9 V) is also similar to

the WFC observed on naphthalene adsorption (-1.95 V) implying similar adsorption geometry, however, the WFC on adsorption of quinoline (-1.45 V) is unexpectedly small. The diffraction results for quinoline and isoquinoline support the contention that these compounds interact with the surface primarily via π-bonding. The WFC observed on adsorption of quinoline suggests that other effects may be occurring; more complete experimental work is necessary before detailed interpretations can be made.

The WFC on adsorption of pyrrole (-1.45 V) indicates that pyrrole is interacting with the surface in a different manner than pyridine. The lone electron pair of the nitrogen is delocalized into the electron deficient aromatic system in pyrrole, therefore the nitrogen is not as basic (electron rich) as the nitrogen in pyridine. The WFC observed for pyrrole is similar to the WFC observed on adsorption of many substituted aromatic compounds. Thus it seems likely that the primary interaction occurs via π-bonding between the aromatic π electrons and the metal surface. This type of interaction implies adsorption parallel or nearly parallel to the metal surface. The diffraction pattern resulting from pyrrole adsorption displays very diffuse half order features, thus the diffraction pattern cannot be interpreted unambiguously.

The adsorption of piperidine on the Pt(111) surface causes a large WFC (-2.1) implying that the nitrogen lone pair is involved in the interaction between the adsorbate and substrate. Comparing the piperidine result with the analogous hydrocarbon, cyclohexane, which causes a WFC of -1.2 V on adsorption accentuates the importance of

the basic nitrogen in the binding. Thus it appears that the primary interaction between substrate and adsorbate occurs through an interaction of the basic nitrogen and the electron deficient metal surface.

3. Nitrogen Heterocycle Adsorption on the Pt(100)-(5×1) Surface.

Pyridine and the dimethypyridines adsorbed on the Pt(100)-(5×1) surface have been discussed in detail in section IV-D. In brief the results for 20°C adsorption show that pyridine and 3,5-dimethylpyridine adsorb perpendicular or nearly perpendicular to the metal surface and interact with the metal surface primarily through their basic nitrogens. Interaction of 2,6-dimethylpyridine occurs through the formation of a π bond with the metal surface since the basic nitrogen is sterically hindered from interaction with the surface by two adjacent methyl groups.

The WFC observed for adsorption of quinoline on Pt(100)-(5×1) surface (-1.7 V) is equal to the WFC on adsorption of naphthalene (-1.7 V) This implies that both interact with the surface in a similar manner and may have similar adsorption geometries. The WFC on adsorption of isoquinoline is unexpectedly large (-2.1 V). This may be the result of a different type of interaction between substrate and adsorbate which may lead to different adsorption geometry for isoquinoline than for quinoline and naphthalene, however, more detailed experiments are necessary before explanations can be made. The adsorbed layers of these compounds appear to be disordered.

Pyrrole adsorption on the Pt(100)-(5×1) surface causes a WFC of -1.6 V. Pyrrole has an electron deficient nitrogen since the nitrogen's lone electron pair is delocalized into the aromatic ring. Since the nitrogen is not very basic the primary interaction might be expected to occur between the π electrons and the electron deficient metal surface. Since the value of the WFC observed is similar to the WFC on adsorption of many of the substituted aromatics is seems likely that the primary interaction is π-bonding and that the molecule adsorbs parallel or nearly parallel to the metal surface. The diffraction information is too diffuse to allow unambiguous interpretation.

Piperidine adsorbed on the Pt(100)-(5×1) surface causes a large WFC (-2.05 V) on adsorption implying that the nitrogen lone pair is involved in the interaction between adsorbate and substrate. Cyclohexane, the analogous hydrocarbon, causes a WFC of -.75 V..

G. Aliphatic Adsorption on the Pt(111) and Pt(100)-(5×1) Surfaces

Cyclohexane, n-hexane, and cyclopentane adsorb on the Pt(111) surface at 20°C with organic vapor fluxes in the range 10^{-8} Torr to 10^{-6} Torr. All three compound undergo an organic vapor pressure induced transitions during which the magnitude of the WFC decreases. Comparison of the WFC data on adsorption of these aliphatics at 20° with the WFC data for adsorption of similar olefins (cyclohexene, and cyclopentene) at 20°C shows that the adsorbed state of these aliphatic molecules is certainly different than the adsorbed state of the olefins. That is, these compounds do not become doubly dehydrogenated and adsorb as olefins. With increased temperature cyclohexane and hexane (cyclopentane

was not studied) apparently become at least partially dehydrogenated as evidenced by the fact that the magnitude of the WFC increases and goes through a maximum above 200°C.

The binding involved between these aliphatics and the metal surface with 20°C adsorption may involve single dehydrogenation followed by covalent bonding and/or Van der Waals type interaction coupled with charge-transfer interaction. The resolution of this question must await the results of further experiments now in progress.[16] However, at this point it seems likely that covalent binding might well be involved in the interaction between aliphatics and low index Pt surface. Recent experiments by L. A. Firment in this laboratory have shown that propane adsorbs on both of these Pt surfaces at 20°C in the pressure rang 10^{-8} to 10^{-6} Torr.[16] This result seems to argue against physisorption since the heat of physisorption would be much smaller for propane than the heat for physisorption of hexane. [On graphitized carbon black a substrate for which physisorption predominates the heat of adsorption for hexane is -11.8 kcal/mole; [17] for propane the heat of adsorption is -5.9 kcal/mole.[17]] The possibility of dehydrogenation is supported by the observation that at elevated temperature these compounds are known to dehydrogenate on platinum.

Several explanations of the transition which occurs with pressure are possible. It seems likely that the final state involves a molecule adsorbed perpendicular or nearly perpendicular to the metal surface. The low pressure adsorbed state may involve either a physisorbed molecule adsorbed parallel to the surface or singly dehydrogenated

molecules covalently bound to the surface but adsorbed parallel or nearly parallel to the metal surface.

REFERENCES

1. D. E. Eastman, Phys. Rev. B. (Solid State) 2, 2 (1970).
2. R. Boiruman, H. P. van Keulen, W. M. H. Sachlter, Ber. Bunsenges Physik Chem. 74, 198 (1970).
3. Landolt-Bornstein Zahlenwerte und Funktionen aus Physik, Chemie, Austronomie, Geophysik und Technik 6th ed. 1(3), 509 (Springer-Verlag, Berlin, 1951).
4. F. A. Cotton, G. Wilkinson, Advanced Inorganic Chemistry, 2nd ed. (Interscience, New York, 1966).
5. R. B. Moyes, K. Baron, R. C. Squire, J. Catalysis 22, 333 (1971).
6. H. C. Brown, D. Ginits, L. Domash, J. Am. Chem. Soc. 78, 5387 (1956).
7. G. E. Calf, J. L. Garnett Aust. J. Chem. 21, 1221 (1968).
8. R. B. Moyes, P. B. Wells, J. Catalysis 21, 86 1971.
9. D. G. Fedak and N. A. Gjostein, Acta. Met. 15, 827 (1967).
10. D. G. Fedak and N. A. Gjostein, Surf. Sci. 8, 17 (1969).
11. P. W. Palmberg, in The Structure and Chemistry of Solid Surfaces Ed. G. A. Somorjai paper 29 (J. Wiley and Sons, New York, 1969).
12. A. E. Morgan, G. A. Somorjai, J. Chem. Phys. 51, 3309 (1969).
13. W. H. Weinberg, H. A. Deans, and R. P. Merrill, submitted to Surf. Sci.
14. D. L. Smith, R. P. Merrill, J. Chem. Phys. 52, 5861 (1970).
15. R. L. Park, in The Structure and Chemistry of Solid Surfaces Ed. G. A. Somorjai, paper 28 (J. Wiley and Sons, New York, 1969).

16. L. A. Firment, J. L. Gland, and G. A. Somorjai, to be submitted to Surf. Sci.

17. D. M. Young, and A. D. Crowell, Physical Adsorption of Gases (Butterworths, London 1962).

APPENDIX

The geometry of some of the molecules studied are shown in Figs. A-1 through A-12. The internuclear distances and bond angles used were taken from a compilation of structures published by the Chemical Society.* The van der Waals radius used for hydrogen is 1.2 Å† and for the methyl group is 2.0 Å†. The thickness of the aromatic ring system is taken as 3.4 Å†. These radii are typical of intermolecular distances in organic solids and have been used as upper limits for the intermolecular distance between adsorbed molecules.

---

*Table of Interatomic Distances and Configurations in Molecules and Ions. Special Publication No. 11 (The Chemical Society London, 1958). Table of Interatomic Distances and Configurations in Molecules and Ions Special Publication No. 18, (The Chemical Society, London, 1965).

†L. Pauling, The Nature of the Chemical Bond 3rd ed. (Cornell University Press, Ithaca, New York, 1960).

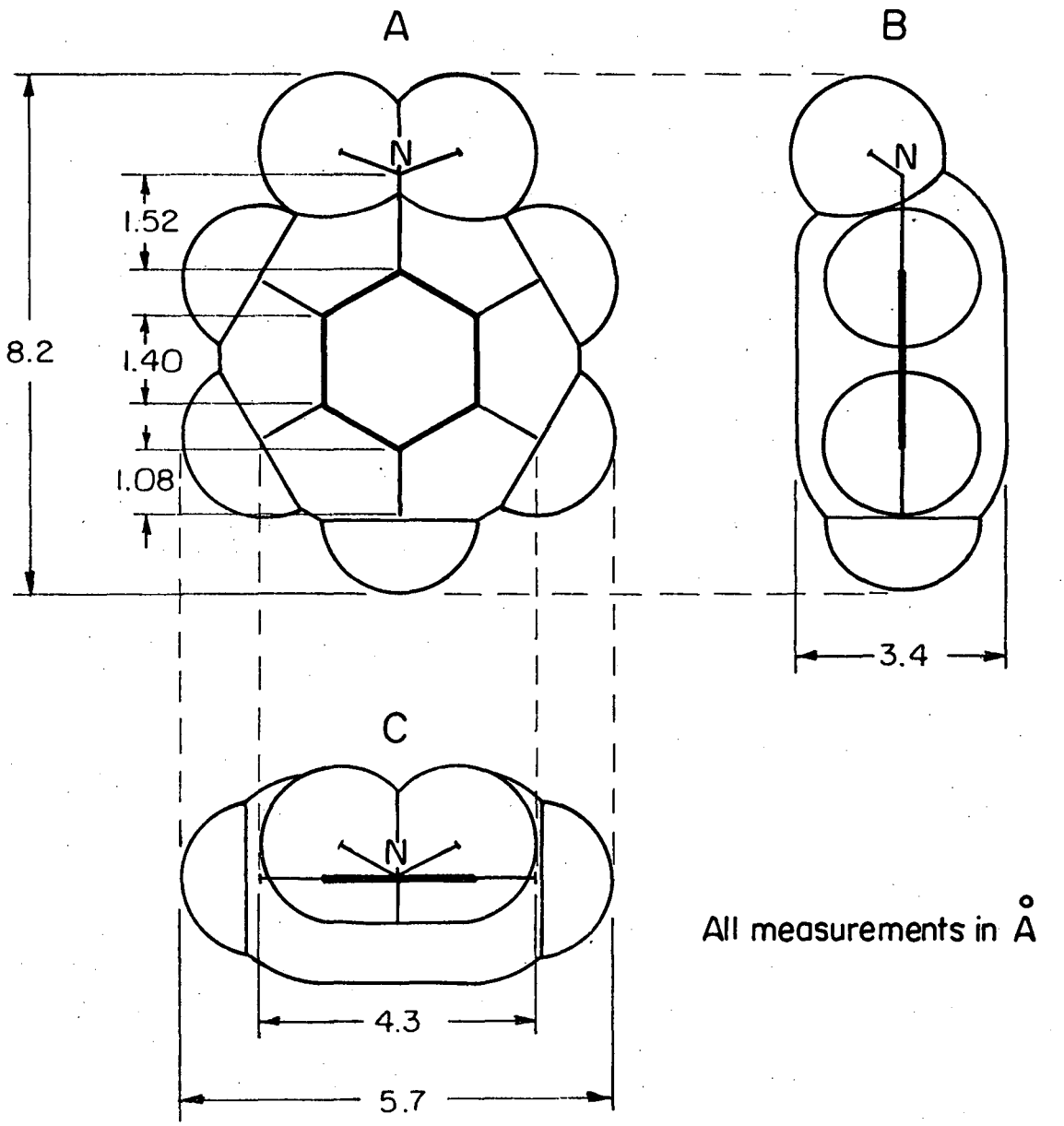

Fig. A-1. The structure of aniline with van der Waals radii shown.

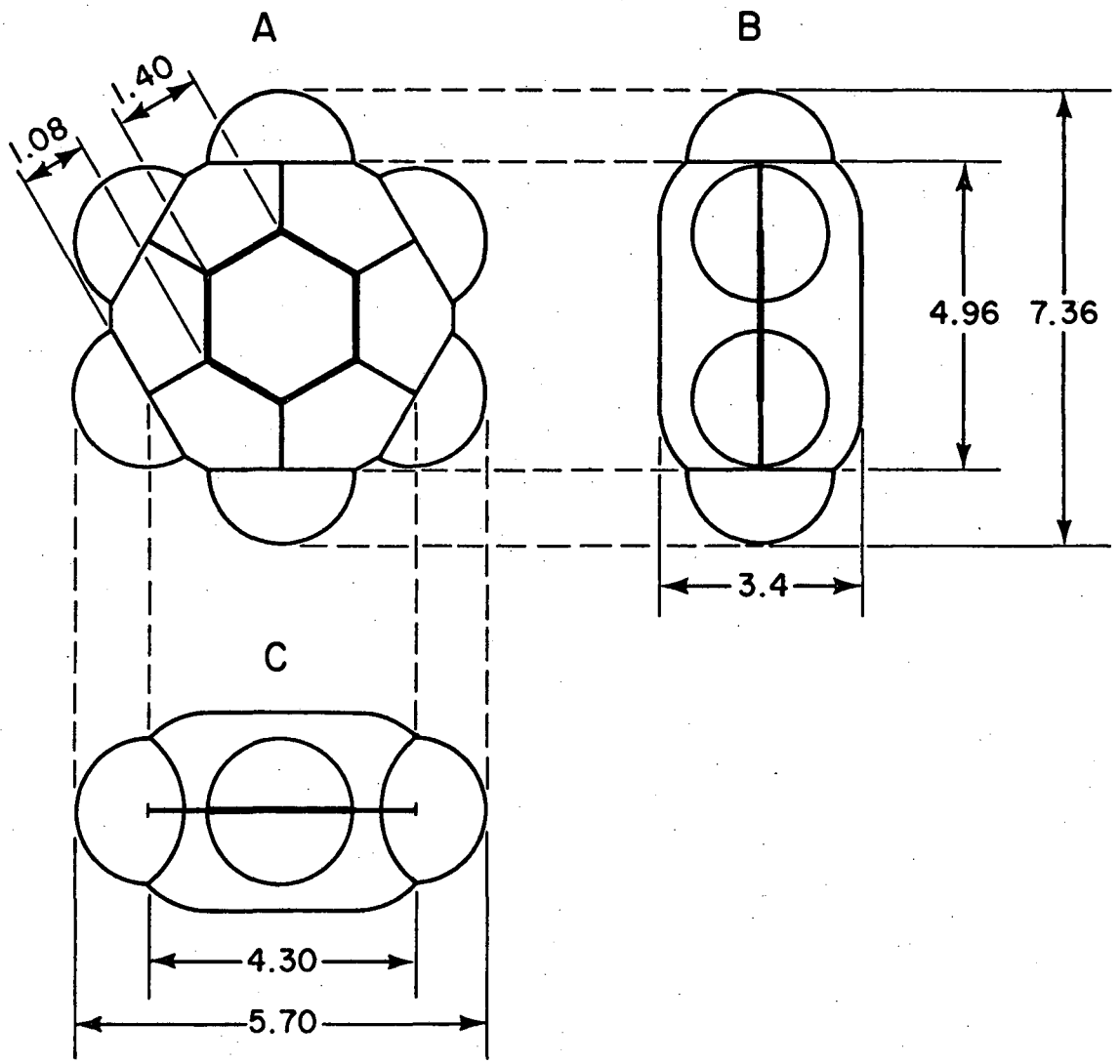

Benzene

XBL7211-7286

Fig. A-2. The structure of benzene with van der Waals radii shown.*

(* = All dimensions are in Angstroms)

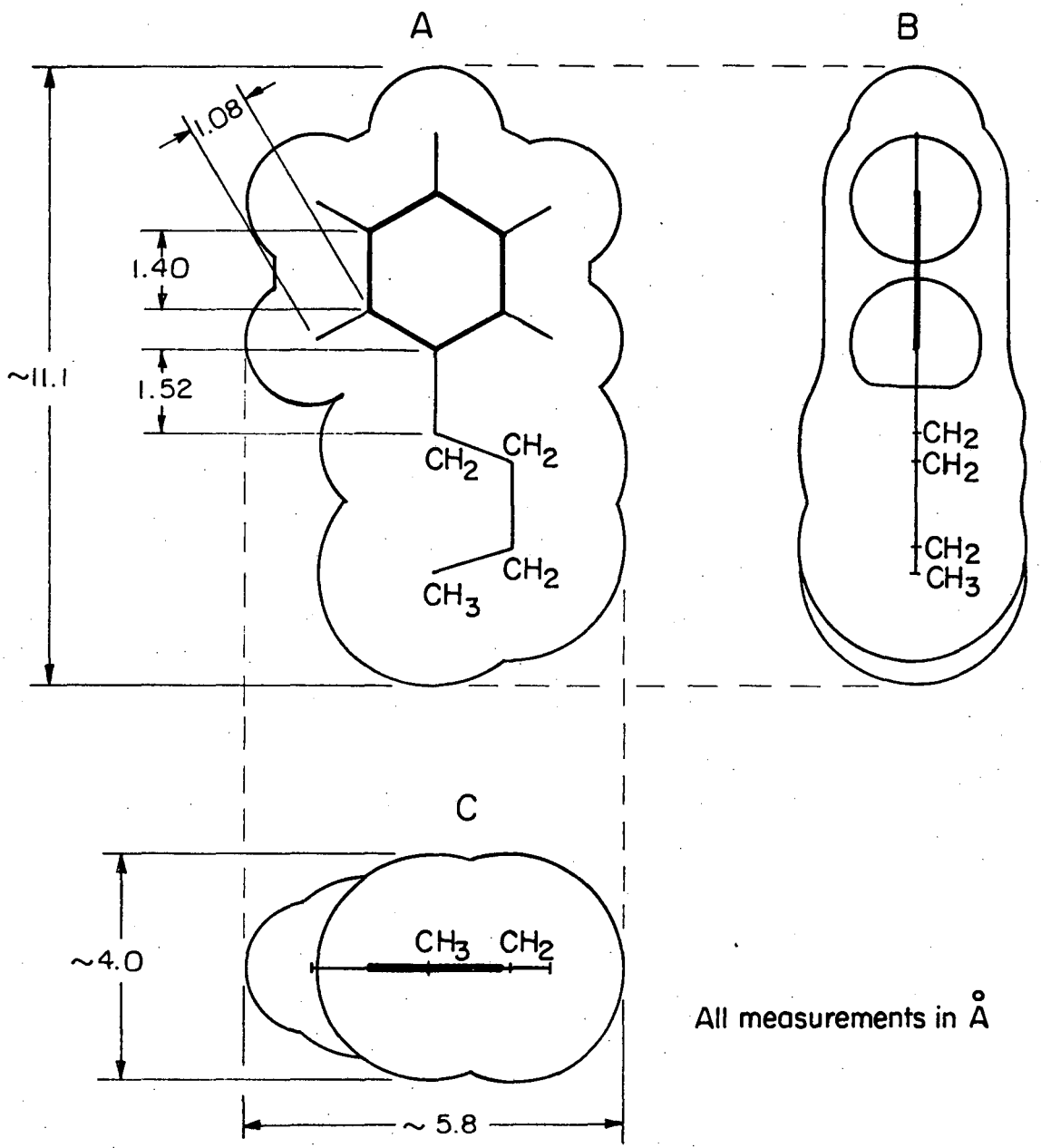

N - Butylbenzene

(one of the possible flat configurations)

XBL 737-6382

Fig. A-3. The structure of n-butylbenzene with van der Waals radii shown.

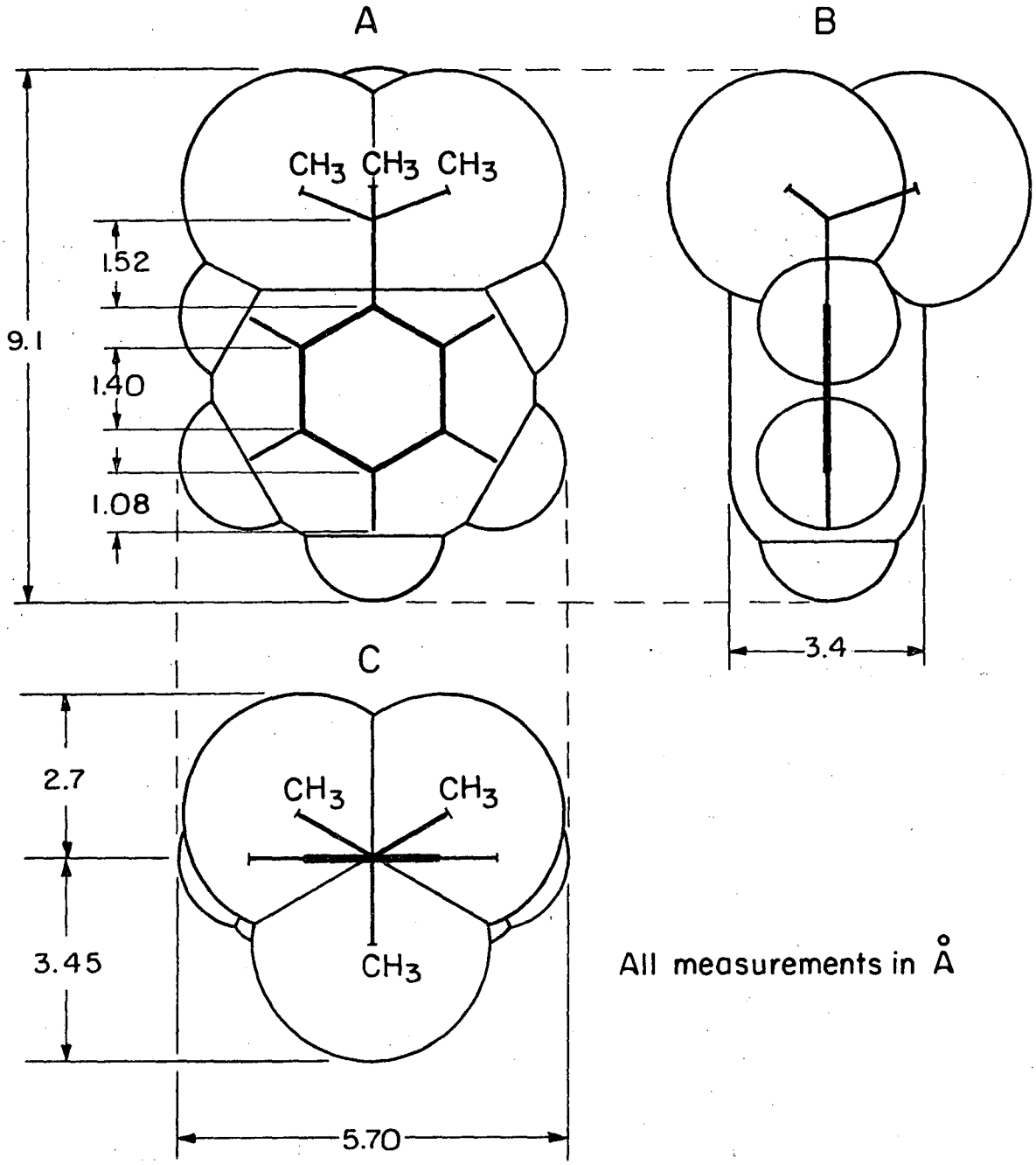

T-Butylbenzene

XBL737-6381

Fig. A-4. The structure of t-butylbenzene with van der Waals radii shown.

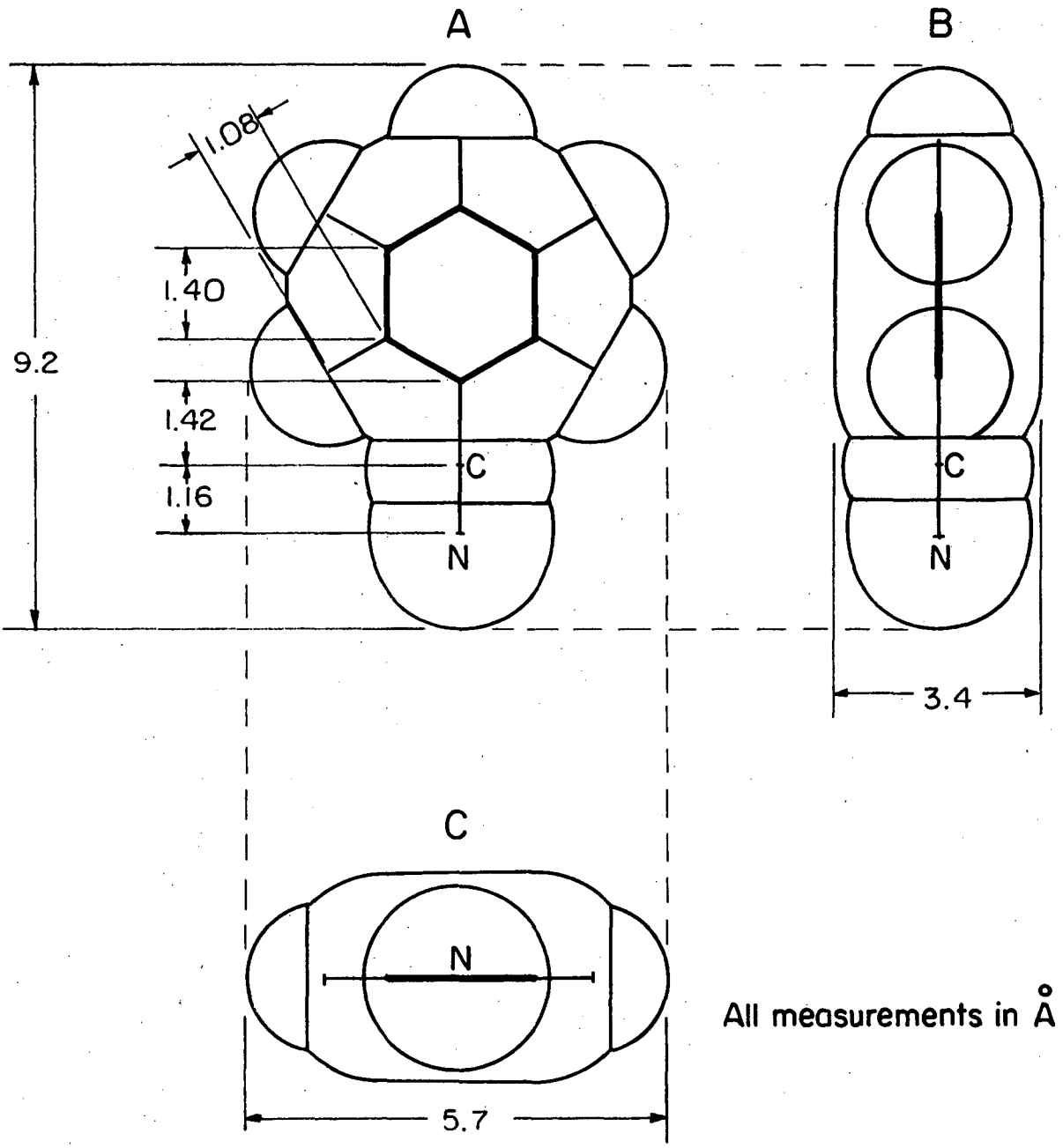

Fig. A-5. The structure of cyanobenzene with van der Waals radii shown.

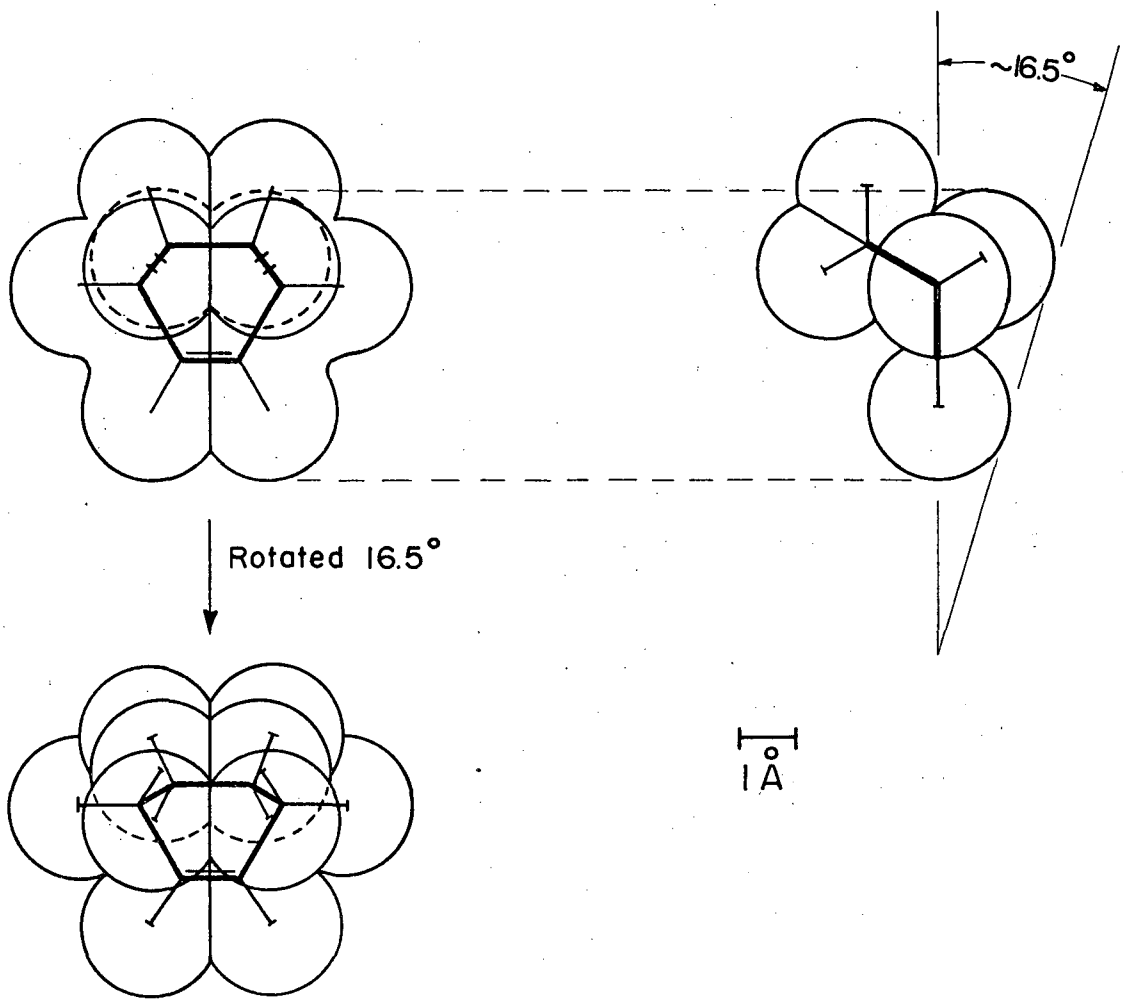

Cyclohexene
(one of the possible orientations)

XBL737-1529

Fig. A-6. The structure of cyclohexene with van der Waals radii shown.

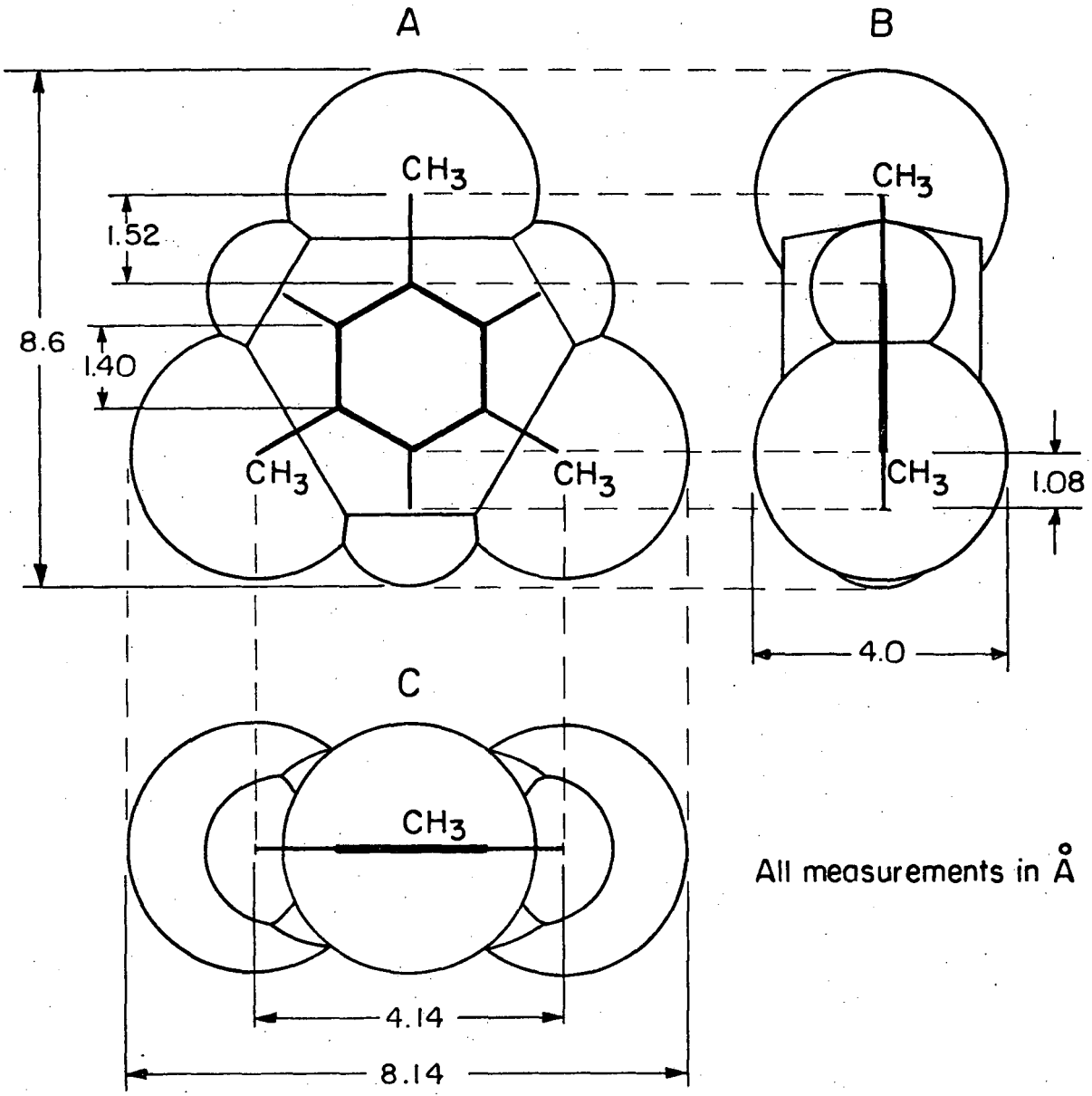

Fig. A-7. The structure of mesitylene with van der Waals radii shown.

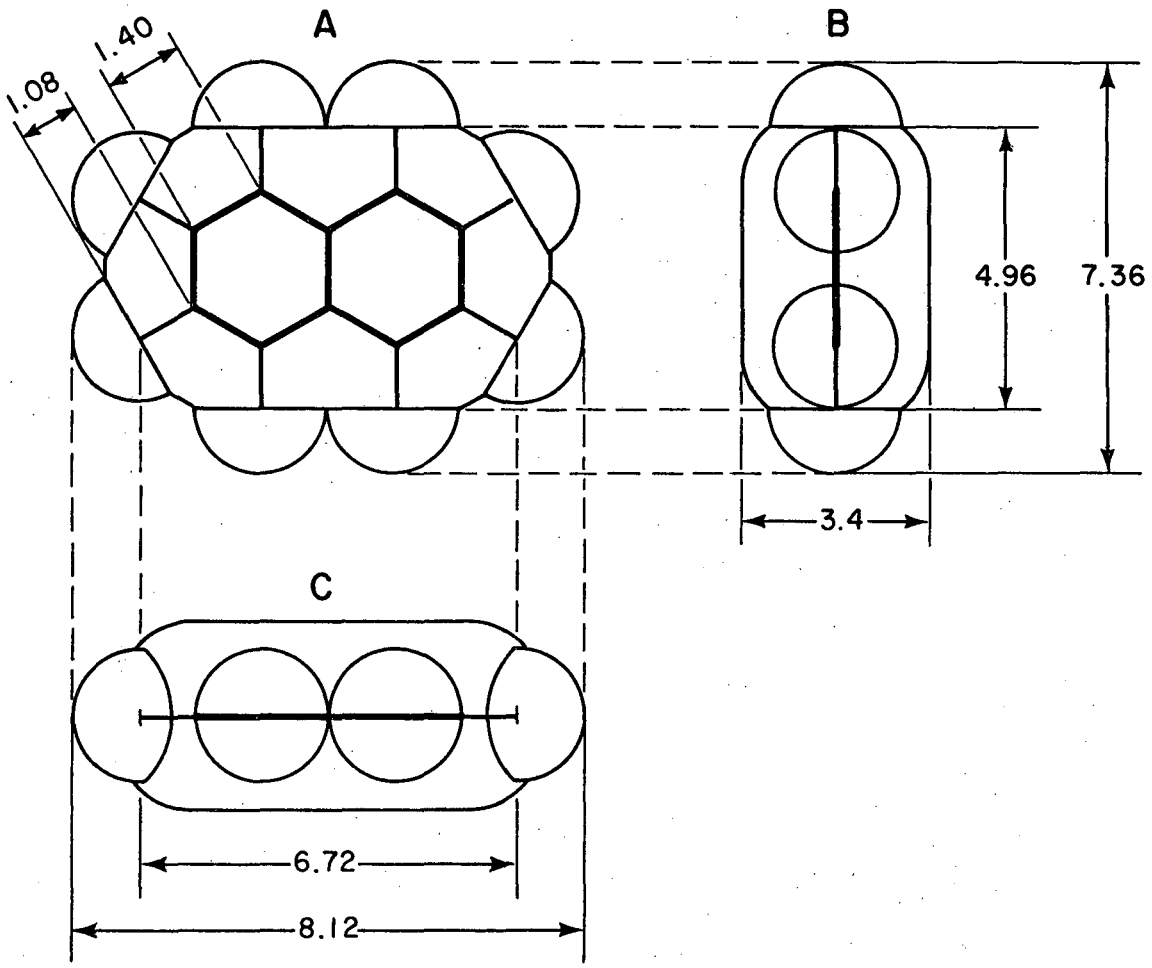

Fig. A-8. The structure of naphthalene with van der Waals radii shown.*
(* = All dimensions are in Angstroms)

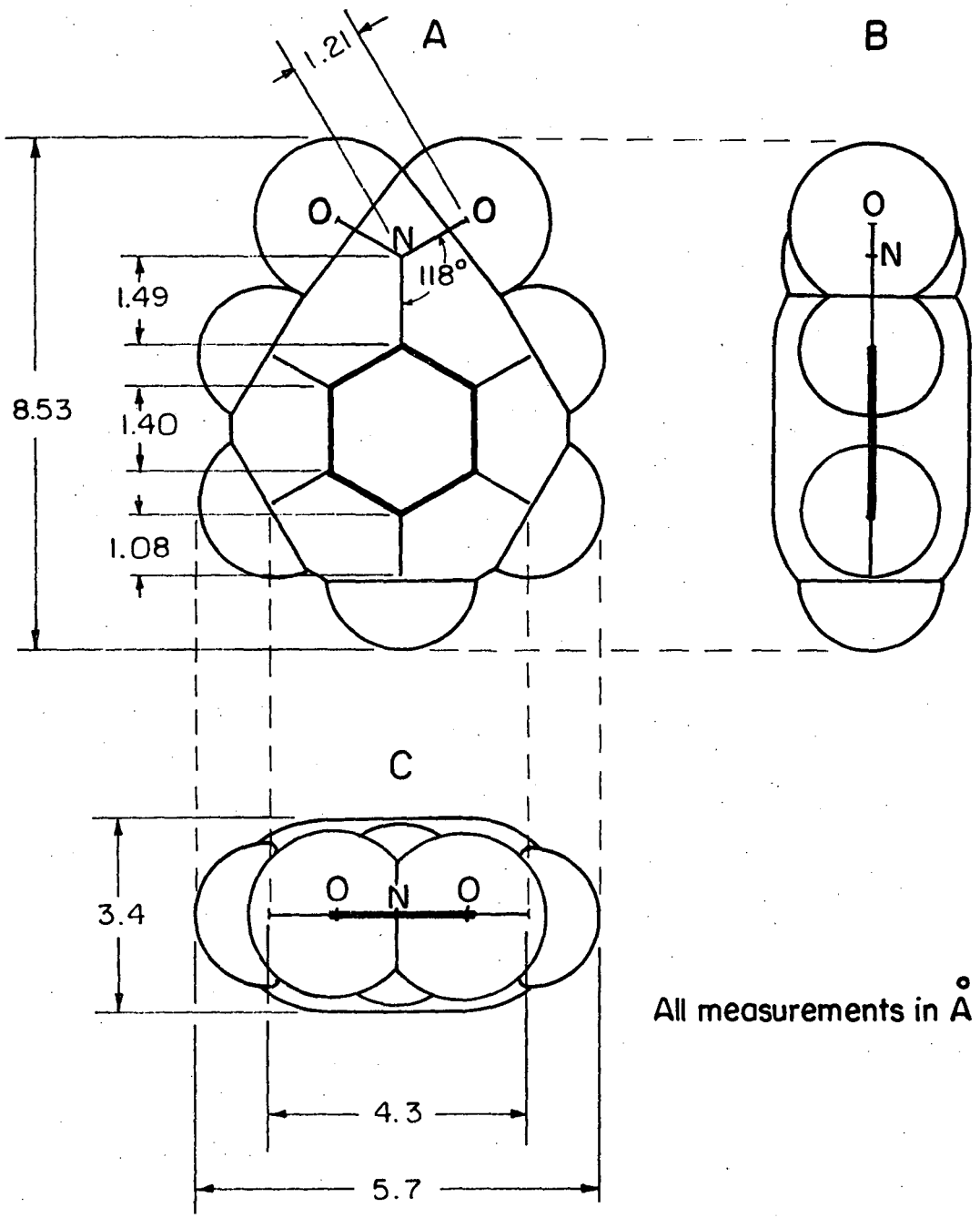

Nitrobenzene

XBL 737-6384

Fig. A-9. The structure of nitrobenzene with van der Waals radii shown.

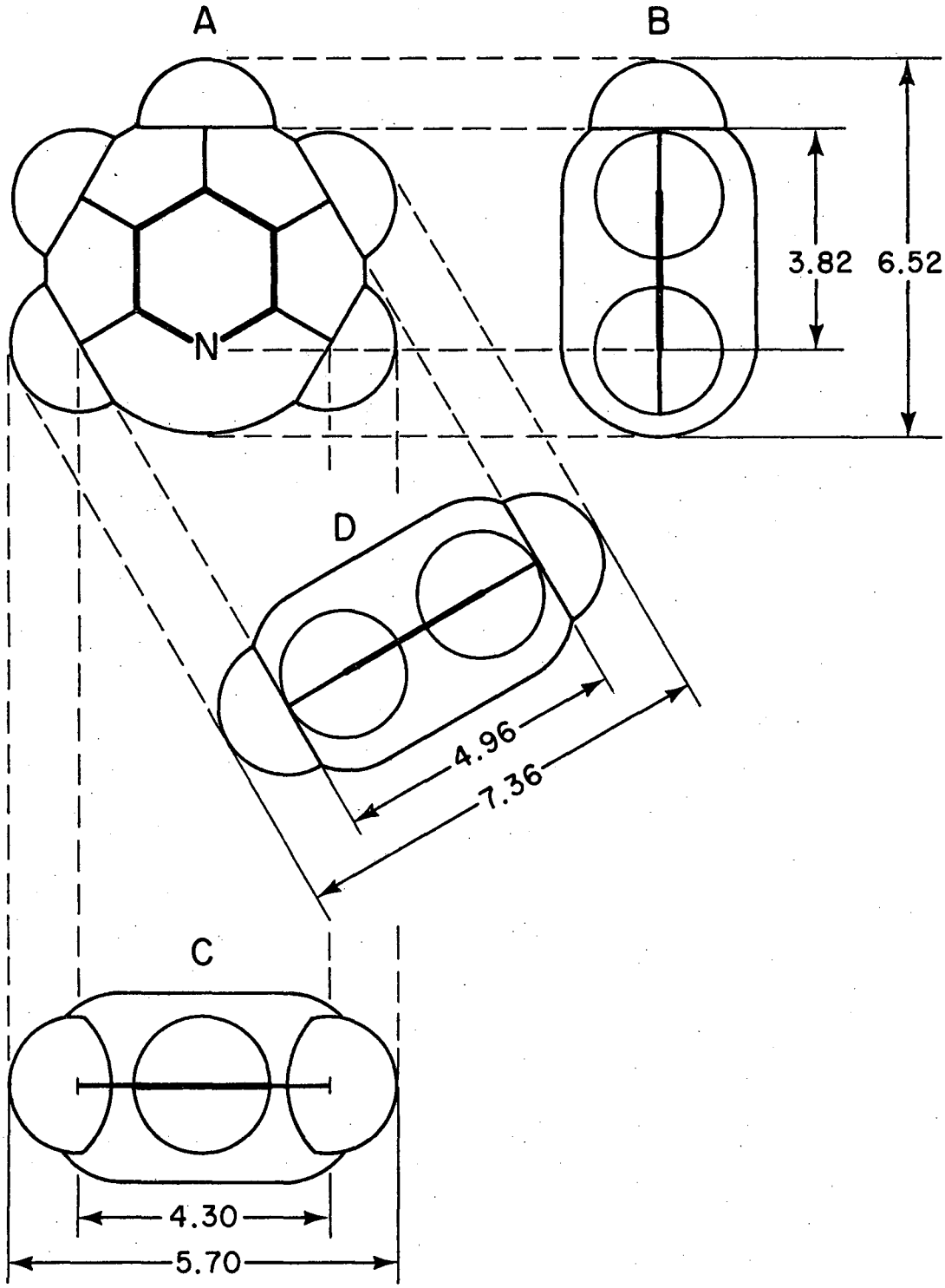

Fig. A-10. The structure of pyridine with van der Waals radii shown.*
(* = All dimensions are in Angstroms)

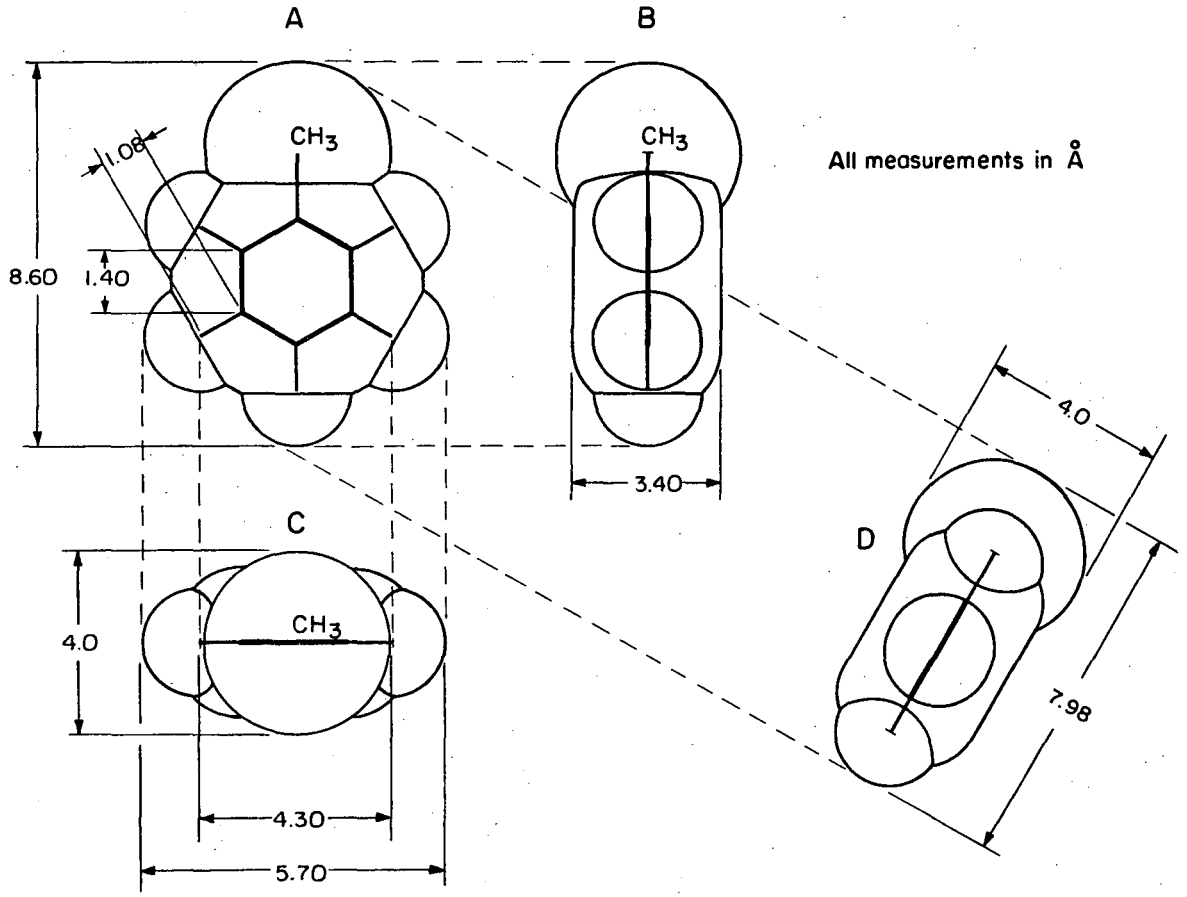

Fig. A-11. The structure of toluene with van der Waals radii shown.

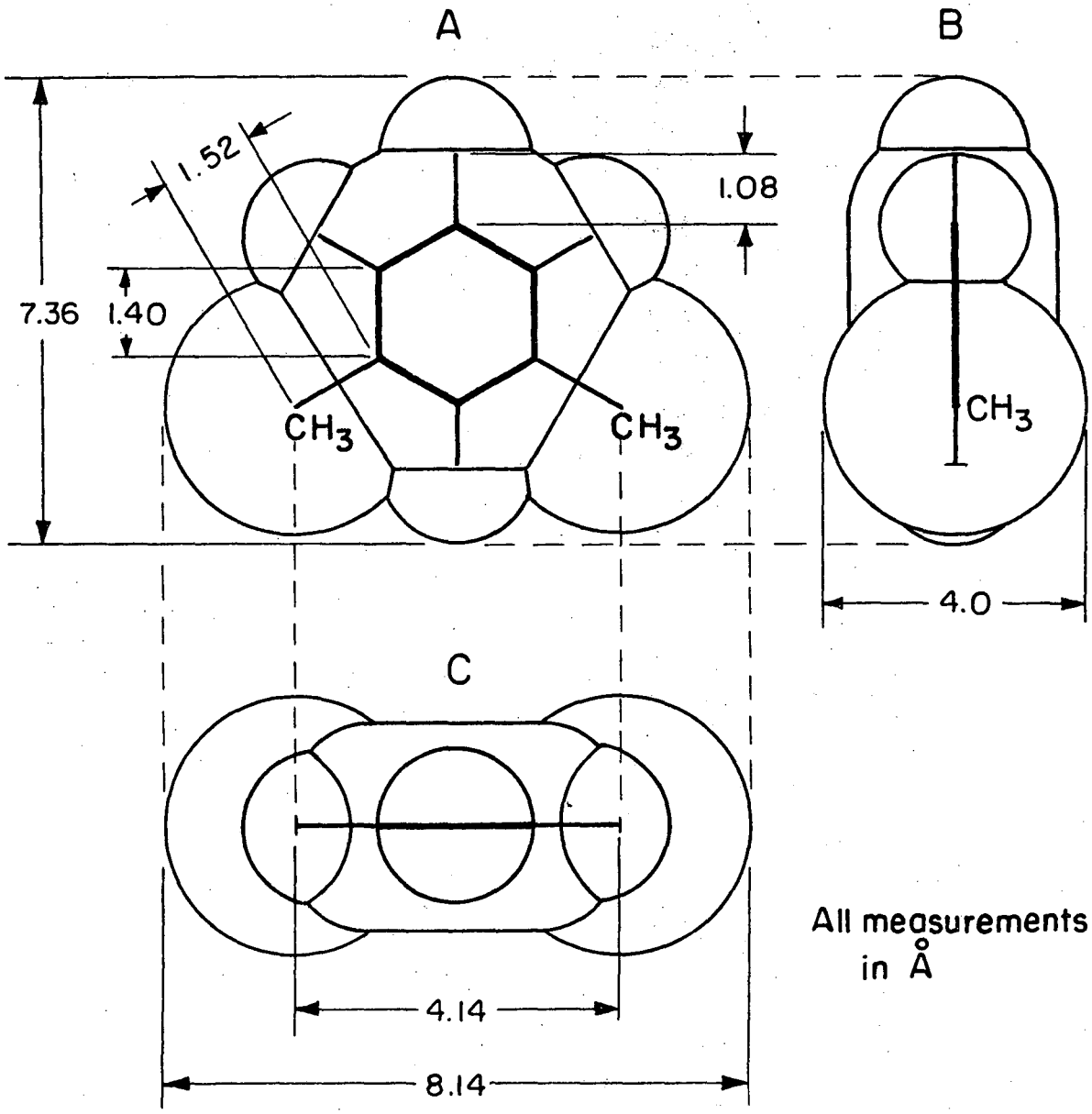

Fig. A-12. The structure of m-xylene with van der Waals radii shown.

ACKNOWLEDGEMENTS

First of all I would like to thank my wife Wanda for her help, patience, and the many sacrifices she has made in helping me through school. I am especially grateful to Gabor A. Somorjai for his guidance and the unfailing enthusiam he has shown in the past four years. Gabor has certainly added a great deal to my experience here in Berkeley with his example of boundless energy and relentless drive.

I would like to thank all the members past and present, of the Somorjai research team. A large part of my graduate education has occurred during informal discussions with group members. I would like to thank "Lenny" F. J. Szalkowski for his friendship and the introduction he gave me concerning surfaces and UHV technology. Al West has also become a good friend and I would particularly like to thank him for introducing me to the techniques involved in molecular beam scattering and sailboat racing. I am grateful to Richard Joyner for introducing me to catalysis and for the many enlightening discussions we had. Steve and Sandy Bernasek have added a great deal to the last two years with their friendship and understanding. I would also like to thank Don Blakely, John Wasilczyk, Reed McFeely, Cliff Megerle and my protegé and heir apparent, Larry Firment for our mutually enlightening experiences. My understanding of catalysis would not have been the same without the help and friendship of Ken Baron.

I would like to express my sincere appreciation to Louis and Opal Gland, my parents, who have encouraged me and helped me throughout my life.

I would like to thank Gerald Nienke for introducing me to the exciting world of chemistry. Dave Westneat and Rolfe Hahne carefully nurtured my interest through my undergraduate years and added considerably to my college experience.

I would like to commend the entire staff of IMRD for being so helpful and kind. I would especially like to thank Phil Eggars who patiently taught me electronics, assisted me with experimental problems, and encouraged me during many trying periods. Emery Kozak wins a special place in the hearts of all the members of our research group; he is a vacuum technician to end all vacuum technicians. I would like to thank him for his patience, guidance, and help during many difficult periods when my ultra-high vacuum had all "leaked out." I would like to thank "Pat" Julien Patenaude for teaching me how to use a machine shop and Del Peterson for teaching me how to build electronic gadgets. I would especially like to thank Alice Ramirez for typing this manuscript and doing a very commendable job.

This work was performed under the auspices of the U. S. Atomic Energy Commission.

TECHNICAL INFORMATION DIVISION
LAWRENCE BERKELEY LABORATORY
UNIVERSITY OF CALIFORNIA
BERKELEY, CALIFORNIA 94720